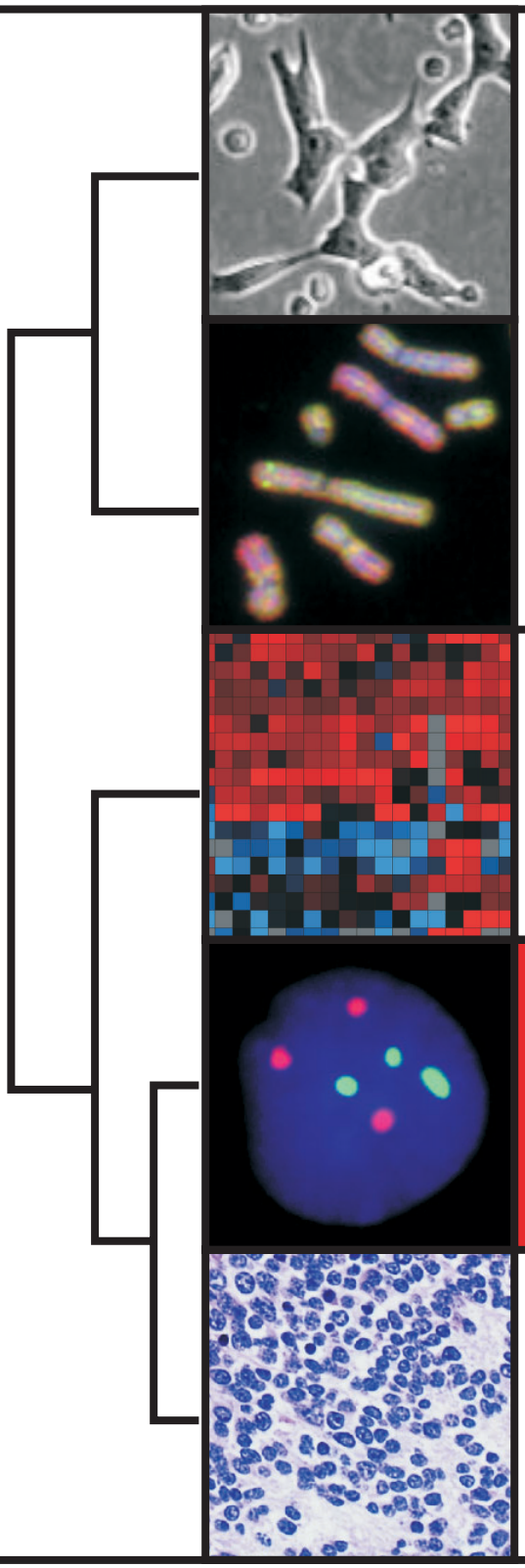

Delineation of the heterogeneous pattern of genomic changes and identification of differentially expressed genes in neuroblastoma

UNIVERSITEIT GENT

Jo Vandesompele

Ghent University, Faculty of Medicine and Health Sciences
Center for Medical Genetics

Delineation of the heterogeneous pattern of genomic changes and identification of differentially expressed genes in neuroblastoma

this thesis is submitted as fulfillment of the requirements for the degree of
Ph.D. in Medical Sciences by ir. Jo Vandesompele, 2002

promotors
Prof. dr. Anne De Paepe, Prof. dr. Frank Speleman

Center for Medical Genetics
Ghent University Hospital, 1K5, De Pintelaan 185, B-9000 Gent, Belgium
+32-9-2405518 (phone)
+32-9-2404970 (fax)
joke.vandesompele@rug.ac.be

to my parents and Ellen, my love
to children diagnosed with neuroblastoma

Thesis submitted to fulfill the requirements for the degree of Doctor in Medical Sciences

May 2002

Promotors: Prof. dr. Frank Speleman
Ghent University, Belgium

Prof. dr. Anne De Paepe
Ghent University, Belgium

Members of the examination committee:

Prof. dr. Marc Mareel
Ghent University, Belgium

Prof. dr. Geneviève Laureys
Ghent University, Belgium

Prof. dr. Joël Vandekerckhove
Ghent University, Belgium

Dr. Geert Berx
Ghent University, Belgium

Prof. dr. Sven Påhlman
Lund University, Sweden

The research described in this thesis was conducted in the Center for Medical Genetics, Ghent University Hospital, Ghent, Belgium.

This work was supported by the Flemish Institute for the Promotion of Scientific Technological Research in Industry (IWT), FWO-grant G.0028.00, GOA-grant 12051397 and BOF-grants 011B4300 and 011F1200.

Publication of this thesis was supported by Bio-Rad en Eurogentec.

TABLE OF CONTENTS

INTRODUCTION

At the start of this doctoral study (October 1997), the molecular (cyto)genetic and clinical picture of neuroblastoma comprised three types of tumors[1, 2]. A first type was typically found in infants (children under the age of 1 year at diagnosis) and characterized by a near-triploid DNA content. Patients with this type of tumor had a high survival probability. A second type of tumor was found in children over the age of 1 year, with a near-diploid or near-tetraploid DNA content, and exhibited *MYCN* amplification (MNA) and deletion of the short arm of chromosome 1. Despite intensive and multi-modal therapy, these patients had a dismal survival probability. A third type of tumor was clinically and genetically less clearly defined. These tumors shared many characteristics of type 2 tumors, but did not exhibit *MYCN* amplification. The prognosis for these patients was difficult to predict, and sometimes referred to as 'intermediate'.

Genetic research on neuroblastoma had mainly focused on the study of the prognostic value and the functional role of *MYCN* amplification, and on the search for tumor suppressor genes located on the distal part of the short arm of chromosome 1. In addition, at least 7 other chromosomal regions were identified that showed frequent loss of heterozygosity (LOH), and in the mid 1990's, fluorescent in situ hybridization (FISH) studies demonstrated the frequent occurrence of unbalanced 17q translocations in cell lines and tumors.
Although these studies yielded significant and valuable insights in the genetic basis of neuroblastoma, the applied FISH and allelotyping methods were limited in the sense that only a few selected regions were studied simultaneously, leaving the majority of the genome unexamined. Furthermore, metaphase cytogenetic analysis of neuroblastoma was often hampered by a low mitotic index of the tumor cells, resulting in a biased analysis of high stage tumors that tended to grow better in vitro. We therefore decided to apply a new method called 'comparative genomic hybridization' (CGH[3, 4]) that allowed detection of gains and losses in the tumor genome. Particular advantages of this technique are the possibility to screen the complete genome in a single FISH experiment, without the need for culturing the tumor cells. The methodology is based on differential labeling of tumor and normal control DNA and simultaneous hybridization on normal metaphase chromosomes fixed on a microscope slide. The ratios of red to green fluorescent intensities along the chromosome axis reflect the relative copy number for each chromosomal region, and pinpoint losses, gains, and DNA amplifications (Figure 1).

Preliminary studies in our laboratory validated the CGH method on well-characterized neuroblastoma cell lines and a small series of primary tumors[5, 6]. Advanced and detailed analyses of multiple large series of primary biopsies are described in Chapter 2.

Despite significant new insights in the genomic heterogeneity described in Chapter 2, only few genes have been recognized to play a role in neuroblastoma, and if so, only in a subgroup of tumors (e.g. *MYCN* and *CASP8*). Therefore, a new strategy was outlined in our laboratory to identify and study differentially expressed transcripts in the various genetic subgroups. It is well known that the transcriptome is the driving force for proliferation, differentiation and apoptosis, and that changes in expression patterns can lead to malignant transformation. Studying these changes can identify genes that are implicated in the complex process of oncogenesis, and might pinpoint genes that have diagnostic or prognostic discriminatory power.

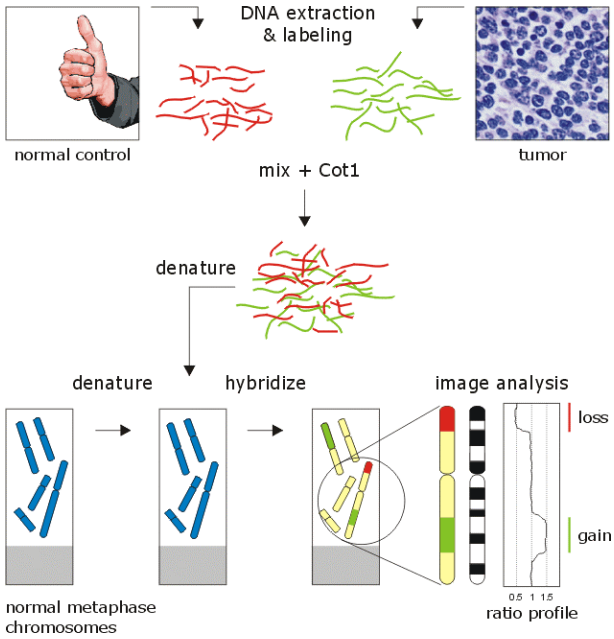

Figure 1 : Comparative genomic hybridization
DNA is extracted from both tumor and reference (normal control) samples and labelled using a green and red fluorescent dye, respectively. The samples are mixed together in the presence of Cot1 DNA, which blocks repetitive sequences. The mixture of DNA is then competitively hybridized onto normal metaphase chromosomes. Fluorescent images are digitally captured and analyzed with specific software to determine the fluorescent ratio along the chromosome axis, which reflects the relative copy number for each chromosomal region in the tumor genome. In this scheme, red segments are underrepresented in the tumor (e.g. due to a deletion), whereas green regions are overrepresented (e.g. duplication). Yellow areas represent regions of the chromosome in which the DNA copy numbers are the same between the two samples.

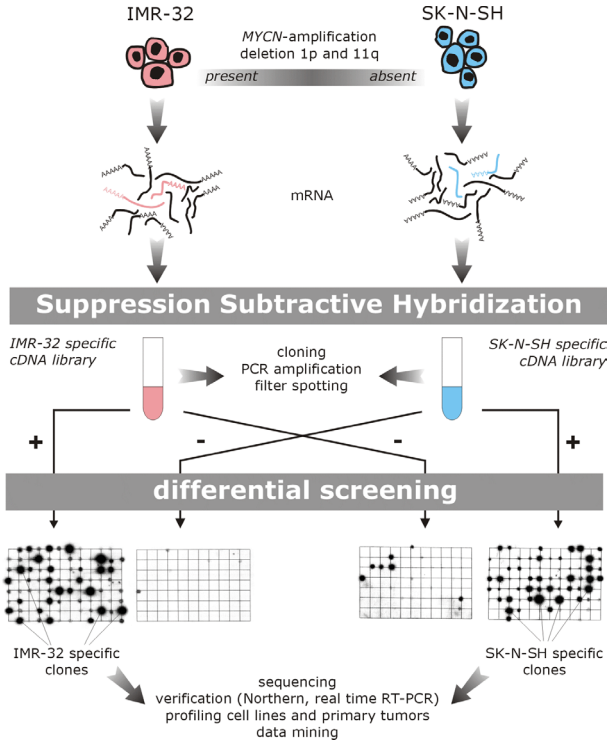

Figure 2 : Subtractive cDNA cloning strategy for identification of differentially expressed genes between cell lines IMR-32 and SK-N-SH, belonging to different genetic subgroups of neuroblastoma. Suppression subtractive hybridization allows specific amplification of transcripts that are specifically expressed in one cell line versus the other. After elimination of false positive clones through differential screening, the differential expression status is verified and the relevance is determined by expression profiling of well characterized cell lines and primary tumor biopsies.

To this purpose, suppression subtractive hybridization (SSH[7]) was applied to extract relevant neuroblastoma genes on a transcriptome wide basis. This PCR based method allows specific amplification of differentially expressed genes, including low abundant transcripts, by comparing two neuroblastoma cell lines that belong to different genetic subgroups (Figure 2).
An important step in the study of differential gene expression analysis based on subtractive cDNA cloning is the verification of the differential expression status of the isolated clones. As Northern blot hybridization requires large amounts of RNA, and constitutes a labor intensive method which is not particularly sensitive, we decided to introduce quantitative RT-PCR[8] in our search for relevant neuroblastoma genes. In Chapter 3, we describe the development of an optimized and validated cost-effective real time RT-PCR assay, and provide an adequate solution for the old problem of gene expression normalization. Based on this technical framework, we screened putative differentially expressed clones in cell lines and primary tumors, and identified new candidate genes and predictors for clinical outcome.

REFERENCES

1. Brodeur, G.M., Maris, J.M., Yamashiro, D.J., Hogarty, M.D. & White, P.S. Biology and genetics of human neuroblastomas. *J Pediatr Hematol Oncol* **19**, 93-101 (1997).
2. Castleberry, R.P. Neuroblastoma. *Eur J Cancer* **33**, 1430-1437; discussion 1437-1438 (1997).
3. du Manoir, S. et al. Detection of complete and partial chromosome gains and losses by comparative genomic in situ hybridization. *Hum Genet* **90**, 590-610 (1993).
4. Kallioniemi, A. et al. Comparative genomic hybridization for molecular cytogenetic analysis of solid tumors. *Science* **258**, 818-821 (1992).
5. Van Gele, M. et al. Sensitive and reliable detection of genomic imbalances in human neuroblastomas using comparative genomic hybridisation analysis. *Eur J Cancer* **33**, 1979-1982 (1997).
6. Van Roy, N. et al. Comparative genomic hybridization analysis of human neuroblastomas: detection of distal 1p deletions and further molecular genetic characterization of neuroblastoma cell lines. *Cancer Genet Cytogenet* **97**, 135-142 (1997).
7. Diatchenko, L. et al. Suppression subtractive hybridization: a method for generating differentially regulated or tissue-specific cDNA probes and libraries. *Proc Natl Acad Sci U S A* **93**, 6025-6030 (1996).
8. Bustin, S.A. Absolute quantification of mRNA using real-time reverse transcription polymerase chain reaction assays. *J Mol Endocrinol* **25**, 169-193. (2000).

chapter 1

CHAPTER 1: NEUROBLASTOMA

CLINICAL ASPECTS

Neuroblastoma is the most frequent extra-cranial solid tumor in children, preceded in frequency by acute lymphoblastic leukemia and brain tumors[1]. Neuroblastoma comprises 10% of all childhood malignancies, with a yearly incidence of 1/100 000 children in the Western world. The median age of diagnosis is less than two years and almost 90% of patients diagnosed by the age of 5 years. Despite recent advances in understanding the biology of this disease, neuroblastoma still accounts for more deaths in childhood than any other cancer[2].

Neuroblastoma tumors arise from primitive sympathetic cells that are derived from the neural crest. During embryonic development, pluripotent cells migrate from the neural crest to give rise to –amongst others- the sympathetic ganglia and the adrenal medulla. Accordingly, the primary tumors are most often found along the abdominal (30%) or thoracic sympathetic chain ganglia (20%) and in the adrenal gland (35%)[1] (Figure 1).

Because neuroblastoma tumors are derived from postganglionic sympathetic neuron precursor cells, they most often show an adrenergic neurotransmitter phenotype. More than 90% of the tumors produce catecholamines, which is an important and relatively easy assessable diagnostic marker, since these products and their metabolites can be measured in serum and urine[3]. Homovanillic acid (HVA) and vanillylmandelic acid (VMA) are the urinary catecholamine metabolites usually measured in neuroblastoma for diagnostic purpose and follow-up.

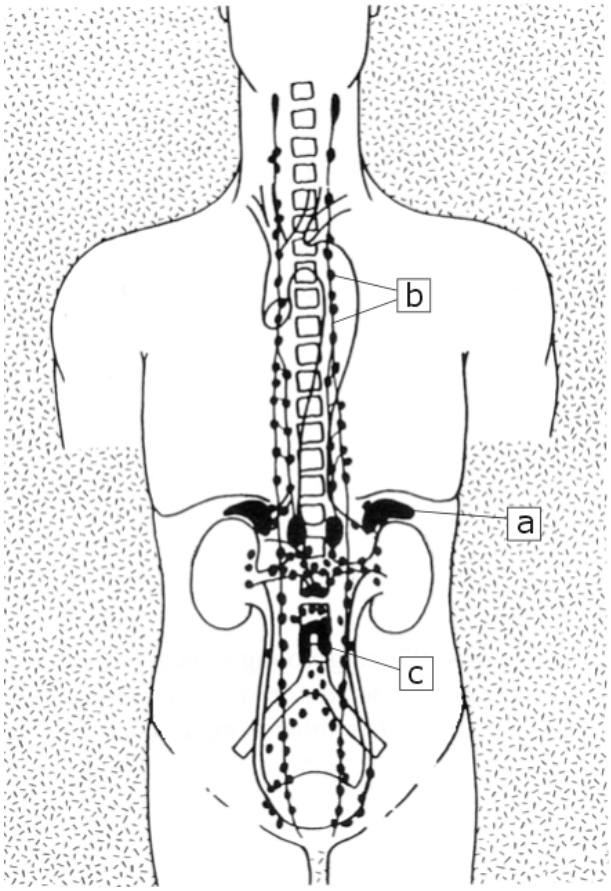

Figure 1: Distribution of the sympathetic nervous system in children, including the adrenal medulla (a), sympathetic side chains and ganglia (b), and the retroperitoneal paraganglia (c) (adapted from source: NKI, Amsterdam, the Netherlands).

Based on the localization of the primary tumor, lymph node involvement and the pattern of metastasis, neuroblastomas can be classified into different stages. The first staging system was proposed in 1971 by Evans and colleagues[4], and evolved into the International Neuroblastoma Staging System in the late 1980s with revisions in 1993[5]. Internationally accepted criteria for confirming the diagnosis of neuroblastoma, initial patient evaluation, and staging are incorporated in this system.

Stage 1 neuroblastomas are localized tumors that allow complete gross excision. Stage 2A and 2B are localized tumors with incomplete gross excision. In stage 2A the ipsilateral nonadherent lymph nodes are negative for tumor microscopically, in stage 2B they are positive. Stage 3 tumors are unresectable unilateral tumors infiltrating across the midline. Stage 4 tumors show remote disease involving the skeleton, liver and other organs, and distant lymph nodes. The group of stage 4S tumors have metastases restricted to liver, skin and/or or bone marrow but not to the skeleton. Stage 4S is limited to infants less than 1 year old.

The most important clinical variables that predict outcome are the stage of disease and the age of the patient at diagnosis. The outcome of infants less than 1 year of age is substantially better than older patients with the same stage of disease, particularly those with more advanced stages of disease. The exception to this is stage 4S, which has –despite widespread metastases- a similar outlook as stages 1 and 2. Based on stage and age, three broad risk groups can be defined[2] (Figure 2). A group of patients who require surgery alone with additional treatment only if there are life- or functioning-threatening symptoms or recurrence, encompasses stage 1, 2 and 4S neuroblastoma, and accounts for one quarter of all patients, with an overall survival rate of 85%. An intermediate group of patients who are treated with conventional chemotherapy and surgical resection of the primary tumor have approximately a 60% probability of survival. This group includes patients with stage 3 neuroblastoma and infants with stage 4 disease, and accounts for approximately one quarter of all children. Patients with poor-prognosis neuroblastoma, defined as stage 4 disease over the age of one year, make up the largest group,

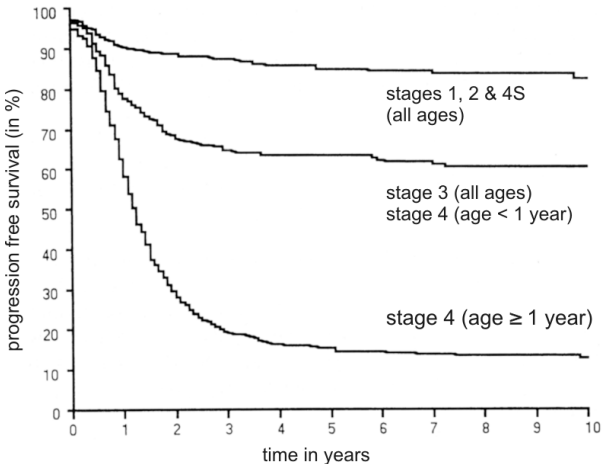

Figure 2: Progression free survival of patients with neuroblastoma, classified according to patient age at diagnosis and tumor stage (adapted from ref. [2]).

comprising half of all patients. Despite multimodal therapy including chemotherapy, surgical resection of the primary tumor and myeloablative therapy with hematopoietic stem cell rescue, only 15-25% of the stage 4 patients are long-term survivors.

In agreement with the above described large differences in individual survival probability, neuroblastoma is often described as enigmatic because the tumor exhibits three distinct patterns of clinical behaviour[6]: life-threatening progression, maturation into ganglioneuroma or ganglioneuroblastoma (see further), or spontaneous regression. The incidence of the latter phenomenon in neuroblastoma is between 10-100 fold more frequent than in any other human cancer. The most striking examples of neuroblastoma regression include cases where primary tumor and metastases disappear without treatment. Spontaneous regression is most often found for the stage 4S neuroblastoma in infants. In addition, post-surgical residual disease from stage 2 neuroblastoma usually regresses completely[7]. It has been postulated that a delayed natural occurring apoptosis mechanism is responsible for the observed regression[8]. Alternatively, immunological cytolytic processes guided by natural IgM antibodies might play a role in the regression of malignant neuroblastoma cells[9].
The regression behavior of clinically manifested neuroblastoma tumors is reminiscent to the naturally occurring or programmed cell death during development of the nervous system. This trimming process, referred to as involution[10, 11] is characterized by massive death of still immature neuroblasts before differentiation. In this context, a very high frequency of microscopic aggregates of immature neural crest cells has been observed inside and outside of the adrenal gland at autopsy of infants younger than 3 months who died of non-tumor-related causes[12]. The incidence of so-called 'neuroblastoma in situ' is by far exceeding the frequency of clinically detected cases of neuroblastoma, implying that these in situ lesions undergo spontaneous regression or involution. It's still an open question whether neuroblastoma in situ represents embryonic remnants of sympathetic nervous system development, or hyperplastic/neoplastic lesions. Likewise, mass screening studies aiming at the preclinical detection of neuroblastoma revealed a doubled frequency in low stage prognostic favorable tumors without a concomitant decrease in advanced stage neuroblastoma[13]. These data demonstrate that mass screening studies result in overdiagnosis of otherwise regressing tumors, and suggest that low stage tumors do not progress to advanced stages of disease. Alternatively, the higher incidence of tumors as a result from screening studies might partially be explained by the detection of nests of non-transformed neuroblasts, not yet eliminated in the normal process of trimming the nervous system.

PATHOLOGY

Neuroblastoma belongs to the small round blue cell tumors of childhood, which is a descriptive category of a number of malignant tumors that tend to occur in childhood with a similar histological appearance of uniformly sized round cells, with large dark nuclei and scant cytoplasm (Figure 3). Other tumors that fit into this category are primitive neuroectodermal tumors (PNET), Ewing's sarcoma, Wilms' tumor, rhabdomyosarcoma, desmoplastic small round blue cell tumor, non-Hodgkin lymphoma and acute leukemia.
A subset of neuroblastomas has the capacity for spontaneous or therapy induced maturation, thus mimicking the physiological pathways of sympathetic neuroblasts. Invading normal Schwann cells in the tumor are believed to play a role in the differentiation process by providing the necessary differentiation factors[14]. Ganglioneuroma is the fully differentiated and benign counterpart of neuroblastoma. It is composed of mature ganglion and Schwann cells. In ganglioneuroblastoma, both mature and immature cells are present. These three classic histopathological patterns of neuroblastic tumors (neuroblastoma, ganglio-neuroblastoma and ganglioneuroma) reflect a continuous spectrum of maturation and differentiation, and are correlated with clinical outcome. Based on age at diagnosis and histological morphology (i.e. the fraction of Schwann stroma, differentiation status of the neuroblastic cells, and the mitosis-karyorrhexis index), an International Neuroblastoma Pathology Classification (INPC) system was developed, in which favorable and unfavorable histological

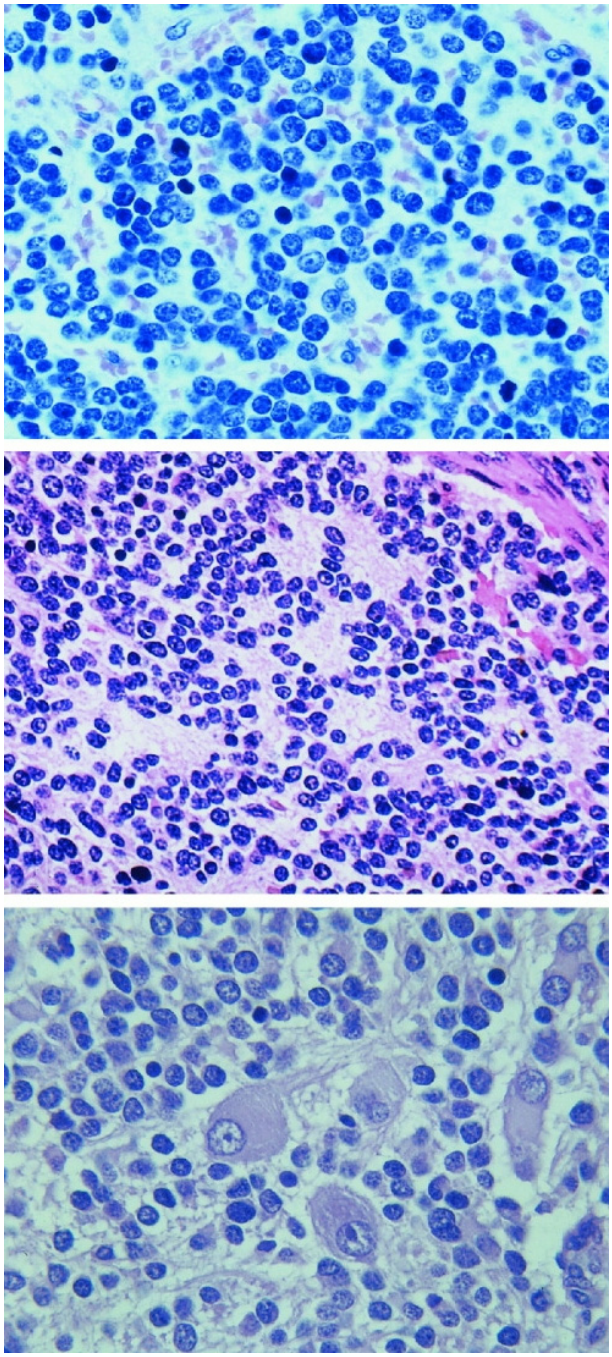

Figure 3: According to the INPC, neuroblastoma is defined as a neuroblastic, Schwannian stroma-poor tumor, with subtype classification depending on the degree of neuroblastic differentiation. Top: undifferentiated subtype, composed of undifferentiated neuroblasts without discernable neuropil (original magnification x200); Middle: poorly differentiated subtype, composed of undifferentiated neuroblastic cells with clearly recognizable neuropil (original magnification x200); Bottom: differentiating subtype, showing both nuclear and cytoplasmic differentiation (original magnification x400) (reproduced from ref.[15]).

groups are distinguished[15, 16] (Figure 3). A recent study assessed the value of this system by multivariate regression analysis including known genetic defects with adverse prognosis (see further), and confirmed the prognostic power of the INPC system[17].

SYMPATHETIC NERVOUS SYSTEM DEVELOPMENT

The human nervous system consists of the central nervous system (CNS) (comprising the brain and the spinal cord) and the peripheral nervous system (PNS), which links the CNS with the body's sense receptors, muscles, and glands. The PNS is divided in two components : the somatic or skeletal nervous system, which controls voluntary movement, and the autonomic nervous system, which regulates inner organ function via the sympathetic, parasympathetic ganglia, or enteric ganglia. The main role of the sympathetic nervous system (SNS) is to control stress response.

The nervous system originates from the neural plate, an embryonic structure evolving from the ectodermal germ layer during the third week of gestation. Little is known with respect to the genes and processes implicated in the early development of the human nervous system. Furthermore, most of the information we currently have on this subject is based on animal systems. There, the process of neural induction is initiated and guided by several growth factors (such as *bone morphogenetic protein*, *fibroblast growth factor*, and *wingless* family members) and transcriptional responses to these factors (belonging to the *Snail*, *Pax* and *Zic* transcription factor families)[18]. During the process of neurulation, the neural plate invaginates ventrally and closes in order to form the neural tube (which will give rise to the CNS).
During this closure, neural crest cells originate at the interface between the closing neural tube and the dorsal ectoderm (Figure 4). These pluripotent migratory cells are unique in that they generate multiple cell types contributing to different functionally unrelated tissues located all over the body, such as melanocytes in the skin, cartilage and facial bones, neurons and support cells of the PNS, and neuroendocrine cells in the adrenal medulla and thyroid[19]. The ultimate cell fate is largely determined by region- and cell-type specific transcription factors, as well as signalling molecules encountered during migration[20, 21].
Important transcription factors that play a role in SNS development are *ARIX (PHOX2A)*, *PMX2B* (*PHOX2B), ASCL1 (HASH1)*, and *HAND2 (dHAND)*.
The adult SNS consists of neuroendrocrine adrenal chromaffin cells, and sympathetic neurons and supportive cells. However, during prenatal and early postnatal life, several additional cell types are present that regress or mature, such as clusters of immature neuroblastic cells in the adrenal gland, and extra-adrenal chromaffin cells that form the

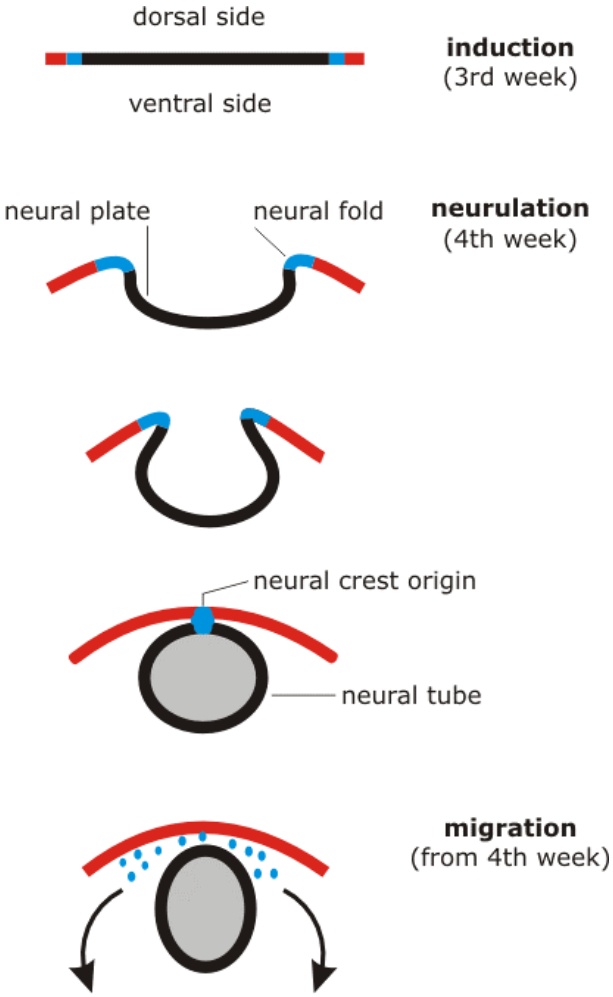

Figure 4: Nervous system development (cross-section): invagination of the dorsal ectoderm, closure of the neural tube, neural crest formation at the interface of the closing neural folds and dorsal ectoderm, and migration of the pluripotent crest cells (human time frame).

paraganglia, or that are found as small intensely fluorescent (SIF) cells in sympathetic ganglia (reviewed in [22]). Expression studies indicated that neuroblastomas share expression patterns with developing SNS cells. Differentiating tumors (having prognostically favorable characteristics) are thought to progress along an extra-adrenal chromaffin lineage, and undifferentiated aggressive tumors display marker expression mirroring that of early sympathetic neuroblasts of the ganglia and adrenal gland[23, 24].

In view of the importance of neurotrophin signalling in normal neural development, a number of studies investigated this pathway in neuroblastoma. Neurotrophins implicated in SNS development include nerve growth factor (NGF), brain-derived neurotrophic factor (BDNF), neurotrophin-3 and neurotrophin-4, and mediate signalling through the high-affinity TRK receptor family of tyrosine kinases, and the low-affinity p75 neurotrophin receptor (p75NTR). Neurotrophin signalling regulates growth, development, survival and repair of the sympathetic nervous system[25, 26].
Differential expression of the TRK receptor kinases is strongly correlated with the biological and clinical features of neuroblastoma (reviewed in ref. [27]). *NTRK1* (*TRKA*) expression is inversely related to disease stage and *MYCN* amplification status (see further), with high *NTRK1* expression hence being a marker for prognostically favorable tumors. The presence of NGF results in terminal differentiation of NTRK1 expressing cells. In contrast, if NGF is limiting, NTRK1 expressing cells will enter a programmed cell death.
Full length *NTRK2* (*TRKB*) is expressed preferentially in advanced stage, *MYCN* amplified neuroblastomas. Many of these tumors also display high BDNF expression, which result in an autocrine pathway promoting growth and survival, even in the absence of exogenous neurotrophins. In favorable tumors, *NTRK2* is expressed as a truncated isoform or in low amounts of the full length isoform. Lastly, *NTRK3* (*TRKC*) shows a similar expression pattern as *NTRK1*.

NEUROBLASTOMA GENETICS

In many neoplasms of adulthood, a multistep process of genetic and epigenetic alterations has been shown to be implicated in tumorigenesis, best exemplified for the progression of colon adenoma to invasive carcinoma[28]. In contrast, for many pediatric tumors, only few or single initiation events, such as oncogene activation due to a specific translocation or loss of tumor suppressor function due to deletion, have been shown to be responsible for tumorigenesis. For neuroblastoma however, the observed genetic changes are heterogeneous, and no single genetic alteration has been identified which is common to all or most tumors.
During the last three decades, a complex pattern of genetic abnormalities has been described in neuroblastoma (Figure 6), some of which delineate distinct genetic subgroups with respect to response to therapy and outcome.

MYCN amplification

The first genetic analyses of neuroblastoma were cytogenetic characterizations of tumor derived cell lines in the 1970s. Biedler and colleagues described double minute chromatin bodies (dmins) and occasional long, homogeneously staining regions within chromosomes[29]. Ten years later, it was shown that these cytogenetic abnormalities were the result of *MYCN* gene amplification[30], a new member of the MYC proto-oncogene family. Brodeur and colleagues were the first to report *MYCN* amplification (MNA) in a substantial subset of primary untreated

neuroblastomas, and demonstrated a correlation with advanced stage of disease[31]. Subsequently, it was shown that MNA was strongly associated with rapid disease progression and a poor prognosis[32]. Hence, assessment of *MYCN* copy number is an important component of disease evaluation for newly diagnosed patients (Figure 5).

Overall, around 20% of neuroblastomas show MNA, all having very high MYCN expression both at the RNA and protein level. Although there is some variation in MYCN levels in tumors without amplification, higher expression in this group is not correlated with a worse outcome[33, 34]. Targeted overexpression of human MYCN in the neuro-ectoderm of transgenic mice produced neuroblastoma tumors in a dose-dependent manner[35], firmly demonstrating a role of *MYCN* in the development of a subset of neuroblastomas.

MYCN is a proto-oncogene located on chromosome band 2p24, and is normally expressed in the developing nervous system as well as in other tissues. Like all MYC family proteins, *MYCN* encodes a transcription factor with a N-terminal transactivation domain (Myc box) and a C-terminal basic helix-loop-helix/leucine zipper (bHLH-LZ) motif. For MYCN to activate transcription, it must first dimerize to MAX by means of the bHLH-LZ domain, upon which the heterodimers bind E-box-related sequences with high affinity. MAX expression is relatively constant, and results in the preferential formation of MAX/MAX homodimers in quiescent cells, which results in transcriptional repression. In addition, heterodimerization of MAX with the MAD family of proteins also represses transcription[36]. With increasing MYCN protein levels (e.g. entrance into the cell cycle, or as a consequence of genomic amplification), heterodimerization of MYCN/MAX occurs, which lead to transcriptional control of -largely unknown- genes involved in amongst others growth and proliferation. Indeed, the molecular mechanism of tumorigenesis caused by overexpression of *MYCN* remains largely unknown.

As the amplicon containing *MYCN* is large, usually between 500-1000 kb, it has been postulated that additional genes located near *MYCN* could contribute to the observed aggressive behavior. High-resolution restriction mapping of the region around *MYCN* indicated that a core domain of 130 kb is consistently amplified[37]. To date, no other gene besides *MYCN* has been identified in this core region[38]. However, two other genes (*DDX1* and *NAG*) have been reported to be coamplified in 40-50% of the *MYCN* amplified tumors[39, 40]. As amplification of *DDX1* and *NAG* has never been observed in *MYCN* single copy tumors, it seems that MYCN is primarily responsible for the formation of the amplicon.

Non-syntenic co-amplification of other genes with *MYCN* is rare in neuroblastoma. Amplification of the *CCND1* and *EMS1* genes at 11q13 have been reported in one primary tumor[41]; amplification of the *SAS, MDM2* and *CDK4* genes (12q13-q14), *RSN* (12q24), and *ZNF133* (20p11) in neuroblastoma cell line NGP[42, 43] (with *MDM2* amplification found in two other cell lines and a tumor[44]); amplification of the *MEIS1* homeobox gene (2p14) in cell line IMR-32[45, 46]; and *MYCL* (1p34) amplification in cell line GOTO[47]. Interestingly, in a *MYCN* single copy neuroblastoma cell line SJNB-12, non-syntenic co-amplification of the *ATBF1* gene, located at 16q22-q23, and the *MYC* proto-oncogene (8q24) was found[48, 49]. The biological significance of these findings in neuroblastoma remains to be determined.

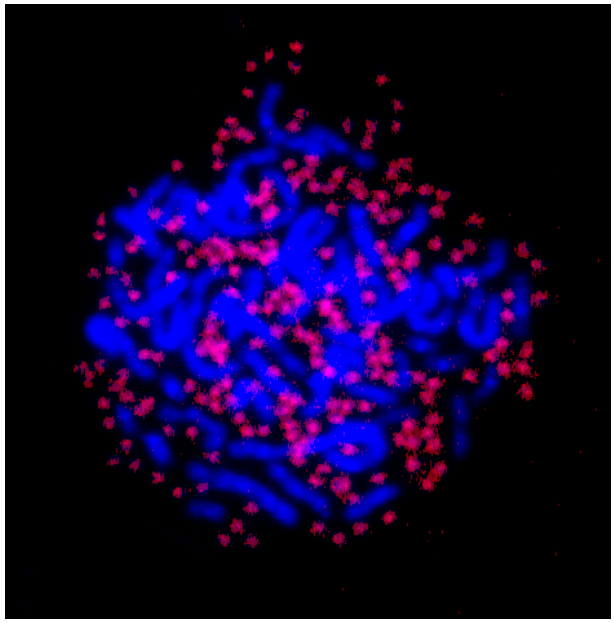

Figure 5: *MYCN* amplification under the form of double minute chromatin bodies (red), as evidenced by FISH analysis for neuroblastoma cell line SMS-KCNR.

Ploidy patterns suggest two biological subtypes

Both cytogenetic and flow-cytometric analyses of neuroblastoma tumor cells have demonstrated the existence of two patterns of ploidy with distinct prognosis for the patient. The majority of the neuroblastoma cell lines and advanced stage tumors have a near-diploid or near-tetraploid chromosome number, whereas favorable neuroblastomas, especially in infants, usually have a hyperdiploid or near-triploid DNA content.

Look and colleagues were the first to describe the association of hyperdiploidy in infants with a better response to chemotherapy and thus a more favorable prognosis[50]. More recent flow-cytometric studies demonstrated that a hyperdiploid DNA content primarily provides important prognostic value in infants, whereas this variable looses its prognostic significance for

patients over two years of age[51, 52]. Near-triploid tumors are characterized by three almost complete haploid sets of chromosomes, with no or only few structural abnormalities. In contrast, the near-diploid or near-tetraploid tumors exhibit structural abnormalities[53, 54].
Recently, comparative genomic hybridization analysis demonstrated that numerical imbalances were predominantly found in lower stage neuroblastoma (1, 2 and 4S), whereas the advanced stage tumors commonly had partial chromosome gains and losses[41]. A subsequent multicenter study provided an accurate description of the typical pattern of numerical imbalances observed in near-triploid neuroblastomas, with whole chromosome 17 gain relative to ploidy found in all tumors with only numerical imbalances[55]. Based on these findings, it has been conceived that the near-triploid tumors have a fundamental defect in mitotic disjunction, while the near-diploid/tetraploid neuroblastomas are characterized by genomic instability leading to various structural chromosome rearrangements (Figure 6).

Unbalanced gain of distal 17q as adverse prognostic marker

In a review of Giemsa-banded karyotypes from 35 neuroblastoma cell lines and tumors, Gilbert and colleagues were the first to report a high frequency of extra copies of the long arm of chromosome 17[56]. These findings however remained unconfirmed until the advent of the fluorescent in situ hybridization (FISH) technique that highlighted the extent and nature of chromosome 17q rearrangements in neuroblastoma cell lines[57, 58], and subsequently in two series of primary tumors[59, 60]. These studies unequivocally demonstrated that unbalanced translocations resulting in gain of 17q and partial loss of the partner chromosome are the most common genetic abnormalities in neuroblastoma. The most frequent partner chromosomes for these translocations are 1p and 11q, with many other partner regions involved, demonstrating the highly promiscuous nature of these 17q translocations.
A further study demonstrated that the chromosome 17 homologue from which the unbalanced translocation had been derived was still present and intact in the neuroblastoma cells. This indicates that the unbalanced 17q translocations occur in the S/G2 phase of the cell cycle[61].
Extensive breakpoint mapping using FISH analysis revealed that the breakpoints are scattered over a large genomic region from 17q11 to 17q23, with a 25 Mb region from 17q23-qter being consistently gained[57, 58, 60, 62]. These findings strongly suggest that this region contains one or multiple genes that -when present in increased copy number- contribute to neuroblastoma tumorigenesis through a gene dosage effect.
More recent comparative genomic hybridization (CGH) studies on all stages of neuroblastoma corroborated and extended the results obtained by FISH[41, 59, 63-65]. Further analysis in a multicenter study of 204 both published and new cases showed that unbalanced 17q gain was present in 70% of the neuroblastomas without whole chromosome 17 gain[55].
These CGH studies and other molecular cytogenetic analyses clearly demonstrated that unbalanced 17q gain is significantly associated with well established indicators of adverse prognosis, such as advanced stage of disease, age at diagnosis over 1 year, 1p deletion (see further), MNA, and ploidy in the near-diploid or near-tetraploid range[66]. To determine the independent prognostic value of 17q gain, a multicenter collaborative compilation of 313 cases with known 17q status was studied[67]. Overall survival at 5 years was 30.6% for the cases with 17q gain, whereas 86.0% of the cases without this feature survived. Furthermore, multivariate analysis showed that unbalanced 17q gain was the most powerful independent prognostic factor, followed by the presence of stage 4 disease and deletion of 1p.

The search for chromosome 1p tumor suppressor genes

Almost 25 years ago, Brodeur and colleagues first reported that deletions of the short arm of chromosome 1 (1p) were a common cytogenetic finding in neuroblastoma cell lines and advanced tumors[68]. Subsequent cytogenetic and molecular genetic studies have confirmed these findings by documenting loss of heterozygosity (LOH) in 20-40% of primary tumors, and until very recently, this feature was considered to be the most frequent genetic aberration in neuroblastoma.
It has rapidly been established that 1p deletions were strongly correlated with high risk factors, such as age at diagnosis greater than 1 year, advanced stages of disease, and MNA. However, there has been ongoing controversy about the independent prognostic value of 1p deletions. In a recent large study, Maris and colleagues have demonstrated that loss of 1p was a significant independent predictor of decreased event free survival (EFS), but had no significant effect on overall survival (OS) probability[69]. These findings suggest that diagnostic assessment of the 1p status may be useful in predicting relapses in otherwise low risk patients.
The frequent finding of 1p deletions in neuroblastoma strongly suggests the implication of a tumor suppressor gene in this region. This has been reinforced by the description of a patient with neuroblastoma who was found to have a constitutional balanced translocation t(1;17) disrupting the 1p36 region[70], and two patients with a constitutional deletion in the 1p36 region who developed neuroblastoma[71, 72].

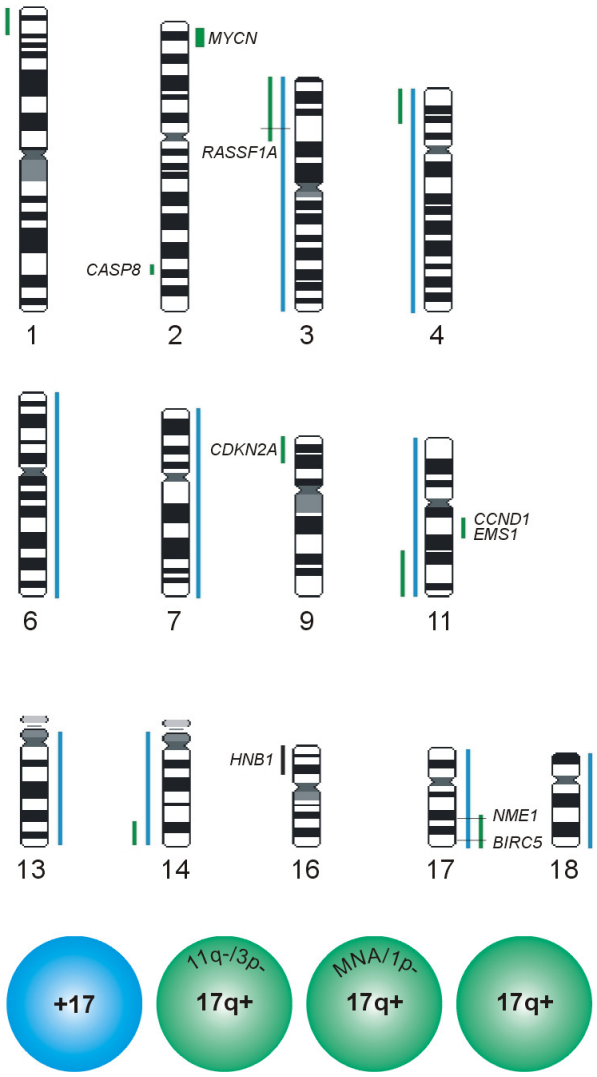

Figure 6: Top: Overview of frequent gains and losses in neuroblastoma, with indication of (putatively) relevant neuroblastoma genes (2q33: *CASP8;* 2p24: *MYCN;* 3p21*: RASSF1A;* 9p21: *CDKN2A;* 11q13: *CCND1/EMS1;* 16p12-p13: *HNB1* (hereditary neuroblastoma locus 1); 17q22: *NME1;* 17q25: *BIRC5*) (bars to the right represent gains, bars to the left losses, bold bar indicates amplification; blue: numerical chromosome changes, each found in more than 40% of the near-triploid tumors; green: structural aberrations found in the near-diploid/near-tetraploid tumors). Bottom: Simplified scheme representing the 4 major genetic subgroups of neuroblastoma (-: loss, +: gain, MNA: *MYCN* amplification).

Further evidence for the presence of a tumor suppressor on 1p came from a chromosome transfer experiment in which the reintroduction of 1p in cell line NGP resulted in morphological differentiation and cell death[73].
Great efforts have been made by many research groups to narrow down the critical region of LOH on 1p in order to find the putative neuroblastoma suppressor gene (reviewed in [74-76]). The observed deletions were generally large, encompassing the telomere and extending to or beyond 1p32. Identification of tumors with small deletions refined the proximal boundary of the shortest region of overlap (SRO), leading to a region of consistent loss on 1p36.3 between markers D1S244 and D1S80[77].
Several lines of evidence indicated that there might be additional 1p neuroblastoma suppressor genes. Schleiermacher and colleagues reported 3 interstitial deletions of 1p32, suggesting the existence of a suppressor gene in this proximal region[78]. Takeda and colleagues reported that tumors with large 1p deletions usually exhibited MNA and poor survival, while tumors with small terminal 1p deletions generally showed normal *MYCN* copy numbers[79]. A similar finding was made by Caron and colleagues, who additionally reported the preferential loss of the maternal allele in the *MYCN* single copy tumors with the smaller deletions[80-82]. These findings suggest the presence of at least two neuroblastoma suppressor genes: an imprinted distal 1p36.3 locus defined by the SRO of all 1p deleted tumors, and a non-imprinted 1p35-p36.1 locus that is lost in *MYCN* amplified aggressive tumors.
Although several genes have been analyzed as possible candidates for the 1p36 neuroblastoma suppressor gene (reviewed in [75]), no mutations have been found in the non-deleted allele of any candidate. However, one has to consider the possibility that loss of one allele results in haploinsufficiency of one or more genes with tumor suppressive function, as shown for the *PTEN* and *APC* gene[83, 84].
Recently, the distal SRO was further refined down to a 1 Mb region between markers D1S2731 and D1S2666[85], which may provide an entrance point for the cloning of candidate genes for neuroblastoma. Additionally, two different homozygous deletions of about 500 kb were identified in two neuroblastoma cell lines, and might pinpoint 1p36 suppressor genes[86, 87].

Chromosome 11q deletions delineate a new genetic subgroup

Several lines of evidence suggest the localization of another important neuroblastoma tumor suppressor gene at chromosome arm 11q. Deletions of the long arm of chromosome 11 have been described in approximately 15-20% of tumor karyotypes[88], and chromosome 11 transfer in cell line NGP with 11q LOH resulted in a more differentiated phenotype[73]. Furthermore, rare cases of constitutional abnormalities of this region in children who developed neuroblastoma have been reported (reviewed in [76]). Molecular genetic studies demonstrated LOH or loss of 11q in approximately one third of the neuroblastoma tumors[41, 59, 64, 65, 89]. It was first reported by Vandesompele and colleagues that 11q deletions were inversely correlated with MNA and loss of 1p. Furthermore, 11q deletions were found significantly associated with loss of 3p and 14q[41].

A subsequent large multicenter CGH study confirmed this pattern and delineated a new genetic subgroup of high stage tumors with 11q loss in the absence of MNA and 1p deletions[55] (Figure 6). Further analysis of this subgroup of neuroblastomas indicated a very high frequency of 11q deletions (60%) in stage 4 tumors without the above mentioned abnormalities[90]. A recent large LOH study on 331 neuroblastomas identified a 2.1 cM consensus region of deletion in chromosome band 11q23.3, flanked by markers D11S1340 and D11S1299[91]. However, further studies are needed to confirm these observations.

Loss of other chromosomal regions

In addition to ploidy changes, 17q gain, MNA, 1p and 11q deletions, losses for several other chromosomal regions were frequently reported, suggesting the existence of additional tumor suppressor genes. There have been reports of frequent LOH at chromosome arms 2q[89, 92], 3p[89, 93], 4p[94], 9p[89, 95, 96], 14q[89, 97-99], and 18q[89, 100]. CGH analyses largely confirmed these PCR based data (except for 2q and 18q) (Figure 6), and demonstrated a significant association between 3p and 11q deletions in *MYCN* single copy tumors, suggestive for a distinct genetic subgroup[55, 90].

The *CASP8* gene has been identified as the putative neuroblastoma tumor suppressor gene for the region of frequent allelic loss at 2q33[101]. This gene encodes for a cysteine protease involved in initiation of apoptosis, and was shown to be preferentially inactivated by deletion or promoter hypermethylation in *MYCN* amplified tumors. As MYCN overexpression sensitizes neuroblastoma cells to apoptotic signals[102], it is suggested that CASP8 acts as a tumor suppressor whose loss is required for survival of MYCN overexpressing cells. However, in a subsequent study, the correlation between lack of CASP8 expression and MNA could not be confirmed[92].

Recently, promoter hypermethylation of the *RASSF1A* gene located on 3p21.3 has been reported in half of the neuroblastoma tumors, and is therefore considered to be a good candidate for the neuroblastoma 3p tumor suppressor gene. However, no mutations have been found as yet. As there was an association between *RASSF1A* and *CASP8* hypermethylation, a subset of neuroblastoma might be characterized by a CpG island methylator phenotype[103].

Mutation status of known tumor suppressor genes

Several tumor suppressor genes frequently implicated in other malignancies have been investigated in neuroblastoma. So far, none of these seems implicated in neuroblastoma tumorigenesis, indicating that one or more hitherto unidentified genetic pathways must play a role in this tumor.

Although *TP53* is inactivated in about half of the human cancers, very few mutations have been reported in primary neuroblastomas at diagnosis[104, 105]. However, recent reports indicate that some neuroblastomas acquire *TP53* mutations during cytotoxic therapy, which can confer high-level multidrug resistance (see further)[106, 107]. Cytoplasmatic sequestration of TP53 has been suggested as an alternative mechanism for accumulation and functional inactivation of p53 in neuroblastoma. However, there are conflicting reports about the cellular localization and functional status of TP53 in neuroblastoma (overview in [108]). In addition, *MDM2* amplification and overexpression (observed in a few neuroblastomas; cf. supra) has also been suggested as a mechanism for TP53 inactivation through ubiquitination and subsequent degradation.

TP73, the first identified *TP53* homolog, was proposed in 1997 as the long sought-after neuroblastoma 1p36 tumor suppressor gene[109], but only two mutations have been reported for a total of 209 tumors from 4 studies[110-113]. This is in keeping with a very low mutation rate of *TP73* in other human cancers[114]. In view of the originally reported monoallelic expression of *TP73*, the loss of a single copy would be sufficient for tumorigenesis. However, more recent studies showed that TP73 is generally biallelicly expressed. Interestingly, abnormal splicing variants of *TP73* and increased *TP73* expression have been described in different human cancers and cancer-derived cell lines, including neuroblastoma[115, 116]. The current hypothesis therefore is that altered *TP73* expression, rather than loss of function, is involved in tumorigenesis. Further studies need to clarify whether some TP73 protein isoforms exhibit a dominant negative gain of function, and if this gene is involved in neuroblastoma.

Although some studies reported an association between neuroblastoma and neurofibromatosis type 1, epidemiological analysis has suggested that this is coincidental[117]. Two studies have documented *NF1* gene mutations in a few neuroblastoma cell lines[118, 119]. Furthermore, a homozygous *NF1* deletion was described in a neuroblastoma tumor from a patient with hereditary neurofibromatosis type 1[120]. Familial neuroblastoma was shown not to be linked to the *NF1* locus[121].

The consensus deletion region at 9p contains the tumor suppressor gene *CDKN2A*, which encodes two different proteins with overlapping reading frames ($p16^{INK4A}$ and $p19^{ARF}$). These cyclin

dependent kinase inhibitors are mutated in many human cancers[122]. Extensive mutation scanning in 6 studies however revealed only one mutation in a series of more than 200 neuroblastoma tumors[75]. A recent study found 4 homozygous deletions of the *CDKN2A* gene in 46 tested neuroblastoma cell lines, suggesting that biallelic inactivation may contribute to tumorigenesis[123]. In contrast, high expression of $p16^{INK4A}$ has been reported in NB cell lines and high stage tumors. Intriguingly, the RB1 protein was nonetheless phosphorylated and functional. It has therefore been suggested that neuroblastoma may bypass the cell cycle block imposed by constitutive expression of wild-type $p16^{INK4A}$ [124-126]. In this respect, the reported amplification of *CCND1* and *CDK4* in a primary tumor and cell line respectively[41, 42], suggest that overexpression of cyclins or cyclin dependent kinases might be part of this mechanism.

Hereditary neuroblastoma

Although the majority of neuroblastoma tumors occur sporadically, 1-2% of patients have a familial history of the disease[127, 128]. In these cases, neuroblastoma is inherited in a autosomal dominant fashion with incomplete penetrance. Familial neuroblastoma patients are usually diagnosed earlier, and have often multiple sites of primary tumors compared to sporadic cases. These clinical characteristics are hallmarks of the two-hit cancer predisposition model first described for retinoblastoma. Linkage analysis has excluded all candidate loci of known allelic loss in neuroblastoma (reviewed in [129]), but has recently identified a putative predisposition locus for familial neuroblastoma at 16p12-p13[130].

ALTERED EXPRESSION OF CANCER RELATED GENES

Multidrug resistance

Half of the patients diagnosed with neuroblastoma present with disseminated disease, and have to be treated with chemotherapeutic agents. Unfortunately, many of these patients respond only transiently or incompletely, often due to acquired resistance to the administered drugs. Furthermore, it appears that these tumors are concomitantly resistant to structurally and functionally unrelated agents, a phenomenon described as multidrug resistance. Classes of chemotherapeutic drugs commonly used to treat neuroblastoma patients, and to which multidrug resistance frequently arises are the anthracyclins (doxorubicin), vinca alkyloids (vincristine), epipodophyllotoxins (etoposide), platinum compounds (cisplatin), and alkylating agents (cyclophosphamide)[131].

The underlying cellular mechanisms that result in multidrug resistance are increased efflux or decreased influx of toxic compounds, activation of detoxification or drug-induced DNA damage repair systems, and disruption of apoptotic signalling pathways[132]. The best characterized mechanism in neuroblastoma involves increased expression of two ATP-binding cassette (ABC) transporters, ABCB1 (MDR1) and ABCC1 (MRP), that pump hydrophobic toxic compounds out of the cell. However, the role of MDR1 in neuroblastoma is controversial (reviewed in[133]), mainly due to different methods used for quantification and the scale of the studies. One study reported *MDR1* overexpression in advanced stage tumors resulting in poor response to chemotherapy[134]. Other studies failed to confirm this, and even showed preferential expression in localized and more differentiated tumors of good clinical prognosis[135-137]. Furthermore, MDR1 might be transcriptionally activated in response to differentiation, rather than chemotherapy[138]. These results suggest that enhanced MDR1 expression is unlikely to be a major cause of acquired drug resistance in neuroblastoma.

A more clear picture is available for the other ABC transporter *MRP*. It was shown that *MRP* expression is strongly correlated with *MYCN* expression and poor survival[137, 139]. Together with the identification of an E-box sequence in the *MRP* promoter region[140], and downregulation of *MRP* expression in a cell line using *MYCN* antisense RNA transcipts[141], these data indicate a mechanistic link between *MYCN* and *MRP*, whereby *MYCN* amplification can result in increased drug resistance.

Telomerase activity

Telomeres are short repetitive stretches of DNA at the end of the chromosomes and are responsible for the chromosomal integrity. During each cell division, the telomeres decrease in size, resulting in cellular senescence and death after 20-80 divisions. Hence, most cancer cells have developed a mechanism to maintain their telomeres by aberrantly expressing telomerase, an RNA dependent DNA polymerase that adds telomeric repeats to the chromosome ends[142]. Telomerase expression is detectable in the majority of neuroblastoma cells, with high levels of expression associated with high stage of disease and poor outcome[143, 144]. The observed telomerase activity in favorable neuroblastoma may reflect the observed expression in developing normal neuroblasts, while markedly increased levels in aggressive neuroblastomas are probably due to reactivation of telomerase in the tumor cells[145].

Metastasis

Two genes that exhibit a differential expression pattern in many cancer types depending on the dissemination status, display an opposite pattern in neuroblastoma. The cell surface glycoprotein

CD44 has been postulated to play a role in cell adhesion and has been shown to be overexpressed in several cancers. For neuroblastoma however, *CD44* expression is undetectable in the majority of cell lines and tumors with dissemination at diagnosis[146-148]. *CD44* expression is inversely correlated with *MYCN* amplification and has been reported as an independent prognostic marker, especially in higher stage tumors[146, 149].

The *NME1* gene encodes a nucleoside diphosphate kinase, for which reduced expression has been correlated with metastases of breast and ovarian carcinomas[150, 151]. For neuroblastoma however, increased expression has been found in advanced stage primary tumors, correlating with a decreased survival probability[152-154]. Furthermore, missense mutations in a highly conserved domain were identified in a subset of these advanced tumors with *NME1* overexpression[153, 155]. The mutated protein displays both decreased enzymatic activity as well as altered protein-binding interactions, suggesting that overexpression of a mutated protein might act in a dominant-negative fashion[156]. Given the chromosomal position of *NME1* at 17q22, further studies are required to determine if there is a mechanistic link between gain of 17q and overexpression of *NME1*.

Apoptosis

During normal fetal and neonatal development of the nervous system, a large number of neuronal cells die via apoptosis. It has been postulated that this apoptotic mechanism is somehow defective in neuroblastoma cells, with the phenomenon of spontaneous regression of some neuroblastoma tumors being a delayed process of naturally occurring apoptosis.

NGF withdrawal is a major signal for apoptosis in the developing sympathetic nervous system, and mediates the elimination of redundant cells. Favorable neuroblastoma tumors usually express high levels of the high-affinity NGF receptor gene *NTRK1*, and differentiate in vitro in response to NGF (cf. supra). In contrast, deprivation of NGF results in tumoral cell death[157]. It was further shown that high expression of caspases *CASP1* and *CASP3* are associated with favorable biologic features (such as *MYCN* single copy number and low stage of disease), suggesting that neuroblastomas prone to undergoing apoptosis are more likely to regress or respond well to therapy[158, 159]. Remarkably, *MYCN* amplification and concurrent overexpression seems to sensitize neuroblastoma cells to apoptotic signals[102]. A recent study however demonstrated that *CASP8* was preferentially inactivated in these *MYCN* amplified tumors, hereby rendering the cells insensitive to programmed cell death[101].

Many cytotoxic agents have been shown in vitro to induce apoptosis in neuroblastoma cells, mediated by the TNFRSF6 (FAS,CD95) and mitochondrial BCL2 pathway. Increased *TNFRSF6* expression appears to be a crucial component of chemotherapy induced apoptosis[160], and the anti-apoptotic BCL2 and BCL2L1 (BCL2-XL) proteins may play an important role in acquired resistance to chemotherapy[161, 162]. BCL2 is expressed in the majority of cell lines and tumors (which have neuronal/ganglionic features) where it is positively correlated to cellular differentiation. In a small subset of tumors with a spontaneous neuronal to neuroendocrine-chromaffin lineage shift, BCL2 expression is high in the neuroblastic cells, but decreases as the cells become increasingly more neuroendocrine, a phenomenon occurring in poorly vascularized areas, adjacent to necrotic zones. There, BCL2 expression is inversely correlated with morphological features of apoptosis[24, 163-167]. Another anti-apoptotic protein BIRC5 (survivin) has been associated with a more aggressive and histologically unfavorable disease[168, 169]. Interestingly, this gene is located at 17q25, and might be the target of consistent gain of 17q in neuroblastoma. Other proteins involved in neuroblastoma apoptosis are the members of the retinoic acid receptor family, which mediate signalling from different retinoids, resulting in differentiation or apoptosis of the cell[170].

REFERENCES

1. Brodeur, G.M. & Castleberry, R.P. in Principles and Practice of Pediatric Oncology, Edn. 2nd. (eds. P.A. Pizzo & D.G. Poplack) (JB Lippincott, Philadelphia; 1993).
2. Pearson, A. & Philip, T. in Neuroblastoma. (eds. G.M. Brodeur, T. Sawada, Y. Tsuchida & P. Voûte) 551-560 (Elsevier, Amsterdam; 2000).
3. LaBrosse, E.H. et al. Urinary excretion of 3-methoxy-4-hydroxymandelic acid and 3-methoxy-4- hydroxyphenylacetic acid by 288 patients with neuroblastoma and related neural crest tumors. *Cancer Res* **40**, 1995-2001 (1980).
4. Evans, A.E., D'Angio, G.J. & Randolph, J. A proposed staging for children with neuroblastoma. Children's cancer study group A. *Cancer* **27**, 374-378 (1971).
5. Brodeur, G.M. et al. Revisions of the international criteria for neuroblastoma diagnosis, staging, and response to treatment. *J Clin Oncol* **11**, 1466-1477 (1993).
6. Jaffe, N. Neuroblastoma: review of the literature and an examination of factors contributing to its enigmatic charcter. *Cancer Treat Rev* **3**, 61-82 (1976).
7. Ninane, J., Pritchard, J., Morris Jones, P.H.,

Mann, J.R. & Malpas, J.S. Stage II neuroblastoma. Adverse prognostic significance of lymph node involvement. *Arch Dis Child* **57**, 438-442 (1982).
8. Pritchard, J. & Hickman, J.A. Why does stage 4s neuroblastoma regress spontaneously? *Lancet* **344**, 869-870 (1994).
9. David, K. et al. Human natural immunoglobulin M antibodies induce apoptosis of human neuroblastoma cells by binding to a Mr 260,000 antigen. *Cancer Res* **59**, 3768-3775 (1999).
10. Oppenheim, R.W. Naturally occurring cell death during neural development. *Trends in Neurosciences* **8**, 487-493 (1985).
11. Hamburger, V. History of the discovery of neuronal death in embryos. *J Neurobiol* **23**, 1116-1123 (1992).
12. Beckwith, J.B. & Perrin, E.V. In-situ neuroblastoma: its contribution to the natural history of neural crest tumors. *Am J Pathol* **43**, 1089-1104 (1963).
13. Woods, W.G. et al. A population-based study of the usefulness of screening for neuroblastoma. *Lancet* **348**, 1682-1687 (1996).
14. Ambros, I.M. et al. Role of ploidy, chromosome 1p, and Schwann cells in the maturation of neuroblastoma. *N Engl J Med* **334**, 1505-1511 (1996).
15. Shimada, H. et al. Terminology and morphologic criteria of neuroblastic tumors: recommendations by the International Neuroblastoma Pathology Committee. *Cancer* **86**, 349-363 (1999).
16. Shimada, H. et al. The International Neuroblastoma Pathology Classification (the Shimada system). *Cancer* **86**, 364-372 (1999).
17. Lastowska, M. et al. Comprehensive genetic and histopathologic study reveals three types of neuroblastoma tumors. *J Clin Oncol* **19**, 3080-3090 (2001).
18. LaBonne, C. & Bronner-Fraser, M. Molecular mechanisms of neural crest formation. *Annu Rev Cell Dev Biol* **15**, 81-112 (1999).
19. Anderson, D.J. Genes, lineages and the neural crest: a speculative review. *Philos Trans R Soc Lond B Biol Sci* **355**, 953-964 (2000).
20. Anderson, D.J. Cellular and molecular biology of neural crest cell lineage determination. *Trends Genet* **13**, 276-280 (1997).
21. Bang, A.G. & Goulding, M.D. Regulation of vertebrate neural cell fate by transcription factors. *Curr Opin Neurobiol* **6**, 25-32 (1996).
22. Pahlman, S. & Hedborg, F. in Neuroblastoma. (eds. G.M. Brodeur, T. Sawada, Y. Tsuchida & P. Voûte) 9-19 (Elsevier, Amsterdam; 2000).
23. Hoehner, J.C. et al. Developmental gene expression of sympathetic nervous system tumors reflects their histogenesis. *Lab Invest* **78**, 29-45 (1998).
24. Hoehner, J.C. et al. A developmental model of neuroblastoma: differentiating stroma-poor tumors' progress along an extra-adrenal chromaffin lineage. *Lab Invest* **75**, 659-675 (1996).
25. Patapoutian, A. & Reichardt, L.F. Trk receptors: mediators of neurotrophin action. *Curr Opin Neurobiol* **11**, 272-280 (2001).
26. Kaplan, D.R. & Miller, F.D. Neurotrophin signal transduction in the nervous system. *Curr Opin Neurobiol* **10**, 381-391 (2000).
27. Nakagawara, A. & Kogner, P. in Neuroblastoma. (eds. G.M. Brodeur, T. Sawada, Y. Tsuchida & P. Voûte) 147-157 (Elsevier, Amsterdam; 2000).
28. Cho, K.R. & Vogelstein, B. Genetic alterations in the adenoma--carcinoma sequence. *Cancer* **70**, 1727-1731 (1992).
29. Biedler, J.L., Helson, L. & Spengler, B.A. Morphology and growth, tumorigenicity, and cytogenetics of human neuroblastoma cells in continuous culture. *Cancer Res* **33**, 2643-2652 (1973).
30. Schwab, M. et al. Amplified DNA with limited homology to myc cellular oncogene is shared by human neuroblastoma cell lines and a neuroblastoma tumour. *Nature* **305**, 245-248 (1983).
31. Brodeur, G.M., Seeger, R.C., Schwab, M., Varmus, H.E. & Bishop, J.M. Amplification of N-myc in untreated human neuroblastomas correlates with advanced disease stage. *Science* **224**, 1121-1124 (1984).
32. Seeger, R.C. et al. Association of multiple copies of the N-myc oncogene with rapid progression of neuroblastomas. *N Engl J Med* **313**, 1111-1116 (1985).
33. Cohn, S.L. et al. MYCN expression is not prognostic of adverse outcome in advanced-stage neuroblastoma with nonamplified MYCN. *J Clin Oncol* **18**, 3604-3613 (2000).
34. Bordow, S.B., Norris, M.D., Haber, P.S., Marshall, G.M. & Haber, M. Prognostic significance of MYCN oncogene expression in childhood neuroblastoma. *J Clin Oncol* **16**, 3286-3294 (1998).
35. Weiss, W.A., Aldape, K., Mohapatra, G., Feuerstein, B.G. & Bishop, J.M. Targeted expression of MYCN causes neuroblastoma in transgenic mice. *Embo J* **16**, 2985-2995 (1997).
36. Zhou, Z.Q. & Hurlin, P.J. The interplay between Mad and Myc in proliferation and differentiation. *Trends Cell Biol* **11**, S10-14 (2001).
37. Reiter, J.L. & Brodeur, G.M. High-resolution mapping of a 130-kb core region of the MYCN amplicon in neuroblastomas. *Genomics* **32**, 97-103 (1996).
38. Reiter, J.L. & Brodeur, G.M. MYCN is the only highly expressed gene from the core

amplified domain in human neuroblastomas. *Genes Chromosomes Cancer* **23**, 134-140 (1998).
39. Wimmer, K. et al. Co-amplification of a novel gene, NAG, with the N-myc gene in neuroblastoma. *Oncogene* **18**, 233-238 (1999).
40. Squire, J.A. et al. Co-amplification of MYCN and a DEAD box gene (DDX1) in primary neuroblastoma. *Oncogene* **10**, 1417-1422 (1995).
41. Vandesompele, J. et al. Genetic heterogeneity of neuroblastoma studied by comparative genomic hybridization. *Genes Chromosomes Cancer* **23**, 141-152 (1998).
42. Van Roy, N. et al. Identification of two distinct chromosome 12-derived amplification units in neuroblastoma cell line NGP. *Cancer Genet Cytogenet* **82**, 151-154 (1995).
43. Heiskanen, M.A. et al. Detection of gene amplification by genomic hybridization to cDNA microarrays. *Cancer Res* **60**, 799-802 (2000).
44. Corvi, R. et al. Non-syntenic amplification of MDM2 and MYCN in human neuroblastoma. *Oncogene* **10**, 1081-1086 (1995).
45. Jones, T.A., Flomen, R.H., Senger, G., Nizetic, D. & Sheer, D. The homeobox gene MEIS1 is amplified in IMR-32 and highly expressed in other neuroblastoma cell lines. *Eur J Cancer* **36**, 2368-2374 (2000).
46. Spieker, N. et al. The MEIS1 oncogene is highly expressed in neuroblastoma and amplified in cell line IMR32. *Genomics* **71**, 214-221 (2001).
47. Jinbo, T., Iwamura, Y., Kaneko, M. & Sawaguchi, S. Coamplification of the L-myc and N-myc oncogenes in a neuroblastoma cell line. *Jpn J Cancer Res* **80**, 299-301 (1989).
48. Vandesompele, J. et al. Co-amplification of *ATBF1* and *MYC* in neuroblastoma cell line SJNB-12. Advances in Neuroblastoma Research, Paris, France (2002).
49. Van Roy, N. et al. Combined M-FISH and CGH analysis allows comprehensive description of genetic alterations in neuroblastoma cell lines. *Genes Chromosomes Cancer* **32**, 126-135 (2001).
50. Look, A.T., Hayes, F.A., Nitschke, R., McWilliams, N.B. & Green, A.A. Cellular DNA content as a predictor of response to chemotherapy in infants with unresectable neuroblastoma. *N Engl J Med* **311**, 231-235 (1984).
51. Look, A.T. et al. Clinical relevance of tumor cell ploidy and N-myc gene amplification in childhood neuroblastoma: a Pediatric Oncology Group study. *J Clin Oncol* **9**, 581-591 (1991).
52. Bourhis, J. et al. Combined analysis of DNA ploidy index and N-myc genomic content in neuroblastoma. *Cancer Res* **51**, 33-36 (1991).
53. Kaneko, Y. et al. Different karyotypic patterns in early and advanced stage neuroblastomas. *Cancer Res* **47**, 311-318 (1987).
54. Christiansen, H. & Lampert, F. Tumour karyotype discriminates between good and bad prognostic outcome in neuroblastoma. *Br J Cancer* **57**, 121-126 (1988).
55. Vandesompele, J. et al. Multicentre analysis of patterns of DNA gains and losses in 204 neuroblastoma tumors: how many genetic subgroups are there? *Med Pediatr Oncol* **36**, 5-10 (2001).
56. Gilbert, F. et al. Human neuroblastomas and abnormalities of chromosomes 1 and 17. *Cancer Res* **44**, 5444-5449 (1984).
57. Savelyeva, L., Corvi, R. & Schwab, M. Translocation involving 1p and 17q is a recurrent genetic alteration of human neuroblastoma cells. *Am J Hum Genet* **55**, 334-340 (1994).
58. Van Roy, N. et al. 1;17 translocations and other chromosome 17 rearrangements in human primary neuroblastoma tumors and cell lines. *Genes Chromosomes Cancer* **10**, 103-114 (1994).
59. Lastowska, M. et al. Comparative genomic hybridization study of primary neuroblastoma tumors. United Kingdom Children's Cancer Study Group. *Genes Chromosomes Cancer* **18**, 162-169 (1997).
60. Meddeb, M. et al. Additional copies of a 25 Mb chromosomal region originating from 17q23.1-17qter are present in 90% of high-grade neuroblastomas. *Genes Chromosomes Cancer* **17**, 156-165 (1996).
61. Caron, H. et al. Recurrent 1;17 translocations in human neuroblastoma reveal nonhomologous mitotic recombination during the S/G2 phase as a novel mechanism for loss of heterozygosity. *Am J Hum Genet* **55**, 341-347 (1994).
62. Lastowska, M. et al. Molecular cytogenetic delineation of 17q translocation breakpoints in neuroblastoma cell lines. *Genes Chromosomes Cancer* **23**, 116-122 (1998).
63. Altura, R.A. et al. Novel regions of chromosomal loss in familial neuroblastoma by comparative genomic hybridization. *Genes Chromosomes Cancer* **19**, 176-184 (1997).
64. Brinkschmidt, C. et al. Comparative genomic hybridization (CGH) analysis of neuroblastomas--an important methodological approach in paediatric tumour pathology. *J Pathol* **181**, 394-400 (1997).
65. Plantaz, D. et al. Gain of chromosome 17 is the most frequent abnormality detected in neuroblastoma by comparative genomic hybridization. *Am J Pathol* **150**, 81-89 (1997).
66. Speleman, F. & Bown, N. in Neuroblastoma.

(eds. G.M. Brodeur, T. Sawada, Y. Tsuchida & P. Voûte) 113-124 (Elsevier, Amsterdam; 2000).
67. Bown, N. et al. Gain of chromosome arm 17q and adverse outcome in patients with neuroblastoma. *N Engl J Med* **340**, 1954-1961 (1999).
68. Brodeur, G.M., Sekhon, G. & Goldstein, M.N. Chromosomal aberrations in human neuroblastomas. *Cancer* **40**, 2256-2263 (1977).
69. Maris, J.M. et al. Loss of heterozygosity at 1p36 independently predicts for disease progression but not decreased overall survival probability in neuroblastoma patients: a Children's Cancer Group study. *J Clin Oncol* **18**, 1888-1899 (2000).
70. Laureys, G., Speleman, F., Opdenakker, G., Benoit, Y. & Leroy, J. Constitutional translocation t(1;17)(p36;q12-21) in a patient with neuroblastoma. *Genes Chromosomes Cancer* **2**, 252-254 (1990).
71. Biegel, J.A. et al. Constitutional 1p36 deletion in a child with neuroblastoma. *Am J Hum Genet* **52**, 176-182 (1993).
72. White, P.S. et al. Detailed molecular analysis of 1p36 in neuroblastoma. *Med Pediatr Oncol* **36**, 37-41 (2001).
73. Bader, S.A., Fasching, C., Brodeur, G.M. & Stanbridge, E.J. Dissociation of suppression of tumorigenicity and differentiation in vitro effected by transfer of single human chromosomes into human neuroblastoma cells. *Cell Growth Differ* **2**, 245-255 (1991).
74. Maris, J.M. & Matthay, K.K. Molecular biology of neuroblastoma. *J Clin Oncol* **17**, 2264-2279 (1999).
75. White, P.S. & Versteeg, R. in Neuroblastoma. (eds. G.M. Brodeur, T. Sawada, Y. Tsuchida & P. Voûte) 57-74 (Elsevier, Amsterdam; 2000).
76. Bown, N. Neuroblastoma tumour genetics: clinical and biological aspects. *J Clin Pathol* **54**, 897-910 (2001).
77. Martinsson, T., Sjoberg, R.M., Hedborg, F. & Kogner, P. Deletion of chromosome 1p loci and microsatellite instability in neuroblastomas analyzed with short-tandem repeat polymorphisms. *Cancer Res* **55**, 5681-5686 (1995).
78. Schleiermacher, G. et al. Two distinct deleted regions on the short arm of chromosome 1 in neuroblastoma. *Genes Chromosomes Cancer* **10**, 275-281 (1994).
79. Takeda, O. et al. There may be two tumor suppressor genes on chromosome arm 1p closely associated with biologically distinct subtypes of neuroblastoma. *Genes Chromosomes Cancer* **10**, 30-39 (1994).
80. Caron, H. et al. Allelic loss of chromosome 1p36 in neuroblastoma is of preferential maternal origin and correlates with N-myc amplification. *Nat Genet* **4**, 187-190 (1993).
81. Caron, H. et al. Chromosome bands 1p35-36 contain two distinct neuroblastoma tumor suppressor loci, one of which is imprinted. *Genes Chromosomes Cancer* **30**, 168-174 (2001).
82. Caron, H. et al. Evidence for two tumour suppressor loci on chromosomal bands 1p35-36 involved in neuroblastoma: one probably imprinted, another associated with N-myc amplification. *Hum Mol Genet* **4**, 535-539 (1995).
83. Yan, H. et al. Small changes in expression affect predisposition to tumorigenesis. *Nat Genet* **30**, 25-26 (2002).
84. Kwabi-Addo, B. et al. Haploinsufficiency of the Pten tumor suppressor gene promotes prostate cancer progression. *Proc Natl Acad Sci U S A* **98**, 11563-11568 (2001).
85. Bauer, A. et al. Smallest region of overlapping deletion in 1p36 in human neuroblastoma: a 1 Mbp cosmid and PAC contig. *Genes Chromosomes Cancer* **31**, 228-239 (2001).
86. Ohira, M. et al. Identification and characterization of a 500-kb homozygously deleted region at 1p36.2-p36.3 in a neuroblastoma cell line. *Oncogene* **19**, 4302-4307 (2000).
87. Chen, Y.Z. et al. Homozygous deletion in a neuroblastoma cell line defined by a high-density STS map spanning human chromosome band 1p36. *Genes Chromosomes Cancer* **31**, 326-332 (2001).
88. Mertens, F., Johansson, B., Hoglund, M. & Mitelman, F. Chromosomal imbalance maps of malignant solid tumors: a cytogenetic survey of 3185 neoplasms. *Cancer Res* **57**, 2765-2780 (1997).
89. Takita, J. et al. Allelotype of neuroblastoma. *Oncogene* **11**, 1829-1834 (1995).
90. Plantaz, D. et al. Comparative genomic hybridization (CGH) analysis of stage 4 neuroblastoma reveals high frequency of 11q deletion in tumors lacking MYCN amplification. *Int J Cancer* **91**, 680-686 (2001).
91. Guo, C. et al. Allelic deletion at 11q23 is common in MYCN single copy neuroblastomas. *Oncogene* **18**, 4948-4957 (1999).
92. Takita, J. et al. Allelic imbalance on chromosome 2q and alterations of the caspase 8 gene in neuroblastoma. *Oncogene* **20**, 4424-4432 (2001).
93. Ejeskar, K., Aburatani, H., Abrahamsson, J., Kogner, P. & Martinsson, T. Loss of heterozygosity of 3p markers in neuroblastoma tumours implicate a tumour-suppressor locus distal to the FHIT gene. *Br J Cancer* **77**, 1787-1791 (1998).
94. Caron, H. et al. Allelic loss of the short arm of chromosome 4 in neuroblastoma suggests a novel tumour suppressor gene locus. *Hum Genet* **97**, 834-837 (1996).
95. Takita, J. et al. Deletion map of

chromosome 9 and p16 (CDKN2A) gene alterations in neuroblastoma. *Cancer Res* **57**, 907-912 (1997).
96. Marshall, B., Isidro, G., Martins, A.G. & Boavida, M.G. Loss of heterozygosity at chromosome 9p21 in primary neuroblastomas: evidence for two deleted regions. *Cancer Genet Cytogenet* **96**, 134-139 (1997).
97. Hoshi, M., Shiwaku, H.O., Hayashi, Y., Kaneko, Y. & Horii, A. Deletion mapping of 14q32 in human neuroblastoma defines an 1,100-kb region of common allelic loss. *Med Pediatr Oncol* **35**, 522-525 (2000).
98. Theobald, M. et al. Sublocalization of putative tumor suppressor gene loci on chromosome arm 14q in neuroblastoma. *Genes Chromosomes Cancer* **26**, 40-46 (1999).
99. Thompson, P.M. et al. Loss of heterozygosity for chromosome 14q in neuroblastoma. *Med Pediatr Oncol* **36**, 28-31 (2001).
100. Kong, X.T. et al. Expression and mutational analysis of the DCC, DPC4, and MADR2/JV18-1 genes in neuroblastoma. *Cancer Res* **57**, 3772-3778 (1997).
101. Teitz, T. et al. Caspase 8 is deleted or silenced preferentially in childhood neuroblastomas with amplification of MYCN. *Nat Med* **6**, 529-535 (2000).
102. Fulda, S., Lutz, W., Schwab, M. & Debatin, K.M. MycN sensitizes neuroblastoma cells for drug-induced apoptosis. *Oncogene* **18**, 1479-1486 (1999).
103. Astuti, D. et al. RASSF1A promoter region CpG island hypermethylation in phaeochromocytomas and neuroblastoma tumours. *Oncogene* **20**, 7573-7577 (2001).
104. Vogan, K. et al. Absence of p53 gene mutations in primary neuroblastomas. *Cancer Res* **53**, 5269-5273 (1993).
105. Komuro, H. et al. Mutations of the p53 gene are involved in Ewing's sarcomas but not in neuroblastomas. *Cancer Res* **53**, 5284-5288 (1993).
106. Keshelava, N. et al. Loss of p53 function confers high-level multidrug resistance in neuroblastoma cell lines. *Cancer Res* **61**, 6185-6193 (2001).
107. Tweddle, D.A., Malcolm, A.J., Bown, N., Pearson, A.D. & Lunec, J. Evidence for the development of p53 mutations after cytotoxic therapy in a neuroblastoma cell line. *Cancer Res* **61**, 8-13 (2001).
108. Tweddle, D.A., Malcolm, A.J., Cole, M., Pearson, A.D. & Lunec, J. p53 cellular localization and function in neuroblastoma: evidence for defective G(1) arrest despite WAF1 induction in MYCN-amplified cells. *Am J Pathol* **158**, 2067-2077 (2001).
109. Kaghad, M. et al. Monoallelically expressed gene related to p53 at 1p36, a region frequently deleted in neuroblastoma and other human cancers. *Cell* **90**, 809-819 (1997).
110. Han, S. et al. Infrequent somatic mutations of the p73 gene in various human cancers. *Eur J Surg Oncol* **25**, 194-198 (1999).
111. Ichimiya, S. et al. p73 at chromosome 1p36.3 is lost in advanced stage neuroblastoma but its mutation is infrequent. *Oncogene* **18**, 1061-1066 (1999).
112. Kovalev, S., Marchenko, N., Swendeman, S., LaQuaglia, M. & Moll, U.M. Expression level, allelic origin, and mutation analysis of the p73 gene in neuroblastoma tumors and cell lines. *Cell Growth Differ* **9**, 897-903 (1998).
113. Ejeskar, K., Sjoberg, R.M., Kogner, P. & Martinsson, T. Variable expression and absence of mutations in p73 in primary neuroblastoma tumors argues against a role in neuroblastoma development. *Int J Mol Med* **3**, 585-589 (1999).
114. Levrero, M. et al. The p53/p63/p73 family of transcription factors: overlapping and distinct functions. *J Cell Sci* **113**, 1661-1670 (2000).
115. Casciano, I., Ponzoni, M., Lo Cunsolo, C., Tonini, G.P. & Romani, M. Different p73 splicing variants are expressed in distinct tumour areas of a multifocal neuroblastoma. *Cell Death Differ* **6**, 391-393 (1999).
116. Zaika, A.I., Kovalev, S., Marchenko, N.D. & Moll, U.M. Overexpression of the wild type p73 gene in breast cancer tissues and cell lines. *Cancer Res* **59**, 3257-3263 (1999).
117. Kushner, B.H., Hajdu, S.I. & Helson, L. Synchronous neuroblastoma and von Recklinghausen's disease: a review of the literature. *J Clin Oncol* **3**, 117-120 (1985).
118. Johnson, M.R., Look, A.T., DeClue, J.E., Valentine, M.B. & Lowy, D.R. Inactivation of the NF1 gene in human melanoma and neuroblastoma cell lines without impaired regulation of GTP.Ras. *Proc Natl Acad Sci U S A* **90**, 5539-5543 (1993).
119. The, I. et al. Neurofibromatosis type 1 gene mutations in neuroblastoma. *Nat Genet* **3**, 62-66 (1993).
120. Martinsson, T., Sjoberg, R.M., Hedborg, F. & Kogner, P. Homozygous deletion of the neurofibromatosis-1 gene in the tumor of a patient with neuroblastoma. *Cancer Genet Cytogenet* **95**, 183-189 (1997).
121. Maris, J.M., Chatten, J., Meadows, A.T., Biegel, J.A. & Brodeur, G.M. Familial neuroblastoma: a three-generation pedigree and a further association with Hirschsprung disease. *Med Pediatr Oncol* **28**, 1-5 (1997).
122. Sharpless, N.E. & DePinho, R.A. The INK4A/ARF locus and its two gene products. *Curr Opin Genet Dev* **9**, 22-30 (1999).
123. Thompson, P.M. et al. Homozygous deletion of CDKN2A (p16INK4a/p14ARF) but not within 1p36 or at other tumor suppressor loci in neuroblastoma. *Cancer Res* **61**, 679-

686 (2001).
124. Easton, J., Wei, T., Lahti, J.M. & Kidd, V.J. Disruption of the cyclin D/cyclin-dependent kinase/INK4/retinoblastoma protein regulatory pathway in human neuroblastoma. *Cancer Res* **58**, 2624-2632 (1998).
125. Omura-Minamisawa, M. et al. p16/p14(ARF) Cell Cycle Regulatory Pathways in Primary Neuroblastoma: p16 Expression Is Associated with Advanced Stage Disease. *Clin Cancer Res* **7**, 3481-3490 (2001).
126. Diccianni, M.B. et al. Frequent deregulation of p16 and the p16/G1 cell cycle-regulatory pathway in neuroblastoma. *Int J Cancer* **80**, 145-154 (1999).
127. Kushner, B.H., Gilbert, F. & Helson, L. Familial neuroblastoma. Case reports, literature review, and etiologic considerations. *Cancer* **57**, 1887-1893 (1986).
128. Knudson, A.G., Jr. & Strong, L.C. Mutation and cancer: neuroblastoma and pheochromocytoma. *Am J Hum Genet* **24**, 514-532 (1972).
129. Maris, J.M. & Tonini, G.P. in Neuroblastoma. (eds. G.M. Brodeur, T. Sawada, Y. Tsuchida & P. Voûte) 125-135 (Elsevier, Amsterdam; 2000).
130. Weiss, M.J. et al. Localization of a hereditary neuroblastoma predisposition gene to 16p12- p13. *Med Pediatr Oncol* **35**, 526-530 (2000).
131. Haber, M. & Kavallaris, M. in Neuroblastoma. (eds. G.M. Brodeur, T. Sawada, Y. Tsuchida & P. Voûte) 207-215 (Elsevier, Amsterdam; 2000).
132. Gottesman, M.M., Fojo, T. & Bates, S.E. Multidrug resistance in cancer: role of ATP-dependent transporters. *Nature Rev Cancer* **2**, 48-58 (2002).
133. Kuttesch, J.F., Jr. Multidrug resistance in pediatric oncology. *Invest New Drugs* **14**, 55-67 (1996).
134. Chan, H.S. et al. P-glycoprotein expression as a predictor of the outcome of therapy for neuroblastoma. *N Engl J Med* **325**, 1608-1614 (1991).
135. Nakagawara, A. et al. Inverse correlation between expression of multidrug resistance gene and N-myc oncogene in human neuroblastomas. *Cancer Res* **50**, 3043-3047 (1990).
136. Dhooge, C.R. et al. Expression of the MDR1 gene product P-glycoprotein in childhood neuroblastoma. *Cancer* **80**, 1250-1257 (1997).
137. Norris, M.D. et al. Expression of the gene for multidrug-resistance-associated protein and outcome in patients with neuroblastoma. *N Engl J Med* **334**, 231-238 (1996).
138. Bates, S.E. et al. Expression of a drug resistance gene in human neuroblastoma cell lines: modulation by retinoic acid-induced differentiation. *Mol Cell Biol* **9**, 4337-4344 (1989).
139. Bordow, S.B. et al. Expression of the multidrug resistance-associated protein (MRP) gene correlates with amplification and overexpression of the N-myc oncogene in childhood neuroblastoma. *Cancer Res* **54**, 5036-5040 (1994).
140. Zhu, Q. & Center, M.S. Cloning and sequence analysis of the promoter region of the MRP gene of HL60 cells isolated for resistance to adriamycin. *Cancer Res* **54**, 4488-4492 (1994).
141. Norris, M.D. et al. Evidence that the MYCN oncogene regulates MRP gene expression in neuroblastoma. *Eur J Cancer* **33**, 1911-1916 (1997).
142. Kim, N.W. et al. Specific association of human telomerase activity with immortal cells and cancer. *Science* **266**, 2011-2015 (1994).
143. Hiyama, E. et al. Correlating telomerase activity levels with human neuroblastoma outcomes. *Nat Med* **1**, 249-255 (1995).
144. Reynolds, C.P. et al. Telomerase expression in primary neuroblastomas. *Eur J Cancer* **33**, 1929-1931 (1997).
145. Hiyama, E. & Reynolds, C.P. in Neuroblastoma. (eds. G.M. Brodeur, T. Sawada, Y. Tsuchida & P. Voûte) 159-174 (Elsevier, Amsterdam; 2000).
146. Favrot, M.C., Combaret, V. & Lasset, C. CD44--a new prognostic marker for neuroblastoma. *N Engl J Med* **329**, 1965 (1993).
147. Shtivelman, E. & Bishop, J.M. Expression of CD44 is repressed in neuroblastoma cells. *Mol Cell Biol* **11**, 5446-5453 (1991).
148. Gross, N. et al. CD44H expression by human neuroblastoma cells: relation to MYCN amplification and lineage differentiation. *Cancer Res* **54**, 4238-4242 (1994).
149. Combaret, V. et al. Clinical relevance of CD44 cell-surface expression and N-myc gene amplification in a multicentric analysis of 121 pediatric neuroblastomas. *J Clin Oncol* **14**, 25-34 (1996).
150. Bevilacqua, G., Sobel, M.E., Liotta, L.A. & Steeg, P.S. Association of low nm23 RNA levels in human primary infiltrating ductal breast carcinomas with lymph node involvement and other histopathological indicators of high metastatic potential. *Cancer Res* **49**, 5185-5190 (1989).
151. Scambia, G. et al. nm23 in ovarian cancer: correlation with clinical outcome and other clinicopathologic and biochemical prognostic parameters. *J Clin Oncol* **14**, 334-342 (1996).
152. Hailat, N. et al. High levels of p19/nm23 protein in neuroblastoma are associated with advanced stage disease and with N-myc gene amplification. *J Clin Invest* **88**, 341-345 (1991).

153. Leone, A. et al. Evidence for nm23 RNA overexpression, DNA amplification and mutation in aggressive childhood neuroblastomas. *Oncogene* **8**, 855-865 (1993).
154. Takeda, O. et al. An increased NM23H1 copy number may be a poor prognostic factor independent of LOH on 1p in neuroblastomas. *Br J Cancer* **74**, 1620-1626 (1996).
155. Chang, C.L. et al. Nm23-H1 mutation in neuroblastoma. *Nature* **370**, 335-336 (1994).
156. Chang, C.L. et al. A nucleoside diphosphate kinase A (nm23-H1) serine 120-->glycine substitution in advanced stage neuroblastoma affects enzyme stability and alters protein-protein interaction. *Oncogene* **12**, 659-667 (1996).
157. Nakagawara, A. et al. Association between high levels of expression of the TRK gene and favorable outcome in human neuroblastoma. *N Engl J Med* **328**, 847-854 (1993).
158. Nakagawara, A. et al. High levels of expression and nuclear localization of interleukin-1 beta converting enzyme (ICE) and CPP32 in favorable human neuroblastomas. *Cancer Res* **57**, 4578-4584 (1997).
159. Ikeda, H. et al. Interleukin-1 beta converting enzyme (ICE) is preferentially expressed in neuroblastomas with favourable prognosis. *Eur J Cancer* **33**, 2081-2083 (1997).
160. Fulda, S., Sieverts, H., Friesen, C., Herr, I. & Debatin, K.M. The CD95 (APO-1/Fas) system mediates drug-induced apoptosis in neuroblastoma cells. *Cancer Res* **57**, 3823-3829 (1997).
161. Dole, M. et al. Bcl-2 inhibits chemotherapy-induced apoptosis in neuroblastoma. *Cancer Res* **54**, 3253-3259 (1994).
162. Dole, M.G. et al. Bcl-xL is expressed in neuroblastoma cells and modulates chemotherapy- induced apoptosis. *Cancer Res* **55**, 2576-2582 (1995).
163. Gestblom, C., Hoehner, J.C., Hedborg, F., Sandstedt, B. & Pahlman, S. In vivo spontaneous neuronal to neuroendocrine lineage conversion in a subset of neuroblastomas. *Am J Pathol* **150**, 107-117 (1997).
164. Hoehner, J.C., Hedborg, F., Wiklund, H.J., Olsen, L. & Pahlman, S. Cellular death in neuroblastoma: in situ correlation of apoptosis and bcl-2 expression. *Int J Cancer* **62**, 19-24 (1995).
165. Hoehner, J.C., Gestblom, C., Olsen, L. & Pahlman, S. Spatial association of apoptosis-related gene expression and cellular death in clinical neuroblastoma. *Br J Cancer* **75**, 1185-1194 (1997).
166. Ikeda, H. et al. Bcl-2 oncoprotein expression and apoptosis in neuroblastoma. *J Pediatr Surg* **30**, 805-808 (1995).
167. Krajewski, S., Chatten, J., Hanada, M. & Reed, J.C. Immunohistochemical analysis of the Bcl-2 oncoprotein in human neuroblastomas. Comparisons with tumor cell differentiation and N-Myc protein. *Lab Invest* **72**, 42-54 (1995).
168. Islam, A. et al. High expression of Survivin, mapped to 17q25, is significantly associated with poor prognostic factors and promotes cell survival in human neuroblastoma. *Oncogene* **19**, 617-623 (2000).
169. Adida, C., Berrebi, D., Peuchmaur, M., Reyes-Mugica, M. & Altieri, D.C. Anti-apoptosis gene, survivin, and prognosis of neuroblastoma. *Lancet* **351**, 882-883 (1998).
170. Melino, G., Thiele, C.J., Knight, R.A. & Piacentini, M. Retinoids and the control of growth/death decisions in human neuroblastoma cell lines. *J Neurooncol* **31**, 65-83 (1997).

chapter 2

CHAPTER 2: GENOME WIDE DETECTION OF CHROMOSOMAL ABERRATIONS AND SUBGROUP DELINEATION

Genetic Heterogeneity of Neuroblastoma Studied by Comparative Genomic Hybridization

Jo Vandesompele,[1] Nadine Van Roy,[1] Mireille Van Gele,[1] Geneviève Laureys,[2] Peter Ambros,[3] Pierre Heimann,[4] Christine Devalck,[5] Ed Schuuring,[6] Penelope Brock,[7] Jacques Otten,[8] Jan Gyselinck,[9] Anne De Paepe,[1] and Frank Speleman[1]*

[1]Department of Medical Genetics, University Hospital, Gent, Belgium
[2]Department of Pediatric Hemato-Oncology, University Hospital, Gent, Belgium
[3]Children's Cancer Research Institute, St. Anna Kinderspital, Vienna, Austria
[4]Department of Cytogenetics, Children's Hospital, Brussels, Belgium
[5]Department of Pediatric Hemato-Oncology, Children's Hospital, Brussels, Belgium
[6]Department of Pathology, Leiden University Medical Center, Leiden, the Netherlands
[7]Department of Pediatric Oncology, University Hospital, Leuven, Belgium
[8]Pediatric Hemato-Oncology Unit, University Hospital, Brussels, Belgium
[9]Department of Pediatric Hemato-Oncology, General Children's Hospital, Antwerp, Belgium

Comparative genomic hybridization (CGH) analysis was performed on 36 neuroblastomas of both low and high stage of disease. This study significantly increases the number of neuroblastoma tumors studied by CGH. Analysis of larger series of tumors is particularly important in view of the different clinical subgroups that are recognized for this tumor. The present data and a comparison with all published CGH data on neuroblastoma provide further insights into the genetic heterogeneity of neuroblastoma. Stage 1, 2, and 4S tumors showed predominantly whole chromosome gains and losses. A similar pattern of whole chromosome imbalances, although less frequent, was observed in stage 3 and 4 tumors, in addition to partial chromosome gains and losses. An increase in chromosome 17 or 17q copy number was observed in 81% of tumors. The most frequent losses, either through partial or whole chromosome underrepresentation, were observed for 1p (25%), 3p (25%), 4p (14%), 9p (19%), 11q (28%), and 14q (31%). The presence of 3p, 11q or 14q deletions defines a genetic subset of neuroblastomas and contributes to the further genetic characterization of stage 3 and 4 tumors without *MYCN* amplification (MNA) and 1p deletion. The present study also provides additional evidence for a possible role of genes at 11q13 in neuroblastoma. In a few cases, 1p deletion or MNA detected by FISH or Southern blotting was not found by CGH, indicating that the use of a second, independent technique for evaluation of these genetic parameters is recommended. *Genes Chromosomes Cancer 23:141–152, 1998.*

INTRODUCTION

Neuroblastoma is the most common extracranial solid tumor in children (Brodeur and Castleberry, 1993). The tumor cells are thought to arise from neuroectodermal stem cells (Ross et al., 1995). Neuroblastoma is a heterogeneous disorder both clinically and genetically. Three subgroups can be distinguished based on the clinical behavior and genetic abnormalities of the tumors. A first group of neuroblastomas with a low stage of disease, most often occurring in children younger than one year of age, shows a hyperdiploid or near-triploid nuclear DNA content with no 1p deletion or *MYCN* amplification (MNA). These patients have a good prognosis. In contrast, older children with disseminated disease and tumors exhibiting 1p deletions and MNA have a poor survival. These neuroblastomas are typically diploid or near-tetraploid. A third group with a so-called intermediate prognosis consists of near-diploid tumors without MNA (Brodeur and Castleberry, 1993).

The variety in the clinical behavior of neuroblastomas and the current knowledge of genetic aberrations occurring in these tumors suggest that disruption or activation of multiple genes that control cell division, differentiation, or apoptosis of neuroblasts is implicated in neuroblastomas. The direct role of *MYCN* in the development of neuroblastoma was recently shown by the occurrence of neuroblastomas in transgenic mice overexpressing the *MYCN* gene in neuroectodermal cells (Weiss et al., 1997). Furthermore, multiple genes on 1p are thought to be involved in the development of neuroblastoma. A strong candidate gene for the imprinted neuroblas-

Supported by: the Vereniging voor Kankerbestrijding (1995–98); Contract Grant number: FWO G0328.95, G.0085.96, GOA 12051397; and the Flemish Institute for the Promotion of Scientific Technological Research in Industry (IWT).

*Correspondence to: Frank Speleman, Center for Medical Genetics, University Hospital, De Pintelaan 185, B-9000 Gent, Belgium. E-mail: franki.speleman@rug.ac.be

Received 14 January 1998; Accepted 20 April 1998

toma suppressor locus, called *p73*, has been identified (Kaghad et al., 1997).

In contrast to the overwhelming data suggesting the involvement of genes on 1p in neuroblastoma, familial predisposition of neuroblastoma was shown not to map to 1p36 (Maris et al., 1996) and thus other regions must also play an important role in neuroblastoma. A number of these chromosomal regions have been identified by their recurrent loss in neuroblastoma, including 3p, 4p, 11q, and 14q (Suzuki et al., 1989, 1991; Fong et al., 1992; Takayama et al., 1992; Srivatsan et al., 1993; Caron et al., 1996; Hallstensson et al., 1997). An allelotype study revealed 2q, 9p, and 18q as additional chromosomal regions exhibiting preferential loss in neuroblastomas (Takita et al., 1995). Extra copies of 17q were observed in most of the investigated neuroblastoma cell lines and disseminated tumors (Caron et al., 1994; Savelyeva et al., 1994; Van Roy et al., 1994, 1995a; Meddeb et al., 1996; Lastowska et al., 1997c). Despite progress in the genetic dissection of neuroblastoma, the genes that play a key role in the development of neuroblastoma remain to be identified and thus alternative approaches for further genetic characterization are needed.

Comparative genomic hybridization (CGH) has been useful in whole tumor genome screening, allowing identification of those chromosome regions that are preferentially lost, overrepresented, or amplified (Kallioniemi et al., 1992; du Manoir et al., 1993). We have previously shown by analyzing genetically well-characterized neuroblastoma cell lines that CGH can reliably detect chromosomal imbalances, including a small interstitial deletion approximately 10 Mb in size (Van Gele et al., 1997; Van Roy et al., 1997). Nevertheless, due to intrinsic limitations of CGH, it is recommended that a second approach should always be used to detect small 1p deletions or low-level/small amplicon MNA.

Only five CGH studies on neuroblastoma tumors have been reported so far (Altura et al., 1997; Brinkschmidt et al., 1997; Lastowska et al., 1997b; Plantaz et al., 1997; Van Gele et al., 1997), one of which involves a small series of familial neuroblastomas (Altura et al., 1997). The number of tumors of each stage that has been analyzed so far is still relatively small. Our aim in this study was to extend the present series of neuroblastomas studied by CGH and to compare our data with those published in order to further characterize genetic subgroups, to gain more information on imbalances that have not been extensively studied so far, and to identify new chromosomal regions involved in neuroblastoma.

MATERIALS AND METHODS

Patients

Thirty-six tumors were analyzed, including 10 tumors for which preliminary CGH data were reported previously (cases 4, 5, 12, 14, 21, 22, 25, 26, 28, and 29) (Van Gele et al., 1997). Clinical and genetic data are summarized in Table 1. Staging was done according to the International Neuroblastoma Staging System (INSS, Brodeur and Castleberry, 1993). Twenty-six unselected tumor samples from which enough tumor material was available (cases 1–12, 14–16, 20–30) were collected from five different Belgian pediatric oncology centers. Ten tumors (cases 13, 17–19, 31–36) were obtained from the Children's Cancer Research Institute (Vienna, Austria).

Comparative Genomic Hybridization (CGH)

Metaphase spreads were prepared from phytohemagglutinin-stimulated lymphocytes from healthy individuals according to standard procedures. Each batch of chromosome preparations was tested by hybridization (reverse painting) with DNA from the neuroblastoma cell line IMR32 with known DNA gains and losses (Van Roy et al., 1997) in order to assess the quality of the slides for CGH. Batches with poor hybridization (e.g., strong contour staining of sister chromatids, heterogeneous or granular staining, etc.) were discarded. Slides were stored in plastic boxes with silica gel at -20°C before use.

Control DNA was extracted from peripheral blood cells from a healthy male individual as described (Sambrook et al., 1989). Primary tumor DNA was extracted from 50 μm cryosections from biopsy specimens stored at -80°C. Evaluation of the tumor percentage was done on H&E-stained 5 μm cryosections. Tumor samples containing less than 60% of tumor material were excluded from further analysis. Labeling of DNA, in situ hybridization, fluorescence microscopy, and digital image acquisition and processing were done according to du Manoir et al. (1993, 1995), with minor modifications (Van Roy et al., 1997). DAPI images of metaphases were recorded prior to hybridization using a Leitz DM microscope, a high-sensitivity integrated monochrome CCD camera (Sony IMAC-CCD S30), and dedicated software (ISIS, MetaSystems, Germany). Further processing of these images for CGH analysis was performed with the ISIS-CGH software (MetaSystems, Altlussheim, Germany). For each

TABLE 1. Clinical and Genetic Data of 36 Primary Neuroblastomas

Case	Stage[a]	MNA[b]	Chromosome 1 status[c]	DNA index	Age at diagnosis[d]	Dead[e]	EFS[f]	S[g]
1	1	−	− (3/3; 5/5)	1.43	17	—	—	70
2	1	−	− (3/3)	nd	10	—	—	13
3	1	−	− (3/3)	1.54	36	—	—	20
4	1	−	− (2/2)	1	12	—	—	24
5	1	nd	nd	nd	7	—	6	61
6	1	−	nd	nd	2 days	—	—	72
7	2	−	− (2/2)	1	185	—	—	45
8	2	−	− (3/3)	1.28	11	—	—	41
9	2	nd	− (3/3)	nd	3	—	—	7
10	2	−	− (3/3; 4/4; 5/5)	nd	1	—	—	80
11	4S	−	+ (2/3)	1.74	3	—	—	61
12	4S	−	+ (2/3)	1.6/1.29	3	—	—	42
13	4S	nd	+ (3/4)	1.0/2.0	2	1.5	—	—
14	3	–	– (1/2)	nd	20	21	19	—
15	3	−	− (3/3)	nd	36	—	—	84
16	3	−	− (3/3)	1.51	8	—	—	19
17	3	+	+ (1/2)	1	25	—	—	25
18	3	−	− (2/2)	nd	10	—	20	114
19	3	+	+ (2/3)	1.0/1.84	20	—	—	46
20	4	−	− (2/2)	nd	101	19	—	—
21	4	nd	nd	nd	31	−	8	64
22	4	−	− (2/2)	nd	65	—	—	40
23	4	nd	nd	nd	32	38	14	—
24	4	−	− (2/2)	nd	47	36	24	—
25	4	+	+ (1/2)	1.13	57	25	24	—
26	4	—	+ (1/2)	nd	63	3	—	—
27	4	−	− (2/2)	1.09	57	21	13	—
28	4	−	nd	nd	49	20	15	—
29	4	−	− (2/2)	1.09	41	—	—	43
30	4	+	nd	nd	32	24	18	—
31	4	+	+ (2/4)	2.01	18	—	—	78
32	4	+	+ (3/4)	1.0/1.93	35	—	—	38
33	4	−	− (2/2)	nd	32	—	—	67
34	4	+	+ (1/2)	1	178	—	—	25
35	4	+	+ (1/2)	1	19	—	—	52
36	4	+	+ (2/3)	1.17	34	—	—	42

[a]According to the International Neuroblastoma Staging System (INSS, Brodeur and Castleberry, 1993).
[b]*MYCN* amplification (+); normal (−); not done (nd).
[c]1p depletion (+); normal (−); not done (nd); (ratio p1–79/pUC1.77 FISH signals).
[d]Months.
[e]Months between first diagnosis and death of patient; still alive (−).
[f]Event free survival, months between first diagnosis and relapse or tumor progression; no relapse or progression (−).
[g]Survival, months between first diagnosis and present time if patient is still alive; patient is dead (−).

case, 10 to 20 metaphase cells were analyzed. For evaluation of CGH data, average ratio profiles with fixed limits at 1.25 and 0.75 and standard deviation limits (the width of the confidence interval being three times the standard deviation), as well as individual ratio profiles, were analyzed. A chromosomal region was considered to be overrepresented (gain) or underrepresented (loss) if the average ratio profile crossed the standard deviation limit. The reliability of the CGH procedure and software analysis was previously tested on well-characterized neuroblastoma cell lines. Particular attention was given in that study to the accuracy for detection of small distal 1p deletions and *MYCN* amplification (Van Roy et al., 1997). As a control, normal-to-normal hybridizations were performed.

Fluorescence In Situ Hybridization (FISH) and Southern Blot Analysis

For cases 1–4, 7–12, 14–16, 20, 22–27, and 29, FISH analysis for the detection of 1p deletion and MNA was performed on tumor cell interphase nuclei on standard unfixed touch slides or by collagenase disaggregation of tumor tissue (1000 U/ml for 1 hr at 37°C). For the latter method, cell clumps were removed by filtering through a 70 μm

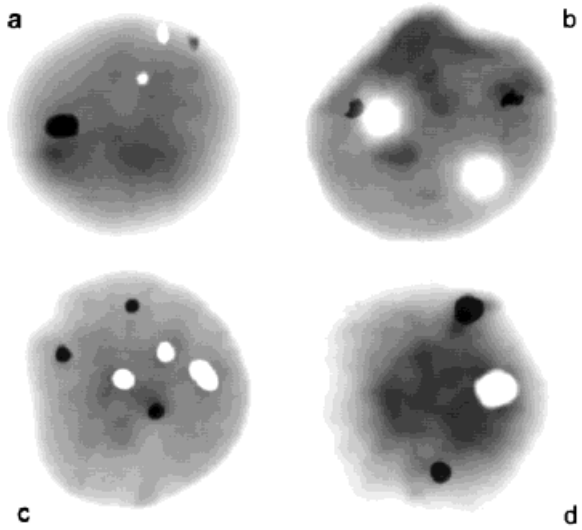

Figure 1. Comparison of interphase nuclei hybridized with biotin-labeled p1–79 (D1Z2) (white) and direct Cy3-labeled pUC1.77 (D1Z1) (black) by use of standard immunocytochemical detection (**a**) versus ultrasensitive detection with the Blast-HRP kit (**b–d**) (see text). a and b: Normal diploid nuclei; c: a nucleus of a triploid neuroblastoma cell without 1p deletion; d: a near-diploid neuroblastoma cell with 1p deletion.

nylon membrane, followed by hypotonic treatment in 0.95% Na citrate for 20 min and subsequent fixation in a 3:1 methanol:acetic acid solution. Probes used for in situ hybridization were Cy3 direct-labeled pUC1.77 (1q12, D1Z1), biotinylated p1–79 (1p36.33, D1Z2), and pNB-9 (*MYCN*). Probe labeling, slide pretreatment, in situ hybridization, and immunocytochemical detection for pNB-9 were performed as described (Van Roy et al., 1994). Probes pUC1.77 and p1–79 were cohybridized for detection of distal 1p deletions and determination of chromosome 1 copy number.

After hybridization, p1–79 was detected using the Blast-HRP kit (NEN-117, Dupont), which allowed a more sensitive detection than conventional biotin-avidin detection and unequivocal interpretation of the presence or absence of the D1Z2 sequence (Fig. 1). Slides were incubated with streptavidin-HRP (diluted 1:500 in 0.5% Blocking Reagent, Boehringer-Mannheim, Mannheim, Germany) for 5 min in a moist chamber at room temperature. Subsequently, slides were rinsed for 3×5 min with 0.1 M Tris-HCl/0.15 M NaCl/0.05% Tween-20 and incubated with biotinyl tyramide (diluted 1:1,000 in amplification diluent concentrate and H_2O) for 1 min. Slides were washed with 0.1 M Tris-HCl/0.15 M NaCl/0.05% Tween-20 for 3×5 min. Finally, slides were incubated with Neutralite-avidin-FITC (Eurogentec) (diluted 1:200 in 0.5% Blocking Reagent) for 5 min. Slides were rinsed for 2×5 min with 0.1 M Tris-HCl/0.15 M NaCl/0.05% Tween-20, 1×5 min in $1 \times$ PBS, and dehydrated through an ethanol series. Slides were embedded in Vectashield (Vector Labs, Burlingame, CA) containing 4,6-diamidino-2-phenylindole (DAPI) for counterstaining. Streptavidin-HRP, biotinyl tyramide, and amplification diluent concentrate were supplied in the Blast-HRP kit (NEN-117, Dupont). For cases 13, 17–19, and 31–36, FISH analysis for chromosome 1 status and *MYCN* copy number was done according to Strehl and Ambros (1993). Detection of *MYCN* amplification by Southern blot analysis for cases 6, 28, and 30 was done according to standard procedures.

Statistical Analysis

Fisher's Exact Test was used to look for significant differences in the frequency of a specific chromosome abnormality between the two groups of neuroblastoma tumors (stages 1, 2, and 4S versus stages 3 and 4). This test was also performed in order to investigate whether two different chromosomal abnormalities occur independently of each other over all the cases. Statistical significance was always defined as $P \leq 0.05$.

RESULTS

To evaluate the presence of genetic abnormalities in neuroblastoma, we performed CGH on 36 primary neuroblastomas. Chromosomal imbalances were found in 34/36 tumors analyzed. The results are summarized in Figure 2. The results for tumors with a low stage of disease (stages 1, 2, and 4S) versus a high stage of disease (stages 3 and 4) are represented on separate ideograms in order to facilitate comparison. Examples of average ratio profiles for specific chromosomes are given in Figure 3.

A total of 237 imbalances were observed (122 partial and 115 whole chromosome abnormalities). DNA copy number abnormalities varied from 1 to 18 per tumor. Although the average number of chromosomal imbalances in stage 1, 2, and 4S versus stage 3 and 4 neuroblastomas is approximately the same (7 vs. 6.3), stage 1, 2, and 4S tumors show highly significantly ($P = 5.48 \times 10^{-6}$) more whole and less partial gains and losses compared to stage 3 and 4 neuroblastomas (4.7 vs. 2.3 average whole abnormalities; 2.3 vs. 4 average partial abnormalities). Most of the partial imbalances in stage 1, 2, and 4S tumors were accounted for by only three tumors (cases 3, 11, and 13).

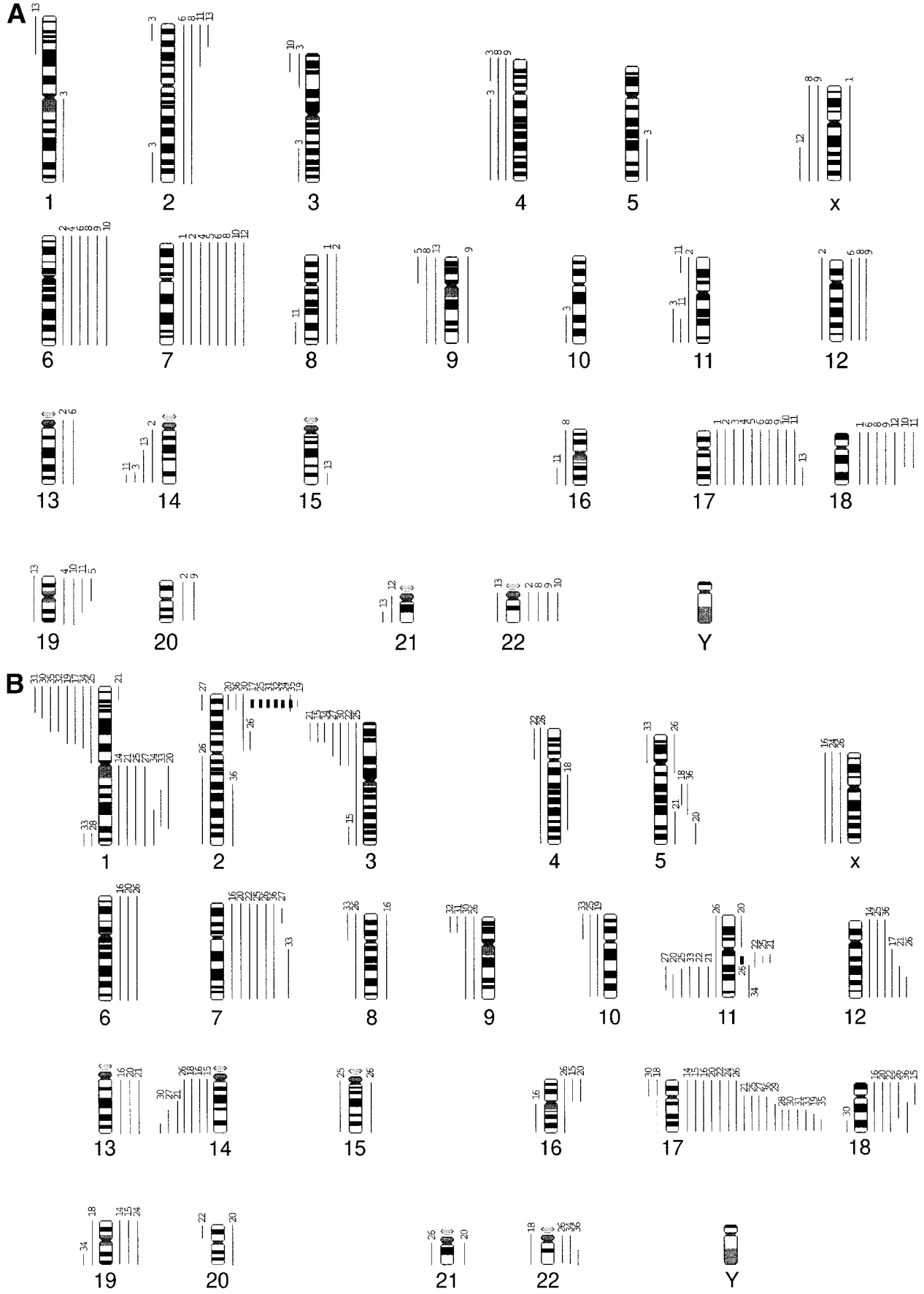

Figure 2. Ideograms of DNA copy number changes in 36 samples of neuroblastoma tumors. Lines on the left side of the ideograms indicate underrepresentations, lines on the right side show overrepresentations, bars on the right side represent high copy number amplification. **A:** 13 stage 1, 2, and 4S neuroblastomas; **B:** 23 stage 3 and 4 neuroblastomas.

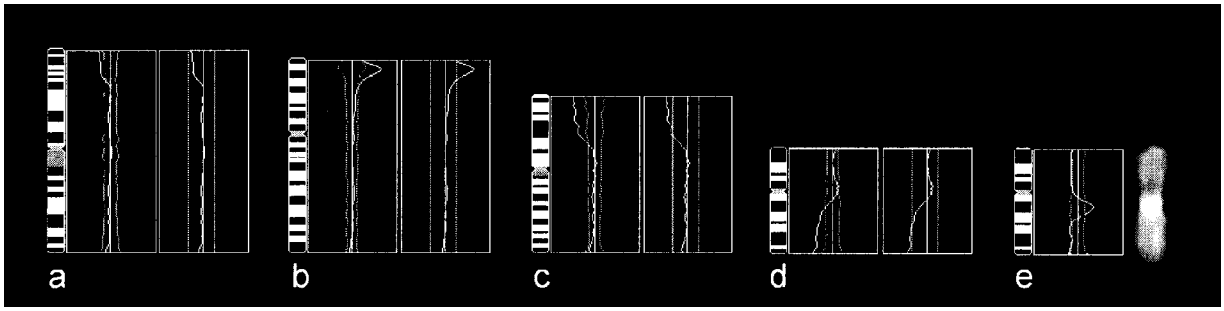

Figure 3. Examples of average ratio profiles with 99% confidence limits and fixed limits (0.75–1.25). **a:** Distal 1p deletion; **b:** MYCN amplification at 2p23–24; **c:** 3p deletion; **d:** 11q deletion; **e:** high-level DNA copy number amplification at 11q13. The strong white staining corresponds to increased fluorescence intensity of tumor DNA detected by FITC.

Whole Chromosome Gains and Losses

Of the 12 stage 1, 2, or 4S neuroblastomas with imbalances, seven tumors (58%) showed only whole chromosome abnormalities. The pattern of imbalances is clearly nonrandom and predominantly consists of gains of chromosomes 17 (10/13, 77%), 7 (8/13, 61%), 6 (6/13, 46%), and 18 (5/13, 38%). The same pattern of whole chromosome gains and losses was apparent in stage 3 and 4 neuroblastomas, although the average number of whole chromosome gains or losses was significantly lower.

Partial Chromosome Gains

Partial chromosome gains were most frequently observed for 17q (12/36, 33%). Extra 17q material was found exclusively in stage 3 and 4 tumors (11/23, 48%) and one stage 4S neuroblastoma. The distal part of 17q was always implicated, with the smallest overrepresented segment being 17q23–qter. Taken together for all stages, overrepresentation of 17q either through 17q gain or whole chromosome 17 gain was observed in 81% of the tumors (29/36). We compared the results of this study with the data reported by Plantaz et al. (1997) on the occurrence of extra chromosome 17 or 17q with respect to the presence or absence of 1p deletion and/or MNA. In both studies, (1) >70% of the neuroblastomas showed an extra chromosome arm 17q or 17 material; (2) the majority of whole chromosome 17 overrepresentations were found in tumors without 1p deletion and/or MNA and was never associated with MNA and 1p deletion; (3) 17q gain was frequently associated with 1p deletion and MNA; and (4) MNA and 1p deletion also occurred in stage 3 and 4 tumors without chromosome 17 abnormalities. A difference between the two studies is the high frequency of extra 17q in stage 1, 2, and 4S tumors reported by Plantaz et al. (1997) (6/17, 35%).

Partial or complete gain of 1q was observed in one stage 1, one stage 3, and six stage 4 tumors. The consensus region for 1q overrepresentation was 1q31.2–32.3. Partial gains were also observed for other chromosomal regions, including 2p (7/36, 19%, consensus region 2p23–pter) and 18q (5/36, 14%, consensus region 18q11.2–12.3).

Partial Chromosome Losses

DNA losses were most frequently observed for 1p (9/36, 25%), 3p (8/36, 22%), 11q (8/36, 22%), 14q (6/36, 17%), and 9p (3/36, 8%). Underrepresentation of 1p involved at least 1p35–36 in all cases. For five neuroblastoma biopsy specimens with a sufficient percentage of tumor cells (cases 11, 12, 14, 26, and 36), a normal ratio profile was observed for 1p, although loss of 1p36.33 was revealed by FISH analysis with probe p1–79. Karyotyping of case 14 revealed the presence of a der(1)t(1;1)(p36;q11), which leads us to assume that, at least in this case, the size of the lost segment was too small to be detected by CGH.

Partial 3p underrepresentation was found in six stage 3 and 4 and two stage 1, 2, and 4S neuroblastomas (Table 2). Four tumors with partial 3p loss and one tumor with whole chromosome 3 loss were found in association with 11q loss ($P = 0.030$). Three of these tumors and two tumors without 11q loss also showed 14q loss. Two tumors with 3p loss had a 1p deletion and MNA. With one exception, all tumors with 3p loss showed chromosome 17 or 17q overrepresentation. For all stages together, 3p loss either through distal 3p underrepresentation or whole chromosome loss (only 1 case) was observed in 25% of the tumors (9 cases).

TABLE 2. Presence (+) or Absence (−) of Chromosome Arm 1p, 3p, 11q, and 14q Deletions, Chromosome 17q Gain, and *MYCN* Amplification in Tumors with 3p, 11q, or 14q Loss[a]

Case	Stage[b]	3p[c]	11q−[c]	14q−[c]	1p−[d]	MNA[e]	17q+[f]
2	1	−	+ WCL	+ WCL	−	−	+ WCG
3	1	+	+	+	−	−	+ WCG
10	2	+	−	−	−	−	+ WCG
15	3	+	−	+ WCL	−	−	+ WCG
16	3	−	−	+ WCL	−	−	+ WCG
18	3	−	−	+ WCL	−	−	−
20	4	−	+	−	−	−	+ WCG
33	4	−	+	−	−	−	+
26	4	−	+ WCL	+ WCL	+ F	−	+ WCG
21	4	+	+	+	−	−	+
27	4	+	+	+	−	−	+
22	4	+	+	−	−	−	+ WCG
25	4	+ WCL	+	−	+	+	+
30	4	+	−	+	+	+ S	+
34	4	+	−	−	+	+	−
11	4S	−	+	+	+ F	2p+	+ WCG
13	4S	−	−	+	+	2p+	+

[a]Gray boxes are used to facilitate visual inspection of different subgroups of tumors.
[b]According to the International Neuroblastoma Staging System (Brodeur and Castleberry, 1993).
[c]WCL, whole chromosome loss.
[d]F, detected by FISH, but not by CGH.
[e]*MYCN* amplification; 2p+, partial gain for 2p, including 2p23–24; S, detected by Southern blot, but not by CGH.
[f]WCG, whole chromosome gain.

Loss of 11q was found in eight tumors (22%): one stage 1, one stage 4S, and six stage 4 tumors. Underrepresentations of 11q were found in association with 1p deletion in only two tumors, one of which was *MYCN*-amplified (Table 2). Four of six 14q losses were found in tumors exhibiting 11q loss, which results in a significant positive association ($P = 0.014$). All cases with 11q loss showed 17q overrepresentation, either through 17q gain only or through whole chromosome 17 gain. Besides eight partial chromosome 11 losses, two additional whole chromosome 11 losses were observed, which brings the total percentage of 11q underrepresentation to 28% of all cases.

Underrepresentation of a small distal segment of chromosome 14 (14q31–qter) was found in a stage 1, 4S, and 4 tumor. Loss of larger distal 14q segments was found in two stage 4 and one stage 4S tumor. The occurrence of 14q loss with or without 1p loss, 3p loss, 11q loss, and MNA is also shown in Table 2. Besides the six partial 14q losses, five additional whole chromosome 14 losses were found (one stage 1, three stage 3, and one stage 4 tumor). This means that 31% of all cases had 14q losses, either through partial or whole chromosome 14 underrepresentation.

Loss of 9p was observed in one stage 1 neuroblastoma and two stage 4 tumors. The two stage 4 tumors also showed 1p deletions and MNA. Besides these three partial losses, four whole chromosome 9 underrepresentations were observed (one stage 2, one stage 4S, and two stage 4 tumors). Among these four cases, one stage 4 tumor was associated with a large 1p deletion and with MNA (case 30), and two tumors showed a 1p deletion (case 13 and 26) without MNA.

DNA Amplification

DNA amplification for the 2p23–24 region detected by CGH was found exclusively in stage 3 and 4 tumors (6/36, 17%) and correlated with the presence of MNA as analyzed by FISH or Southern blot analysis. In three tumors with MNA as determined by Southern blot analysis (cases 19, 30, and 36), gain of 2p was observed by CGH, but there was no DNA amplification at 2p23–24. In two of these three tumors, a large 1p deletion was also found. Repeated independent experiments yielded similar results. We are currently investigating the amplicon size and copy number in order to explain this discrepancy.

As reported (Van Gele et al., 1997), in one stage 4 tumor (case 26), DNA amplification at 11q13 was observed in the absence of MNA. Southern blot analysis using probes for the *EMS1/cortactin* and *cyclin D1* genes located at 11q13 showed significant amplification of both genes (approximately 10-fold), thus confirming the CGH observation.

Comparison of Present and Published Neuroblastoma CGH Data

Figure 4 shows the cumulative percentage of whole and partial imbalances for each chromosome in the present study and in other CGH analyses reported by Brinkschmidt et al. (1997), Lastowska et al. (1997b), and Plantaz et al. (1997). The figure shows that, although the overall pattern of gains and losses is quite similar, there are a number of differences between the individual studies, either in the proportion of whole versus partial gains and losses for certain chromosomes or in the frequency of specific imbalances. The study by Plantaz et al. (1997) showed a higher proportion of whole chromosome losses as compared to the other studies. In the former study, a very high percentage of whole chromosome 11 losses was observed, whereas in this study a high proportion of 11q loss was detected. Furthermore, in this study, chromosome 4 loss was found in only 16% of tumors, versus nearly 30% in the other studies. Imbalances for whole chromosomes 6, 14, and X were much more frequently observed by Plantaz et al. (1997) than in the other studies. Similarly, Brinkschmidt et al. (1997) found a higher percentage of chromosome 15 loss. Lastowska et al. (1997b) showed few chromosome 7 gains and no chromosome 18 gains, both of them imbalances that were observed frequently in the other studies. The same authors also more frequently detected partial chromosome 13 losses, 11q13 gain, and chromosome 12 gain.

DISCUSSION

In this study, chromosomal imbalances were observed in 34/36 tumors, confirming the presence of DNA gains and losses in the majority of neuroblastomas (Altura et al., 1997; Brinkschmidt et al., 1997; Lastowska et al., 1997b; Plantaz et al., 1997). Predominantly gains of whole chromosomes 17, 7, 6, and 18 (in order of frequency) and losses of whole chromosomes 14, 9, and 4 were observed in tumors in a low stage of disease. This pattern of whole chromosome gains and losses correlated with a DNA content in the triploid range for most tumors on which this information was available. Most of these patients were diagnosed when they were younger than one year and are still alive, except one patient with a stage 4S tumor bearing a 1p deletion (case 13). A favorable outcome for hyperploid neuroblastomas was previously demonstrated by DNA content analysis (Look et al., 1991) and cytogenetic investigation (Hayashi et al., 1988). A similar pattern of whole chromosome imbalances was observed for stage 3 and 4 tumors, but in a significantly lower number as compared to low stages of disease, and associated with partial gains and losses.

In the present study, gain of chromosome 17 or 17q was found in 81% of tumors, confirming that this is the most frequent imbalance observed by CGH in neuroblastoma (Brinkschmidt et al., 1997; Lastowska et al., 1997b; Plantaz et al., 1997). In stage 1, 2, and 4S tumors, only whole chromosome 17 gains were found except for one 4S tumor, whereas in stages 3 and 4 both chromosome 17 and 17q gain were frequently observed. Like CGH analysis, karyotyping of near-triploid neuroblastomas (Hayashi et al., 1988) revealed that additional copies (more than three) are found most frequently for chromosome 17. The distribution for the other chromosomes was different, however. This discrepancy could be related to the fact that the karyotyped tumors were identified by vanillylmandelic acid (VMA) mass screening. CGH analysis of this particular group of tumors should be performed in order to validate whether differences in patterns of whole chromosome imbalances exist in clinically diagnosed low stage tumors versus those identified by mass screening programs.

The occurrence of chromosome 17 abnormalities in neuroblastomas was first described by Gilbert et al. (1984) and confirmed by FISH and molecular studies by Caron et al. (1994), Savelyeva et al. (1994), Van Roy et al. (1994), Meddeb et al. (1996), and Lastowska et al. (1997c). The present data and those published by Plantaz et al. (1997) showed that 83% of tumors with 17q gain also had 1p loss, 11q loss, or 1p loss and MNA. It is of interest that the remaining 17% of tumors with 17q gain showed only one (2 cases) or no additional partial imbalances (2 cases). Of these patients, 3/4 are alive without disease and one has died (case 28, in whom 17q gain was the only detectable abnormality). This analysis shows that 17q gain can be found in tumors with a favorable prognosis, without 1p loss, 11q loss, or MNA, although a recent study by Lastowska et al. (1997a) indicated that patients who had a tumor with partial 17q gain had an unfavorable prognosis. The high incidence of chromosome arm 17q gain in all stages of neuroblastoma suggests that a dosage effect of genes located in this region could play a role in the development of this tumor. Possible candidate genes on 17q include *NME2* and *survivine* (Leone et al., 1993; Ambrosini et al., 1997).

One of the major challenges in the genetic analysis of neuroblastoma is the identification of

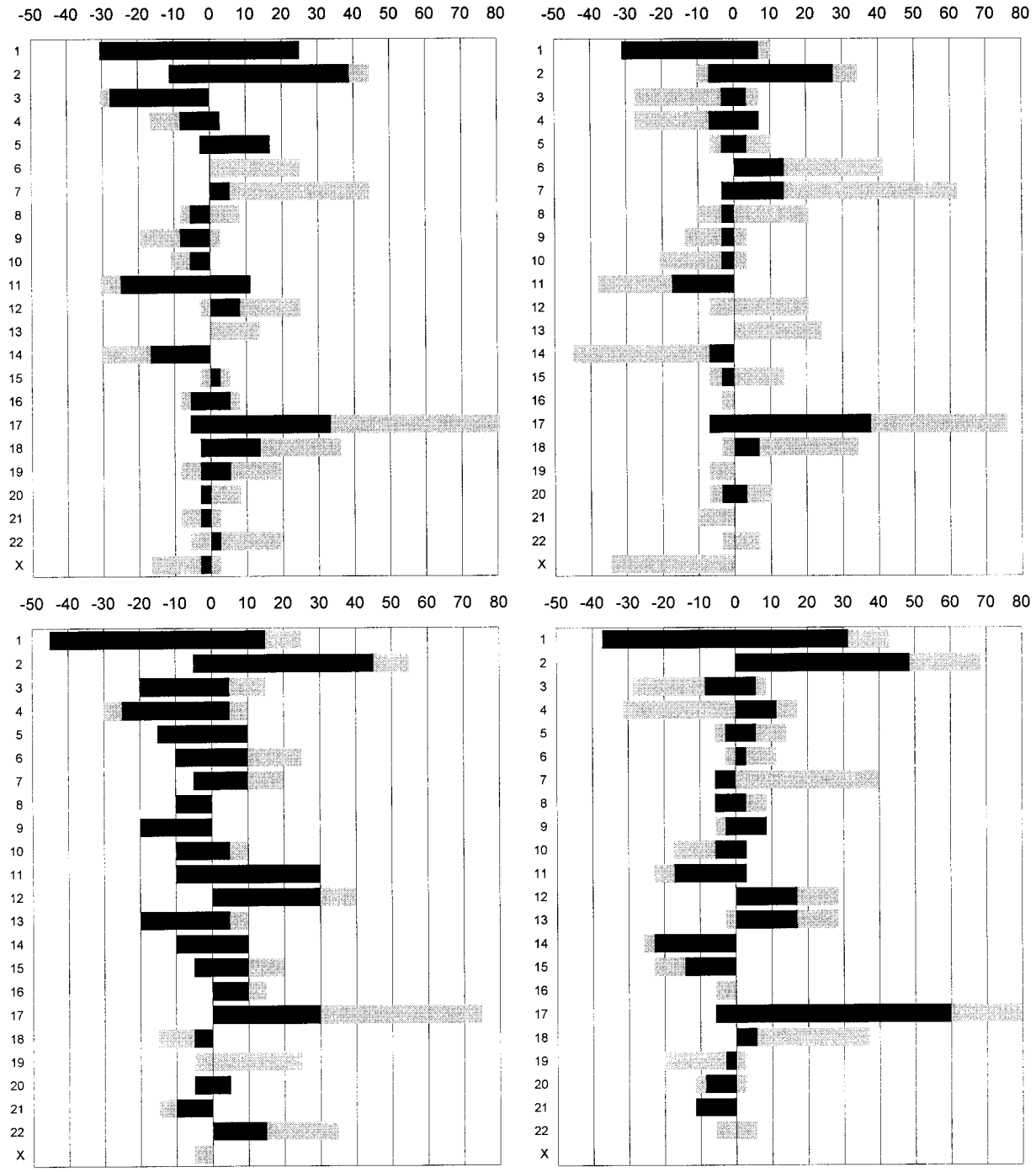

Figure 4. Cumulative percentages of whole (gray) and partial (black) chromosome abnormalities versus chromosome number: Plantaz et al. (1997) (**top right**); Brinkschmidt et al. (1997) (**bottom right**); this study (**top left**); and Lastowska et al. (1997b) (**bottom left**).

particular gains and losses in stage 3 and 4 tumors without 1p deletion and/or MNA. In this study, loss of 11q was found in 28% of predominantly stage 3 and 4 tumors without 1p deletion and/or MNA (consensus region 11q22–q24). In addition, statistical analysis showed a significant positive association between losses of 11q and 14q or 11q and 3p. This pattern of imbalances is found in a large proportion of stage 3 and 4 tumors without 1p and/or MNA, thus possibly defining a distinct genetic subgroup.

As was the case for 1p, the observed recurrent losses of 3p, 11q, and 14q material suggest that tumor suppressor genes located in these regions play a role in neuroblastoma.

Previous CGH studies revealed loss of 11q in 17%, 10%, and 10% in the studies by Brinkschmidt et al. (1997), Lastowska et al. (1997b), and Plantaz et al. (1997), respectively. Loss of 11q has previously been studied in neuroblastoma by LOH (Srivatsan et al., 1991, 1993; Fong et al., 1992). The incidence of 11q loss as studied by LOH varied considerably. Srivatsan et al. (1993) found 11q loss in as many as 26% of tumors, whereas in the study of Fong et al. (1992) only 5% of tumors showed 11q loss (one tumor in a series of 20 informative cases). Although the data by Srivatsan et al. (1993), Brinkschmidt et al. (1997), and Plantaz et al. (1997) suggest that 11q loss occurs in prognostically unfavorable tumors, we found $\geq$ 3-year survival of more than 60% of patients with 11q deletion.

Involvement of 3p deletions is a relatively new finding in neuroblastoma. Using LOH analysis, Hallstensson et al. (1997) found 3p deletions in 9 of 58 low-stage neuroblastomas and in 8 of 43 additional tumors of varying stages. In their CGH studies, Brinkschmidt et al. (1997) and Plantaz et al. (1997) could only detect one tumor each with 3p loss, whereas Altura et al. (1997) found 3p deletions in three of six tumors in patients with familial neuroblastoma and Lastowska et al. (1997b) found four cases (20%) of 3p loss. In the present study, we identified 8/36 (22%) tumors of both high and low stage of disease with 3p deletion. Underrepresentation of the entire chromosome 14 or the distal part of arm 14q was found in 31% of stage 1, 2, and 4S tumors and 30% of stage 3 and 4 tumors. Previous LOH studies revealed a similar incidence of chromosome 14 deletions in advanced stages, predominantly without 1p deletion or MNA (Suzuki et al., 1989, 1991; Fong et al., 1992).

By using reverse painting and CGH, we have previously shown that regions other than 2p24 can be amplified in neuroblastoma. This was shown to be the case for regions 12q13–15 (implicating the *SAS* and *MDM2* oncogenes) and 12q24 in cell line NGP and regions 2p23 and 2p13 in IMR32 (Van Roy et al., 1995b, 1997). Other CGH studies have also identified new regions of amplification in neuroblastoma, including 3q24–26, 4q33–35, and 6p11–12 (Brinkschmidt et al., 1997; Plantaz et al., 1997).

In one particular tumor included in this study, we previously reported for the first time in neuroblastoma the presence of DNA amplification of the 11q13 region. Southern blot analysis using probes for the *EMS1/cortactin* and *cyclin D1* genes located at 11q13 showed significant amplification for both genes (approximately 10-fold), thus confirming the CGH observation (Van Gele et al., 1997). In the present study, gain of 11q13 was observed in three additional tumors. A similar observation was previously made by Lastowska et al. (1997b) in six tumors. Amplification of the *EMS1/cortactin*, *cyclin D1*, *HST1/FGF4*, and *INT2/FGF3* genes located at 11q13 has been reported frequently (13–30% of the cases) in carcinomas of the breast, head and neck, bladder, and lung (Schuuring et al., 1995), but, interestingly, only low-copy DNA amplification ($<$10 copies) has been observed in these tumors. Therefore, a modest increase in the copy number of genes located at 11q13 may play a role in the biology and clinical behavior of subsets of neuroblastomas. We are currently investigating the incidence of low-level DNA amplification of 11q13 genes in more detail by using more sensitive methods for detection.

DNA amplification for the 2p23–24 region harboring the *MYCN* gene was observed in 6/36 (17%) tumors. All tumors typically displayed large 1p deletions with breakpoints ranging from 1p12 to 1p32. In three tumors, with MNA demonstrated by Southern blot analysis, gain of 2p (always including the *MYCN* region) was demonstrated by CGH, instead of DNA amplification. Thus, as for detection of 1p deletions, a second independent method in addition to CGH should be used for detection of MNA.

Survival of patients in this study of *MYCN*-amplified tumors is remarkably high and may reflect the use of improved treatment protocols. A similar observation was made by Lastowska et al. (1997a), who found no significant difference in survival between patients with *MYCN*-amplified vs. *MYCN*-nonamplified tumors.

In this study, DNA loss of the chromosome 1 short arm was seen in 25% of tumors, and always in association with MNA, except in one tumor. In five tumors with normal 1p ratio profiles, 1p deletions were detected by FISH. In one case, a patient who died 21 months after diagnosis, karyotypic analysis revealed an unbalanced translocation, der(1)t(1;1)(p36;q21). CGH analysis revealed the expected 1q gain in addition to gains for chromosomes 12, 17, and 19, but no 1p loss. In view of the distal localization of the 1p breakpoint, it is possible that the segment lost upon translocation was too small to be detected by CGH. This case illustrates that small distal 1p deletions can be missed by CGH

and thus a second independent technique, like FISH or LOH analysis, should be performed. In this study, we employed a recently developed method for ultrasensitive FISH by using peroxidase-mediated deposition of biotin tyramides for the detection of 1p deletions in interphase nuclei. Instead of clusters of small, distinct spots, the signals for the 1p36 DNA probe for locus D1Z2 appear as large, strong hybridization spots, which greatly facilitated the scoring of interphase nuclei.

Comparison of the present with previously published CGH data on neuroblastoma reveals a similar overall pattern of gains and losses. At the same time, differences are found in either the frequency of certain chromosome imbalances or the proportion of whole and partial imbalances for a specific chromosome. A number of explanations can account for this observation. The high frequency of whole chromosome abnormalities in the study by Plantaz et al. (1997), where 59% of the tumors were stage 1, 2, or 4S, compared to 36–40% in the other studies, can be explained by the higher relative number of tumors in a low stage of disease. The relatively small sampling size and the genetic heterogeneity of neuroblastoma tumors can also account for some discrepancies. Finally, subtle differences in the CGH procedure and the interpretation of gain and loss may explain some of the observed discrepancies.

In conclusion, the present study provides further support for the heterogeneity of neuroblastoma. In tumors in a low stage of disease, whole chromosome imbalances predominate, whereas partial gains and losses are more frequent in stage 3 and 4 tumors. The high incidence of chromosome 17 overrepresentation in both high- and low-stage neuroblastomas is now firmly established. Tumors with 11q and/or 14q and/or 3p loss may identify a genetic subgroup of neuroblastomas that contributes to a further genetic characterization of stage 3 and 4 tumors without MNA or 1p deletion. This study adds 11q13 to the list of regions that may be amplified in neuroblastoma. Although the results of the CGH studies on neuroblastomas performed so far are generally comparable, our data also reveal a number of discrepancies. The study of additional tumors with well-documented molecular and clinical data will be necessary for further characterization of discrete subgroups of neuroblastoma such as those carrying 3p, 11q, or 14q deletions.

ACKNOWLEDGMENTS

The authors thank A. Uyttebroeck and R. Sciot for providing clinical data and tumor material. N.V.R. is a postdoctoral researcher of the Fund for Scientific Research, Flanders.

REFERENCES

Altura RA, Maris JM, Li H, Boyett JM, Brodeur GM, Look AT (1997) Novel regions of chromosomal loss in familial neuroblastoma by comparative genomic hybridization. Genes Chromosomes Cancer 19:176–184.

Ambrosini G, Adida C, Altieri DC (1997) A novel antiapoptosis gene, survivine, expressed in cancer and lymphoma. Nature Med 3:917–921.

Brinkschmidt C, Christiansen H, Terpe HJ, Simon R, Boecker W, Lampert F, Stoerkel S (1997) Comparative genomic hybridization (CGH) analysis of neuroblastomas: An important methodological approach in paediatric tumour pathology. J Pathol 181:394–400.

Brodeur GM, Castleberry RP (1993) Neuroblastoma. In Pizzo PA, Poplack DG (eds): Principles and Practice of Pediatric Oncology, 2nd ed. Philadelphia: Lippincott, pp 739–761.

Caron H, van Sluis P, Van Roy N, de Kraker J, Speleman F, Voute PA, Westerveld A, Slater R, Versteeg R (1994) Recurrent 1;17 translocations in human neuroblastoma reveal nonhomologous mitotic recombination during the S/G2 phase as a novel mechanism for loss of heterozygosity. Am J Hum Genet 55:341–347.

Caron H, van Sluis P, Buschman R, Pereira-do-Tanque R, Maes P, Beks L, de Kraker J, Voute PA, Vergnaud G, Westerveld A, Slater R, Versteeg R (1996) Allelic loss of the short arm of chromosome 4 in neuroblastoma suggests a novel tumour suppressor gene locus. Hum Genet 97:834–837.

du Manoir S, Speicher MR, Joos S, Schrock E, Popp S, Dohner H, Kovacs G, Robert-Nicoud M, Lichter P, Cremer T (1993) Detection of complete and partial chromosome gains and losses by comparative genomic in situ hybridization. Hum Genet 90:590–610.

du Manoir S, Schrock E, Bentz M, Speicher MR, Joos S, Ried T, Lichter P, Cremer T (1995) Quantitative analysis of comparative genomic hybridization. Cytometry 19:27–41.

Fong CT, White PS, Peterson K, Sapienza C, Cavenee WK, Kern SE, Vogelstein B, Cantor AB, Look AT, Brodeur GM (1992) Loss of heterozygosity for chromosomes 1 or 14 defines subsets of advanced neuroblastomas. Cancer Res 52:1780–1785.

Gilbert F, Feder M, Balaban G, Brangman D, Lurie DK, Podolsky R, Rinaldt V, Vinikoor N, Weisband J (1984) Human neuroblastomas and abnormalities of chromosomes 1 and 17. Cancer Res 44:5444–5449.

Hallstensson K, Tholin S, Aburatani H, Hippo Y, Martinsson T (1997) RDA and LOH studies detect 3p deletions in neuroblastoma. Eur J Cancer 33:1966–1970.

Hayashi Y, Inaba T, Hanada R, Yamamoto K (1988) Chromosome findings and prognosis in 15 patients with neuroblastoma found by VMA mass screening. J Pediatr 112:567–571.

Kaghad M, Bonnet H, Yang A, Creancier L, Biscan JC, Valent A, Minty A, Chalon P, Lelias JM, Dumont X, Ferrara P, McKeon F, Caput D (1997) Monoallelically expressed gene related to p53 at 1p36, a region frequently deleted in neuroblastoma and other human cancers. Cell 90:809–819.

Kallioniemi A, Kallioniemi OP, Sudar D, Rutovitz D, Gray JW, Waldman F, Pinkel D (1992) Comparative genomic hybridization for molecular cytogenetic analysis of solid tumors. Science 258:818–821.

Lastowska M, Cotterill S, Pearson AD, Roberts P, McGuckin A, Lewis I, Bown N (1997a) Gain of chromosome arm 17q predicts unfavourable outcome in neuroblastoma patients. U.K. Children's Cancer Study Group and the U.K. Cancer Cytogenetics Group. Eur J Cancer 33:1627–1633.

Lastowska M, Nacheva E, McGuckin A, Curtis A, Grace C, Pearson A, Bown N (1997b) Comparative genomic hybridization study of primary neuroblastoma tumors. United Kingdom Children's Cancer Study Group. Genes Chromosomes Cancer 18:162–169.

Lastowska M, Roberts P, Pearson ADJ, Lewis I, Wolstenholme J, Bown N (1997c) Promiscuous translocations of chromosome arm 17q in human neuroblastomas. Genes Chromosomes Cancer 19:143–149.

Leone A, Seeger RC, Hong CM, Hu YY, Arboleda MJ, Brodeur GM, Stram D, Slamon DJ, Steeg PS (1993) Evidence for nm23 RNA overexpression, DNA amplification and mutation in aggressive childhood neuroblastomas. Oncogene 8:855–865.

Look AT, Hayes FA, Shuster JJ, Douglass EC, Castleberry RP, Bowman LC, Smith EI, Brodeur GM (1991) Clinical relevance of

tumor cell ploidy and N-myc gene amplification in childhood neuroblastoma: A Pediatric Oncology Group study. J Clin Oncol 9:581–591.

Maris JM, Kyemba SM, Rebbeck TR, White PS, Sulman EP, Jensen SJ, Allen C, Biegel JA, Yanofsky RA, Feldman GL, Brodeur GM (1996) Familial predisposition to neuroblastoma does not map to chromosome band 1p36. Cancer Res 56:3421–3425.

Meddeb M, Danglot G, Chudoba I, Venuat AM, Benard J, Avet-Loiseau H, Vasseur B, Le-Paslier D, Terrier-Lacombe MJ, Hartmann O, Bernheim A (1996) Additional copies of a 25 Mb chromosomal region originating from 17q23.1–17qter are present in 90% of high-grade neuroblastomas. Genes Chromosomes Cancer 17:156–165.

Plantaz D, Mohapatra G, Matthay KK, Pellarin M, Seeger RC, Feuerstein BG (1997) Gain of chromosome 17 is the most frequent abnormality detected in neuroblastoma by comparative genomic hybridization. Am J Pathol 150:81–89.

Ross RA, Spengler BA, Domenech C, Porubcin M, Rettig WJ, Biedler JL (1995) Human neuroblastoma I-type cells are malignant neural crest stem cells. Cell Growth Differ 6:449–456.

Sambrook J, Fritsch EF, Maniatis T (1989) Molecular Cloning: A Laboratory Manual, 2nd ed. Cold Spring Harbor, NY: Cold Spring Harbor Laboratory.

Savelyeva L, Corvi R, Schwab M (1994) Translocation involving 1p and 17q is a recurrent genetic alteration of human neuroblastoma cells. Am J Hum Genet 55:334–340.

Schuuring E (1995) The involvement of the chromosome 11q13 region in human malignancies: *Cyclin D1* and *EMS1* are two new candidate oncogenes—a review. Gene 159:83–96.

Srivatsan ES, Murali V, Seeger RC (1991) Loss of heterozygosity for alleles on chromosomes 11q and 14q in neuroblastoma. Prog Clin Biol Res 366:91–98.

Srivatsan ES, Ying KL, Seeger RC (1993) Deletion of chromosome 11 and of 14q sequences in neuroblastoma. Genes Chromosomes Cancer 7:32–37.

Strehl S, Ambros PF (1993) Fluorescence in situ hybridization combined with immunohistochemistry for highly sensitive detection of chromosome 1 aberrations in neuroblastoma. Cytogenet Cell Genet 63:24–28.

Suzuki T, Yokota J, Mugishima H, Okabe I, Ookuni M, Sugimura T, Terada M (1989) Frequent loss of heterozygosity on chromosome 14q in neuroblastoma. Cancer Res 49:1095–1098.

Suzuki T, Mugishima H, Fujisawa T, Okuni M, Okabe I, Yokota J, Terada M (1991) Loss of heterozygosity on chromosome 14 in neuroblastoma. Prog Clin Biol Res 366:135–145.

Takayama H, Suzuki T, Mugishima H, Fujisawa T, Ookuni M, Schwab M, Gehring M, Nakamura Y, Sugimura T, Terada M. (1992) Deletion mapping of chromosomes 14q and 1p in human neuroblastoma. Oncogene 7:1185–1189.

Takita J, Hayashi Y, Kohno T, Shiseki M, Yamaguchi N, Hanada R, Yamamoto K, Yokota J (1995) Allelotype of neuroblastoma. Oncogene 11:1829–1834.

Van Gele M, Van Roy N, Jauch A, Laureys G, Schelfhout V, De Potter CR, Brock P, Uyttebroeck A, Sciot R, Schuuring E, Versteeg R, Speleman F (1997) Sensitive and reliable detection of genomic imbalances in human neuroblastomas using comparative genomic hybridization analysis. Eur J Cancer 33:1979–1982.

Van Roy N, Laureys G, Cheng NC, Willem P, Opdenakker G, Versteeg R, Speleman F (1994) 1;17 translocations and other chromosome 17 rearrangements in human primary neuroblastoma tumors and cell lines. Genes Chromosomes Cancer 10:103–114.

Van Roy N, Cheng NC, Laureys G, Opdenakker G, Versteeg R, Speleman F (1995a) Molecular cytogenetic analysis of 1;17 translocations in neuroblastoma. Eur J Cancer 31A:530–535.

Van Roy N, Forus A, Myklebost O, Cheng NC, Versteeg R, Speleman F (1995b) Identification of two distinct chromosome 12-derived amplification units in neuroblastoma cell line NGP. Cancer Genet Cytogenet 82:151–154.

Van Roy N, Jauch A, Van Gele M, Laureys G, Versteeg R, De Paepe A, Cremer T, Speleman F (1997) Comparative genomic hybridization analysis of human neuroblastomas: Detection of distal 1p deletions and further molecular genetic characterization of neuroblastoma cell lines. Cancer Genet Cytogenet 82:151–154.

Weiss WA, Aldape K, Mohapatra G, Feuerstein BG, Bishop JM (1997) Targeted expression of MYCN causes neuroblastoma in transgenic mice. Embo J 16:2985–2995.

Medical and Pediatric Oncology 36:5–10 (2001)

Multicentre Analysis of Patterns of DNA Gains and Losses in 204 Neuroblastoma Tumors: How Many Genetic Subgroups Are There?

Jo Vandesompele, MSc,[1] Frank Speleman, PhD,[1]* Nadine Van Roy, PhD,[1] Geneviève Laureys, MD, PhD,[2] Christian Brinkschmidt, MD, PhD,[5] Holger Christiansen, MD,[6] Fritz Lampert, MD,[7] Maria Lastowska, MD, PhD,[8] Nick Bown, MSc,[8] Andy Pearson, MD,[8] James C. Nicholson, DM, MA, MD,[10] Fiona Ross, PhD, MD,[10] Valérie Combaret, PhD,[11] Olivier Delattre, MD, PhD,[12] Bert G. Feuerstein, MD, PhD,[4] and Dominique Plantaz, MD, PhD[3]

Procedure. Analysis of comparative genomic hybridization (CGH) data of 120 tumors from four different studies, and data of 84 previously unpublished tumors, allowed delineation of at least six different genetic subsets of neuroblastomas. ***Results and Conclusions.*** A small number of tumors show no detectable imbalances. A second group of tumors presents with gains and losses of whole chromosomes and is found predominantly in prognostically favorable stage 1 and 2 tumors. The remaining groups are characterized by the presence of partial chromosome imbalances, and are found mostly in stage 3, 4, and 4S tumors. The third group shows 17q gain without 11q loss, 1p loss, or *MYCN* amplification (MNA). The fourth group has 1p deletion or MNA, and finally, a fifth group shows 11q loss without 1p deletion or MNA, and is found mainly in stage 4 tumors. The latter group is significantly associated with losses of 3p, 4p, and 14q. Med. Pediatr. Oncol. 36: 5–10, 2001.

Key words: neuroblastoma; CGH; genetic subgroup

INTRODUCTION

The genetic study of neuroblastoma was initiated in the early seventies. Cytogenetic data were mainly obtained for a subset of tumors which typically presented with *MYCN*-amplification (MNA) and/or 1p-deletions [1]. Analysis of tumor DNA ploidy identified tumors with a near triploid DNA content, predominantly in young children (age <1 year) with lower stages of disease and good prognosis [2]. In contrast, near diploid or near tetraploid DNA was found most often in stage 3 and 4 tumors. Molecular studies defined the critical regions on the short arm of chromosome 1, which are lost in subsets of neuroblastomas [3,4]. In addition to 1p36, other genomic regions were shown to be involved in neuroblastoma. Recurrent losses were observed for 3p, 4p, 9p, 11q, and 14q [5–12], as well as frequent gain of chromosome 17 or the chromosome 17q arm [13–20]. A drawback of many molecular and molecular cytogenetic studies is that they do not provide a complete overview of all genomic imbalances occurring in tumors. CGH can circumvent this problem. It allows the detection of DNA gains and losses for the entire tumor genome within one experiment, and thus provides information of all, albeit large (>10 Mb), genomic imbalances, which are present in each investigated tumor [21]. This technique has been successfully applied for genome-wide screening of neuroblastomas by several investigators [22–28]. The aim of these studies was:

[1]Department of Medical Genetics, Ghent University Hospital, Ghent, Belgium

[2]Paediatric Oncology, Ghent University Hospital, Ghent, Belgium

[3]Department of Paediatrics, University Hospital Centre of Grenoble, Grenoble, France

[4]Department of Laboratory Medicine, Division of Molecular Cytometry, University of California, San Francisco, California, USA

[5]Gerhard-Domagk-Institute of Pathology, University of Münster, Münster, Germany

[6]Department of Paediatrics, University of Marburg

[7]Department of Paediatrics, Haematology and Oncology, Univ.-Kinderklinik of Gießen, Gießen, Germany

[8]Department of Human Genetics, University of New Castle upon Tyne, New Castle upon Tyne, United Kingdom

[9]Department of Child Health, University of New Castle upon Tyne, New Castle upon Tyne, United Kingdom

[10]Wessex Regional Genetics Laboratory, Salisbury District Hospital, Salisbury, United Kingdom

[11]Department of Tumor Biology, Centre Léon Bérard, Lyon, France

[12]Department of Pediatric Oncology, Institut Curie, Paris, France

Grant sponsor: The Parthenon Trust; Grant sponsor: The Wessex Cancer Trust; Grant sponsor: R&D Committee of the Northern & Yorkshire Regional Health Authority; Grant sponsor: FWO; Grant number: G.0085.96; Grant sponsor: Vereniging voor Kankerbestrijding 1995–1998; Grant sponsor: GOA; Grant number: 12051397; Grant sponsor: Flemish Institute for the Promotion of Scientific Technological Research in Industry (IWT); Grant sponsor: Forschungshilfe Station Peiper.

*Correspondence to: F. Speleman, Department of Medical Genetics, Ghent University Hospital, De Pintelaan 185, B-9000 Ghent, Belgium

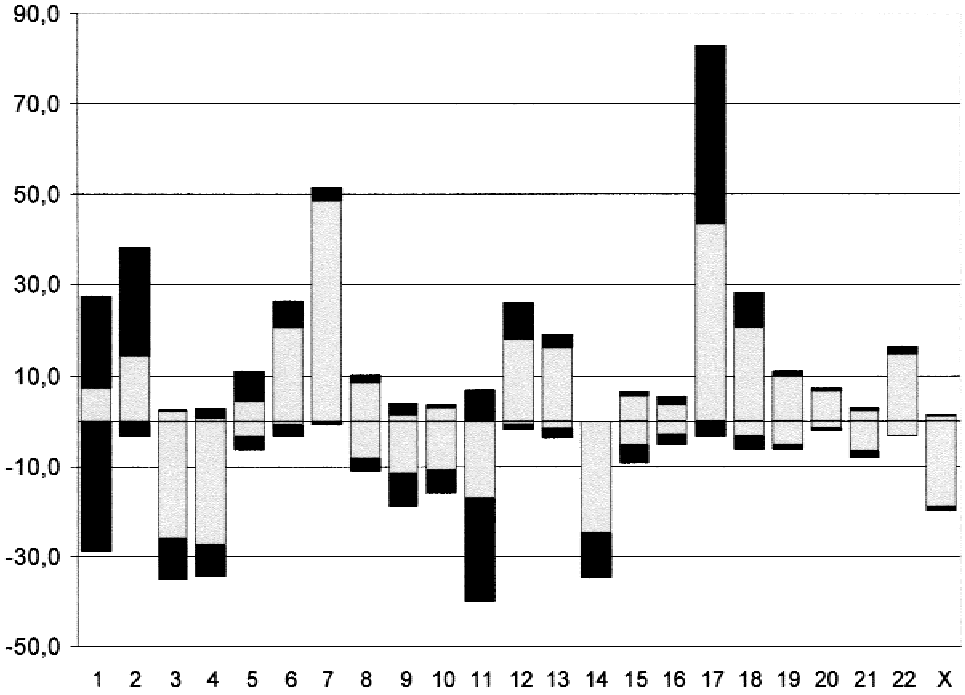

Fig. 1. Cumulative percent of whole (gray) and partial (black) chromosome imbalances detected by CGH in 204 neuroblastomas (bars above horizontal axis indicate gains, bars below indicate losses).

1. To identify previously unrecognised gains, losses, or amplifications, and thus new regions which could harbour genes implicated in neuroblastoma.
2. To look for associations between frequently occurring imbalances, and thus identify new genetic subgroups.
3. To study the response to therapy and survival for these subgroups.

As it was not possible to evaluate genomic imbalances for individual tumors for all published CGH data, we decided to collect all data on these 120 tumors and re-evaluate them in one single study. Moreover, data from 84 unpublished cases are included in this study. This multicentre study thus yielded an unprecedented overview of the pattern of genomic imbalances occurring in 36 stage 1, 30 stage 2, 31 stage 3, 68 stage 4, and 39 stage 4S tumors.

MATERIALS AND METHODS

Patients

In total, 204 different tumors were studied by five different centres (Department of Medical Genetics and Paediatric Oncology, Ghent University Hospital, Belgium, 36 cases; Department of Paediatrics, University Hospital Centre of Grenoble, France, 82 cases; Gerhard-Domagk-Institute of Pathology, University of Münster and Department of Paediatrics, University of Marburg, Germany, 51 cases; Department of Human Genetics, University of Newcastle upon Tyne, UK, 22 cases; Wessex Regional Genetics Laboratory, Salisbury District Hospital, UK, 13 cases). Detailed survival data have been published or will be published elsewhere.

CGH

CGH was performed according to du Manoir et al. [29], or Kallioniemi et al. [30]. For digital image analysis, different image acquisition equipment and software programs were used [23,24,27,28]. For data analysis, DNA copy number changes for individual cases were represented on separate ideogram charts.

RESULTS

Chromosomal imbalances were observed in most tumors (92%). Figure1 shows the cumulative percentages of whole and partial imbalances for each chromosome for the 204 analysed tumors. Detailed data on the gains and losses observed for each individual tumor and survival data can be found at http://allserv.rug.ac.be/neubla/cgh.htm.

Whole Chromosome Gains and Losses

Most tumors with lower stages of disease showed exclusively whole chromosome gains and losses. Pooling of all data from 51 tumors with only numerical imbalances revealed a nonrandom pattern of gains for chromosomes 1, 2, 6, 7, 8, 12, 13, 17, 18, and 22, and losses for chromosomes 3, 4, 9, 11, 14, and X (Fig. 2). This pattern was observed in the majority of all stage 1 and 2 tumors (50 and 60%, respectively), in a small portion of stage 3 and 4S tumors (16 and 15%, respectively), and in a few cases of stage 4 tumors (6%) (Fig. 3). This char-

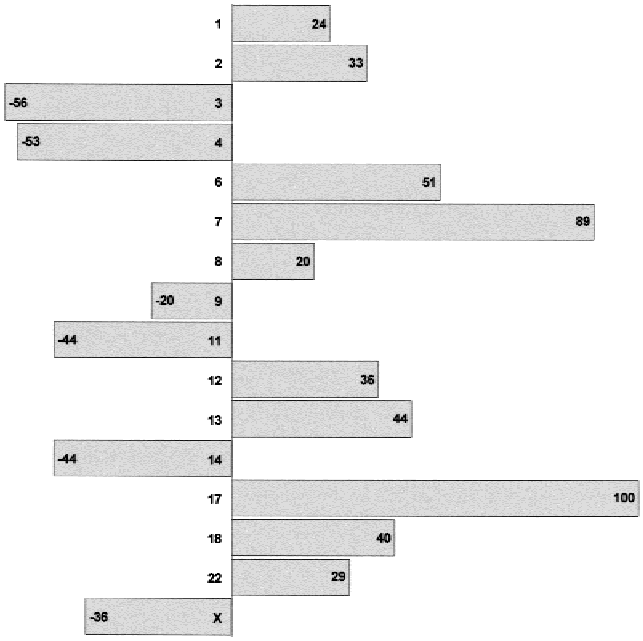

Fig. 2. Characteristic pattern of whole chromosome gains (bars to the right, in percentage) and losses (bars to the left) in 51 neuroblastomas with only numerical imbalances (chromosomes that show abnormalities in less than 20% in this subgroup are not included).

acteristic pattern of whole chromosome imbalances was typically observed in infants (61% $\leq$ 1 year of age at diagnosis), with high survival rates (only 3 of 51 patients died). Seventy percent of these tumors for which information on DNA index was available showed a DNA content in the near triploid range. The highest incidence of whole chromosomal imbalance taken together for all stages was observed for chromosome 17 gain (89/204, 44%; Fig.1).

Partial Chromosomal Imbalances

Partial chromosome gains were most frequently observed for 17q (80/204, 39%). Gain of 17q either through over-representation of a complete chromosome 17 or (partial) gain of the long arm only, thus occured in 83% of all examined tumors. Seventeen-q gain was exclusively found in tumors with 1p loss and/or MNA or 11q loss in stage 2 ($P = 2.10^{-6}$) and 3 ($P = 2.10^{-7}$) and was significantly associated with 1p loss and/or MNA or 11q loss in stage 4 ($P = 0.01$). The majority of stage 3 tumors with partial chromosomal imbalance showed MNA, and most often but not exclusively 1p-deletion and 17q over-representation. The same pattern emerged in stage 2 tumors but in a much smaller proportion. Most stage 4 tumors showed 17q over-representation in combination with 1p-deletion, 1p-deletion and MNA, 11q-deletion with or without 3p- and/or 14q-deletion, or without any of these aforementioned additional changes. Survival analysis for patients with or without 17q gain is described in an accompanying paper (Bown et al., this issue).

Although indicative from data of some individual studies, pooling of all data clearly defines a subset of tumors with 11q-deletion (Fig. 3). Loss of 11q was found in a few cases of stage 1(2 of 36), 2 (2 of 30), 3 (3of 31), and 4S (3 of 39) tumors and in 19 out of 68 stage 4 tumors. These 11q losses typically occurred in stage 4 tumors without 1p deletion or MNA. Within this subgroup of tumors (15 cases), losses of 3p, 4p, 14q, and 9p were frequently observed (53%, 27%, 27%, and 13%, respectively).

Loss of 1p was observed in 59 tumors (29%). No 1p loss was found in stage 1 tumors. Only three cases were observed in stage 2 tumors, two of which had MNA. Seventy-three percent of tumors with 1p loss also showed MNA.

Other regions for which loss was observed included 3p, 4p, 9p, and 14q. Losses of 3p, 4p, and 14q showed a highly significant association with 11q loss ($P = 1.10^{-6}$, $P = 0.016$, and $P = 4.10^{-4}$, respectively). Loss of 3p (18 cases, 9%) was found in all stages, but most frequently in stage 4 tumors with 11q loss (see above). Loss of 4p was observed in eight tumors (four of which were stage 4 tumors with 11q loss). Loss of 9p material was observed in 12 cases (6%), three of which were stage 1 tumors with otherwise good prognostic features.

Partial loss for chromosome arm 14q was found in 10% of tumors (20 cases), mainly stage 4 and 4S. Partial 14q loss was found in only 1 out of 25 stage 4 tumors with 1p deletion and MNA and in 4 out of 15 (27%) stage 4 tumors with 11q loss without 1p deletion or MNA.

MNA was observed in 49 tumors (24%). Additionally, the five different CGH studies identified seven new regions of amplification: 2p23, 3q24-26, 4q33-35, 6p11-12, 10p13, 10q25, and 11q13. For each of these chromosomal regions, high level DNA amplification was observed only once, indicating that amplifications of these sites in neuroblastoma are rare events. One exception may be the 11q13 region, for which over-representation (but not amplification) was observed in 11 additional cases. In the tumor with 11q13 amplification, copy number increase of *CCND1* and *EMS1* was confirmed by Southern blot analysis.

DISCUSSION

As cytogenetic analysis is often unsuccessful in the analysis of neuroblastoma, CGH is a valuable alternative for genome-wide screening of whole or partial chromosomal gains and losses and gene amplification. Recently, several investigators have successfully applied CGH to the genetic study of neuroblastoma [22–27]. In Vandesompele et al. [28], the authors compared the published data with their own series of analysed tumors. The major

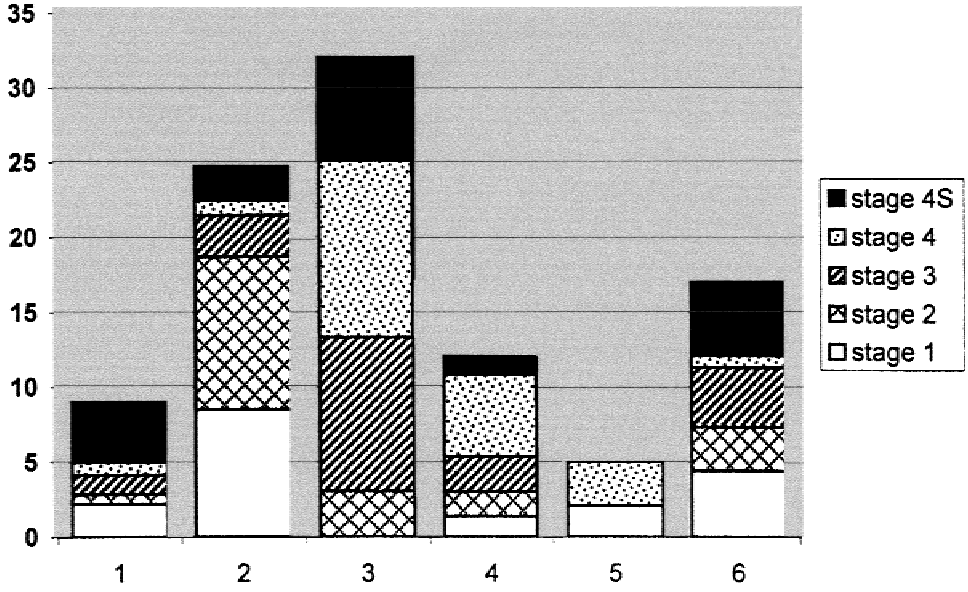

Fig. 3. Normalised distribution (in percent) of clinical stages for each genetic subgroup of neuroblastoma as defined by CGH. **1:** No detectable abnormalities; **2:** Only numerical imbalances; **3:** 1p loss and/or MNA; **4:** 11q loss (no 1p loss or MNA); **5:** 17q gain (no 1p loss or MNA or 11q loss); **6:** Others (mainly tumors with numerical imbalances and few structural changes).

findings in all individual studies were concordant, but from this analysis it was apparent that, although significant numbers of tumors were studied, the total number of tumors of clinical and genetic subgroups was relatively small in the individual studies. Moreover, simultaneous occurrence of particular imbalances in individual tumors could not be analysed from published data in all cases. For this reason, we decided to collect and re-evaluate all individual tumor CGH data. In addition, a significant number of previously unpublished data was included in this analysis. Many of the previously observed characteristic CGH findings from individual studies were confirmed and strengthened by pooling of all data. This includes the typical pattern of gains for chromosomes 1, 2, 6, 7, 8, 12, 13, 17, 18, and 22, and losses for chromosomes 3, 4, 9, 11, 14, and X. These tumors are typically triploid and occur in children with favorable prognosis and age less than one year. Particular patterns of whole chromosome gains and losses have also been observed in other pediatric tumors with good prognosis, including acute lymphoblastic leukemia [31]. The biological significance of these numerical chromosome changes is unknown, and it is puzzling that most of the chromosomes that are underrepresented in low stage tumors also show partial losses in high stage tumors. Similarly, gain of chromosome 17 and extra 17q are the most frequently observed chromosomal imbalances in low and high stage tumors, respectively.

The frequent finding of chromosome 17q gain in neuroblastoma is an interesting observation that is receiving increasing attention. In early cytogenetic studies preferential involvement of 17q was noted [13], but these initial findings were not further explored until the introduction of FISH analysis [14–16]. Using this approach, it became clear that unbalanced translocations result in extra 17q copies and loss of chromosomal material in the partner chromosome. The observation that chromosomes 1 and 11 were frequently implicated as partner chromosomes with resulting 1p and 11q loss led to the suggestion that these translocations could act as a mechanism which lead to simultaneous loss of tumor suppressor genes on 1p and 11q and extra copies of genes on 17q, controlling growth, differentiation, or apoptosis [16,20]. An accompanying paper shows that 17q gain is a powerful prognostic predictor of adverse outcome (Bown et al., this issue). Whether genes on 17q, and in particular an imbalance of 17p versus 17q genes, is responsible for a more aggressive tumor phenotype, or whether 17q is an innocent bystander in association with known or possibly prognostically unfavorable genetic parameters such as MNA and 1p and 11q deletion, remains to be determined.

The present analysis of a large set of tumors showed that 11q loss defines a distinct genetic subgroup of stage 4 tumors. Eleven-q loss was found in almost half of stage 4 tumors without 1p deletion and/or MNA. A high proportion of 3p, 4p, and 14q losses was observed within this newly defined genetic subgroup, and furthermore 17q gain was consistently present. Literature on incidences of 11q loss in neuroblastoma is scarce and conflicting. Srivatsan et al. [8], Takita et al. [10], and Takeda et al. [32] found 11q loss in 26%, 24%, and 19% of analysed tumors, respectively, whereas Fong et al. [6] reported 11q loss in only 5% of tumors (one tumor in a series of 20 informative cases). Recently, a LOH study

with 11q markers on a series of 267 neuroblastomas was conducted by Maris et al. (this issue). These authors found 11q loss in 43% of tumors, a frequency that is much higher than that observed by CGH. If we assume that their tumors could also represent near-triploid tumors with whole chromosome 11 loss (61 cases), partial 11q-loss occurred in only 20% of tumors, a figure that is in keeping with our findings. Inclusion of near-triploid tumors in the series of Maris et al. may also explain why no correlation with clinical stage was found.

The present study and previous 11q LOH studies strongly suggest that one or more tumor suppressor genes on 11q play an important role in the development of this subgroup of neuroblastomas. An essential first step towards the identification of this gene is the delineation of a shortest region of overlap for 11q deletions. Based upon the ratio-profiles of cases with partial 11q loss, an SRO was assigned to 11q21→q22. Caution is needed, however, in the positioning of breakpoints based upon CGH profiles, and further molecular analysis of the cases with small 11q deletions is warranted to verify the exact chromosomal localization of these deletions. Interphase FISH-, CGH- and LOH-analyses on larger series of stage 4 tumors without 1p-deletion and/or MNA could allow further refinement of this SRO, which should facilitate the selection of positional and functional candidate tumor suppressor genes within this region for further analysis. Eight out of the 15 patients with tumors with 11q deletions described in this study died and one patient relapsed, thus indicating a poor survival for patients with tumors belonging to this genetic subgroup. Additional patients need to be studied in order to obtain more reliable survival estimate figures.

CGH is a technique that is particularly suited for identification of new amplicons in tumors. The CGH studies that have been performed so far on neuroblastoma show that amplification of chromosomal regions other than 2p23-24 is a rare event. Several additional regions for which high level DNA amplification was noted were identified by CGH. One region, 11q13 is particularly interesting, as it is known to be implicated in many other malignancies, including carcinoma of the breast, head, neck, bladder, lung [33]. The observation of 11q13 gain (not amplification) in additional neuroblastomas, and the fact that low-copy 11q13 DNA amplification (<10 copies) occurs in other tumors opens the possibility that 11q13 gain or amplification plays a role in a subset of neuroblastomas.

In conclusion, this study further illustrates the significance of CGH in the characterization of genetics subgroups in neuroblastoma. We were able to define the pattern of whole chromosome gains and losses in the genetic subgroup of tumors with whole chromosome imbalances only. Furthermore, we defined a new genetic subgroup of tumors with 11q loss within the subset of stage 4 tumors without 1p deletion or MNA. As this group represents almost one-third of all stage 4 tumors, a search for a tumor suppressor gene on 11q is warranted, as the identification of this gene may improve our understanding of the behavior of this subgroup of tumors, and may ultimately lead to new therapeutic approaches and increased survival for these patients.

ACKNOWLEDGMENTS

We would like to acknowledge following people: Dr. J.A. Kohler, Dr. I. Moore, UK Children's Cancer Study Group, Rosel Engel. Nadine Van Roy is a postdoctoral researcher from the Fund for Scientific Research, Flanders.

REFERENCES

1. Brodeur GM, Fong CT. Molecular biology and genetics of human neuroblastoma. Cancer Genet Cytogenet 1989;41:153–174.
2. Look AT, Hayes FA, Shuster JJ, et al. Clinical relevance of tumor cell ploidy and N-myc gene amplification in childhood neuroblastoma: a Pediatric Oncology Group study. J Clin Oncol 1991;9: 581–591.
3. Versteeg R, Caron H, Cheng NC, et al. 1p36: every subband a suppressor? Eur J Cancer 1995;31A:538–541.
4. Schwab M, Praml C, Amler LC. Genomic instability in 1p and human malignancies. Genes Chrom Cancer 1996;16:211–229.
5. Suzuki T, Yokota J, Mugishima H, et al. Frequent loss of heterozygosity on chromosome 14q in neuroblastoma. Cancer Res 1989; 49:1095–1098.
6. Fong CT, White PS, Peterson K, et al. Loss of heterozygosity for chromosomes 1 or 14 defines subsets of advanced neuroblastomas. Cancer Res 1992;52:1780–1785.
7. Takayama H, Suzuki T, Mugishima H, et al. Deletion mapping of chromosomes 14q and 1p in human neuroblastoma. Oncogene 1992;7:1185–1189.
8. Srivatsan ES, Ying KL, Seeger RC. Deletion of chromosome 11 and of 14q sequences in neuroblastoma. Genes Chrom Cancer 1993;7:32–37.
9. Caron H, van-Sluis P, Buschman R, et al. Allelic loss of the short arm of chromosome 4 in neuroblastoma suggests a novel tumor suppressor gene locus. Hum Genet 1996;97:834–837.
10. Takita J, Hayashi Y, Kohno T, et al. Allelotype of neuroblastoma. Oncogene 1995;11:1829–1834.
11. Takita J, Hayashi Y, Kohno T, et al. Deletion map of chromosome 9 and p16 (CDKN2A) gene alterations in neuroblastoma. Cancer Res 1997;57:907–912.
12. Hallstensson K, Thulin S, Aburatani H, et al. Representational difference analysis and loss of heterozygosity studies detect 3p deletions in neuroblastoma. Eur J Cancer 1997;33:1966–1970.
13. Gilbert F, Feder M, Balaban G, et al. Human neuroblastomas and abnormalities of chromosomes 1 and 17. Cancer Res 1984;44: 5444–5449.
14. Savelyeva L, Corvi R, Schwab M. Translocation involving 1p and 17q is a recurrent genetic alteration of human neuroblastoma cells. Am J Hum Genet 1994;55:334–340.
15. Van Roy N, Laureys G, Cheng NC, et al. 1;17 translocations and other chromosome 17 rearrangements in human primary neuroblastoma tumors and cell lines. Genes Chrom Cancer 1994;10: 103–114.
16. Van Roy N, Cheng NC, Laureys G, et al. Molecular cytogenetic

analysis of 1;17 translocations in neuroblastoma. Eur J Cancer 1995;31A:530–535.
17. Caron H, van Sluis P, Van Roy N, et al. Recurrent 1;17 translocations in human neuroblastoma reveal nonhomologous mitotic recombination during the S/G2 phase as a novel mechanism for loss of heterozygosity. Am J Hum Genet 1994;55:341–347.
18. Meddeb M, Danglot G, Chudoba I, et al. Additional copies of a 25 Mb chromosomal region originating from 17q23.1-17qter are present in 90% of high-grade neuroblastomas. Genes Chrom Cancer 1996;17:156–165.
19. Lastowska M, Roberts P, Pearson AD, et al. Promiscuous translocations of chromosome arm 17q in human neuroblastomas. Genes Chrom Cancer 1997;19:143–149.
20. Van Roy N, Laureys G, Van Gele M, et al. Analysis of 1;17 translocation breakpoints in neuroblastoma: implications for mapping of neuroblastoma genes. Eur J Cancer 1997;33:1974–1978.
21. Bentz M, Plesch A, Stilgenbauer S, et al. Minimal sizes of deletions detected by comparative genomic hybridization. Genes Chrom Cancer 1998;21:172–175.
22. Altura RA, Maris JM, Li H, et al. Novel regions of chromosomal loss in familial neuroblastoma by comparative genomic hybridization. Genes Chrom Cancer 1997;19:176–184.
23. Brinkschmidt C, Christiansen H, Terpe HJ, et al. Comparative genomic hybridization (CGH) analysis of neuroblastomas—an important methodological approach in paediatric tumor pathology. J Pathol 1997;181:394–400.
24. Lastowska M, Nacheva E, McGuckin A, et al. Comparative genomic hybridization study of primary neuroblastoma tumors. United Kingdom Children's Cancer Study Group. Genes Chrom Cancer 1997;18:162–169.
25. Van Gele M, Van Roy N, Jauch A, et al. Sensitive and reliable detection of genomic imbalances in human neuroblastomas using comparative genomic hybridization analysis. Eur J Cancer 1997; 33:1979–1982.
26. Van Roy N, Jauch A, Van Gele M, et al. Comparative genomic hybridization analysis of human neuroblastomas: detection of distal 1p deletions and further molecular genetic characterization of neuroblastoma cell lines. Cancer Genet Cytogenet 1997;97:135–142.
27. Plantaz D, Mohapatra G, Matthay KK, et al. Gain of chromosome 17 is the most frequent abnormality detected in neuroblastoma by comparative genomic hybridization. Am J Pathol 1997:150:81–89.
28. Vandesompele J, Van Roy N, Van Gele M, et al. Genetic heterogeneity of neuroblastoma studied by comparative genomic hybridization. Genes Chrom Cancer 1998;23:141–152.
29. du Manoir S, Speicher MR, Joos S, et al. Detection of complete and partial chromosome gains and losses by comparative genomic in situ hybridization. Hum Genet 1993;90:590–610.
30. Kallioniemi A, Kallioniemi OP, Sudar D, et al. Comparative genomic hybridization for molecular cytogenetic analysis of solid tumors. Science 1992;258:818–821.
31. Raimondi SC. Current status of cytogenetic research in childhood acute lymphoblastic leukemia. Blood 1993:81:2237–2251.
32. Takeda O, Handa M, Uehara T, et al. An increased NM23H1 copy number may be a poor prognostic factor independent of LOH on 1p in neuroblastomas. Br J Cancer 1996;74: 1620–1626.
33. Schuuring E. The involvement of the chromosome 11q13 region in human malignancies: cyclin D1 and EMS1 are two new candidate oncogenes—a review. Gene 1995;159:83–96.

Int. J. Cancer: **91,** 680–686 (2001)

Publication of the International Union Against Cancer

COMPARATIVE GENOMIC HYBRIDIZATION (CGH) ANALYSIS OF STAGE 4 NEUROBLASTOMA REVEALS HIGH FREQUENCY OF 11Q DELETION IN TUMORS LACKING *MYCN* AMPLIFICATION

D. PLANTAZ[1]*, J. VANDESOMPELE,[2], N. VAN ROY[2], M. ŁASTOWSKA[3], N. BOWN[3], V. COMBARET[4], M.C. FAVROT[1,4], O. DELATTRE[5], J. MICHON[6], J. BÉNARD[7], O. HARTMANN[8], J.C. NICHOLSON[9], F.M. ROSS[9], C. BRINKSCHMIDT[10], G. LAUREYS[2], H. CARON[11], K.K. MATTHAY[12], B.G. FEUERSTEIN[13] and F. SPELEMAN[2]

[1]*Department of Paediatrics, and Laboratory of Cancer Biology. University Hospital Centre of Grenoble, Grenoble, France*
[2]*Departments of Medical Genetics and Paediatric Oncology, Ghent University Hospital, Ghent, Belgium*
[3]*Departments of Human Genetics and Child Health, University of Newcastle Upon Tyne, Newcastle Upon Tyne, UK*
[4]*Laboratory of Tumour Biology, Centre Léon Bérard, Lyon, France*
[5]*Inserm U 434, Institut Curie, Paris, France*
[6]*Paediatric Department, Institut Curie, Paris, France*
[7]*Laboratory of Molecular Biology, Institut Gustave-Roussy, Villejuif, France*
[8]*Paediatric Department, Institut Gustave-Roussy, Villejuif, France*
[9]*Wessex Regional Genetics Laboratory, Salisbury District Hospital, Salisbury, UK*
[10]*Gerhard-Domagk-Institute of Pathology, University of Münster, Münster, Germany*
[11]*Department of Human Genetics and Paediatric Oncology, Academic Medical Centre, Amsterdam, The Netherlands*
[12]*Department of Paediatrics, University of California, San Francisco, CA, USA*
[13]*Department of Laboratory Medicine (Division of Molecular Cytometry), University of California, San Francisco, CA, USA*

We have studied the occurrence and association of 11q deletions with other chromosomal imbalances in Stage 4 neuroblastomas. To this purpose we have performed comparative genomic hybridization (CGH) analysis on 50 Stage 4 neuroblastomas and these data were analyzed together with those from 33 previously published cases. We observed a high incidence of 11q deletion in Stage 4 neuroblastoma without *MYCN* amplification (59%) whereas 11q loss was only observed in 15% of neuroblastomas with *MYCN*-amplification ($p = 0.0002$) or 11% of cases with 1p deletion detected by CGH ($p = 0.0001$). In addition, 11q loss showed significant positive correlation with 3p loss ($p = 0.0002$). Event-free survival was poor and not significantly different for patients with or without 11q deletion. Our study provides further evidence that Stage 4 neuroblastomas with 11q deletions represent a distinct genetic subgroup that typically shows no *MYCN*-amplification nor 1p deletion. Moreover, it shows that neuroblastomas with 11q deletion also often present 3p deletion. This genetic subgroup shows a similar poor prognosis as *MYCN* amplified 4 neuroblastomas.

Key words: *Stage 4 neuroblastoma; comparative genomic hybridization; 11q deletion; MYCN; 1p deletion; genetic subgroup*

Neuroblastoma (NB) is an embryonal solid tumour of childhood believed to originate from immature neural crest cells.[1] The disease has a variable clinical course, ranging from spontaneous regression to malignant progression with complete resistance to therapy. Genetic investigations further supported the heterogeneous nature of this tumour. Based upon these clinical and genetic findings, three prognostically distinct groups were recognized.[2] One group includes hyperdiploid tumors that lack 1p deletion and *MYCN*-amplification (MNA). These patients are often infants with less advanced disease, and prognosis is usually excellent. A second group includes near-diploid or near-tetraploid tumors that lack MNA. These patients are usually over 1 year of age and present with advanced stage disease. Although their overall outcome is poor, these patients tend initially to respond to treatment. The third group is also near-diploid or near-tetraploid, but with both MNA and 1p deletion. These patients tend to respond poorly to therapy, and die within months.

Recent studies have illustrated the power of CGH in whole genome screening for partial and whole chromosome imbalances in NB, in particular for the analysis of low stage NB for which little genetic information was available apart from ploidy, 1p and *MYCN* status. One of the striking findings of CGH analyses was the occurrence of whole chromosome 17 or 17q gain as the most frequent chromosome abnormality in low and high stage NB, respectively.[3–6] Gain of 17q was subsequently shown to be a strong indicator for unfavorable prognosis.[7]

Genetically, the subgroup of Stage 4 NB lacking *MYCN* amplification has remained poorly defined. CGH studies revealed 11q loss in these tumors, but the number of cases in the individual studies was too small to draw significant conclusions.[5,6] In a larger multicenter study on 204 NB, preferential occurrence of 11q deletion in Stage 4 NB without MNA was observed, but the latter group of tumors was still relatively small (33 Stage 4 tumors). In a recent loss of heterozygosity (LOH) study, Guo *et al.*[8] found a high incidence of 11q loss in all NB stages. To further evaluate the occurrence of 11q deletions in *MYCN* non-amplified Stage 4 neuroblastomas and its correlation with other chromosomal imbalances in *MYCN* amplified or non-amplified Stage 4 neuroblastomas, we performed CGH analysis on 50 additional Stage 4 tumors. These data were compiled with data from 33 previously published unselected Stage 4 NB (for details see Material and Methods). A second objective was to assess the prognostic value of 11q deletion in metastatic neuroblastomas.

Nadine Van Roy is a post-doctoral researcher of the Fund for Scientific Research Flanders.

Grant sponsor: University Hospital Center of Grenoble, France; Grant sponsor: GOA; Grant number: 12053397; Grant sponsor: FWO; Grant number: 3G002800; Grant sponsor: Flemish Institute for the Promotion of Scientific Technological Research in Industry (IWT) Fund for Scientific Research Flanders; Grant sponsor: R&D Committee of the Northern and Yorkshire Regional Health Authority; Grant sponsor: Wessex Cancer Trust; Grant sponsor: Parthenon Trust; Grant sponsor: Children's Cancer Group; Grant sponsor: Alfred and Ursula Kuhlemann-Stiftung, Marburg; Grant sponsor: University of Münster; Grant number: BR 119830.

---

*Correspondence to: Department of Paediatrics, University Hospital Centre of Grenoble, BP 217X, 38045 Grenoble, France. Fax: +33 4 76 76 58 30. E-mail: dominique.plantaz@ujf-grenoble.fr

---

Received 7 July 2000; Revised 15 September 2000; Accepted 25 September 2000

MATERIAL AND METHODS

Data from 50 unpublished Stage 4 neuroblastomas (23 unselected, 27 selected for absence of *MYCN*-amplification) were included in our study as well as data on 33 unselected Stage 4 NB from previously published CGH studies.3–6 Indeed, as genetic imbalances are now well known in tumors with MNA, we extended the series of Stage 4 tumors with a selection of 27 non-amplified Stage 4 tumors, to better define genetic abnormalities in this putative subgroup; Table I gives an overview of clinical, genetic and CGH data on all cases. In total 83 Stage 4 tumors were studied by 6 different research laboratories from the following institutions: University of Grenoble, France (27 cases); University of California San Francisco, USA (20 cases); University of Ghent, Belgium (16 cases); University of Newcastle upon Tyne, UK (8 cases); Salisbury District Hospital, UK (7 cases); University of Munster, Germany (5 cases).

The median age of the 83 patients was 39 months (range 1–216). Clinical follow-up data were available from 77 patients. Forty-seven of them relapsed and 43 died with a median follow-up of 20 months (range 3–80).

Genetic data including at least the *MYCN* status were available for 80 patients. Twenty-six of these 80 tumors (33%) showed MNA as determined by FISH, Southern blot or PCR analysis.

CGH was performed according to Kallioniemi *et al.*[9] or du Manoir *et al.*[10] techniques with minor modifications. For digital image analysis, each group used particular image acquisition equipment and software programs, that have been individually validated.[3–6] For data analysis, DNA copy number changes for all individual cases were represented on ideogram charts. We chose upper (indicating gains) and lower (indicating loss) fluorescence ratio thresholds of 1.2 and 0.8 respectively. Amplifications were defined by a ratio >1.5 in a subchromosomal region.

RESULTS

Seventy-eight (94%) cases had partial chromosome gains or losses. Forty-seven of these 78 (60%) cases with partial imbalances also had whole chromosome gains or losses. Five out of 83 cases (6%) solely exhibited whole chromosome abnormalities. The modal number of partial imbalances was 4 per tumour (range 0–11).

Partial chromosomal gains were most often detected for chromosomes 17q (65/83) (78%), 2p (34/83) (41%) (24 cases of 2p23–25 amplification and 10 cases of 2p16–25 simple gain) and 1q (23/83) (28%). Partial chromosomal losses were observed for chromosomes 11q (36/83) (43%), 1p (32/83) (39%), 3p (18/83) (22%), 4p (13/83) (16%), 9p (8/83) (10%), and 14q (9/83) (11%). Figure 1 shows the relative percentage of partial gains of chromosome 1q, 2p and 17q and partial losses of chromosome 1p, 3p and 11q, with the distinction according to the *MYCN* status of the tumour. The interrelationship between MNA and deletion of 1p and 11q is illustrated in Figure 2. The majority of the 65 tumors with 17q gain (54/65, 83%) had either 1p deletion or 11q deletion.

DNA losses

CGH identified 36 tumors with 11q deletion. These deletions were found in 32 of 54 (59%) tumors without MNA and only in 4 of 26 (15%) tumors with MNA determined by Southern blot analysis($p = 0.0002$). Thirty-one (86%) of these 36 tumors also had a 17q gain. Only 4 of these 36 tumors (11%) presented with a 1p deletion by CGH. In 9 of these 36 (25%) tumors 1q gain was noted. Within this subgroup defined by 11q deletion, losses of 3p, 4p, 9p, or 14q were frequently observed [14/36 (39%), 7/36 (19%), 4/36 (11%) and 6/36 (17%) respectively]. Fisher's exact test revealed a significant positive correlation between deletion of 11q and 3p ($p = 0.0002$). A significant inverse correlation was found between 11q deletion and MNA ($p = 0.0002$) and between deletions of 1p and 11q ($p = 0.0001$). Figure 3 gives an overview of all CGH results for chromosome arms 3p and 11q. The 11q deletions were generally large with breakpoints being most frequently located at chromosome bands 11q14 to 11q22, except for a single case that showed an interstitial deletion 11q14–q21.

CGH identified 32 tumors deleted at 1p with breakpoints in the 1p12–p36 region. Twenty-seven of these 32 (83%) tumors with 1p deletion had a 17q gain. Twenty-two of these 32 (69%) had evidence for MNA. Nineteen of these 32 (59%) tumors with 1p deletion had both 17q gain and MNA. CGH detected a gain involving chromosome 1q in 23 cases. These 1q gains were associated with a 1p deletion in 13 cases (56%) and with an 11q deletion in 8 different cases (35%). The 1q gains usually involved the whole q arm.

The third most frequent deletion found was a 3p deletion, occurring in 18 cases. Fifteen of these 18 cases (83%) also had an 11q deletion, whereas only 4 of these 18 cases (22%) presented with a 1p deletion ($p = 0.04$).

Nine tumors had a 14q deletion; 6 of them also had an 11q deletion. Only 1 of the 9 tumors with 14q deletion had MNA (not statistically different).

Gene amplification and gains

High level amplifications at 2p23–25, corresponding to MNA were found in 24 cases (29%); 22 of these 24 (92%) tumors had a 1p loss and 20/24 (83%) a 17q gain. Nineteen of the 24 (79%) tumors with MNA had both 1p deletion and 17q gain. In 10 other cases (12%), CGH detected an apparently simple gain (duplication) of the 2p distal region (2p16–25) clearly distinct from the typical pattern that emerges in MNA tumors. Eight of these 10 tumors with a simple 2p gain had a 17q gain, 3/10 had a 1p deletion and 6/10 had an 11q deletion.

Among the 83 cases, 5 regions of high level amplification at another locus than 2p23–25 were identified by CGH: 4q33–35 (2 cases), 10p13 (1 case), 10q25 (1 case), 11q13 (1 case) and 14q12–13 (1 case). Except for the 10p13 and 10q25 amplification, these tumors showed no MNA. It is interesting to note that besides 11q13 amplification found in 1 case, 6 tumors show local gain at 11q13 and 2 tumors have 11q gain encompassing the 11q13 locus (see also Fig. 3).

Other chromosomal imbalances

Twenty tumors among the 83 (24%) cases with chromosomal imbalances at one or more loci had neither 1p nor 11q deletion. Five of these 20 had only whole chromosome copy number changes and triploid DNA content. Fourteen of the 15 remaining tumors had a 17q gain. Three of these 15 had MNA. MNA was the sole imbalance detected by CGH in only 1 case.

Survival

The 3-year event-free survival (EFS) (Kaplan–Meier) for the 77 patients with a known follow-up was 31% (±7%). EFS was not significantly different between patients whose tumour had an 11q deletion (36%) (±6%) and patients whose tumour showed no 11q deletion (29%, ±7%) ($p = 0.9$). Among 54 patients with a known follow-up and whose tumour was not amplified for *MYCN*, EFS was 37% (±6%) for patients whose tumour showed an 11q deletion and 33% (±7%) ($p = 0.9$) for patients whose tumour had no 11q deletion.

DISCUSSION

Our study presents the largest genome wide screening of gains and losses by comparative genomic hybridization in Stage 4 neuroblastomas. CGH is now well recognized as a valuable and powerful method for genetic analysis of this tumour. Thus far, however, each individual published CGH study of NB included only a limited number of Stage 4 cases (6 to 17 cases per study)[3–6,11] and thus particular genetic subgroups may have remained unnoticed or poorly defined.

In the present study, we compared the pattern of chromosomal imbalances between Stage 4 NB with MNA and those without this

TABLE I – CLINICAL DATA AND OVERVIEW OF CGH ABNORMALITIES ON 83 STAGE 4 NEUROBLASTOMA TUMOURS

No.	Age[1]	MNA[2]	Event[3]	Fol-up event[1]	Death[4]	Fol-up death[4]	Overview CGH abnormalities[5]
1	61	0	1	5	1	10	−11q21-25, +17q21-25
2	34	0	1	3	1	5	−1p11-36, +1q11-44, −4p11-16//+7, +13, −3, −8, −9, −10, −11, −16
3	36		1	6	1	7	−1p34-36, −4p15-16
4	54	0	1	7	1	20	+2p14-25, −9p12-24, −11q14-25, +17q11-25//+13
5	29	0	1	14	1	16	−11q14-25, +17q22-25
6	12	0	1	8	1	8	−11q14-25, +17q11-25
7	88	0	1	2	1	4	−3p11-26, −11q21-25, −17p11-13
8	27	0	1	10	1	10	+17q11-25//+2, +7, −8, −9, −11
9	38	0	1	11	1	11	−3p11-26, −4p14-16, +6q23-37, −8p11-23, +11p11-15, −11q14-25, +17q11-25
10	64	0	0	6	0	6	+2p22-25, −3p21-26, −4p15-16, −11q14-25, +13q21-34, +17q22-25
11	57	0	0	8	0	8	+7q21-36, −11q14-25, +17q21-25//+18
12	41	0	1	19	1	20	−3p11-26, −11q14-25, −14q24-32, −17p11-13, +17q11-25//+13, +18, −10
13	38	0	0	9	0	9	−4q31-35, +6p22-25, +7p11-14, +7q11-36, +17q11-25//+13
14	9	0	0	51	0	51	−11q14-25
15	2	0	ND	ND	ND	ND	+6, +7, +13, +17, −3, −4, −5, −9, −11, −14, −15
16	6	0	ND	ND	ND	ND	+7, +17, −3, −4, −9, −11, −16, −X
17	29	0	1	12	1	12	−1p35-36, +1q11-44, +6p11-25, −6q11-27, +17q22-25//+7, +18, +22, −X
18	61	1	0	26	0	26	−1p35-36, +1q11-44, ++2p24-25, +17q21-25//+7, +X, −3, −5, −10, −15
19	20	0	1	10	1	15	−1p11-36, +1q11-44, ++4q34-35, +8q22-24, −8q24, −9p21-24
20	45	1	1	14	1	19	−1p35-36, ++2p24-25, +6p11-25, −6q21-27, +11q21-25, +17q23-25
21	31	ND	1	8	0	64	+1p35-36, +1q11-44, −3p22-26, +5p31-35, −11q14-25, +11q13, −14q22-32, +17q11-25//+13
22	32	0	0	67	0	67	+1q43-44, −5p11-15, +7q21-36, −8p11-23, −10p11-15, −11q14-25, +17q22-25
23	32	1	1	18	1	24	−1p32-36, +2p11-25, −3p13-26, −17p11-13, +17q22-25, −18q21-23//−9
24	57	1	1	24	1	25	−1p11-36, +1q11-44, ++2p24-25, −11q14-25, +11q13, +17q11-25//+7, +12, −3, −10, −15
25	49	0	1	15	1	20	−1q42-44, +17q22-25
26	34	1	0	42	0	42	+2p22-25, +2q23-37, +5q14-23, +17q21-25, +18q11-23//+7, +12, +22
27	57	0	1	13	1	21	+1q11-44, −2p24-25, −3p21-26, +7p15-22, −11q13-25, −14q24-32, +17q21-25
28	63	0	1	1	1	3	+2p11-15, +5p11-15, ++11q13, +12q22-24//+6, +7, +15, +16, +17, +18, −4, −8, −9, −11, −14, −21, −X
29	178	1	0	25	0	25	−1p13-36, +1q31-44, ++2p24-25, −3p22-26, +11q13-25//+22
30	19	1	0	52	0	52	−1p22-36, ++2p24-25, +17q22-25
31	101	0	1	1	1	19	+1q11-44, +2p22-25, +5p31-35, +11p11-15, −11q21-25, +16p11-13//+6, +7, +13, +17, +18, +20
32	47	0	1	24	1	36	+17, +19, −X
33	65	0	0	40	0	40	−3p13-26, −4p11-16, −11q14-25, +11q13, −20p11-13//+7, +17, +18
34	18	1	0	78	0	78	−1p33-36, ++2p24-25, −9p21-24, +17q21-25
35	35	1	0	38	0	38	−1p32-36, ++2p24-25, −9p22-24
36	41	0	0	43	0	43	+17q21-25
37	39	0	1	6	1	6	−11q14-25, +17q21-25//+7, +18
38	60	0	1	32	1	40	+1q11-44, −10q23-26, −11q21-25, +17q11-25//+7, +8, +18, −9, −Y
39	9	0	0	68	0	68	+17q22-25//+6, +7, +12, +13
40	60	0	0	54	0	54	−3p21-26, −4p15-16, −11q14-25, +11q13, +17q21-25//+7, +19, −21
41	28	0	0	14	0	14	−1p32-36, +2p22-25, −4p12-16, +7q21-36, −10p11-15, −14q22-34, +17q21-25
42	19	0	0	16	0	16	−4p14-16, +4q11-35, +5q11-23, +13q14-34, −17p11-13//−16, −19, −20, −22
43	65	0	1	10	0	22	−6q24-27, +12q21-24, −17p11-13, +17q11-25
44	44	0	1	22	0	22	+1q11-44, −9p11-24, −11q14-25, +13q33-34, −16q11-24, +17q11-25
45	36	0	0	8	0	8	+2p15-25, +7q21-26, −11q14-25, +17q11-25
46	156	0	0	67	0	67	+2p21-25, −3q11-29, −6p11-25, +10p11-15, −11q14-25, ++14q12-13, +17q11-25, +Xp11-22//+17, +18
47	84	0	0	22	0	22	+2p16-25, +7q22-26, −11q21-25, −14q22-32//−3
48	96	0	0	41	0	41	−14q22-32, +17q21-25
49	84	0	0	6	0	6	−3p14-26, +17q21-25, +Xp11-22//+18
50	47	0	1	1	1	4	−11q14-25, +17q21-25//+13
51	12	0	ND	ND	ND	ND	−3p21-26, −11q13-25, +17q21-25
52	67	0	0	10	0	10	−1p32-36, ++2p24-25, −4p11-16, +7q11-26, +16q22-24, −17p11-13, +17q11-25//+12, −11

TABLE I – CLINICAL DATA AND OVERVIEW OF CGH ABNORMALITIES ON 83 STAGE 4 NEUROBLASTOMA TUMOURS (CONTINUED)

No.	Age[1]	MNA[2]	Event[3]	Fol-up event[1]	Death[4]	Fol-up death[4]	Overview CGH abnormalities[5]
53	33	1	1	9	1	17	−1p11-36, +1q11-44, ++2p24-25, +17q21-25//−8, −11
54	38	1	1	1	1	10	−1p32-36, +1q11-44, ++2p24-25, +17q21-25, −18p11.1-11.3, +18q22-23//+3, +5
55	57	1	1	22	1	34	−1p11-36, +1q11-44, ++2p24-25, +13q21-31, +17q11-25//+2, +7, −3, −8, −9, −11, −14, −15, −18, −X
56	9	1	1	12	1	16	−1p11-36, ++2p24-25, +17q11-25
57	41	1	1	1	1	15	−1p34-36, +1q11-44, ++2p24-25, +18q11-23
58	19	0	1	6	1	9	+1q11-44, +17q21-25, +18q11-23//+2, +16
59	47	0	0	79	0	79	−4q31-35, −11q14-25, +17q11-25//+22
60	38	0	1	8	1	8	−3p21-26, +11p11-15, −11q11-25, +16q21-24, +17q21-25
61	51	1	0	4	0	4	−1p32-36, ++2p24-25, +3q25-29, +4q11-35, +7q11-36, −11q22-25, +13q14-34, −16q23-24, −17p11-13, +17q21-25//−10, −19
62	12	1	ND	ND	ND	ND	−1p36, ++2p24-25, −11q11-25, +13q11-21, −14q22-34, +17q21-25//+7, −18, −19
63	66	0	0	28	0	28	−5q11-35, +6q11-27, +7q21-36, −11q22-25, −12q23-24, +17q21-25//+18, −3
64	3	0	0	19	0	19	+17, −3, −11, −14, −15
65	30	1	1	1	1	11	−1p35-36, ++2p24-25, +11q12-14, +17q11-25//+19
66	24	ND	1	11	1	11	−1p11-34, +2q22-37, −3p21-26, −5p11-15, +5q32-35, +6p21-22, −9p21-24, −11q14-25, +12q23-24, +13q21-34, ++17q12-21//+17, +19, +22
67	24	1	1	1	1	9	−1p21-36, ++2p24-25, +17q21-25//−X
68	42	0	1	10	1	15	+1p32-36, +1q11-44, −9p13-24, +17q11-25//+7, +19, −14, −21
69	12	0	1	30	1	30	−1p34-36, +2p22-25, −3p11-26, −4p11-16, +17q22-25, −18q22-23//+6, +12, −14, −2
70	90	1	1	1	1	29	−1p11-36, ++2p24-25, −10q11-26, +17q21-25, +18p21-25//+7, −X
71	156	0	1	1	1	3	−3p24-26, −4p13-16, −9q33-34, −11q22-25, +12q23-24, +17q22-25
72	216	0	1	18	1	25	−1p32-36, +1q11-44, −4q11-28, +6p22-25, −6q21-27, −14q22-32, +17q21-25//+12, −3, −X
73	67	0	1	17	1	20	−3p14-26, −4p14-16, +4q26-35, +5q31-35, −11q13-25, −14q22-32, +17q21-25//+18, −2, −8
74	5	1	1	18	1	41	−1p34-36, ++2p24-25, +6p11-22, +6q11-27, +17q11-25//−10
75	20	1	1	7	1	9	−1p31-36, +1q23-44, ++4q33-35, +17q21-25
76	16	0	0	45	0	45	+1, +6, +7, +8, +13, +17, −3, −11
77	66	1	ND	ND	ND	ND	++2p24-25, +10p13-15, −10q25-26, +17q11-25//−X
78	23	1	1	12	0	12	−1p32-36, ++2p24-25, +17q11-25
79	84	0	0	23	0	23	−2p24-25, −3p14-26, −4p11-16, +7p21-22, +7q11-36, +8p11-23, −11q14-25, +17q11-25//−X
80	14	1	0	12	0	12	−1p31-36, ++2p24-25, +3q11-29, −15q11-13, +17q11-25, +19p11-13, −19q11-13
81	58	1	ND	ND	ND	ND	−1p32-36, +1q11-44, ++2p24-25, −11p12-14, −11q14-21, −15q11-13, +17q11-25//+2, −3, −9, −13, −14
82	66	0	1	20	1	20	+1q22-25, +7q22-36, −9p13-24, −11q14-25, +17q11-25//−Y
83	69	1	1	6	1	14	++2p24-25

[1]In months.–[2]1, MYCN-amplification; 0, no MYCN-amplification; ND, no data.–[3]0, no event at all; 1, relapse, progression or toxic death; ND, no data.–[4]0, alive at last follow-up; 1, death; ND, no data.–[5]+, gain; −, loss; ++, amplification.

genetic change. This analysis revealed a remarkably high incidence of 11q deletions in tumors without MNA (59%) whereas in Stage 4 NB with MNA, 11q deletion was observed in only 15% of cases. All except one of the 11q deletions were large, encompassing more than half of the distal end of 11q. The subgroup defined by the 11q deletion was also characterized by the infrequent 1p deletion by CGH. In addition to typical absence of MNA and 1p deletion, Stage 4 NB with 11q deletions were significantly associated with 3p deletion. The present data therefore strongly suggest that 11q deletions identify a distinct genetic subgroup of Stage 4 NB. In two previous, studies an association between 11q and 14q loss was reported, albeit less stronger than the association between 11q and 3p.[6,11] In our study on a larger series of tumors with 11q deletion the association between 11q and 14q loss was not statistically significant.

Standard cytogenetic studies of neuroblastoma did not reveal 11q deletion as a recurrent cytogenetic abnormality.[12] More recently, a compilation of reported neuroblastoma karyotypes however showed a rate of 11q deletion in approximately 15% of cases.[13] Initial studies analyzing loss of 11q by LOH were conflicting.[14–17] In some LOH studies 11q loss was found in up to 19 to 26% of cases, whereas others found only 5% of tumors with 11q loss (1 case in a series of 20 informative cases). Recently, in a large LOH study on a series of 310 primary neuroblastomas LOH was found for multiple 11q loci in as much as 43% of cases,[8] with a smallest region of overlap (SRO) in the 11q23.3 chromosomal region. As in our study, there was a strong inverse relationship of 11q LOH and MNA. The authors did not find a negative correlation with 1p deletion. The highest percentage of 11q allelic loss was observed in Stage 4 tumors (48%) but surprisingly, a high proportion of Stage 1, 2 and 3 tumors also showed 11q loss (30%, 45% and 45%, respectively). In previous CGH studies a much lower incidence of 11q deletion was observed but whole loss of chromosome 11 was a frequent finding in near triploid low stage NB.[3–6] Further studies by Guo *et al.*,[8] including microsatellite loci from the short arm of 11p confirmed (as CGH) difference between whole chromosome 11 losses in the low stage tumors and chromosome 11q losses in high stage tumors.

The frequent occurrence of 11q deletions in this subset of Stage 4 NB, strongly suggests that one or more tumour suppressor genes residing on 11q are implicated in the biology of these tumors. This was previously suggested by chromosome 11 transfer experiments that resulted in induction of differentiation of neuroblastoma cells.[19] Guo *et al.*[8] defined an SRO on 11q23.3. Interestingly, this region falls within a constitutional 11q23–qter deletion reported in a patient with NB.21 Deletions found in our study were large and

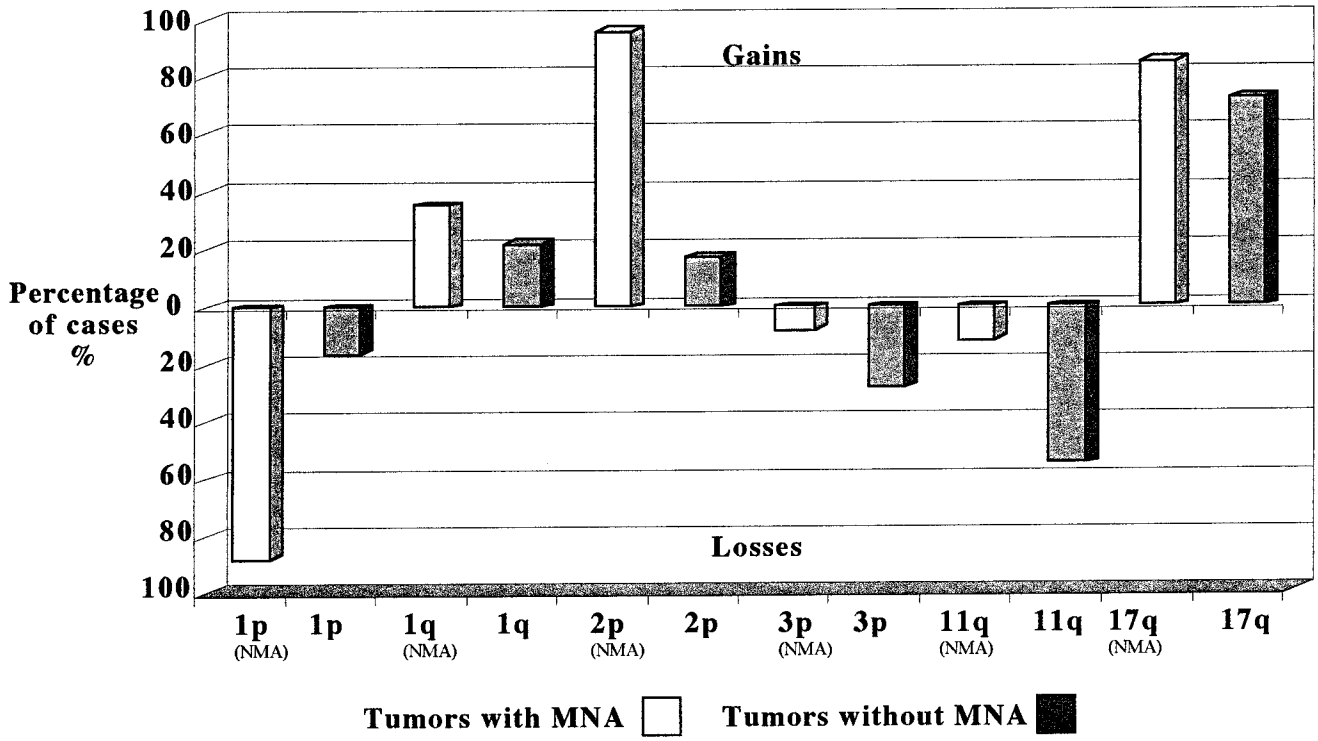

FIGURE 1 – Relative percentage of partial gains of chromosome 1q, 2p and 17q (above the horizontal axis) and partial losses of chromosome 1p, 3p and 11q (below the horizontal axis) . Bars in white indicate tumors with *MYCN* amplification (MNA); bars in gray indicate tumors without *MYCN* amplification (MNNA).

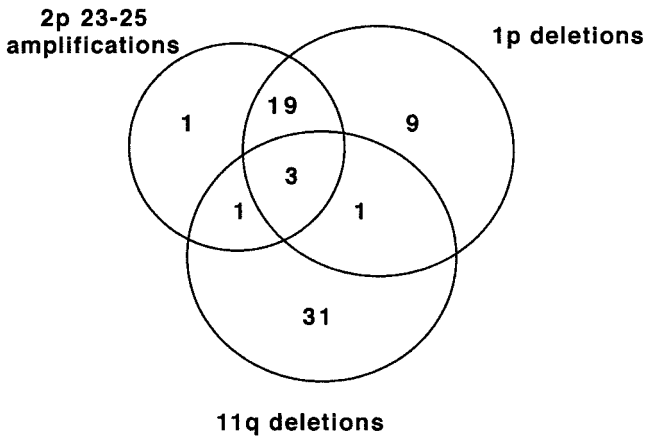

FIGURE 2 – Interrelationship between *MYCN*-amplification, 1p deletion and 11q deletion (as determined by CGH).

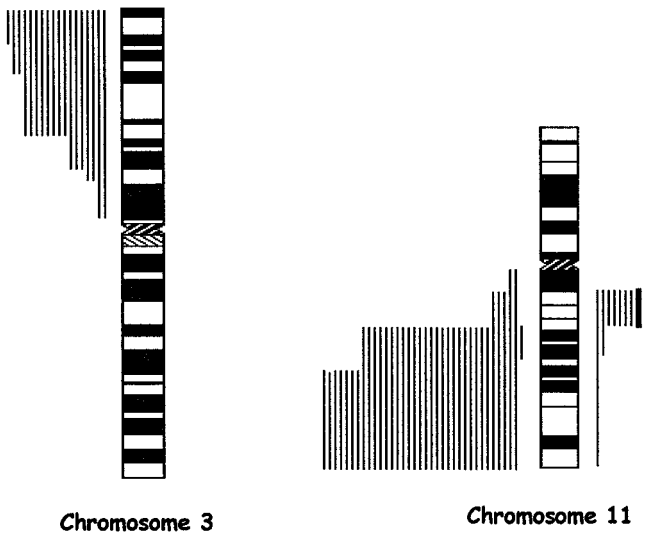

FIGURE 3 – Overview of CGH results for chromosome arms 3p and 11q. Lines on the left side of the ideogram represent losses, lines on the right gains; bold bars represent amplification.

terminal, except for one tumour that showed an interstitial 11q13–q21 deletion. This interstitial deletion overlaps with a previous cytogenetically detected 11q13–q21 deletion.[21] Confirmation of this putative second more proximal located SRO at 11q13–q21 awaits further investigations.

The present study shows a positive correlation between the presence of deletion of 3p in NB tumors with 11q deletion and without MNA. The occurrence of 3p loss was previously observed by representational difference and LOH analysis.[22] A further study confirmed this finding and showed the presence of 3p deletion in 15% of investigated NB. The consensus region was defined by markers D3S1286 and D3S1295 (3p25.3–p14.3), distal to the *FHIT* gene.[23] Our study provides further support for the non-random involvement of 3p loss in neuroblastoma and also delineates a critical region located in the distal part of 3p (3pter–p24).

The negative correlations between 11q loss and MNA and between 11q loss and 1p deletion are particularly striking. On the other hand, 11q loss is by necessity linked to gain of 17q due to the well established prevalence of unbalanced translocation der(11)t(11q;17q).[24] This rearrangement, that results in concurrent loss of distal 11q and gain of distal 17q, may account for up to 50% of 11q loss events. Because 17q gain is an important predictor of

adverse outcome,[7,25] this physical interaction between 11q and 17q is an important factor in considering the prognostic significance of 11q loss.

An interesting observation was the presence of 11q13 gain in 7 tumors and amplification in one. For the latter, previous molecular analysis showed the presence of *CCND1* amplification.[26] In the study of Breen *et al.*[11] 11q13 amplification was noted in 2 tumors. Also, SAGE analyses of neuroblastoma cell lines confirmed the occurrence of *CCND1* overexpression.[27] In 5 out of 7 cases 11q13 gain coincided with more distal 11q loss. The significance of this observation remains to be resolved by study of additional tumors.

We also evaluated the prognostic significance of 11q deletions among patients with Stage 4 neuroblastoma. More than 50% of patients over 1 year of age with Stage 4 neuroblastoma will relapse and die within 5 years after diagnosis and treatment. For some long term survivors, however, favorable genetic prognostic factor(s) remain to be identified. Compared with patients with 11q non-deleted NB (mainly represented by patients harboring tumors with 1p deleted or *MYCN* amplified NB), the prognosis of patients with 11q deleted tumors is statistically similar and poor in our study of Stage 4 tumors.

Guo *et al.*[8] found a significantly better survival for patients without vs. those with 11q deletion in tumors without *MYCN* amplification (91% vs. 75% 3-year overall survival) in a cohort of different stages. As CGH detected 11q deletion in only 7% of localized tumors (Stage 1, 2 and 3 tumors), however, the 75% 3-year survival reported by Guo *et al.*[8] seems high for tumors with 11q deletions. In the same way that the rate of 11q LOH seems high for low stage tumors, the 75% survival in the study of Guo *et al.*[8] may be explained by the presence of near triploid low stage tumors with whole chromosome 11 loss and typical favorable prognosis. Most recently, Guo *et al.*[18] have extended the analysis of 11q LOH with the inclusion of 11p markers to segregate whole chromosome loss from rearrangements resulting in unbalanced deletion of distal 11q. With this distinction, 11q unbalanced LOH is now highly correlated with age over 1 year at diagnosis and Stage 4 disease. The 11q deletion prognostic value will need further studies for metastatic patients treated with new treatment regimes such as retinoic acid[28] and for non-metastatic patients who relapsed from tumors without *MYCN* amplification.

In conclusion, CGH showed 11q deletions in more than 50% of Stage 4 neuroblastomas without *MYCN* amplification. This genetic subgroup is also characterized by a positive correlation with 3p deletions and an inverse correlation with 1p deletion. Although 11q deletion currently has no prognostic value in metastatic neuroblastoma, further studies remain necessary to evaluate its impact for patients treated with new therapeutic regimens. Molecular studies are required to identify a putative 11q suppressor gene involved in neuroblastoma development.

ACKNOWLEDGEMENTS

Our study was supported by grants from: the Association "Ligue contre le Cancer" and "Clinical Research Direction" University Hospital Center of Grenoble. France; GOA grant number 12053397, FWO grant 3G002800, the Flemish Institute for the Promotion of Scientific Technological Research in Industry (IWT) Fund for Scientific Research Flanders; R&D Committee of the Northern and Yorkshire Regional Health Authority, Wessex Cancer Trust and Parthenon Trust and the Children's Cancer Group; Alfred and Ursula Kuhlemann-Stiftung, Marburg. The study of the German centre (C.B.) was in part supported by the research program IMF (Innovative medizinische Forschung) by the University of Münster (grant BR 119830). Nadine Van Roy is a post-doctoral researcher of the Fund for Scientific Research Flanders.

REFERENCES

1. Cooper MJ, Hutchins GM, Cohen PS, Helman LJ, Mennie RJ, Israel MA. Human neuroblastoma tumour cell lines correspond to the arrested differentiation of chromaffin adrenal medullary neuroblasts. Cell Growth Differ 1990;1:149–59.
2. Brodeur GM, Castleberry RP. Neuroblastoma. In: Pizzo PA, Poplack DG, editors. Principles and practice of pediatric oncology, 2nd ed. Philadelphia: Lippincott 1993:739–61.
3. Brinkschmidt C, Christiansen H, Terpe HJ, Simon R, Boecker W, Lampert F, et al. Comparative genomic hybridization (CGH) analysis of neuroblastomas—an important methodological approach in pediatric tumour pathology. J Pathol 1997;181:394–400.
4. Łastowska M, Nacheva E, McGuckin A, Curtis A, Grace C, Pearson A, et al. Comparative genomic hybridization study of primary neuroblastoma tumors. United Kingdom Children's Cancer Study Group. Genes Chromosomes Cancer 1997;18:162–9.
5. Plantaz D, Mohapatra G, Matthay KK, Pellarin M, Seeger RC, Feuerstein BG. Gain of chromosome 17 is the most frequent abnormality detected in neuroblastoma by comparative genomic hybridization. Am J Pathol 1997;150:81–9.
6. Vandesompele J, Van Roy N, Van Gele M, Laureys G, Ambros P, Heimann P, et al. Genetic heterogeneity of neuroblastoma studied by comparative genomic hybridization. Genes Chromosomes Cancer 1998;23:141–52.
7. Bown N, Cotterill S, Łastowska M, O'Neill S, Pearson ADJ, Plantaz D, et al. Gain of chromosome arm 17q and adverse clinical outcome in neuroblastoma. N Engl J Med 1999;24:1954–61.
8. Guo C, White PS, Weiss MJ, Hogarty MD, Thompson PM, Stram DO, et al. Allelic deletion at 11q23 is common in MYCN single copy neuroblastomas. Oncogene 1999;18:4948–57.
9. Kallioniemi A, Kallioniemi OP, Sudar D, Rutowitz D, Gray JW, Waldman F, et al. Comparative genomic hybridization for molecular cytogenetic analysis of solid tumors. Science 1992;258:818–21.
10. du Manoir S, Speicher MR, Joos S, Schrock E, Popp S, Dohner H, et al. Detection of complete and partial chromosome gains and losses by comparative genomic in situ hybridization. Hum Genet 1993;90:590–610.
11. Breen CJ, O'Meara A, McDermott M, Mullarkey M, Stallings RL. Coordinate deletion of chromosome 3p and 11q in neuroblastoma detected by comparative genomic hybridization. Cancer Genet Cytogenet 2000;120:44–9.
12. Brodeur GM, Fong CT. Molecular biology and genetics of human neuroblastoma. Cancer Genet Cytogenet 1989;41:153–74.
13. Mertens F, Johansson B, Hoglund M, Mitelman F. Chromosomal imbalance maps of malignant solid tumors: a cytogenetic survey of 3185 neoplasms. Cancer Res 1997;57:2765–80.
14. Fong CT, White PS, Peterson K, Sapienza C, Cavenee WK, Kern SE, et al. Loss of heterozygosity for chromosomes 1 or 14 defines subsets of advanced neuroblastomas. Cancer Res 1992;52:1780–5.
15. Srivatsan ES, Yink KL, Seeger RC. Deletion of chromosome 11 and of 14q sequences in neuroblastoma. Genes Chromosomes Cancer 1993;7:32–7.
16. Takita J, Hayashi Y, Kohno T, Shiseki M, Yamaguchi N, Hanada R, et al. Allelotype of neuroblastoma. Oncogene 1995;11:1829–34.
17. Takeda O, Handa M, Uehara T, Maseki N, Sakashita A, Sakurai M, et al. An increased NM23H1 copy number may be a poor prognostic factor independent of LOH on 1p in neuroblastomas. Br J Cancer 1996;74:1620–6.
18. Guo C, Lee JY, White PS, Hogarty MD, Brodeur GM, Maris JM. Deletion of 11q23 is a frequent event in the evolution of MYCN single copy, high-risk neuroblastomas. Med Pediatr Oncol 2000;35:544–6.
19. Bader SA, Fashing C, Brodeur GM, Stanbridge EJ. Dissociation of suppression of tumorigenicity and differentiation in vitro effected by transfer of single human chromosomes into human neuroblastoma cells. Cell Growth Differ 1991;2:245–55.
20. Koiffmann CP, Gonzales CH, Vianna-Morgante AM, Kim CA, Odone-Fiho V, Wajntal A. Neuroblastoma in a boy with MCA/MR syndrome, deletion 11q, and duplication 12q. Am J Med Genet 1995;58:46–9.
21. Christiansen H, Lampert F. Tumour karyotype discriminates between good and bad prognostic outcome in neuroblastoma. Br J Cancer 1988;57:121–6.
22. Hallstensson K, Thulin S, Aburatani H, Hippo Y, Martinsson T. Representational difference analysis and loss of heterozygosity studies detect 3p deletions in neuroblastoma. Eur J Cancer 1997;12:1966–70.
23. Ejeskar K, Aburatani H, Abrahamson J, Kogner P, Martinsson T. Loss of heterozygosity of 3p markers in neuroblastoma tumors implicate a tumour-suppressor locus distal to the FHIT gene. Br J Cancer 1998;11:1787–91.

24. Meddeb M, Danglot G, Chudoba I, Venuat AM, Benard J, Avet-Loiseau H, et al. Additional copies of a 25 Mb chromosomal region originating from 17q23.1–17qter are present in 90% of high grade neuroblastomas. Genes Chromosomes Cancer 1996;17:156–65.
25. Caron H, Hogenbirk K, Van Sluis P, De Kraker J, Bras JH, Voûte PA, et al. Relative prognostic value of genetic factors in neuroblastoma. Med Pediatr Oncol 1998;31:298.
26. Van Gele M, Van Roy N, Jauch A, Laureys G, Schelfout V, De Potter CR, et al. Sensitive and reliable detection of genomic imbalances in human neuroblastomas using comparative genomic hybridization analysis. Eur J Cancer 1997;33:1979–82.
27. Boon K, Caron H, Voûte PA, Van Asperen R, Hermus M-C, Van Sluis P, et al. SAGE profiles of neuroblastoma: identification of MYCN downstream pathways. Med Ped Oncol 2000;35;735.
28. Matthay KK, Villablanca JG, Seeger RC, Stram DO, Harris RE, Ramsay NK, et al. Treatment of high-risk neuroblastoma with intensive chemotherapy, radiotherapy, autologous bone marrow transplantation, and 13-cis-retinoic acid. N Engl J Med 1999;341: 1165–73.

The New England Journal of Medicine

Volume 340:1954-1961 June 24, 1999 Number 25

Gain of Chromosome Arm 17q and Adverse Outcome in Patients with Neuroblastoma

Nick Bown, M.Sc., Simon Cotterill, B.A., Maria Łastowska, M.D., Ph.D., Seamus O'Neill, Ph.D., Andrew D.J. Pearson, M.D., Dominique Plantaz, M.D., Mounira Meddeb, M.D., Ph.D., Gisele Danglot, M.D., Christian Brinkschmidt, M.D., Holger Christiansen, M.D., Genevieve Laureys, M.D., Ph.D., Frank Speleman, Ph.D., James Nicholson, M.B., B.Chir., Alain Bernheim, M.D., David R. Betts, B.Sc., Jo Vandesompele, Ph.D., and Nadine Van Roy, Ph.D.

ABSTRACT

Background Gain of genetic material from chromosome arm 17q (gain of segment 17q21–qter) is the most frequent cytogenetic abnormality of neuroblastoma cells. This gain has been associated with advanced disease, patients who are ≥ 1 year old, deletion of chromosome arm 1p, and amplification of the N-*myc* oncogene, all of which predict an adverse outcome. We investigated these associations and evaluated the prognostic importance of the status of chromosome 17.

Methods We compiled molecular cytogenetic analyses of chromosome 17 in primary neuroblastomas in 313 patients at six European centers. Clinical and survival information were collected, along with data on 1p, N-*myc,* and ploidy.

Results Unbalanced gain of segment 17q21–qter was found in 53.7 percent of the tumors, whereas the chromosome was normal in 46.3 percent. The gain of 17q was characteristic of advanced tumors and of tumors in children ≥ 1 year of age and was strongly associated with the deletion of 1p and amplification of N-*myc.* No tumor showed amplification of N-*myc* in the absence of either deletion of 1p or gain of 17q. Gain of 17q was a significant predictive factor for adverse outcome in univariate analysis. Among the patients with this abnormality, overall survival at five years was 30.6 percent (95 percent confidence interval, 21 to 40 percent), as compared with 86.0 percent (95 percent confidence interval, 78 to 91 percent) among those with normal 17q status. In multivariate analysis, gain of 17q was the most powerful prognostic factor, followed by the presence of stage 4 disease and deletion of 1p (hazard ratios, 3.4, 2.3, and 1.9, respectively).

Conclusions Gain of chromosome segment 17q21–qter is an important prognostic factor in children with neuroblastoma.

GAIN OF CHROMOSOME ARM 17q AND ADVERSE OUTCOME IN PATIENTS WITH NEUROBLASTOMA

NICK BOWN, M.SC., SIMON COTTERILL, B.A., MARIA ŁASTOWSKA, M.D., PH.D., SEAMUS O'NEILL, PH.D., ANDREW D.J. PEARSON, M.D., DOMINIQUE PLANTAZ, M.D., MOUNIRA MEDDEB, M.D., PH.D., GISELE DANGLOT, M.D., CHRISTIAN BRINKSCHMIDT, M.D., HOLGER CHRISTIANSEN, M.D., GENEVIEVE LAUREYS, M.D., PH.D., AND FRANK SPELEMAN, PH.D.

ABSTRACT

Background Gain of genetic material from chromosome arm 17q (gain of segment 17q21–qter) is the most frequent cytogenetic abnormality of neuroblastoma cells. This gain has been associated with advanced disease, patients who are ⩾1 year old, deletion of chromosome arm 1p, and amplification of the N-*myc* oncogene, all of which predict an adverse outcome. We investigated these associations and evaluated the prognostic importance of the status of chromosome 17.

Methods We compiled molecular cytogenetic analyses of chromosome 17 in primary neuroblastomas in 313 patients at six European centers. Clinical and survival information were collected, along with data on 1p, N-*myc,* and ploidy.

Results Unbalanced gain of segment 17q21–qter was found in 53.7 percent of the tumors, whereas the chromosome was normal in 46.3 percent. The gain of 17q was characteristic of advanced tumors and of tumors in children ⩾1 year of age and was strongly associated with the deletion of 1p and amplification of N-*myc.* No tumor showed amplification of N-*myc* in the absence of either deletion of 1p or gain of 17q. Gain of 17q was a significant predictive factor for adverse outcome in univariate analysis. Among the patients with this abnormality, overall survival at five years was 30.6 percent (95 percent confidence interval, 21 to 40 percent), as compared with 86.0 percent (95 percent confidence interval, 78 to 91 percent) among those with normal 17q status. In multivariate analysis, gain of 17q was the most powerful prognostic factor, followed by the presence of stage 4 disease and deletion of 1p (hazard ratios, 3.4, 2.3, and 1.9, respectively).

Conclusions Gain of chromosome segment 17q21–qter is an important prognostic factor in children with neuroblastoma. (N Engl J Med 1999;340:1954-61.)

GENETIC studies have an important role in formulating the prognosis in children with neuroblastoma, because certain acquired genetic abnormalities in the tumor cells correlate closely with the clinical outcome.[1] Established indicators of the aggressiveness of the tumor and poor outcome include the deletion of the short arm of chromosome 1 (1p),[2] the amplification of the N-*myc* gene,[3] and near diploidy or near tetraploidy.[2] Conversely, the presence of 1p, single copies of N-*myc,* near triploidy, and expression of the *TRK* gene[4] are significantly associated with a favorable prognosis.

Rearrangements of chromosome 17 in neuroblastoma cells, particularly those resulting in a gain of material from the long arm of the chromosome (17q), were first described in the early 1980s,[5,6] but the extent of such abnormalities in neuroblastoma cells was not apparent until fluorescence in situ hybridization and comparative genomic hybridization were used to study neuroblastoma cells.[7-15] These methods revealed that the gain of material from chromosome 17 is the most frequent genetic abnormality of neuroblastoma cells, with an incidence ranging from 63 to 83 percent. This gain may consist of an entire chromosome 17 (e.g., tetrasomy 17 in a triploid tumor) or of only the distal segment of the long arm, 17q21–qter. Such a partial gain is strongly associated with risk factors: age of more than one year, presence of advanced disease, deletion of 1p, amplification of the N-*myc* gene, and unfavorable ploidy.

The principal mechanism underlying partial gain of 17q is an unbalanced translocation, with a variety of partner chromosomes.[7-9,15] The segment on the partner chromosome distal to the breakpoint is lost, and a segment of 17q translocates to that site. The translocated segment is in effect an extra copy, because the cell also contains two or more normal chromosomes 17. Hence, these translocations result in unbalanced gain of the distal segment of 17q. The most common site of the translocation is 1p, where the gain of the distal portion of 17q is linked with the loss of 1p (Fig. 1A and 1B).

In 1995, Caron[16] reported that 20 of 53 neuro-

From the Department of Human Genetics (N.B., M.Ł., S.O.) and the Institute of Child Health (S.C., A.D.J.P.), University of Newcastle upon Tyne, Newcastle upon Tyne, United Kingdom; the Department of Pediatrics, University Hospital Center, Grenoble, France (D.P.); Institut Gustave-Roussy, Villejuif, France (M.M., G.D.); Gerhard-Domagk Institute of Pathology, University of Munster, Munster, Germany (C.B.); the Department of Pediatric Hematology and Oncology, Kinderklinik, University of Marburg, Marburg, Germany (H.C.); and the Department of Pediatric Oncology (G.L.) and the Center for Medical Genetics (F.S.), University Hospital, Ghent, Belgium. Address reprint requests to Mr. Bown at the Department of Human Genetics, University of Newcastle upon Tyne, 19-20 Claremont Pl., Newcastle upon Tyne NE2 4AA, United Kingdom, or at nicholas.bown@ncl.ac.uk.

Other authors were James Nicholson, M.B., B.Chir., University of Southampton, Southampton, United Kingdom; Alain Bernheim, M.D., Institut Gustave-Roussy, Villejuif, France; David R. Betts, B.Sc., University Children's Hospital, Zurich, Switzerland; and Jo Vandesompele, Ph.D., and Nadine Van Roy, Ph.D., University Hospital, Ghent, Belgium.

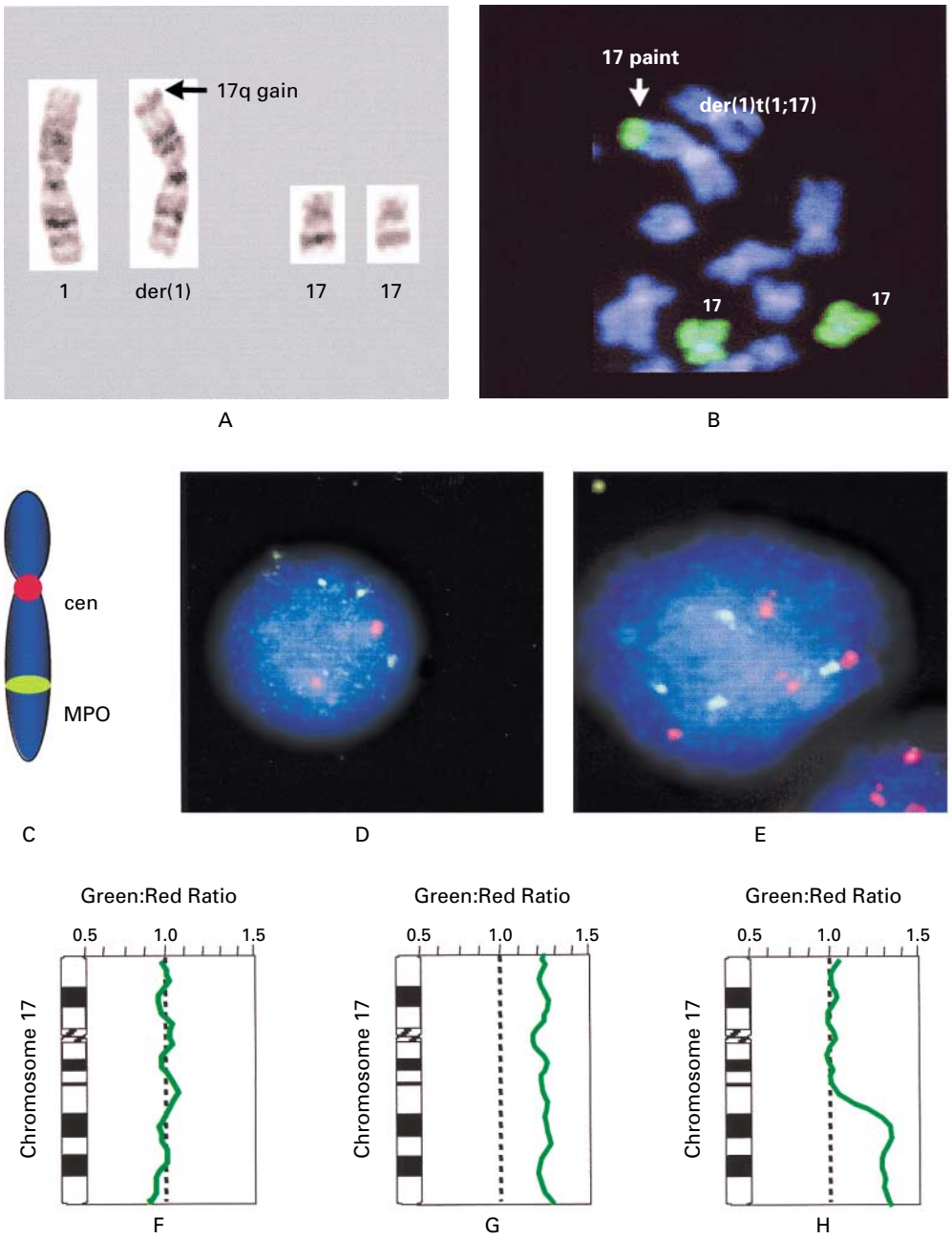

Figure 1. Techniques Used to Determine Chromosome 17 Status.

Panel A shows the results obtained with cytogenetic analysis. G-banding identifies a gain of 17q12–qter as an unbalanced translocation with 1p. Panel B shows the results obtained with fluorescence in situ hybridization of cells in metaphase. A paint probe for chromosome 17 identifies a gain of genetic material from chromosome 17 on the short arm of chromosome 1 in addition to two normal copies of chromosome 17. Panel C shows the results obtained with fluorescence in situ hybridization of cells in interphase in which rhodamine-labeled centromeric probe and fluorescein-labeled myeloperoxidase (MPO) probe have been used. Panel D shows the nucleus of a tumor with 17q gain by fluorescence in situ hybridization of cells in interphase (2 centromeric signals [cen], 3 MPO signals). Panel E shows a whole chromosome gain in a triploid tumor, also by fluorescence in situ hybridization of cells in interphase (4 centromeric signals, 4 MPO signals). Panel F shows the results of comparative genomic hybridization for chromosome 17 with a green:red ratio of 1.0, indicating no gain with respect to ploidy. In Panel G the color ratio shifted to 1.25, indicating gain of a whole chromosome. Panel H shows results of comparative genomic hybridization indicating gain of distal q arm (q21–qter).

blastomas (38 percent) had gain of 17q and that patients with such tumors had a significantly worse event-free survival at two years than those without this feature. However, when the series was expanded sufficiently to allow multivariate analysis,[17] the predictive power of the 17q gain was marginal and was not apparent when 1p or N-*myc* status was added to the model. Using cytogenetic techniques and fluorescence in situ hybridization, Łastowska et al.[18] identified 17q gain in 28 of 45 neuroblastomas (62 percent) and found that overall survival for patients with 17q gain was 13.5 percent at three years, as compared with 100 percent for those without this abnormality. Multivariate analysis revealed a powerful independent effect of 17q gain after other clinical and genetic variables were taken into account.

In this study, we sought to confirm the association of unbalanced 17q gain with other indicators of high risk in patients with neuroblastoma and to test the hypothesis that this abnormality is an independent predictor of tumor aggressiveness and poor clinical outcome. To this end, we assembled a large series of analyses in which the status of chromosome 17 was known and related this information to well-established clinical and genetic risk factors and to rates of relapse and mortality.

METHODS

Tumors

Inclusion in the study was based solely on the ability to define the status of chromosome 17. The data on 313 patients with neuroblastoma for which the status of chromosome 17 in tumor cells was established were collected from six European centers. The tumor stage was classified according to the International Neuroblastoma Staging System.[19] Similar treatment regimens were used in the various centers for patients of the same age and with the same stage of disease.

Genetic Analysis

Four centers provided results of comparative genomic hybridization. A complete description of this procedure is reported elsewhere.[10-14,20,21] In brief, tumor DNA and normal DNA from reference tissue were extracted and labeled by nick translation for differential fluorescence detection (fluorescein vs. rhodamine). Equal amounts of tumor and reference DNA were mixed and hybridized to lymphocytes in metaphase. Images were captured by a photomultiplying camera, and image-analysis software was used to calculate the ratio of red to green fluorescence along chromosome lengths. Control experiments (competitive hybridization of differentially labeled samples of normal DNA) were carried out to establish the fluorescence-ratio thresholds for gain or loss of chromosome regions.

Three centers contributed results from cytogenetic analysis supplemented by fluorescence in situ hybridization.[9,15] Chromosomes were prepared and banded according to standard protocols. In some cases, the status of chromosome 17 was confirmed by fluorescence in situ hybridization of cells in metaphase by using chromosome 17 paints in conjunction with either Oncor myeloperoxidase probe, which maps to 17q21.3–q23, or yeast artificial-chromosome probes mapping to 17q.

Oncor probes for either TP53 (locus 17p13) or chromosome 17 centromere in combination with differentially labeled myeloperoxidase probe were used for interphase fluorescence in situ hybridization at one center. Determining relative numbers of red and green signals in tumor nuclei allows a balanced status of 17q to be distinguished from unbalanced gain (Fig. 1C, 1D, and 1E).

Examples of the results obtained with these techniques are shown in Figure 1. Genetic factors other than the status of 17q were assessed at individual centers by combinations of techniques. The status of 1p was determined by comparative genomic hybridization or by fluorescence in situ hybridization with the use of combinations of a pericentromeric probe for chromosome 1 with probes derived from the 1p36 region,[22] analysis of DNA microsatellite markers by the polymerase chain reaction,[23] or cytogenetic analysis. The status of N-*myc* was determined by comparative genomic hybridization, fluorescence in situ hybridization, or Southern blotting, and ploidy was determined by flow cytometry or cytogenetic analysis.

Definition of the Status of Chromosome 17

The status of chromosome 17 was defined as either gain of 17q or normal. Gain of 17q denoted the gain of segment 17q21–qter. The defining characteristics of 17q gain were a breakpoint in 17q11–q21 and an extra copy of the 17q segment distal to this breakpoint in the chromosomal complement of the cell, resulting in an increase in the number of copies of distal 17q as compared with 17p. These gains almost always result from unbalanced translocations. Normal status denoted no unbalanced gain of 17q relative to 17pter–q12. It included tumors showing no gain or loss of any part of chromosome 17 (e.g., two intact copies of 17 in a diploid nucleus or three in a triploid nucleus) and tumors showing gain of an entire chromosome 17 in relation to the ploidy level of the cell (e.g., four copies in a triploid nucleus). In these cases there is no chromosome breakpoint, and there is a normal ratio of 17p to 17q.

Statistical Analysis

Logistic-regression analysis was used to test the consistency of the findings from the various centers. Descriptive statistical analysis used χ^2 tests to identify the biologic characteristics of the combined data set. In particular, the distribution of 17q gain was determined in relation to established clinical and genetic factors.

The Kaplan–Meier method[24] and the log-rank test were used to estimate survival and progression-free survival. The predictive significance of age, tumor stage, ploidy, and 1p, N-*myc,* and 17q status were tested in univariate analyses. After performing a stratified subgroup analysis, we applied a stepwise Cox proportional-hazards model (successively rejecting nonsignificant variables) to test the hypothesis that 17q status has an independent influence on outcome and to quantify the influence of 17q status with respect to other clinical and genetic factors. In a separate analysis, a multivariate model incorporating tumor stage, age, and N-*myc* status was extended to include 17q status in order to test the additional predictive power that the variable of 17q status provides.

RESULTS

Most of the data were compiled from the results of comparative genomic hybridization (68.7 percent); in the remaining 31.3 percent of cases, the status of chromosome 17 was determined by standard cytogenetic analysis supplemented with metaphase fluorescence in situ hybridization or by two-color interphase fluorescence in situ hybridization. Data on 154 of the 313 tumors (49.2 percent) have been previously reported.[9-12,14,15]

The median age of the patients at the time of diagnosis was 2.2 years. The median duration of follow-up for survivors was 2.5 years (interquartile range, 1.0 to 4.4). Of the 313 tumors, 119 were from infants less than one year of age and 194 were from children

TABLE 1. CLINICAL AND GENETIC CHARACTERISTICS OF 313 PATIENTS WITH NEUROBLASTOMA ACCORDING TO 17q STATUS.*

CHARACTERISTIC	NORMAL 17q (N=145)	GAIN OF 17q (N=168)	P VALUE†
	no. of patients (%)		
Tumor stage‡			
1, 2, or 4S	100 (69)	24 (14)	
3	24 (17)	25 (15)	
4	21 (14)	119 (71)	<0.001
Age			
<1 yr	88 (61)	31 (18)	
≥1 yr	57 (39)	137 (82)	<0.001
Chromosome 1p			
Normal	97 (79)	44 (31)	
Deleted	26 (21)	98 (69)	<0.001
Not evaluated	22	26	
N-*myc* gene			
Single copy	126 (91)	84 (52)	
Amplified	13 (9)	78 (48)	<0.001
Not evaluated	6	6	
Ploidy‡			
Diploid	21 (42)	47 (62)	<0.001
Tetraploid	3 (6)	19 (25)	<0.001
Triploid	26 (52)	10 (13)	
Not evaluated	95	92	

*Percentages include all patients who could be evaluated for a particular characteristic.

†P values were calculated with the χ^2 test.

‡The test for trend with 2 df was used for tumor stage and ploidy.

one or more years of age. According to the criteria of the International Neuroblastoma Staging System, 44 of the tumors were classified as stage 1, 35 as stage 2, 49 as stage 3, 140 as stage 4, and 45 as stage 4S.

Supplementary analyses established the status of 1p in 265 of the tumors (84.7 percent); of these, 124 (46.8 percent) showed 1p deletion. Assessment of the number of N-*myc* copies was performed for 301 (96.2 percent), and gene amplification was detected in 91 of these tumors (30.2 percent). Ploidy could be classified in 126 tumors (40.3 percent); of these, 68 (54.0 percent) were within the near-diploid range, 36 (28.6 percent) were near-triploid, and 22 (17.5 percent) were near-tetraploid.

Of the 313 tumors, 145 (46.3 percent) had a normal 17q status and 168 (53.7 percent) showed 17q gain. Twenty-six percent of the neuroblastomas from the patients less than one year old showed 17q gain, as compared with 71 percent of the tumors from the older children. The proportions with 17q gain according to tumor stage were as follows: 20 percent in stage 1, 17 percent in stage 2, 51 percent in stage 3, 85 percent in stage 4, and 20 percent in stage 4S.

To assess the consistency of the data among centers, the results of genetic analyses (the status of 1p, N-*myc* and 17q) were studied by logistic-regression analysis. No significant differences between laboratories were detected ($P>0.1$ for all analyses).

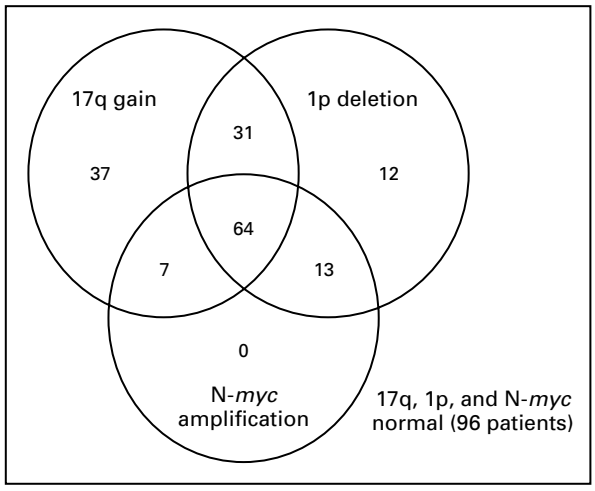

Figure 2. Interrelation of 17q Gain, 1p Deletion, and N-*myc* Amplification in 260 Patients with Neuroblastoma.

Correlations with Other Clinical and Genetic Prognostic Factors

Table 1 shows the relation between clinical and genetic factors and the status of 17q. Gain of 17q was strongly associated with stage 4 disease ($\chi^2=114$, $P<0.001$ for the comparison with all other stages combined). It was also significantly associated with an age of one year or more at presentation ($\chi^2=59$, $P<0.001$). Gain of 17q was strongly associated with 1p deletion ($\chi^2=61$, $P<0.001$), N-*myc* amplification ($\chi^2=53$, $P<0.001$), and diploidy or tetraploidy ($\chi^2=24$, $P<0.001$), but not triploidy. Figure 2 shows the interrelation of 17q gain, N-*myc* amplification, and 1p deletion for the 260 tumors in which the presence or absence of all three abnormalities was known. The status of 17q, 1p, and N-*myc* was normal in 96 tumors, but these tumors had other acquired genetic changes.

Univariate Analysis of Survival

At five years, the overall survival for the 313 children was 55.9 percent (95 percent confidence interval, 48 to 63 percent), and progression-free survival was 46.4 percent (95 percent confidence interval, 39 to 54 percent). With a median follow-up of 24 months, the projected overall 5-year survival of the 168 patients with 17q gain was 30.6 percent (95 percent confidence interval, 21 to 40 percent), as compared with 86.0 percent (95 percent confidence interval, 78 to 91 percent) for the 145 patients whose tumors had normal 17q (Fig. 3A). This difference was significant ($P<0.001$).

In a univariate analysis of survival, age, tumor stage, 1p status, N-*myc* status, and ploidy were all signifi-

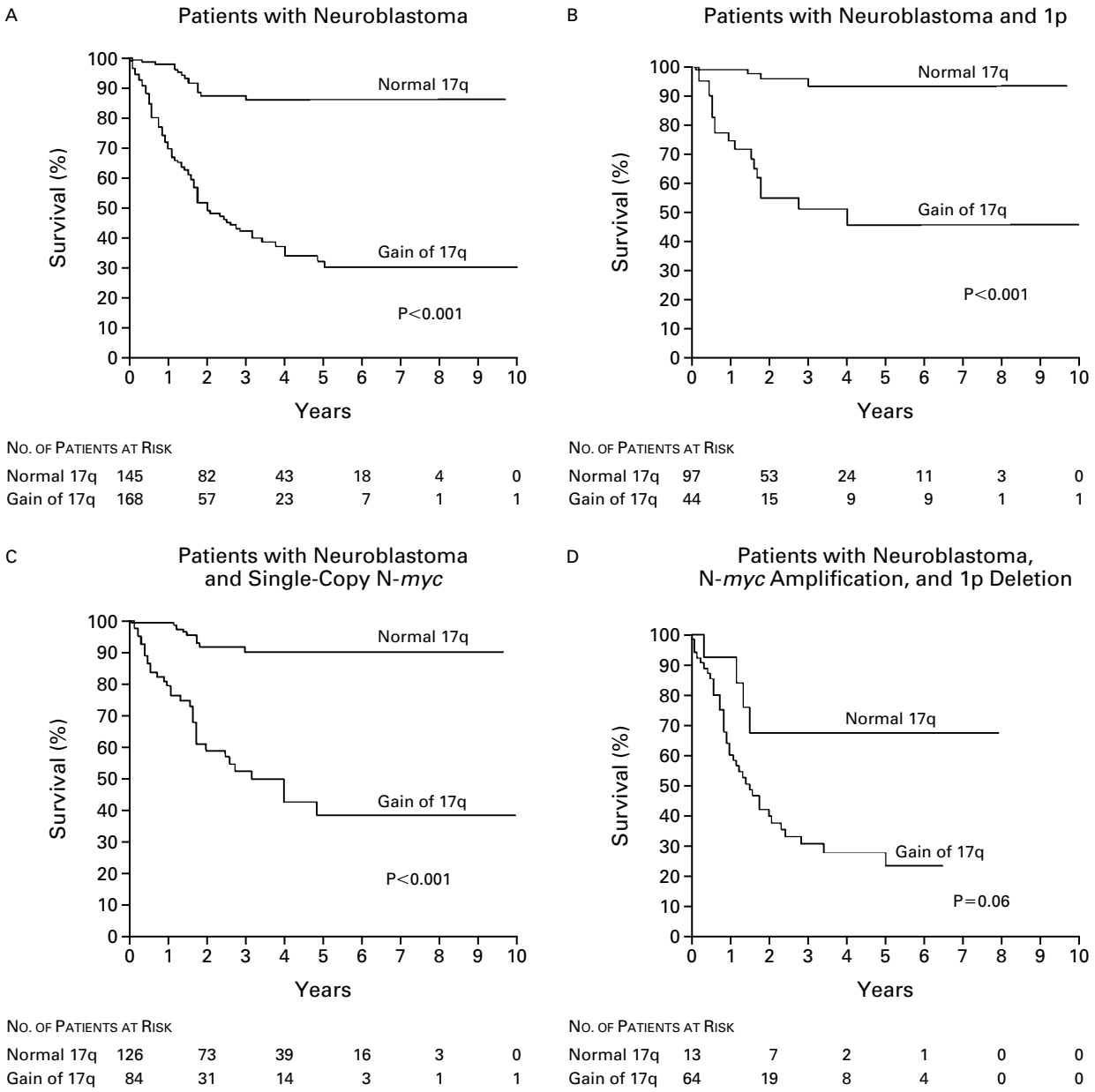

Figure 3. Survival Rates According to the Status of Chromosome 17q.

cantly associated with outcome ($P<0.01$ according to the likelihood-ratio test) (Table 2). The discriminative power of the status of 17q was significant in subgroups in which 1p was not deleted (Fig. 3B) or N-*myc* was not amplified (Fig. 3C) ($P<0.001$ for both). Gain of 17q in tumor cells was associated with significantly poorer outcomes in patients of any age and with tumors of stages 1, 2, 3, or 4S (Table 3). In the subgroup of tumors showing simultaneous 1p deletion and N-*myc* amplification, there was a nonsignificant trend toward additional adverse effects with 17q gain (Fig. 3D).

Multivariate Analysis of Survival

A stepwise Cox proportional-hazard procedure was applied, incorporating age, tumor stage, and status of 1p, 17q, and N-*myc*, to the 260 cases in which all three genetic factors were known. Ploidy was not in-

TABLE 2. SURVIVAL RATES OF 313 PATIENTS WITH NEUROBLASTOMA ACCORDING TO CLINICAL AND GENETIC FACTORS IN UNIVARIATE ANALYSIS.*

VARIABLE AND CATEGORY	NO. OF PATIENTS	5-YEAR SURVIVAL	P VALUE†
		% (95% CI)‡	
Age			
<1 yr	119	82 (72–89)	
≥1 yr	194	42 (33–51)	<0.001
Tumor stage§			
1, 2, or 4S	124	91 (84–95)	
3	49	62 (44–76)	
4	140	25 (16–36)	<0.001
Chromosome 17q			
Normal	145	86 (78–91)	
Unbalanced gain	168	31 (21–40)	<0.001
Chromosome 1p			
Normal	141	77 (67–85)	
Deleted	124	31 (21–42)	<0.001
N-*myc* gene			
Single copy	210	69 (60–77)	
Amplified	91	28 (16–41)	<0.001
Ploidy§			
Diploid	68	35 (21–50)	0.008
Tetraploid	22	44 (13–72)	
Triploid	36	88 (71–95)	

*Survival estimates and comparisons exclude patients who were not evaluated for the particular category.

†P values were calculated with the log-rank test.

‡CI denotes confidence interval.

§Comparisons of tumor stage and ploidy were calculated by the log-rank test for trend.

TABLE 3. SURVIVAL RATES OF 313 PATIENTS WITH NEUROBLASTOMA STRATIFIED ACCORDING TO 17q STATUS AND CLINICAL AND GENETIC FACTORS.*

VARIABLE AND CATEGORY	NO. OF PATIENTS	5-YEAR SURVIVAL		P VALUE†
		NORMAL 17q	17q GAIN	
		% (95% CI)‡		
Age				
<1 yr	119	94 (84–98)	49 (26–69)	<0.001
≥1 yr	194	77 (61–87)	27 (17–38)	<0.001
Tumor stage				
1, 2, or 4S	124	95 (87–98)	75 (50–89)	0.01
3	49	81 (50–94)	45 (22–66)	0.01
4	140	52 (26–74)	22 (13–33)	0.09
Chromosome 1p				
Normal	141	93 (82–98)	45 (26–62)	<0.001
Deleted	124	63 (40–79)	22 (12–35)	0.01
N-*myc* gene				
Normal	210	90 (81–95)	38 (21–54)	<0.001
Amplified	91	67 (34–86)	22 (12–36)	0.05
Ploidy				
Diploid	68	83 (57–94)	19 (7–34)	<0.001
Tetraploid	22	100	35 (7–66)	0.4
Triploid	36	100	49 (13–78)	0.001

*Survival estimates and comparisons exclude patients who were not evaluated for the particular category.

†P values were calculated with the log-rank test.

‡CI denotes confidence interval.

cluded in the multivariate analysis because of the relative paucity of data (ploidy was established for only 40 percent of the tumors). Age and the status of N-*myc* were excluded from the final model (score test, $P=0.4$ and $P=0.2$, respectively). Remaining predictors of adverse outcomes were 1p deletion (hazard ratio, 1.9; 95 percent confidence interval, 1.1 to 3.2; $P=0.02$), stage 4 disease (hazard ratio 2.3; 95 percent confidence interval, 1.3 to 4.0; $P=0.004$), and 17q gain (hazard ratio, 3.4; 95 percent confidence interval, 1.7 to 6.6; $P<0.001$). When a multivariate model incorporating age, tumor stage, and N-*myc* status was extended to include the status of 17q, a significant increase in predictive power was apparent (likelihood-ratio statistic, +15.0; $P<0.001$).

DISCUSSION

The selection of the 313 neuroblastomas that were included in this series was based on the ability to determine the status of chromosome 17. With regard to clinical characteristics, this series of patients is broadly typical of other series of patients with this tumor.[25] We found that 54 percent of the tumors showed gain of 17q12–qter (i.e., a gain of chromosomal material from the distal end of the long arm of chromosome 17), whereas 46 percent had either no gain of chromosome 17 or an additional copy of the whole chromosome.

Our results confirm that 17q gain in neuroblastoma is associated with advanced-stage disease and with tumors in older children rather than infants. Gain of 17q was very strongly linked to both 1p deletion and N-*myc* amplification; indeed, N-*myc* amplification was not found in any tumor without 1p deletion, 17q gain, or both.

In the univariate analysis of survival, the status of 17q was a significant predictor of clinical outcome, as were other clinical and genetic factors. In subgroup analyses, 17q gain was a significant predictive factor within tumor stage, in both infants and children one year old or more, and in cases in which N-*myc* was not amplified or 1p was not deleted. In the stepwise multivariate analysis, the status of 17q was the most significant predictive factor for clinical outcome, followed by stage 4 disease and the status of 1p. The status of N-*myc* and age were not statistically significant in this analysis.

Although neuroblastoma cells contain a variety of chromosomal aberrations, abnormalities of chromosome 17 are the most common. Moreover, gain of 17q21–qter is strongly associated with tumor progression. We found significant correlations between

17q gain and established clinical and genetic risk factors. As noted previously,[6-9,15] a direct relation between 1p deletion and 17q gain is the well-recognized unbalanced translocation t(1p;17q); it seems likely that this rearrangement accounts for a high proportion of 1p deletions in patients with neuroblastoma. Further cytogenetic data will be necessary to clarify the contribution of translocations of 17q to other sites of reported loss of heterozygosity in neuroblastoma cells.

In this study, N-*myc* amplification was not found in any tumor without concurrent 1p deletion, 17q gain, or both. Caron also showed N-*myc* amplification to be a subcategory of 1p loss and 17q gain, albeit in a much smaller number of tumors.[16] This finding suggests that N-*myc* amplification is a late event in the sequence of genetic lesions contributing to neuroblastoma.

The relation between 17q gain and N-*myc* amplification is obscure. Juxtaposition of amplified N-*myc* and 17q material has repeatedly been observed in neuroblastoma cell lines,[7,8] but this finding is very rare in primary tumors, in which N-*myc* amplification usually takes the form of double minute chromosomes; involvement of 17q in these structures has not been demonstrated. The functional interrelations of 17q and N-*myc* (and 1p) remain to be clarified.

A number of potentially important genes, such as *nm23-H1* and the survivin gene (which are involved in inhibiting apoptosis) and the gene for nerve growth factor receptor (which is underexpressed in neuroblastoma cells),[26] are located in the commonly gained segment of 17q. Investigations of such genes may reveal the mechanism of the effect of 17q gain on the behavior of neuroblastoma cells. Preliminary mapping has identified at least seven breakpoints within the proximal half of 17q in neuroblastomas and neuroblastoma cell lines[9,26]; this finding argues against a specific gene event (e.g., gene fusion), but coupled with the gain of 17q material, may implicate a gene dose effect. Loss of heterozygosity at the translocation partner sites may also be important.

The implications of our findings for clinical management follow from the increasing tendency to tailor therapy on an individual basis according to risk factors detected at the time of diagnosis. The objective is to direct the most intensive treatments to children with the most aggressive tumors, while sparing other children from the adverse effects of unnecessarily intensive therapy. For neuroblastoma, N-*myc* gene amplification has an important role in determining risk and is used internationally to stratify therapy for infants and for children with localized tumors. Specifically, infants with stage 4S disease without N-*myc* amplification who are clinically well are simply observed, whereas those with N-*myc* amplification with identical clinical features receive intensive chemotherapy followed by surgery, radiotherapy, and consolidation with myeloablative therapy.[27,28] However, the presence of N-*myc* amplification does not ensure completely accurate prognostic grouping, since 20 percent of infants with metastatic disease and N-*myc* amplification in the tumor are long-term survivors and 20 percent of patients without N-*myc* amplification have recurrence of tumors (Gerrard M: personal communication).

The ongoing Localized Neuroblastoma European Study is investigating the hypothesis that 1p allelic loss is predictive of tumor recurrence in patients with localized resectable (stage 2) neuroblastomas without N-*myc* amplification. Preliminary results suggest that not all recurring tumors have 1p deletion. Therefore, additional molecular genetic markers are needed to identify which tumors with normal 1p and no amplification of N-*myc* are likely to recur.

In our series, gain of 17q emerged as a more important indicator of adverse outcome than any other clinical or genetic factor, including 1p deletion and N-*myc* amplification. The presence of this abnormality identified a larger proportion of aggressive tumors and was more closely linked to outcome than other markers. Furthermore, the status of 17q was informative in all tumor stages and was predictive of the outcome in infants and older children with neuroblastoma and in patients with tumors in which N-*myc* and 1p were both normal. We propose that the detection of 17q gain in individual tumors at the time of diagnosis should be accorded a priority equal to that of the determination of the status of 1p and N-*myc*. In addition, we suggest that investigation of the status of chromosome 17 should be incorporated into future clinical trials in patients with neuroblastoma.

Supported in part by the Neuroblastoma Society; the Wessex Cancer Trust; the Parthenon Trust; Vereniging voor Kankerbestrijding; the Flemish Institute for the Promotion of Scientific Technological Research in Industry; Innovative Medizinische Forschung, University of Munster; Forschungshilfe Station Peiper; Alfred and Ursula Kulemann Stiftung; and Zürcher Vereinigung zur Unterstützung Krebskranker Kinder. Dr. Van Roy is a postdoctoral researcher of the Fund for Scientific Research, Flanders, Belgium.

We are indebted to the U.K. Children's Cancer Study Group and the U.K. Cancer Cytogenetics Group for providing data; to B. Feuerstein of the University of California for help with comparative genomic hybridization conducted at the University Hospital Center in Grenoble, France; to V. Combaret, O. Delattre, and J. Michon from the University Hospital Center in Grenoble, France, for providing tumor samples and clinical data; and to J. Wolstenholme for his support of this research.

REFERENCES

1. Brodeur GM, Maris JM, Yamashiro DJ, Hogarty MD, White PS. Biology and genetics of human neuroblastomas. J Pediatr Hematol Oncol 1997;19:93-101.

2. Ambros IM, Zellner A, Roald B, et al. Role of ploidy, chromosome 1p, and Schwann cells in the maturation of neuroblastoma. N Engl J Med 1996;334:1505-11.

3. Seeger RC, Brodeur GM, Sather H, et al. Association of multiple copies of the N-*myc* oncogene with rapid progression of neuroblastomas. N Engl J Med 1985;313:1111-6.

4. Nakagawara A, Arima-Nakagawara M, Scavarda NJ, Azar CG, Cantor AB, Brodeur GM. Association between high levels of expression of the

TRK gene and favorable outcome in human neuroblastoma. N Engl J Med 1993;328:847-54.
5. Biedler JL, Ross RA, Shanske S, Spengler BA. Human neuroblastoma cytogenetics: search for significance of homogeneously staining regions and double minute chromosomes. In: Evan AE, ed. Advances in neuroblastoma research. New York: Raven Press, 1980:81-96.
6. Gilbert F, Feder M, Balaban G, et al. Human neuroblastomas and abnormalities of chromosomes 1 and 17. Cancer Res 1984;44:5444-9.
7. Savelyeva L, Corvi R, Schwab M. Translocation involving 1p and 17q is a recurrent genetic alteration of human neuroblastoma cells. Am J Hum Genet 1994;55:334-40.
8. Van Roy N, Laureys G, Cheng NC, et al. 1;17 Translocations and other chromosome 17 rearrangements in human primary neuroblastoma tumors and cell lines. Genes Chromosomes Cancer 1994;10:103-14.
9. Meddeb M, Danglot G, Chudoba I, et al. Additional copies of a 25 Mb chromosomal region originating from 17q23.1-17qter are present in 90% of high-grade neuroblastomas. Genes Chromosomes Cancer 1996;17:156-65.
10. Brinkschmidt C, Christiansen H, Terpe HJ, et al. Comparative genomic hybridization (CGH) analysis of neuroblastomas — an important methodological approach in paediatric tumour pathology. J Pathol 1997; 181:394-400.
11. Plantaz D, Mohapatra G, Matthay KK, Pellarin M, Seeger RC, Feuerstein BG. Gain of chromosome 17 is the most frequent abnormality detected in neuroblastoma by comparative genomic hybridization. Am J Pathol 1997;150:81-9.
12. Łastowska M, Nacheva E, McGuckin A, et al. Comparative genomic hybridization study of primary neuroblastoma tumors. Genes Chromosomes Cancer 1997;18:162-9.
13. Van Gele M, Van Roy N, Jauch A, et al. Sensitive and reliable detection of genomic imbalances in human neuroblastomas using comparative genomic hybridisation analysis. Eur J Cancer 1997;33:1979-82.
14. Vandesompele J, Van Roy N, Van Gele M, et al. Genetic heterogeneity of neuroblastoma studied by comparative genomic hybridization. Genes Chromosomes Cancer 1998;23:141-52.
15. Łastowska M, Roberts P, Pearson ADJ, Lewis I, Wolstenholme J, Bown N. Promiscuous translocations of chromosome arm 17q in human neuroblastomas. Genes Chromosomes Cancer 1997;19:143-9.
16. Caron H. Allelic loss of chromosome 1 and additional chromosome 17 material are both unfavorable prognostic markers in neuroblastoma. Med Pediatr Oncol 1995;24:215-21.
17. Caron H, van Sluis P, de Kraker J, et al. Allelic loss of chromosome 1p as a predictor of unfavorable outcome in patients with neuroblastoma. N Engl J Med 1996;334:225-30.
18. Łastowska M, Cotterill S, Pearson ADJ, et al. Gain of chromosome arm 17q predicts unfavorable outcome in neuroblastoma patients. Eur J Cancer 1997;33:1627-33.
19. Brodeur GM, Pritchard J, Berthold F, et al. Revisions of the international criteria for neuroblastoma diagnosis, staging, and response to treatment. J Clin Oncol 1993;11:1466-77.
20. du Manoir S, Speicher MR, Joos S, et al. Detection of complete and partial chromosome gains and losses by comparative genomic in situ hybridization. Hum Genet 1993;90:590-610.
21. Kallioniemi A, Kallioniemi OP, Sudar D, et al. Comparative genomic hybridization for molecular cytogenetic analysis of solid tumors. Science 1992;258:818-21.
22. Strehl S, Ambros PF. Fluorescence in situ hybridization combined with immunohistochemistry for highly sensitive detection of chromosome 1 aberrations in neuroblastoma. Cytogenet Cell Genet 1993;63:24-8.
23. Peter M, Michon J, Vielh P, et al. PCR assay for chromosome 1p deletion in small neuroblastoma samples. Int J Cancer 1992;52:544-8.
24. Kaplan EL, Meier P. Nonparametric estimation from incomplete observations. J Am Stat Assoc 1958;53:457-81.
25. Bernstein ML, Leclerc JM, Bunin G, et al. A population-based study of neuroblastoma incidence, survival, and mortality in North America. J Clin Oncol 1992;10:323-9. [Erratum, J Clin Oncol 1992;10:1202.]
26. Łastowska M, Van Roy N, Bown N, et al. Molecular cytogenetic delineation of 17q translocation breakpoints in neuroblastoma cell lines. Genes Chromosomes Cancer 1998;23:116-22.
27. Matthay KK. Stage 4S neuroblastoma: what makes it special? J Clin Oncol 1998;16:2003-6.
28. Katzenstein HM, Bowman LC, Brodeur GM, et al. Prognostic significance of age, *MYCN* oncogene amplification, tumor cell ploidy, and histology in 110 infants with stage D(S) neuroblastoma: the Pediatric Oncology Group experience — a Pediatric Oncology Group study. J Clin Oncol 1998;16:2007-17.

DISCUSSION

In this Chapter, we applied comparative genomic hybridization (CGH) in order to obtain a genome wide overview of genetic aberrations in neuroblastoma, and to gain insights in the genetic heterogeneity of this enigmatic childhood tumor.

In Paper I, we analyzed 36 primary untreated neuroblastoma tumors of both high and low stage. The major aims of this study were to identify new frequently involved genetic aberrations in neuroblastoma, to gain more information on imbalances not extensively studied so far, and to further characterize the genetic heterogeneity of this tumor. During the course of this work, 4 CGH studies on neuroblastoma were published, including a small series of 6 familial tumors[1-4]. Our aims were therefore extended to a thorough comparison of all published results.

One of the major findings in our study was the presence of predominantly whole chromosome gains and losses in low stage tumors (stages 1, 2 and 4S), while high stage (3 and 4) tumors displayed mainly partial chromosome imbalances. In addition, one or two extra copies of a complete chromosome 17, and gain of the distal part of the long arm of chromosome 17 were found to be the most frequent abnormalities in the low and high stage tumors, respectively. With one exception, unbalanced 17q gain was only found in stage 3 and 4 tumors, in association with loss of 11q, or 1p and/or MNA. Partial chromosome losses were most frequently observed for 1p, 3p and 11q. Remarkably, 11q deletions were mainly found in stage 4 tumors, often in association with 3p or 14q deletions. Paper I was the first to pinpoint at a possible new genetic subgroup of aggressive neuroblastomas characterized by 11q deletion in the absence of 1p deletion or MNA.

In one primary tumor without evidence for MNA, amplification of the 11q13 region was detected. Subsequent Southern blot analysis demonstrated amplification of the *CCND1* (Cyclin D1) and *EMS1* genes, often found amplified in breast cancer and squamous cell carcinomas of the head and neck[5]. Recently, three other primary tumors with 11q13 amplification were found (ref.[6] and unpublished results provided by Dr. Boavida, Lisbon, Portugal). Furthermore, the observation of 11q13 gain (not amplification) in approximately 5% of the primary tumors (see Paper II), and the fact that low-copy 11q13 DNA amplification (< 10 copies) occurs in other tumor types opens the possibility that 11q13 gain or amplification plays a role in a subset of neuroblastomas.

Comparison of our results with 3 published CGH reports revealed that the major findings in all individual studies were concordant, but from this analysis, it was apparent that the total number of tumors in clinical and genetic subgroups was relatively small for each individual study. Moreover, associations between particular imbalances in individual tumors could not always be determined in the published reports due to the applied data format. These observations indicated the need for a larger sampling size and a uniform data presentation, in order to delineate more accurately the different genetic subgroups, and to draw significant conclusions.

In Paper II, we therefore decided to collect 120 published CGH results from 4 studies[1-3, 7], and re-evaluate them together with data from 84 new cases. This multicenter study yielded a unprecedented overview of the genomic imbalances in 204 primary untreated neuroblastoma tumors. Many of the previously observed characteristic CGH findings from individual studies were confirmed and strengthened by pooling all data. In addition, five major genetic subgroups could be distinguished. The largest and hitherto most well known subgroup contained one third of all tumors, and was characterized by unbalanced 17q gain, and 1p deletion and/or MNA. The second subgroup comprised one fourth of all tumors, and showed only numerical imbalances, revealing for the first time a nonrandom pattern of gains for chromosomes 1, 2, 6, 7, 8, 12, 13, 17, 18, and 22, and losses for chromosomes 3, 4, 9, 11, 14, and X. This pattern of numerical imbalances was typically observed in low stage tumors (showing a near-triploid DNA content) from infants with high survival rates. Particular patterns of whole chromosome losses and gains have also been observed in other pediatric tumors with good prognosis, such as acute lymphoblastic leukemia[8]. The biological significance of these numerical chromosome changes is unknown, but it's remarkable that most of the chromosomes that are underrepresented in low stage neuroblastomas also show partial losses in high stage tumors. It's therefore possible that LOH of the same (set of) gene(s) plays a role in both subtypes. Similarly, gain of chromosome 17 and unbalanced 17q gain are the most frequently observed chromosomal imbalances in low and high stage tumors, respectively.

This study further confirmed the existence of a new third subgroup defined by 11q loss and unbalanced 17q gain, in the absence of 1p loss and/or MNA. The majority of these tumors belonged to stage 4, and were significantly correlated with loss of 3p, 4p and 14q. A fourth subgroup contained tumors with predominantly numerical chromosome changes in combination with a few structural aberrations (excluding loss of 1p, 11q or MNA). A last small subgroup presented with unbalanced 17q gain only.

The initial observation in Paper I and confirmation in Paper II of a subgroup of (mainly stage 4) tumors with 11q deletion provided more insight in the thus far ill defined genetic

background of high stage tumors lacking MNA. However, this group of tumors was still relatively small in Paper II (19 stage 4 tumors with 11q loss). In order to draw more reliable conclusions and assess the prognostic value of 11q deletion, a European multicenter study was set up where 50 additional stage 4 tumors were analyzed and pooled with 33 published stage 4 cases (Paper III).

In this study, 36 tumors were identified that exhibited a partial 11q deletion, always encompassing more than half of the distal end of 11q. Approximately 60% of stage 4 tumors without MNA exhibited 11q deletions, whereas loss of 11q was found in only a minority of samples with MNA and/or 1p deletion. In addition to typical absence of MNA and 1p deletion, stage 4 neuroblastomas with loss of 11q were significantly associated with 3p deletions. These data therefore strongly suggest that 11q deletions define a distinct genetic subgroup of advanced stage tumors. Survival analysis demonstrated that patients with an 11q deleted tumor had no significantly different survival probability compared to patients whose tumor bears intact chromosomes 11. The same holds true after stratification for MNA, indicating that the 11q status has no prognostic value in stage 4 patients. However, further studies remain necessary to evaluate the impact of the 11q status for patients treated with new therapeutic regimens. In this respect, tumors with MNA or 11q deletion should be considered as separate groups in optimization of treatment protocols, and in evaluation of clinical results.

In a recent and large LOH study on a series of 310 primary neuroblastomas of all stages, LOH was found for several 11q loci in as much as 43% of the cases, with an SRO in the 11q23.3 region[9]. As in our study, there was a strong inverse correlation between 11q LOH and MNA. However, a significant rate of 11q LOH was found in stage 1 and 2 (30 and 45%, respectively), as well as a much higher survival probability for patients with 11q LOH (3 year survival of 75% vs. 35% in our study). This may be explained by the presence of near triploid low stage tumors in their series, which often present with whole chromosome 11 loss and favorable prognosis, as shown in Paper II. Recently, the aforementioned LOH study was extended with 11p markers to segregate whole chromosome 11 loss from rearrangements leading to deletion of distal 11q[10]. With this distinction, unbalanced 11q LOH was found in 22% of the cases – a figure in keeping with Paper II - and was highly correlated with age over 1 year at diagnosis and stage 4 disease, confirming the conclusions from Paper III.

As mentioned in Chapter 1, several lines of evidence point at the presence of an 11q tumor suppressor gene in neuroblastoma. Molecular (cyto)genetic analyses (including this study) revealed loss of 11q in approximately 15-30% of the tumors. Furthermore, rare cases of constitutional abnormalities of this region in children who developed neuroblastoma have been reported (reviewed in ref.[11]), and chromosome 11 transfer experiments in cell line NGP (harboring an 11q deletion) resulted in a more differentiated phenotype[12]. Further molecular studies are thus required to narrow down the critical region of LOH and to identify the putative tumor suppressor gene on 11q involved in neuroblastoma development or progression.

One of the most striking findings in the CGH analyses of neuroblastoma was the frequent occurrence of extra chromosomes 17 or unbalanced 17q gain in low and high stage tumors, respectively. In view of the reported association of unbalanced 17q gain with adverse prognostic factors, we sought to test the hypothesis that this abnormality was an independent predictor for poor outcome (Paper IV). To this end, clinical information and genetic data (obtained by FISH and CGH) on at least the 17q, 1p, and *MYCN* status for 313 patients with neuroblastoma were collected at six European centers.

Unbalanced 17q gain was found in half of all tumor samples, and was confirmed to be strongly associated with stage 4 disease, age at diagnosis over 1 year, DNA content in the diploid/tetraploid range, MNA, and 1p deletion. In univariate analyses of survival, the 17q status as well as the above mentioned genetic and clinical factors were significant predictors for patient outcome. However, in a multivariate analysis with age, stage, 1p, MNA and 17q as factors, 17q was the most significant predictor for clinical outcome, followed by stage 4 disease and 1p deletion. In this analysis, MNA and age were no independent prognostic factors. The lack of independent discriminative power of MNA might be explained by the fact that this genetic alteration was not found in any tumor without concurrent 1p deletion, 17q gain, or both. This suggests that MNA is a later event in the sequence of genetic alterations that lead to a clinically manifest tumor.

Cytogenetic and metaphase FISH studies have demonstrated that the principle mechanism underlying partial gain of 17q is an unbalanced translocation, with a variety of partner chromosomes[13-16]. These translocations typically result in concurrent loss of the partner chromosome distal to the breakpoint, and gain of a distal 17q segment. The most common sites of these translocations are chromosome arms 1p and 11q, and account for approximately half of all 1p and 11q deletion events in neuroblastoma (reviewed in ref.[11]). Similar 17q translocations have been observed on many other chromosome arms, including 3p, 4p, 9p, and 14q. The significance of unbalanced 17q gain as a mechanism for LOH on the partner chromosome remains to be investigated, but could possibly account for the observed adverse prognosis

associated with partial 17q gain. Alternatively, in view of the different survival probabilities for patients whose tumor displays an extra copy of the complete chromosome 17 or the distal 17q fragment only, an imbalance of genes located on opposite sides of the 17q breakpoint could be responsible for the aggressive behavior.
The molecular mechanism leading to preferential involvement of 17q in unbalanced translocations is unknown. Recently, the 17q breakpoint of a constitutional balanced t(1;17) in a patient who developed neuroblastoma was located in a 25 kb sequenced region, which is thought to be genetically unstable[17]. The cloning and sequencing of additional 17q breakpoints could indicate whether sequences at or near these breakpoints share homologous stretches that are particularly prone to recombination in developing neuroblasts. So far, breakpoint mapping in tumors and cell lines has revealed that the 17q breakpoints are scattered along the proximal half of the long arm[18, 19], which argues against a specific gene effect (e.g. fusion gene). Although it cannot be ruled out that functionally related genes belonging to the same family are implicated in these different breakpoints, the mapping data strongly suggest that a gene dosage effect of one or more genes on distal 17q are involved in neuroblastoma development. Possible candidate genes include the *NME1/2* genes at 17q21.3 and the *BIRC5* (survivin) gene at 17q25. Increased expression of the metastasis related *NME1* gene was observed in advanced stage neuroblastomas[20-22], with missense mutations in a small subset of these tumors[21, 23]. Furthermore, the *NME1/2* genes were recently found to be MYCN downstream genes[24], which provides further support for a possible role of these genes in unfavorable neuroblastomas. Another gene which might be the target of consistent gain of 17q in neuroblastoma is *BIRC5*. This anti-apoptotic protein has been associated with a more aggressive tumor phenotype, and promotion of cell survival[25, 26]. Clearly, additional studies are required to substantiate a role of these genes in neuroblastoma, or to identify other 17q candidate genes responsible for tumor development or progression.
Similar oncogenic mechanisms whereby an extra copy of a single gene lead to specific cancer types have been reported. A recent study demonstrated that an extra copy of the *ATR* gene due to isochromosome 3q formation contributes to rhabdomyosarcoma[27]. Likewise, duplication of a chromosome 7 carrying a mutated *MET* allele is implicated in hereditary papillary renal cell carcinoma[28], and patients with Down's syndrome have a 10-20 fold increased risk of developing leukemia[29]. The presence of extra copies of 17q in the majority of both low (due to whole chromosome gain) and high stage tumors implies that genes on 17q are involved in the initiating steps of neuroblastoma development. Further research is warranted to elucidate the biological role of chromosome 17 alterations in neuroblastoma.
In conclusion, the 17q status was shown to be a more important indicator of adverse outcome than any other clinical or genetic factor, and it allowed identification of a larger proportion of prognostically poor tumors than any other marker. We therefore suggest that assessment of the 17q status in neuroblastoma should be incorporated into future clinical trials.

In conclusion, Chapter 2 has illustrated the power of CGH in whole genome screening for structural and numerical chromosome aberrations in neuroblastoma, in particular for the analysis of localized tumors for which little genetic information was available apart from ploidy, 1p and *MYCN* status. A nonrandom pattern of whole chromosome gains and losses was defined for these tumors, with extra copies of chromosome 17 present in most cases. In contrast, partial gain of 17q was the most frequently observed abnormality in high stage tumors, and was shown to be the most significant independent factor for poor outcome. Within this group of high stage tumors, two genetically distinct subgroups could be delineated : a first well-known group of tumors with 1p deletion, MNA or both; and a newly identified group of tumors with loss of 11q, often in association with loss of 3p.

REFERENCES

1. Plantaz, D. et al. Gain of chromosome 17 is the most frequent abnormality detected in neuroblastoma by comparative genomic hybridization. *Am J Pathol* **150**, 81-89 (1997).
2. Lastowska, M. et al. Comparative genomic hybridization study of primary neuroblastoma tumors. United Kingdom Children's Cancer Study Group. *Genes Chromosomes Cancer* **18**, 162-169 (1997).
3. Brinkschmidt, C. et al. Comparative genomic hybridization (CGH) analysis of neuroblastomas--an important methodological approach in paediatric tumour pathology. *J Pathol* **181**, 394-400 (1997).
4. Altura, R.A. et al. Novel regions of chromosomal loss in familial neuroblastoma by comparative genomic hybridization. *Genes Chromosomes Cancer* **19**, 176-184 (1997).
5. Schuuring, E. The involvement of the chromosome 11q13 region in human malignancies: cyclin D1 and EMS1 are two new candidate oncogenes--a review. *Gene* **159**, 83-96 (1995).

6. Breen, C.J., O'Meara, A., McDermott, M., Mullarkey, M. & Stallings, R.L. Coordinate deletion of chromosome 3p and 11q in neuroblastoma detected by comparative genomic hybridization. *Cancer Genet Cytogenet* **120**, 44-49 (2000).
7. Vandesompele, J. et al. Genetic heterogeneity of neuroblastoma studied by comparative genomic hybridization. *Genes Chromosomes Cancer* **23**, 141-152 (1998).
8. Raimondi, S.C. Current status of cytogenetic research in childhood acute lymphoblastic leukemia. *Blood* **81**, 2237-2251 (1993).
9. Guo, C. et al. Allelic deletion at 11q23 is common in MYCN single copy neuroblastomas. *Oncogene* **18**, 4948-4957 (1999).
10. Guo, C. et al. Deletion of 11q23 is a frequent event in the evolution of MYCN single- copy high-risk neuroblastomas. *Med Pediatr Oncol* **35**, 544-546 (2000).
11. Bown, N. Neuroblastoma tumour genetics: clinical and biological aspects. *J Clin Pathol* **54**, 897-910 (2001).
12. Bader, S.A., Fasching, C., Brodeur, G.M. & Stanbridge, E.J. Dissociation of suppression of tumorigenicity and differentiation in vitro effected by transfer of single human chromosomes into human neuroblastoma cells. *Cell Growth Differ* **2**, 245-255 (1991).
13. Lastowska, M. et al. Promiscuous translocations of chromosome arm 17q in human neuroblastomas. *Genes Chromosomes Cancer* **19**, 143-149 (1997).
14. Meddeb, M. et al. Additional copies of a 25 Mb chromosomal region originating from 17q23.1-17qter are present in 90% of high-grade neuroblastomas. *Genes Chromosomes Cancer* **17**, 156-165 (1996).
15. Van Roy, N. et al. 1;17 translocations and other chromosome 17 rearrangements in human primary neuroblastoma tumors and cell lines. *Genes Chromosomes Cancer* **10**, 103-114 (1994).
16. Savelyeva, L., Corvi, R. & Schwab, M. Translocation involving 1p and 17q is a recurrent genetic alteration of human neuroblastoma cells. *Am J Hum Genet* **55**, 334-340 (1994).
17. Van Roy, N. et al. Localisation of the 17q breakpoint of a constitutional 1;17 translocation in a patient with neuroblastoma within a 25 kb segment located between the ACCN1 and TLK2 genes and near the distal breakpoints of two microdeletions in NF1 patients. *Genes Chromosomes Cancer* (in press).
18. Van Roy, N. et al. Molecular cytogenetic analysis of 1;17 translocations in neuroblastoma. *Eur J Cancer* **31A**, 530-535 (1995).
19. Lastowska, M. et al. Molecular cytogenetic delineation of 17q translocation breakpoints in neuroblastoma cell lines. *Genes Chromosomes Cancer* **23**, 116-122 (1998).
20. Hailat, N. et al. High levels of p19/nm23 protein in neuroblastoma are associated with advanced stage disease and with N-myc gene amplification. *J Clin Invest* **88**, 341-345 (1991).
21. Leone, A. et al. Evidence for nm23 RNA overexpression, DNA amplification and mutation in aggressive childhood neuroblastomas. *Oncogene* **8**, 855-865 (1993).
22. Takeda, O. et al. An increased NM23H1 copy number may be a poor prognostic factor independent of LOH on 1p in neuroblastomas. *Br J Cancer* **74**, 1620-1626 (1996).
23. Chang, C.L. et al. Nm23-H1 mutation in neuroblastoma. *Nature* **370**, 335-336 (1994).
24. Godfried, M.B. et al. The N-myc and c-myc downstream pathways include the chromosome 17q genes nm23-H1 and nm23-H2. *Oncogene* **21**, 2097-2101 (2002).
25. Adida, C., Berrebi, D., Peuchmaur, M., Reyes-Mugica, M. & Altieri, D.C. Anti-apoptosis gene, survivin, and prognosis of neuroblastoma. *Lancet* **351**, 882-883 (1998).
26. Islam, A. et al. High expression of Survivin, mapped to 17q25, is significantly associated with poor prognostic factors and promotes cell survival in human neuroblastoma. *Oncogene* **19**, 617-623 (2000).
27. Smith, L. et al. Duplication of ATR inhibits MyoD, induces aneuploidy and eliminates radiation-induced G1 arrest. *Nat Genet* **19**, 39-46 (1998).
28. Zhuang, Z. et al. Trisomy 7-harbouring non-random duplication of the mutant MET allele in hereditary papillary renal carcinomas. *Nat Genet* **20**, 66-69 (1998).
29. Fong, C.T. & Brodeur, G.M. Down's syndrome and leukemia: epidemiology, genetics, cytogenetics and mechanisms of leukemogenesis. *Cancer Genet Cytogenet* **28**, 55-76 (1987).

chapter 3

CHAPTER 3: DIFFERENTIAL GENE EXPRESSION ANALYSIS

NOTES & TIPS

Elimination of Primer–Dimer Artifacts and Genomic Coamplification Using a Two-Step SYBR Green I Real-Time RT-PCR[1]

Jo Vandesompele, Anne De Paepe, and Frank Speleman[2]

Center for Medical Genetics, Ghent University Hospital, B-9000 Ghent, Belgium

Received September 5, 2001; published online

Gene expression analysis plays an increasingly important role in many fields of biological research. The recently developed real-time PCR quantification method has many advantages over the conventional quantifications in terms of accuracy, sensitivity, dynamic range, high-throughput capacity, and absence of post-PCR manipulations (1, 2). Sequence-specific fluorescence-labeled probes (e.g., TaqMan) have been considered as a standard detection format in many diagnostic and research applications (3, 4), but are not very well suited for quantification of a large number of different sequences, because a new and relatively expensive probe is generally required for each amplicon under investigation. We have therefore optimized and validated a reverse transcriptase PCR (RT-PCR) assay for accurate expression profiling using the double stranded DNA-binding dye SYBR green I, which is a much more economical alternative to quantify any given transcript in a reaction. Using such a generic dye, different PCR amplicons and/or nonspecific amplification products could accurately be distinguished by the generation of so-called DNA melting curves and first-derivative melting peaks (5).

During initial one-step RT-PCR reactions, we observed extensive accumulation of primer–dimers (PD)[3] in no-template-control (NTC) tubes. This might obscure the true result in quantitative assays using generic DNA dyes, especially in samples where the gene of interest is of low abundance and PD are readily formed. A two-step RT-PCR protocol was therefore introduced and eliminated this problem. Further validation of the real-time PCR illustrated the prerequisite and efficacy of DNase treatment of RNA samples prior to cDNA synthesis. This step resulted in a significantly facilitated primer design for RT-PCR as the position of the primers no longer has to be considered to control for genomic contamination. We finally addressed important issues of reproducibility by determination of the intra- and interassay variation of our established method. It was shown that DNase treatment, cDNA synthesis, and RT-PCR are very reproducible. In conclusion, a two-step real-time quantitative RT-PCR based on SYBR Green I detection chemistry and DNase-treated RNA samples is the method of choice for sensitive, reproducible, and large-scale measurements of gene expression levels.

In accordance with previous successful results obtained in our laboratory with one-step quantitative RT-PCR assays using a TaqMan probe as detection format, it was initially decided to apply a one-step RT-PCR for gene expression measurements using SYBR green I (i.e., cDNA synthesis using gene-specific primers and real-time PCR amplification are sequentially performed in the same tube). All primers were designed with PrimerExpress 1.0 software (Applied Biosystems) using the default TaqMan parameters, with modified minimum amplicon length requirements (75 bp). An additional requirement was a maximum GC content of 40% for the five last 3′ end nucleotides. Primer sequences can be obtained from the authors on request. To determine the minimum primer concentrations giving the lowest threshold cycle (C_t) and maximum amplification efficiency while minimizing nonspecific amplification, nine different combinations of reverse and forward primer concentrations were tested (two-by-two combinations of 100, 300, or 900 nM). For each combination, a no-template control was included. SYBR green I amplification mixtures (25 μl) contained 25 ng total RNA, 2× SYBR Green I Master Mix buffer (12.5 μl) (Applied Biosystems), 0.125 μl MuLV-RT enzyme (50 U/μl) (Applied Biosystems), 0.125 μl RNasin (40 U/μl) (Promega), and varying concentrations of for-

[1] This study was supported by a grant from the Flemish Institute for the Promotion of Scientific Technological Research in Industry (IWT), GOA Grant 12051397, FWO Grant G.0028.00, and BOF Grant 011B4300.

[2] To whom correspondence and reprint requests should be addressed at Center for Medical Genetics, Ghent University Hospital, 1K5 De Pintelaan 185, B-9000 Ghent, Belgium. Fax: +32-9-2404970. E-mail: franki.speleman@rug.ac.be.

[3] Abbreviations used: PD, primer–dimers; NTC, no-template controls.

Analytical Biochemistry
doi:10.1006/abio.2001.5564
0003-2697/02 $35.00

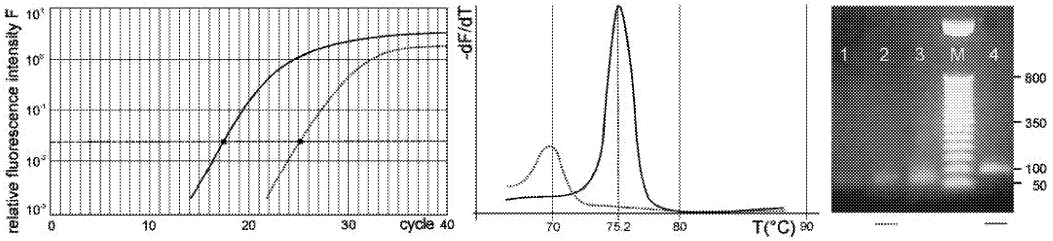

FIG. 1. Primer–dimer accumulation during one-step RT-PCR. Left, amplification plots of no-template control (dotted line, loaded in gel lane 2) and 50 ng input of total RNA (solid line, gel lane 4) using 300 nM of each primer. Middle, melting peaks of same products as in left panel ($-dF/dT$, negative first derivative of fluorescence intensity with respect to temperature T). Right, agarose gel electrophoresis; lanes 1–3, no-template controls (increasing *MME* primer concentrations, respectively, 100, 300, and 900 nM each); lane M, 50-bp DNA marker; and lane 4, 98-bp *MME* amplicon.

ward and reverse primer. Reactions were run on a ABI Prism 5700 sequence detector (Applied Biosystems). The cycling conditions comprised a cDNA synthesis step at 48°C for 30 min, 10 min of polymerase activation at 95°C, and 40 cycles at 95°C for 15 s and 60° C for 1 min. Upon analysis, amplification products were readily observed in all NTCs. DNA melting curve analysis (using the built-in feature in the software for automatic fluorescence data capturing during gradual temperature increase from 60 to 95°C) and agarose gel electrophoresis of PCR products demonstrated extensive PD accumulation in NTC tubes during one-step RT-PCR. This phenomenon was found for five genes tested and was more pronounced with increasing primer concentrations (Fig. 1). To the best of our knowledge, extensive PD formation during a quantitative one-step RT-PCR in NTCs has not been reported yet, probably because most assays use a TaqMan probe that does not detect this kind of nonspecific amplification. Although no general mechanism for the formation of PDs is described, primers appear to be tail-to-tail oriented in sequenced PDs (6).

In an attempt to reduce PD formation, we introduced a two-step protocol, i.e., cDNA synthesis and PCR amplification in separate tubes. First-strand cDNA was synthesized from 1 μg total RNA using random hexamers (AP Biotech) and SuperScriptII reverse transcriptase (RTase) according to the manufacturer (Invitrogen). After synthesis, cDNA was diluted with 60 μl RNase-free water (Sigma) to obtain a concentration 12.5 ng/μl. The one-step amplification protocol was altered by leaving out the 30-min incubation step at 48°C and the RTase, and RNA was substituted for by 25 ng of cDNA. In the two-step NTC reactions, no amplification of PD was observed, in contrast to presence of PDs in the one-step NTCs that were run in parallel as controls (data not shown). It was further shown that for all tested genes, combinations of 300 nM forward and reverse primer resulted in optimal amplification. Besides elimination of PDs, a two-step protocol with oligo(dT) or random hexamer primers for cDNA synthesis has additional advantages. It allows amplification of multiple targets from the same cDNA pool while variation in RT efficiency other than sample-to-sample variation is controlled for as the cDNA mixture is diluted and split to quantify the different genes of interest. Furthermore, the two-step approach eliminates the need to perform repeated housekeeper amplifications for normalization, which is a prerequisite in the one-step method, in the absence of any other controls.

To investigate the nature of the observed PD accumulation, the MuLV RTase and the RNase inhibitor RNasin were omitted separately from NTC reactions during one-step RT-PCR. PDs were only absent in the tubes without the RTase. Two other widely used RTases (SuperScriptII, Invitrogen; AMV, Promega) were also tested for this phenomenon. According to the manufacturer's guidelines, the temperature of the cDNA synthesis step was altered from 48 to 42°C. PD accumulation was also clearly observed for these two RTases (data not shown). These observations suggest that the reported DNA-dependent polymerase activity of RTases on DNA templates and RNA:DNA hybrids—although not significant—accounts for the initial formation of PDs that are subsequently and efficiently amplified by the DNA polymerase during PCR.

Another critical aspect of quantitative RT-PCR with respect to accurate results is the presence of trace amounts of genomic DNA within the RNA samples to be tested. Virtually no extraction method can guarantee the isolation of DNA-free RNA. PCR primers spanning an exon–exon boundary are often designed to control for genomic contamination. However, this strategy can no longer be used if processed pseudogenes are present in the genome. Furthermore, intron–exon boundary information is not available (yet) for the majority of the genes, nor is it often known in advance

if putative pseudogenes of the gene under investigation reside in the genome. Initial interpretation of the sequence data from human chromosomes 21 and 22 indicated that about 20% of the coding sequences turned out to be pseudogenes (7, 8). Therefore, RNase-free DNase treatment of RNA samples is a prerequisite for accurate RT-PCR results. To illustrate the requirement and efficacy of a DNase treatment of the RNA samples prior to cDNA synthesis, real-time SYBR green I PCR reactions were tested for 25 genes in reaction tubes with RNA (−RT controls) or cDNA (+RT controls) as template (both before and after DNase treatment of RNA) and no-template controls. RNA samples from various tissues (RNeasy extraction, Qiagen) were treated with the RQ1 RNase-free DNase according to the manufacturer (Promega). Treated RNA samples were desalted prior to cDNA synthesis using Microcon-100 spin columns (Millipore). DNase treatment of RNA resulted in complete elimination of amplification in tubes with treated RNA as template, while preserving specific amplification in the cDNA controls (Fig. 2). Together with improved accuracy for RT-PCR, primer design is facilitated (as exon–exon spanning primers are no longer required) and the choice of a housekeeping gene for normalization is no longer restricted to those genes without any known pseudogenes. So far, we have analyzed 10 different housekeeping genes belonging to different functional and abundance classes in various tissues and cells. We clearly observed that no gene is really constantly expressed and multiple housekeeping genes are required for an accurate normalization (Vandesompele *et al.*, submitted for publication).

One-step RT-PCR reactions are often preferred over two-step reactions, because of a presumed minimization of experimental variation, as all enzymatic steps occur in the same tube under controlled thermocycler

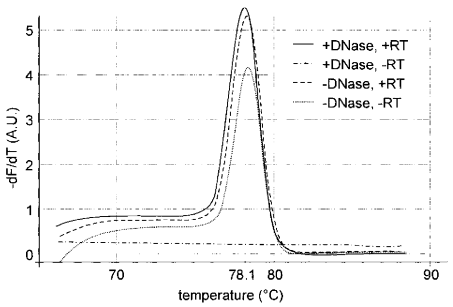

FIG. 2. Efficacy of removal of contaminating DNA in RNA preparations as evidenced by melting peak analysis of generated PCR products, here shown for a representative 91-bp *RPS25* amplicon (+DNase, RNA was DNase treated; −DNase, no DNase treatment; +RT, RT was added for cDNA synthesis; −RT, RT was omitted).

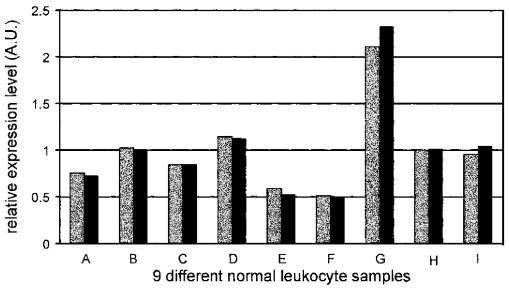

FIG. 3. Relative *HMBS* gene expression levels in nine normal leukocyte samples of which RNA was subjected to two parallel rounds (black and gray) of DNase treatment and cDNA synthesis.

conditions. To address the issue of reproducibility, we determined the interassay variation of our established two-step RT-PCR protocol. We have therefore subjected nine different RNA samples to two parallel rounds of DNase treatment and cDNA synthesis and quantified the relative expression levels of each of four housekeeping genes (*HMBS, UBC, ACTB,* and *HPRT1*) in all samples using the comparative C_t method. The two-step protocol is highly reproducible with Pearson correlation coefficients ranging from 0.974 to 0.988 between the expression levels of the two parallel series of cDNA samples for the four tested genes, of which one is shown in Fig. 3. The interassay variation was calculated as the median coefficient of variation (standard deviation divided by the arithmetic mean) for the paired relative quantities obtained in the two parallel series for the four genes and amount to 7.7%. This figure is only slightly higher than the observed median intraassay variation of 5.8% (reflecting the variation between duplicated reactions in the same PCR run; based on 25 different genes tested on 30 samples, data not shown) and demonstrates the reproducibility of the two-step approach.

To summarize, SYBR green I is the detection format of choice for accurate and reproducible real-time transcript abundance measurements of a large series of genes. Obscuring PD observed in one-step RT-PCR reactions were eliminated by the use of a two-step and DNase treatment of RNA prior to cDNA synthesis was shown to be a prerequisite for accurate RT-PCR and facilitated primer design.

Acknowledgments. We thank Johanna Iso-Oja and Filip Pattyn for their excellent technical assistance.

REFERENCES

1. Higuchi, R., Fockler, C., Dollinger, G., and Watson, R. (1993) Kinetic PCR analysis: real-time monitoring of DNA amplification reactions. *Biotechnology (N. Y.)* **11,** 1026–1030.

2. Heid, C. A., Stevens, J., Livak, K. J., and Williams, P. M. (1996) Real time quantitative PCR. *Genome Res* **6,** 986–994.
3. Bustin, S. A. (2000) Absolute quantification of mRNA using real-time reverse transcription polymerase chain reaction assays. *J. Mol. Endocrinol.* **25,** 169–193.
4. Lie, Y. S., and Petropoulos, C. J. (1998) Advances in quantitative PCR technology: 5′ nuclease assays. *Curr. Opin. Biotechnol.* **9,** 43–48.
5. Ririe, K. M., Rasmussen, R. P., and Wittwer, C. T. (1997) Product differentiation by analysis of DNA melting curves during the polymerase chain reaction. *Anal. Biochem.* **245,** 154–160.
6. Brownie, J., Shawcross, S., Theaker, J., Whitcombe, D., Ferrie, R., Newton, C., and Little, S. (1997) The elimination of primer–dimer accumulation in PCR. *Nucleic Acids Res.* **25,** 3235–3241.
7. Dunham, I., Shimizu, N., Roe, B. A., Chissoe, S., Hunt, A. R., Collins, J. E., Bruskiewich, R., Beare, D. M., Clamp, M., Smink, L. J., Ainscough, R., Almeida, J. P., Babbage, A., Bagguley, C., Bailey, J., Barlow, K., Bates, K. N., Beasley, O., Bird, C. P., Blakey, S., Bridgeman, A. M., Buck, D., Burgess, J., Burrill, W. D., O'Brien, K. P., *et al.* (1999) The DNA sequence of human chromosome 22. *Nature* **402,** 489–495.
8. Hattori, M., Fujiyama, A., Taylor, T. D., Watanabe, H., Yada, T., Park, H. S., Toyoda, A., Ishii, K., Totoki, Y., Choi, D. K., Soeda, E., Ohki, M., Takagi, T., Sakaki, Y., Taudien, S., Blechschmidt, K., Polley, A., Menzel, U., Delabar, J., Kumpf, K., Lehmann, R., Patterson, D., Reichwald, K., Rump, A., Schillhabel, M., and Schudy, A. (2000) The DNA sequence of human chromosome 21: The chromosome 21 mapping and sequencing consortium. *Nature* **405,** 311–319.

Accurate normalization of real-time quantitative RT-PCR data by geometric averaging of multiple internal control genes

Jo Vandesompele, Katleen De Preter, Filip Pattyn, Bruce Poppe, Nadine Van Roy, Anne De Paepe and Frank Speleman

Address: Center for Medical Genetics, Ghent University Hospital 1K5, De Pintelaan 185, B-9000 Ghent, Belgium

Correspondence : Frank Speleman, E-mail: franki.speleman@rug.ac.be

Abstract

Background: Gene expression analysis plays an increasingly important role in many fields of biological research, with real-time RT-PCR becoming the method of choice for high-throughput and accurate expression profiling of selected genes. Given the increased sensitivity, reproducibility and large dynamic range of this methodology, the requirements for a proper internal control gene for normalization have become increasingly stringent. Although it has been reported that housekeeping gene expression can vary considerably, no systematic survey has thoroughly determined the errors related to the common practice of using only one control gene, nor presented an adequate workaround.

Results: We outlined a robust and innovative strategy to identify the most stably expressed control genes in a given set of tissues, and to determine the minimal number of genes required for calculation of a reliable normalization factor. We have evaluated 10 housekeeping genes from different abundance and functional classes in various human tissues, and demonstrated that the conventional practice of using only a single gene for normalization leads to relatively large errors in a significant proportion of tested samples. Furthermore, the geometric mean of multiple carefully selected housekeeping genes was validated as an accurate normalization factor by analyzing publicly available microarray data.

Conclusions: The presented normalization strategy is a prerequisite for accurate RT-PCR expression profiling, which, amongst others, opens the possibility to study the biological relevance of small expression differences.

Background

Gene expression analysis plays an increasingly important role in many fields of biological research. Understanding patterns of expressed genes is expected to provide insight into the complex regulatory networks and will most probably lead to the identification of genes relevant to new biological processes. Two recently developed methods to measure transcript abundance have gained much popularity and are frequently applied. Microarrays allow the parallel analysis of thousands of genes in two differentially labeled RNA populations [1], while real-time reverse transcriptase PCR (RT-PCR) provides the simultaneous measurement of gene expression in many different samples for a limited number of genes, and is especially suited when only a small number of cells are available [2-4]. Both techniques have the advantage of speed, throughput and a high degree of potential automation compared to conventional quantification methods, such as Northern blot analysis, ribonuclease protection assay, or competitive RT-PCR. Nevertheless, these novel approaches require the same kind of normalization as for the traditional methods of mRNA quantification.

Several variable factors need to be controlled for during gene expression analysis, such as the amount of starting material, enzymatic efficiencies, and differences between tissues or cells in overall transcriptional activity. Various strategies have been applied to normalize these variations. Under controlled conditions of reproducible extraction of good quality RNA, the gene transcript number is ideally standardized to the number of cells, but accurate enumeration of cells is often precluded, e.g. when starting from solid tissue. Another frequently applied normalization scalar is the RNA mass quantity, especially in Northern blot analysis. Several arguments

against the use of mass quantity can be raised. The quality of RNA and related efficiency of the enzymatic reactions are not taken into account. Moreover, in some instances it is impossible to quantify this parameter, e.g. when only minimal amounts of RNA are available from microdissected tissues. Probably the strongest argument against the use of total RNA mass for normalization is the fact that this consists predominantly of ribosomal RNA (rRNA) molecules that are not always representative for the messenger RNA (mRNA) fraction, which was recently evidenced by a significant imbalance between ribosomal and messenger RNA content in approximately 7.5% of mammary adenocarcinomas [5]. Also, it has been reported that rRNA transcription is affected by biological factors and drugs [6-8]. Further drawbacks to the use of 18S or 28S rRNA molecules as standards are their absence in mRNA purified samples, and their high abundance compared to target mRNA transcripts, the latter making it difficult to accurately subtract the baseline value in real-time RT-PCR data analysis.

To date, internal control genes are most frequently used to normalize the mRNA fraction. This internal control –often referred to as housekeeping gene– should not vary in the tissues or cells under investigation, or in response to experimental treatment. However, many studies make use of these constitutively expressed control genes without a proper validation of their presumed expression stability. It is shown in the literature though that housekeeping gene expression – although occasionally constant in a given cell type or experimental condition – may vary considerably (reviewed in [9-12]). With the increased sensitivity, reproducibility and large dynamic range of real-time RT-PCR methods, the requirements for a proper internal control gene have become increasingly stringent. In this study, we performed an extensive evaluation of 10 commonly used housekeeping genes in 13 different human tissues, and outlined a procedure for calculation of a normalization factor based on multiple control genes for more accurate and reliable normalization of gene expression data. Furthermore, this normalization factor was validated in a comparative study with frequently applied microarray scaling factors using publicly available microarray data.

Results

Expression profiling of housekeeping genes

Primers were designed for ten commonly used housekeeping genes (*ACTB*, *B2M*, *GAPD*, *HMBS*, *HPRT1*, *RPL13A*, *SDHA*, *TBP*, *UBC* and *YWHAZ*) (see Table 1 for full gene name, alias, chromosomal localization and function; and Table 2 for primer sequences). Special attention was paid to select genes that belong to different functional classes, which significantly reduces the chance that genes might be co-regulated. The expression level of these ten internal control genes was determined in 34 independently prepared neuroblastoma cell lines, 20 short term cultured normal fibroblast samples from different individuals, 13 normal leukocyte samples, 9 normal bone marrow samples, and 9 additional normal human tissues from pooled organs (heart, brain, fetal brain, lung, trachea, kidney, mammary gland, small intestine and uterus). The raw expression values are available as a tab delimited file (raw_data.txt).

Single control normalization error

To determine the possible errors related to the common practice of using only one housekeeping gene for normalization, we calculated the ratio of the ratios of two control genes in two different samples (from the same tissue panel) and termed it the single control normalization error *E* (see Materials & Methods). For two ideal internal control genes (constant ratio between the genes in all samples), *E* equals 1. In practice, observed *E* values are larger than one and constitute the erroneous *E*-fold expression difference between two samples depending on the specific housekeeping gene used for normalization. For all 45 two-by-two combinations of control genes and 865 two-by-two sample combinations within the available tissue panels (neuroblastoma, fibroblast, leukocyte, bone marrow and a series of normal tissues from Clontech) (i.e. a total of 38,925 data points), *E*-values were calculated (Figure 1). In addition, the systematic error distribution was calculated by analysis of repeated runs of the same control gene. The average 75th and 90th percentile *E* values are 3.0 (range 2.1 - 3.9), and 6.4 (range 3.0 - 10.9), respectively.

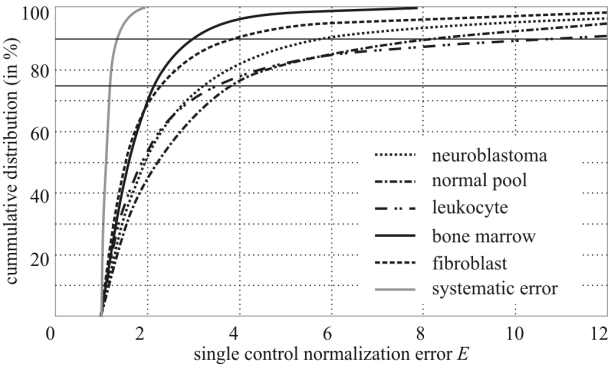

Figure 1: Cumulative distribution plot of single control normalization error values (*E*) for the different tissue panels.

Gene stability measure and ranking of selected housekeeping genes

It is generally accepted that gene expression levels should be normalized by a carefully selected stable internal control gene. However, to validate the presumed stable expression of a given control gene, prior knowledge of a reliable measure to normalize this gene in order to remove any non-specific variation is required. To address this circular problem, we developed a gene stability measure to determine the expression stability of control genes based on non-normalized expression levels. This measure relies on the principle that the expression ratio of two ideal internal control genes is identical in all samples, regardless of the experimental condition or cell type. In this way, variation of the expression ratios of two real life housekeeping genes reflects the fact that one (or both) of the genes is (are)

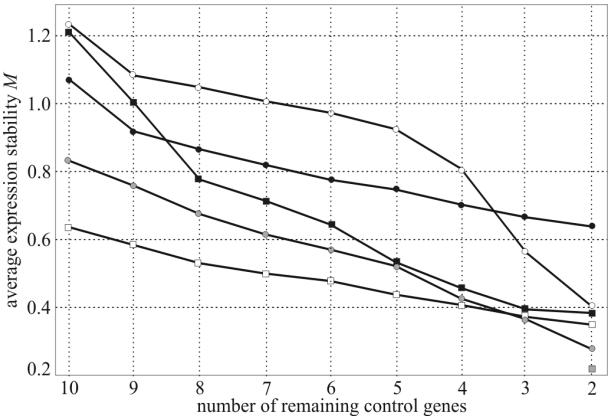

Figure 2: Average expression stability values (*M*) of remaining control genes during stepwise exclusion of the least stable control gene in the different tissue panels (black circle: neuroblastoma; white circle: normal pool; white square: bone marrow; black square: leukocyte; gray circle: fibroblast, gray square: systematic error) (see also Table 3 for the ranking of the genes according to their expression stability).

not constantly expressed, with increasing ratio variation according to decreasing expression stability. For every control gene, we determined the pairwise variation with all other control genes as the standard deviation of the logarithmic transformed expression ratios, and defined the internal control gene stability measure *M* as the average pairwise variation of a particular gene with all other control genes. Genes with the lowest *M* values have the most stable expression. Assuming that the control genes are not co-regulated, stepwise exclusion of the gene with the highest *M* value results in a combination of two constitutively expressed housekeeping genes that have the most stable expression in the tested samples. To manage the large number of calculations, we have written a Visual Basic Application (VBA) for Microsoft Excel -termed *geNorm*- that automatically calculates the expression stability measures *M* for all control genes in a given set of samples (*geNorm* can be obtained from the authors on request). The program allows elimination of the worst scoring housekeeping gene (i.e. with the highest *M* value) and recalculation of new *M* values for the remaining genes. Using this VBA applet, we ranked the 10 control genes in the 5 tested tissue panels according to their expression stability (Figure 2, and Table 3). In addition, the systematic variation was calculated as the pairwise variation *V* for repeated RT-PCR experiments of the same gene, reflecting the inherent machine, enzymatic and pipet variation.

Normalization factor calculation based on the geometric mean of multiple control genes

From the above we concluded that in order to measure expression levels accurately, normalization by multiple instead of one single housekeeping gene is required. Consequently, a normalization factor based upon the expression levels of the best performing housekeeping genes must be calculated. For accurate averaging of the control genes, we propose to use the

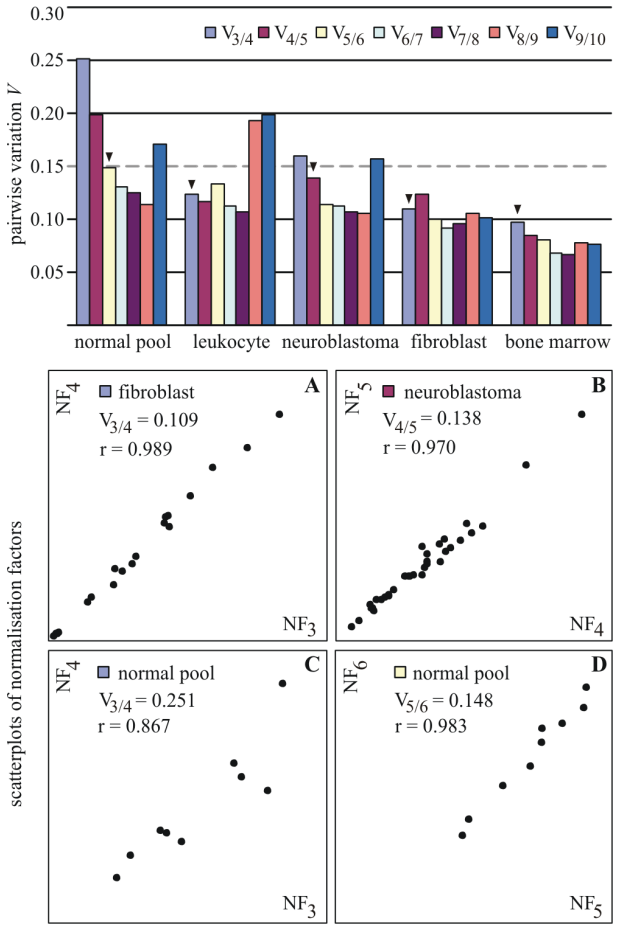

Figure 3: Top: Pairwise variation ($V_{n/n+1}$) analysis between the normalization factors NF_n and NF_{n+1} to determine the number of control genes required for accurate normalization (arrowhead = optimal number of control genes for normalization). Bottom: Selected scatterplots of normalization factors before (x-axis) and after (y-axis) inclusion of an $(n+1)^{th}$ control gene (r = Spearman rank correlation coefficient). Low variation values *V* correspond to high correlation coefficients. It is clear that there is no need to include more than 3, 4 or 5 control genes for fibroblast (A), neuroblastoma (B) and the normal pooled tissues (D), respectively. In contrast, panel C demonstrates that inclusion of at least a fourth gene is required for the normal pooled tissues.

geometric mean instead of the arithmetic mean, as the former controls better for possible outlying values and abundance differences between the different genes. The number of genes used for geometric averaging is a trade off between practical considerations and accuracy. It is obvious that an accurate normalization factor should not include the rather unstable genes that were observed in some tissues. On the other hand, it remains relatively impractical to quantify e.g. 8 control genes when only a few target genes need to be studied, or when only minimal amounts of RNA are available. Furthermore, it is a waste of resources to quantify more genes than necessary if all genes are relatively stably expressed and if the normalization factor do not significantly change whether or not more genes are included. Considering all

Table 1: Internal control genes evaluated in this study

symbol	name	function	localization	alias	IMAGE*
ACTB	beta actin	cytoskeletal structural protein	7p15-p12		510455
B2M	beta-2-microglobulin	beta-chain of major histocompatibility complex class I molecules	15q21-q22		51940
GAPD	glyceraldehyde-3-phosphate dehydrogenase	oxidoreductase in glycolysis and gluconeogenesis	12p13		510510
HMBS	hydroxymethylbilane synthase	heme synthesis, porphyrin metabolism	11q23	porphobilinogen deaminase	245564
HPRT1	hypoxanthine phosphoribosyltransferase 1	purine synthesis in salvage pathway	Xq26		345845
RPL13A	ribosomal protein L13a	structural component of the large 60S ribosomal subunit	19q13	23 kD highly basic protein	-
SDHA	succinate dehydrogenase complex, subunit A	electron transporter in the TCA cycle and respiratory chain	5p15		375812
TBP	TATA box binding protein	general RNA polymerase II transcription factor	6q27		280735
UBC	ubiquitin C	protein degradation	12q24		510582
YWHAZ	tyrosine 3-monooxygenase/tryptophan 5-monooxygenase activation protein, zeta polypeptide	signal transduction by binding to phosphorylated serine residues on a variety of signaling molecules	2p25	phospholipase A2	416026

* IMAGE cDNA clone number according to [14]

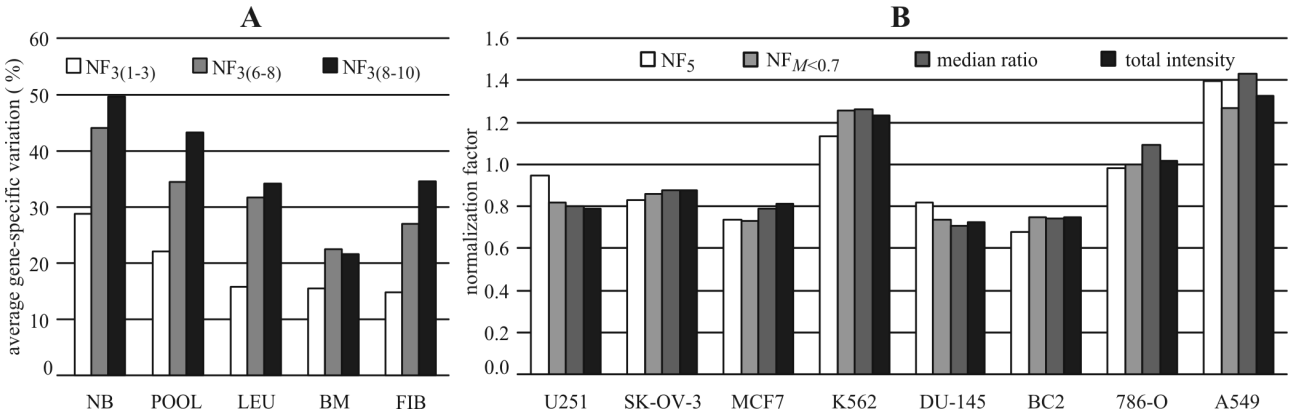

Figure 4: Validation of the gene stability measure (A) and geometric averaging of carefully selected control genes for normalization (B). A: Average gene-specific variation (determined as coefficient of variation, in %) for the 3 control genes with the smallest variation within each tissue panel after normalization with 3 different factors calculated as the geometric mean of the 3 control genes with the lowest ($NF_{3(1-3)}$), highest ($NF_{3(8-10)}$) and intermediate ($NF_{3(6-8)}$) gene stability values (as determined by *geNorm*) (NB: neuroblastoma, POOL: normal pooled tissues, LEU: leukocytes, BM: bone marrow, FIB: fibroblasts). B: Comparison of frequently applied microarray scaling factors and the proposed RT-PCR normalization factor based on the geometric mean of selected control genes (NF_5: geomean of the 5 control genes with the lowest *M* value, $NF_{M<0.7}$: geomean of control genes with *M* value lower than 0.7; see Result section), calculated for 8 hybridizations from publicly available microarray data [14].

the above, we recommend the minimal use of the 3 most stable internal control genes for calculation of an RT-PCR normalization factor (NF_n, n=3), and stepwise inclusion of more control genes until the $(n+1)^{th}$ gene has no significant contribution to the newly calculated normalization factor (NF_{n+1}). To determine the possible need or use of including more than 3 genes for normalization, the pairwise variation $V_{n/n+1}$ was calculated between the two sequential normalization factors (NF_n and NF_{n+1}) for all samples within the same tissue panel (with $a_{ij}=NF_{n,i}$ and $a_{ik}=NF_{n+1,i}$, *n* the number of genes used for normalization ($3 \leq n \leq 9$), and *i* the sample index; see Equation 2 and 3). A large variation means that the added gene has a significant effect and should preferably be included for calculation of a reliable normalization factor. For all tissue types, normalization factors were calculated for the three most stable control genes (i.e. with the lowest *M* value) and for 7 additional factors by stepwise inclusion of the most stable remaining control gene. Pairwise variations were subsequently calculated for every series of NF_n and NF_{n+1} normalization factors, reflecting the effect of adding an $(n+1)^{th}$ gene (Figure 3 top). It is apparent that the inclusion of a 4^{th} gene has no significant effect (i.e. low $V_{3/4}$ value) for leukocytes, fibroblasts and bone marrow. This is also illustrated by the nearly perfect correlation between NF_3 and NF_4 values, as shown for fibroblasts in Figure 3 bottom. Based on these data, we decided to take 0.15 as a cut-off value, below which the inclusion of an additional control gene is not required. For neuroblastoma and the pool of normal tissues, one and two additional genes, respectively, are necessary for reliable normalization (see also Figure 3 bottom). The high $V_{8/9}$ and $V_{9/10}$ values for the normal pool, neuroblastoma, and leukocyte panel corroborate very well the findings obtained by stepwise exclusion of the worst scoring control gene (Figure 2). This analysis showed an initial steep decrease in average *M* value,

Table 2: Primer sequences internal control genes

symbol †	forward primer	reverse primer
ACTB	CTGGAACGGTGAAGGTGACA	AAGGGACTTCCTGTAACAATGCA
B2M	TGCTGTCTCCATGTTTGATGTATCT	TCTCTGCTCCCCACCTCTAAGT
GAPD	TGCACCACCAACTGCTTAGC	GGCATGGACTGTGGTCATGAG
HMBS *	GGCAATGCGGCTGCAA	GGGTACCCACGCGAATCAC
HPRT1	TGACACTGGCAAAACAATGCA	GGTCCTTTTCACCAGCAAGCT
RPL13A	CCTGGAGGAGAAGAGGAAAGAGA	TTGAGGACCTCTGTGTATTTGTCAA
SDHA	TGGGAACAAGAGGGCATCTG	CCACCACTGCATCAAATTCATG
UBC	ATTTGGGTCGCGGTTCTTG	TGCCTTGACATTCTCGATGGT
YWHAZ	ACTTTTGGTACATTGTGGCTTCAA	CCGCCAGGACAAACCAGTAT

† *TBP* primer sequences are described in [23]

* *HMBS* primer sequences kindly provided by E Mensink and L van de Locht (Nijmegen, The Netherlands)

Table 3: Ranking of control genes according to their expression stability (increasing from top to bottom) *

neuroblastoma	fibroblast	leukocyte	bone marrow	normal pool
B2M	*HMBS*	*ACTB*	*ACTB*	*B2M*
RPL13A	*B2M*	*HMBS*	*B2M*	*ACTB*
ACTB	*RPL13A*	*HPRT1*	*HMBS*	*YWHAZ*
TBP	*SDHA*	*SDHA*	*TBP*	*RPL13A*
YWHAZ	*TBP*	*TBP*	*SDHA*	*UBC*
HMBS	*ACTB*	*RPL13A*	*GAPD*	*TBP*
UBC	*UBC*	*GAPD*	*HPRT1*	*HPRT1*
SDHA	*YWHAZ*	*B2M*	*YWHAZ*	*HMBS*
HPRT1 - GAPD	*HPRT1 - GAPD*	*UBC - YWHAZ*	*UBC - RPL13A*	*SDHA - GAPD*

* the two most stable control genes can't be further ranked due to the required use of gene ratios for expression stability measurements

pointing at two aberrantly expressed control genes for leukocytes and one unstable gene for neuroblastoma and the pool of normal tissues. Furthermore, the need to include additional control genes for these last two tissue panels is in keeping with the high variation in control gene expression as evidenced from Figure 2.

Validation of proposed real-time RT-PCR normalization factors

To assess the validity of the established gene stability measure, i.e. that genes with the lowest *M* values have indeed the most stable expression, we determined the gene-specific variation for each control gene as the variation coefficient of the expression levels after normalization. This coefficient should be minimal for proper housekeeping genes. Three different normalization factors were calculated, based on the geometric mean of 3 genes with respectively the lowest ($NF_{3(1-3)}$), the highest ($NF_{3(8-10)}$), and intermediate *M* values ($NF_{3(6-8)}$) (as determined by *geNorm*). We subsequently determined the average gene-specific variation of the 3 genes with the most stable expression (i.e. the lowest variation coefficient) for each normalization factor and within each tissue panel (Figure 4A). It is clear that the gene-specific variation in all tissue panels is by far the smallest when the data are normalized to $NF_{3(1-3)}$. This demonstrates that the gene stability measure effectively identified the control genes with the most stable expression. To verify that a high *M* value is characteristic for an unstable or differentially expressed gene, we analyzed the expression level of *MYCN* –a highly differentially expressed proto-oncogene in neuroblastoma with prognostic value [13]– together with the set of 10 housekeeping genes. *MYCN* was readily identified as the most differentially expressed gene, with an *M* value of 6.02 compared to 2.17 for the least stable control gene *B2M* in neuroblastoma. It was further observed that normalization with a single control gene consistently resulted in significantly higher gene-specific variations of the other control genes (data not shown), which underscores the improved normalization by using multiple housekeeping genes.

To further validate the accuracy of geometric averaging of carefully selected control genes for normalization, the geometric means of housekeeping gene expression levels from publicly available microarray data were compared with commonly applied

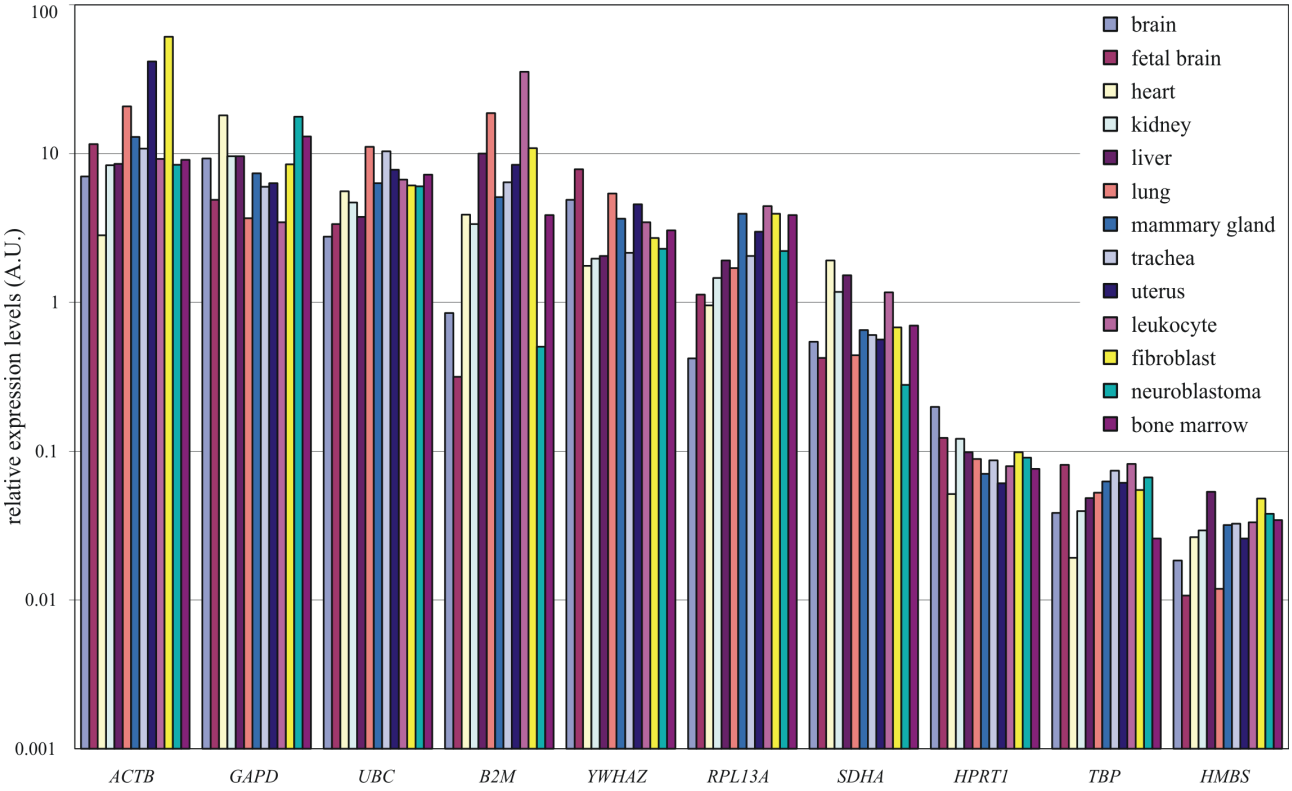

Figure 5: Logarithmic histogram of the expression levels of 10 internal control genes determined in 13 different human tissues.

microarray normalization factors calculated for the same data. To this purpose, an 8000 gene array data set [14] was chosen containing 9 of the 10 control genes evaluated in this RT-PCR study. Two commonly applied microarray normalization factors (based on median ratio normalization, and total intensity normalization) [15-17] were determined for 8 randomly selected hybridization sets. Subsequently, for each hybridization set, the background corrected expression levels of 9 housekeeping genes for the two fluorescence channels were imported in *geNorm* and ranked as described for the RT-PCR data. As these microarray data originate from hybridizations of cell lines from various histological origin versus a reference pool of multiple cell lines, we have calculated the geometric mean of the 5 most stable control genes (NF_5) for each hybridization set, in accordance to the recommendations for reliable normalization within a heterogeneous tissue panel (see previous paragraph). Alternatively, internal control genes were stepwise excluded until the *M* values of the remaining genes were below 0.7 (experimental value shown to eliminate the most variable and outlying genes in this microarray dataset). Depending on the hybridization set, 7 to 9 genes fitted this criterion, upon which the geometric mean was calculated ($NF_{M<0.7}$). Both normalization factors (NF_5 and $NF_{M<0.7}$) were shown to be similar to the calculated microarray normalization factors (Figure 4B).

Tissue specific housekeeping gene expression

In order to compare the control gene expression levels within the heterogeneous group of all 13 tested tissues, the same set of control genes should be used for normalization. We therefore calculated the geometric mean of 6 control genes that were withheld from the set of 10 genes after elimination of the two genes with the highest *M* value within each tissue panel (i.e. *B2M*, *RPL13A*, *ACTB* and *HMBS*) (see Table 3). Given the large variety of tested tissues, this is the optimal strategy to eliminate most variation, and to allow direct comparison between the different samples. Under the assumption of equal PCR threshold cycle values for equal transcript numbers of different genes, an estimation of the transcript abundance of the various control genes can be made. Figure 5 shows that the 10 tested genes belong to various abundance classes, with an approximately 400 fold expression difference between the most abundant (*ACTB*) and most rare (*HMBS*) transcript. Although the overall abundance of a given control gene in the different tissues is relatively similar, we clearly observe tissue specific expression differences, e.g. *B2M* is 112 fold higher expressed in leukocytes compared to fetal brain, and *ACTB* shows an expression difference of 22 fold between fibroblasts and heart tissue. It is also clear that some genes display a relatively constant expression level (e.g. *UBC* and *HPRT1*) compared to the differential expression pattern of others (e.g. *B2M* and *ACTB*).

Discussion

Accurate normalization of gene expression levels is an absolute prerequisite for reliable results, especially

when the biological significance of subtle gene expression differences is studied. Still, little attention has been paid to the systematic study of normalization procedures and the impact on the conclusions. For RT-PCR, there is a general consensus of using a single control gene for normalization purposes. A comprehensive literature analysis of expression studies published in high impact journals during 1999 indicated that *GAPD*, *ACTB*, 18S and 28S rRNA were used as single control genes for normalization in more than 90% of the cases [11]. As numerous studies reported that housekeeping gene expression can vary considerably [6, 9-12], the validity of the conclusions is highly dependent on the applied control. Some laboratories have tried to find the optimal control gene for their experimental system, and often rRNA molecules were proposed as best references. Caution has to be taken with these studies, as often only the expression variation of tested genes with respect to the mass loading of total RNA was assessed. As the rRNA molecules make up the bulk of total RNA, they should indeed correlate very well with the total RNA mass, but that does not necessarily make them good control genes. As outlined in the introduction, total RNA and ribosomal RNA levels are no proper references, due to the observed imbalance between ribosomal and messenger RNA fractions.

In addition to the search for a stable control gene, we aimed at determining the errors related to the common practice of single control normalization. In this study, we have provided evidence that a conventional normalization strategy based on a single housekeeping gene leads to erroneous normalization up to 3.0 and 6.4 fold in 25% and 10% of the cases, respectively, with sporadic cases showing error values above 20. This analysis demonstrated that a few control genes were unstable and significantly differentially expressed in some tissue panels, as evidenced from the 5.9 to 4.5 decrease in 90th percentile single control normalization error value for neuroblastoma by leaving out the *B2M* gene (not shown). This finding is in keeping with the reported differential expression of *B2M* in neuroblastoma, corresponding to the stage of differentiation of the tumor cells [18]. The error distribution curves not only reflect the expression stability of the applied controls, but also the sample heterogeneity within a tissue panel, as noticed from the less steeper curve for the heterogeneous set of normal pooled tissues compared to the other relatively homogeneous tissue panels. With regard to this, the issue has been raised that finding proper control genes is even more important when working with tissues from different histological origin [9].

The single control normalization error values point at inherent noisy oscillations in expression level of the control genes, a finding which has been corroborated in other large scale reports where several thousand genes were measured in different cells or tissues by means of microarray analysis. No gene was found on an 8000 feature array that did not vary by ratios of at least 2 fold across a panel of 60 cell lines [14], and a set of genes frequently used for normalization (including *GAPD* and *ACTB*) was found to vary in expression by 7- to 23-fold [9]. Taken all together, our data and these studies clearly demonstrate that ideal and universal control genes do not exist. This warrants the search for stably expressed genes in each experimental system, and for the development of an accurate normalization strategy.

In order to validate the expression stability of tested control genes without any prior assumption of metric for standardization, we had initially measured the correlation between the raw, non-normalized expression levels of any two control genes, which should be nearly perfect for proper control genes. We observed however that the data range between the minimum and maximum expression levels, or any outlying value could have a profound influence on the slope of the regression line, and consequently on the value of the correlation coefficient. This made Pearson and Spearman correlation coefficients not suitable for this kind of analysis. We have therefore developed a new stability measure, based on the principle that the expression ratio of two proper control genes should be identical in all samples, regardless of the experimental condition or cell type, with increasing ratio variation according to decreasing expression stability of one (or both) of the tested genes. The proposed standard deviation of log transformed control gene ratios is a robust measure for the variation between two control genes, as it does not impose any requirements for normality or homoscedasticity of the data points. Furthermore, this measure is independent of the abundance difference between the genes, and equally affected by any outlying or extreme ratio (i.e. outliers for a sample with low or high overall expression, or outliers caused by an upregulated or downregulated gene have an equivalent increase in pairwise variation *V*). Logarithmic transformation of the ratios is required for symmetrical distribution of the data around zero, resulting in equal absolute values (but opposite signs) for a given ratio and the inverse ratio. As a result, the standard deviation of log transformed ratios is identical to the standard deviation of log transformed inverse ratios, which makes this measure characteristic for every combination of two genes.

Having established a robust measure to assess the expression variation between two control genes, we subsequently defined a gene stability measure *M* as the average pairwise variation between a particular gene and all other control genes. Using our in-house developed VBA applet *geNorm*, we ranked 10 commonly used housekeeping genes belonging to different functional and abundance classes according to their expression stability in 5 tested tissue panels. The clear decrease of the average gene stability measure *M* value of the remaining control genes during stepwise exclusion of the worst scoring gene points at gene-specific expression stability differences and demonstrates that the remaining genes are more stably expressed compared to the excluded genes. Some tissue panels show a relatively steep initial decline, which reflect the exclusion of one or more aberrantly expressed control genes (e.g. *ACTB* and *HMBS* for leukocytes), as also noticed from the single control normalization error analyses (cf. supra). The average gene stability values of the remaining genes during stepwise elimination of the least stable control genes also indicates tissue specific differences, with bone marrow and the pool of normal tissues having the lowest and highest overall

expression variation, respectively. The latter is no surprise, given the larger tissue heterogeneity in this panel. The question if the observed high variation for neuroblastoma is a cancer related phenomenon of deregulated expression is currently under further investigation. From these analyses, it is clear that there is no universal control gene suitable for all cell types. *ACTB* and *B2M* appear to be the worst scoring genes, while *UBC*, *GAPD* and *HPRT1* seem to be the best overall control genes, each belonging to the four most stable genes in 4 out of 5 tested tissues. However, caution has to be taken with these generalizations. *B2M* appears to be one of the least stable control genes, but nevertheless is a good choice for normalization of leukocyte expression levels. This clearly demonstrates that a proper choice of housekeeping genes is highly dependent on the tissues or cells under investigation. This point is even made stronger when considering the transcript abundance differences of some control genes between the various tissues. The large expression differences between the tested tissues for *B2M* and *ACTB* for instance would definitely result in large normalization errors when used for standardization. Interestingly, the observed tissue specific expression of these control genes is in keeping with their known role or function: high *B2M* expression in leukocytes, where it's a major cell surface marker, and relatively low non-muscle cytoskeletal *ACTB* expression in heart tissue that is predominantly of muscular origin.

With the ability to rank control genes according to their expression stability, and given the observed inherent expression variation (resulting in relatively large single control normalization errors), we proposed the use of at least 3 proper control genes for calculation of a normalization factor. We also presented a procedure to determine whether or not more than 3 control genes were required for reliable normalization. This analysis clearly showed that 3 stable control genes sufficed for accurate normalization of samples with relatively low expression variation (e.g. leukocytes, fibroblasts and bone marrow). For the other tissue panels, a fourth and fifth control gene were required to capture the observed variation in neuroblastoma and the pool of normal human tissues, respectively.

The purpose of normalization is to remove the sampling differences (such as input amount and RNA quality) in order to identify real gene-specific variation. For proper internal control genes, this variation should be minimal or nihil. To validate the expression stability measure *M* and the *geNorm* algorithm to identify the most stable control genes in a set of samples, we have calculated the gene-specific variation for each gene as the coefficient of variation of normalized expression levels. To this purpose, the raw expression values were standardized to different normalization factors, calculated as the geomean of the most, intermediate or least stable control genes (as determined by *geNorm*). The rationale of this analysis is that a normalization factor based on proper internal control genes should remove all non-specific variation. In contrast, unstable control genes cannot completely remove the non-specific variation, and even add additional variation, resulting in larger so-called gene-specific variations for the tested control genes. This analysis clearly demonstrated that most non-specific variation was removed when the most stable control genes (as determined by *geNorm*) were used for normalization, which proves that the novel stability measure and presented strategy effectively allowed the assessment of gene expression stability in the different tissue panels.

Further validation demonstrated that the geometric mean of carefully selected control genes is an accurate estimate for the mRNA transcript fraction, as determined by comparison with frequently applied microarray normalization factors. Although both RT-PCR normalization factors based on geometric averaging are relatively similar, the one based on at least 7 control genes (i.e. $NF_{M<0.7}$) is slightly more equivalent to the microarray scaling factors. Two possible explanations can account for this observation. First of all, the 5 most stable control genes as determined by *geNorm* are based on only 2 RNA samples (i.e. a Cy3 labeled reference pool, and a Cy5 labeled test sample), in contrast to the RT-PCR data, where 9 to 34 samples were used, resulting in more reliable estimation of the expression stability. Secondly, recent technical reports clearly state that array hybridization analyses experience considerable –often underestimated– variation and uncertainty at several levels. Accurate background fluorescence correction and spot quality assessment, amongst others, have been described as critical issues for reliable ratio estimation [19-21]. The higher variability associated with array hybridization results might thus explain the need for more control genes to normalize the data. Nevertheless, this study clearly showed that normalization based on the geometric mean of carefully selected control genes result in equivalent ratio estimation compared to commonly applied array scale factors, which validates its use for RT-PCR normalization. In addition, the presented method could easily be applied to normalize gene expression levels resulting from microarray hybridization experiments, where only a limited number of genes are spotted, including some housekeeping genes.

In conclusion, we described and validated a procedure to identify the most stable control genes in a given set of tissue samples, and to determine the optimal number of genes required for reliable normalization of RT-PCR data. The presented strategy can be applied to any number or kind of genes or tissues, and should allow more accurate gene expression profiling. This is of utmost importance for studying the biological significance of subtle expression differences, and for confirmative and/or extended analyses of microarray results by means of RT-PCR.

Materials and Methods

Sample preparation

Thirty-four neuroblastoma cell lines were grown to subconfluency according to standard culture conditions. RNA was isolated using the RNeasy Midi Kit (Qiagen) according to the manufacturer's instructions. Nine RNA samples from pooled normal human tissues (heart, brain, fetal brain, lung, trachea, kidney, mammary gland, small intestine and uterus) were obtained from Clontech. Blood and fibroblast biopsies were obtained from 13 and

14 different normal healthy individuals, respectively. Thirteen leukocyte samples were isolated from 5 ml fresh blood using Qiagen's erythrocyte lysis buffer. Fibroblast cells from 20 upper arm skin biopsies were short time cultured (3-4 passages) according to standard procedures. Bone marrow samples were obtained from 9 patients with no hematological malignancy. Total RNA of leukocyte, fibroblast and bone marrow samples was extracted using the Trizol reagent (Invitrogen), according to the manufacturer.

Real-time RT-PCR

DNase treatment, cDNA synthesis, primer design and SYBR Green I RT-PCR were performed as described [22]. In brief, two micrograms of each total RNA sample was treated with the RQ1 RNase-free DNase according to the manufacturer (Promega). Treated RNA samples were desalted prior to cDNA synthesis using Microcon-100 spin columns (Millipore). First strand cDNA was synthesized using random hexamers and SuperscriptII RT-enzyme according to the manufacturer (Invitrogen), and subsequently diluted with nuclease free water (Sigma) to 12.5 ng/μl cDNA. RT-PCR amplification mixtures (25 μl) contained 25 ng template cDNA, 2X SYBR Green I Master Mix buffer (12.5 μl) (Applied Biosystems) and 300 nM of forward and reverse primer. Reactions were run on an ABI PRISM 5700 Sequence Detector (Applied Biosystems). The cycling conditions comprised 10 min polymerase activation at 95° C and 40 cycles at 95° C for 15s and 60° C for 60s. Each assay included (in duplicate): a standard curve of 4 serial dilution points of SK-N-SH or IMR-32 cDNA (ranging from 50 ng to 50 pg), a no-template control, and 25 ng of each test cDNA. Sequence Detection Software (version 1.3) (Applied Biosystems) results were exported as tab delimited text files and imported in Microsoft Excel for further analysis. The median coefficient of variation (based on calculated quantities) of duplicated samples was 6%.

Single control normalization error E

For any given *m* tissue samples, real-time RT-PCR gene expression levels a_{ij} of *n* internal control genes are measured. For every combination of two tissue samples *p* and *q*, and every combination of two internal control genes *j* and *k*, the single control normalization error *E* was calculated (1). This is the fold expression difference between samples *p* and *q* when normalized to housekeeping gene *j* or *k*.

$(\forall j,k \in [1,n],\ \forall p,q \in [1,m],\ j \neq k$ and $p \neq q)$:

$$R_{jkpq} = \frac{a_{qj}}{a_{qk}} \cdot \frac{a_{pk}}{a_{pj}}$$ (if $R<1$, then $E=R^{-1}$, else $E=R$) (1)

Internal control gene stability measure M

For every combination of two internal control genes *j* and *k*, an array A_{jk} of *m* elements is calculated which consist of $\log_2$ transformed expression ratios a_{ij}/a_{ik} (2). We define the pairwise variation V_{jk} for the control genes *j* and *k* as the standard deviation of the A_{jk} elements (3). The expression stability measure M_j for control gene *j* is the arithmetic mean of all pairwise variations V_{jk} (4).

Array data normalization

Publicly available raw microarray data [14] were downloaded as tab delimited files. Eight hybridization data sets were randomly selected and imported in Microsoft Excel software for further manipulation (MCF7, DU-145, 786-0, BC2, K562, A549, U251,and SK-OV-3). For each hybridization array, all spots with Cy3 or Cy5 fluorescence intensities below the average overall background level plus one standard deviation were discarded. Subsequently, a local background correction for each spot was applied. Two scale factors were calculated for each slide based on median ratio normalization (median ratio set to 1) and total intensity normalization (equalized sum of fluorescence intensities for both channels). Nine housekeeping genes were identified by BLAST similarity or keyword search against the database of cDNA clones present on the array (see IMAGE clones listed in Table 1).

Acknowledgments

We would like to thank H De Preter for writing the Visual Basic application for Microsoft Excel; G Berx (Ghent, Belgium) for critical reading of the manuscript; and M Vidaud (Paris, France) and E Mensink / A van de Locht (Nijmegen, The Netherlands) for providing us with *TBP* and *HMBS* primer sequences respectively; L Nuytinck for the fibroblast RNA samples, and G De Vos and P Degraeve (Ghent, Belgium) for culturing the cell lines. KDP and BP are supported by a grant from the FWO. NVR is a postdoctoral researcher from the FWO. This study was also supported by the Flemish Institute for the Promotion of Scientific Technological Research in Industry (IWT), FWO-grant G.0028.00, GOA-grant 12051397 and BOF-grants 011B4300 and 011F1200.

$(\forall j,k \in [1,n]$ and $j \neq k)$:

$$A_{jk} = \left\{ \log_2\left(\frac{a_{1j}}{a_{1k}}\right), \log_2\left(\frac{a_{2j}}{a_{2k}}\right), \cdots, \log_2\left(\frac{a_{mj}}{a_{mk}}\right) \right\} = \left\{ \log_2\left(\frac{a_{ij}}{a_{ik}}\right) \right\}_{i=1\to m} \quad (2)$$

$$V_{jk} = st.dev\,(A_{jk}) \quad (3)$$

$$M_j = \frac{\sum_{k=1}^{n} V_{jk}}{n-1} \quad (4)$$

References

1. Schena M, Shalon D, Davis RW, Brown PO: **Quantitative monitoring of gene expression patterns with a complementary DNA microarray**. *Science* 1995, **270**:467-470.
2. Fink L, Seeger W, Ermert L, Hanze J, Stahl U, Grimminger F, Kummer W, Bohle RM: **Real-time quantitative RT-PCR after laser-assisted cell picking**. *Nat Med* 1998, **4**:1329-1333.
3. Heid CA, Stevens J, Livak KJ, Williams PM: **Real time quantitative PCR**. *Genome Res* 1996, **6**:986-994.
4. Higuchi R, Fockler C, Dollinger G, Watson R: **Kinetic PCR analysis: real-time monitoring of DNA amplification reactions**. *Biotechnology (NY)* 1993, **11**:1026-1030.
5. Solanas M, Moral R, Escrich E: **Unsuitability of using ribosomal RNA as loading control for Northern blot analyses related to the imbalance between messenger and ribosomal RNA content in rat mammary tumors**. *Anal Biochem* 2001, **288**:99-102.
6. Spanakis E: **Problems related to the interpretation of autoradiographic data on gene expression using common constitutive transcripts as controls**. *Nucleic Acids Res* 1993, **21**:3809-3819.
7. Johnson ML, Redmer DA, Reynolds LP: **Quantification of lane-to-lane loading of poly(A) RNA using a biotinylated oligo(dT) probe and chemiluminescent detection**. *Biotechniques* 1995, **19**:712-715.
8. Warner JR: **The economics of ribosome biosynthesis in yeast**. *Trends Biochem Sci* 1999, **24**:437-440.
9. Warrington JA, Nair A, Mahadevappa M, Tsyganskaya M: **Comparison of human adult and fetal expression and identification of 535 housekeeping/maintenance genes**. *Physiol Genomics* 2000, **2**:143-147.
10. Thellin O, Zorzi W, Lakaye B, De Borman B, Coumans B, Hennen G, Grisar T, Igout A, Heinen E: **Housekeeping genes as internal standards: use and limits**. *J Biotechnol* 1999, **75**:291-295.
11. Suzuki T, Higgins PJ, Crawford DR: **Control selection for RNA quantitation**. *Biotechniques* 2000, **29**:332-337.
12. Bustin SA: **Absolute quantification of mRNA using real-time reverse transcription polymerase chain reaction assays**. *J Mol Endocrinol* 2000, **25**:169-193.
13. Maris JM, Matthay KK: **Molecular biology of neuroblastoma**. *J Clin Oncol* 1999, **17**:2264-2279.
14. Ross DT, Scherf U, Eisen MB, Perou CM, Rees C, Spellman P, Iyer V, Jeffrey SS, Van de Rijn M, Waltham M*, et al.*: **Systematic variation in gene expression patterns in human cancer cell lines**. *Nat Genet* 2000, **24**:227-235.
15. Quackenbush J: **Computational analysis of microarray data**. *Nat Rev Genet* 2001, **2**:418-427.
16. Hess KR, Zhang W, Baggerly KA, Stivers DN, Coombes KR: **Microarrays: handling the deluge of data and extracting reliable information**. *Trends in Biotechnology* 2001, **19**:463-468.
17. Duggan DJ, Bittner M, Chen Y, Meltzer P, Trent JM: **Expression profiling using cDNA microarrays**. *Nat Genet* 1999, **21**:10-14.
18. Cooper MJ, Hutchins GM, Mennie RJ, Israel MA: **Beta 2-microglobulin expression in human embryonal neuroblastoma reflects its developmental regulation**. *Cancer Res* 1990, **50**:3694-3700.
19. Tseng GC, Oh MK, Rohlin L, Liao JC, Wong WH: **Issues in cDNA microarray analysis: quality filtering, channel normalization, models of variations and assessment of gene effects**. *Nucleic Acids Res* 2001, **29**:2549-2557.
20. Yang MC, Ruan QG, Yang JJ, Eckenrode S, Wu S, McIndoe RA, She JX: **A statistical method for flagging weak spots improves normalization and ratio estimates in microarray**. *Physiol Genomics* 2001, **7**:45-53.
21. Brown CS, Goodwin PC, Sorger PK: **Image metrics in the statistical analysis of DNA microarray data**. *Proc Natl Acad Sci U S A* 2001, **98**:8944-8949.
22. Vandesompele J, De Paepe A, Speleman F: **Elimination of primer-dimer artefacts and genomic co-amplification using a two-step SYBR Green I real-time RT-PCR**. *Anal Biochem* (2002)
23. Bieche I, Laurendeau I, Tozlu S, Olivi M, Vidaud D, Lidereau R, Vidaud M: **Quantitation of MYC gene expression in sporadic breast tumors with a real-time reverse transcription-PCR assay**. *Cancer Res* 1999, **59**:2759-2765.

Subtractive expression profiling of neuroblastoma: identification of new candidate genes and predictors for clinical outcome

Jo Vandesompele, et al. (in preparation)

INTRODUCTION

Neuroblastoma is one of the most frequent pediatric solid tumors, and accounts for more deaths in childhood than any other cancer. Despite significant new insights in the genomic heterogeneity of this malignancy, only few genes have been recognized to play a role in neuroblastoma, and if so, only in a subgroup of tumors. In this respect, amplification and overexpression of the proto-oncogene *MYCN*, and concurrent deletion or silencing of the *CASP8* gene have been reported in a subset of aggressive high stage tumors[1, 2]. Clearly, additional hitherto unidentified genes must be involved in this subgroup, as deletion of the distal part of chromosome arm 1p, and gain of distal 17q are almost invariably found in these tumours[3]. Furthermore, the critical genes located in other regions that show frequently loss of heterozygosity (such as 3p, 4p, 9p, 11q, 14q and 18q) remain to be identified (for overview see ref. [4]). Of particular importance are deletions of chromosome 11q and 3p, which were recently shown to delineate a distinct genetic subgroup of high stage tumors in the absence of *MYCN* amplification, 1p deletion, or both[5-7].

In an attempt to identify relevant neuroblastoma genes on a transcriptome wide basis, we performed subtractive expression profiling between two neuroblastoma cell lines that belong to different genetic subgroups (i.e. presence or absence of *MYCN* amplification, 1p- and 11q-deletion). This PCR based strategy allows selective cloning of cDNA fragments that are specifically expressed in each of the two cell lines[8]. The main advantages of this method are the possibility to identify as yet unknown and low abundant differentially expressed genes, and the physical availability of the isolated cDNA clones for downstream applications such as Northern blot and microarray analysis. A non-redundant cDNA library of 300 different genes was generated, of which 50 were used for real-time RT-PCR expression profiling of neuroblastoma cell lines and primary tumors. In addition, we determined the expression level of 26 genes that were selected as candidate neuroblastoma genes located in critical regions, *MYCN* transcriptional target genes, markers for sympathetic nervous system development, prognostic markers, or genes with a reported differential expression pattern in neuroblastoma. All together, this resulted in an unprecedented number of neuroblastoma specific differentially expressed genes that were studied on a large panel of both cell lines and primary tumors. The major aims of this study were to find genes whose expression pattern was correlated with known biological and clinical features, and improve tumor classification and prediction of prognosis; to test the validity of the SSH procedure to generate neuroblastoma specific differentially expressed cDNA libraries for downstream applications; and to assess the power of real-time RT-PCR based expression profiling of a limited number of carefully selected differentially expressed genes. Furthermore, the simultaneous analysis of both SSH clones and literature based genes that were mostly studied as separate entities in previous reports allowed us to determine associations between these genes, and interpret and validate the expression data from hitherto unknown genes in neuroblastoma biology.

MATERIAL & METHODS

Cell lines and tissues

Thirty-three neuroblastoma cell lines and one Ewing sarcoma line SK-N-MC (Table 1) were karyotyped according to standard procedures. FISH-analysis with region specific probes and chromosome paints were reported earlier for 15 cell lines[9, 10]. CGH data and M-FISH results on 16 cell lines have been published[11, 12]. Cell lines were tested for 1p-, 3p- and 11q deletion by FISH, and tested for *MYCN*-amplification by FISH and Q-PCR analysis as described[9, 13]. Twenty-seven primary NB tumors were staged according to the INSS[14] (Table 2). All samples were validated by the pathologist, contained more than 70% tumor cells and were analyzed for 1p-deletion and *MYCN*-amplification as described above. Real-time PCR demonstrated marker gene expression of *GAP43* and *HAND2* in all tumor samples. Nine normal control RNAs were obtained from Clontech: adult brain (A), heart (B), kidney (C), liver (D), lung (E), trachea (F), fetal brain (G), mammary gland (H), and uterus (I).

RNA extraction

Cell lines were grown to subconfluency in RPMI 1640 (Invitrogen) supplemented with antibiotics, 15% fetal calf serum and 1% L-glutamine. Cells from 4 tissue culture flasks (75 cm^2) were pelleted, quick frozen in liquid N2 and stored at –80° C. Tumor biopsies were homogenized with an Ultra-Turrax T25 (IKA-Werke) in 2ml RNeasy lysis buffer (Qiagen). Total RNA of cell lines and biopsies was isolated using the RNeasy Midi Kit (Qiagen), and mRNA was extracted from SK-N-SH and IMR-32 with the FastTrack kit (Invitrogen), both according to the manufacturer's instructions. RNA was quantified using the Ribogreen reagent (Molecular Probes) on a TD-360 fluorometer (Turner Designs).

Suppression subtractive hybridization (SSH)

Starting from 2 µg of mRNA from cell lines SK-N-SH and IMR-32, SSH was performed with the PCR-Select cDNA Subtraction kit (Clontech) as described by the manufacturer. The PCR product mixture of putative differentially expressed genes was subcloned into the pGEM-T Easy vector (Promega) and propagated in DH5α E. coli. Up to 1920 clones were picked, grown in twenty 96-well plates and stored as glycerol stocks at -80° C for further analysis.
Differential screening to eliminate possible false positive clones was performed according to the guidelines described in the Differential Screening kit (Clontech).

DNA sequencing and analysis

SSH clones were PCR amplified using SP6 and T7 vector specific sequences flanking the cloning site. PCR products were exonuclease/phosphatase treated and cycle sequenced using BigDyeTerminator chemistry on an ABI377 (Applied Biosystems) with primers that annealed to the SP6 or T7 sequences. Similarity searches were performed using the BLAST algorithm after removing vector and masking repeat sequences (RepeatMasker). Sequence alignment and EST contig building were performed using the freely available BioEdit package[15].

Northern blot hybridization

Fifteen µg of total RNA was mixed with an equal volume of denaturing buffer (66% DMSO, 12% glyoxal, 33 mM sodium phosphate buffer (pH 7.0)), incubated for 1 hr at 50° C, chilled on ice, mixed with 1/10th volume of loading buffer, separated on 1% agarose gel prepared in 20 mM sodium phosphate buffer (pH 7.0) and blotted onto Hybond-N+ nylon membranes (Amersham Biosciences). Methylene blue staining of blots was carried out to ensure equal RNA loading. Blotted membranes were hybridized overnight at 65 °C in 1 mM EDTA, 0.5 M sodium phosphate (pH 7.2), 1% BSA and 7% SDS. DNA probes for hybridization were obtained by PCR amplification of SSH clones of interest. After purification of PCR products on a QIAquick column (Qiagen), probes were labeled with αP32-dCTP by random primer labeling (MEGAprime, Amersham Biosciences) and purified on a Micro Bio-spin P-30 column (Bio-Rad). After hybridization, membranes were washed four times at 65° C for 30 min in buffers with 1 mM EDTA, 1% SDS and decreasing concentrations of sodium phosphate (pH 7.2) (500 mM, 250 mM, 100 mM and 50 mM). Washed membranes were exposed to a phosphor imaging screen and scanned on a Personal FX phosphorimager (Bio-Rad).

Real-time PCR

Gene copy determination using real-time quantitative PCR based on SYBR Green I chemistry and two reference genes (*BCMA* and *SDC4*) was performed as described[13].

Relative gene expression levels were determined using an optimized two-step SYBR Green I RT-PCR assay[16] with minor modifications. After establishment of amplification efficiencies >95% for all primer pairs, the comparative Ct method was used for quantification. PCR reagents were obtained from Applied Biosystems or Eurogentec as SYBR Green I mastermixes and used according to the manufacturer's instructions. Reactions were run on an ABI5700 (Applied Biosystems) or I-Cycler (Bio-Rad). Gene expression levels were normalized using the geometric mean of the 4 most stable internal control genes in neuroblastoma (i.e. *UBC*, *HPRT1*, *SDHA* and *GAPD*) as reported previously[17].

Based on chromosomal localization and possible function, 50 SSH clones were initially selected for further study of their expression pattern in neuroblastoma. Furthermore, 26 additional known genes were also quantified. Of these, 7 genes were selected based on their reported differential expression pattern in neuroblastoma, 10 genes were neural crest or (sympathetic) lineage marker genes, 7 genes were selected as candidate neuroblastoma genes in critical regions of frequent loss or gain, and 2 were reported *MYCN* transcriptional target genes. The expression levels of all 76 genes were determined in the cell line and normal tissue panel. Due to minimal amounts of available biopsy RNA, only 37 genes (of which 27 SSH clones) were quantified in the primary tumors. These genes were predominantly selected as genes with the highest coefficient of variation in expression level observed in the cell lines. The complete expression data matrix is available as tab delimited file from the authors on request. Primer sequences for all tested genes are also available and will be deposited in a public database for real-time PCR primers, which is under construction (www.realtimepcr.ht.st).

Expression data mining

Univariate survival analysis was performed with the Kaplan-Meier method and log-rank statistic. The predictive significance of multiple variables were tested through Cox proportional hazards modelling. Hierarchical cluster analysis and visualization was performed with Cluster and TreeView[18]. The gene expression data matrix for cluster analysis was log transformed and subsequently mean centered for the rows (genes). The SAM algorithm was used for supervised identification of differentially expressed genes between predefined sample goups[19]. Principal component analysis was performed using the java-based J-Express package[20], to reduce the dimensionality into two or three viewable dimensions, representing linear combinations of genes that account for most variance in the original data set. Non-parametric Mann-Whitney testing was used for identification of significantly differentially expressed genes between samples with or without a specific genetic defect (a two-sided p value below 0.05 was considered statistically significant).

RESULTS

Subtractive cDNA cloning and non-redundant library generation

In order to isolate specifically expressed genes in each cell line, two parallel subtractions were carried out with IMR-32 as tester and SK-N-SH as driver, and vice versa. From each subtraction, a cDNA library of 960 clones was generated. After differential screening, 281 and 265 cDNA clones were retained as IMR-32 or SK-N-SH specific transcripts, respectively, and sequenced. BLAST similarity searches querying the nr and human EST database resulted in a non-redundant list of 241 known genes, 47 UniGene clusters, and 15 anonymous ESTs (of which 7 showed no similarity with clones present in the human EST database). For each unique gene or transcript, a representative clone was selected and re-arrayed.

Interestingly, a large fraction of the isolated clones are implicated in processes related to tumor biology or development, such as genes coding for transcription factors, homeobox genes, cell cycle controllers, cell adhesion proteins, proto-oncogenes, tumor suppressor genes, and genes involved in signal transduction or chromatin remodelling. A detailed list of all clone entries will be published elsewhere.

Validation of the subtracted cDNA library

Thirty-six randomly selected cDNA clones belonging to different genes or transcripts were used as a probe for Northern blot analysis of SK-N-SH and IMR-32 (Figure 1). Five and 7 clones were exclusively expressed in SK-N-SH and IMR-32, respectively. Thirteen and 3 clones were at least 3 fold higher expressed in SK-N-SH and IMR-32, respectively. Eight clones were equally abundant in both cell lines. Summarizing, 78% (28/36) of the isolated SSH clones were differentially expressed in one or the other cell line. The identification of cDNA clones belonging to genes known to be amplified and overexpressed in IMR-32 (i.e. *MYCN*, *DDX1*, *NAG*) further demonstrated the validity of the library. Seventy percent of the non-redundant database entries contained only 1 cDNA clone, highlighting the normalizing power of the subtractive procedure which results in equalized clone abundance.

Characterization of the cell line panel

Hierarchical cluster analysis of the cell line and normal tissue expression data matrix with different similarity measures and cluster algorithms systematically resulted in grouping of the normal samples as expected, and clustering of three neuroblastoma cell lines together with the Ewing sarcoma line SK-N-MC (i.e. NB-3, NN-1 and STA-NB-9) (data not shown). Interestingly, these cell lines displayed a relatively low expression of *HAND2*, a typical neural crest derived and neuroblastoma gene expression marker[21]. To investigate if these cell lines were of true neuroblastic origin, additional neural crest, (sympathetic) nervous system and other lineage specific marker genes (*ARIX*, *PMX2B*, *KIT*, *NPY*, *CHGA*, *NOTCH1*, *HRY*, and *GAP43*) and a Ewing sarcoma specific marker (*MIC2*) were quantified. Subsequent multiclass SAM analysis of the complete gene expression data matrix based on 3 predefined sample classes (i.e. normal human tissues, the 4 above mentioned cell lines, and the remaining neuroblastoma cell lines) resulted in a list of 25 genes that were significantly differentially expressed in at least one sample class ($q<0.01$). Hierarchical cluster and principal component analysis of this gene set clearly demonstrated separate grouping of the 4 above mentioned cell lines (Figure 2). In addition, two other cell lines (GI-M-EN and SJNB-12) also displayed a deviating expression profile and clustered away form the remaining neuroblastoma cell lines. Careful examination of the expression patterns indicated that NN-1, NB-3, STA-NB-9, GI-M-EN, and SK-N-MC completely lacked any sympathetic marker normally expressed in neuroblastoma cell lines. In contrast, SJNB-12 exhibits expression of some genuine neuroblastoma and/or early neural crest markers, such as the transcription factors *ARIX* and *PHOX2B.*

Additional evidence that corroborates the observed deviating expression patterns comes from cytogenetic and immunocytochemical analyses of these cell lines. Chromosome karyotyping and (M)-FISH studies indicated that NN-1, NB-3 and STA-NB-9 either do not exhibit any chromosomal aberration, or no genetic defect typically observed in a neuroblastoma cell line (e.g. gain of 17q, *MYCN* amplification, or deletion of 1p or 11q) (data not shown). Furthermore, cell line SJNB-12 was shown to have *MYC* amplification (unpublished data), which has never been reported before in a neuroblastoma tumor. Immunocytochemical APAAP assays

demonstrated absence of GD2 disialoganglioside molecules in NN-1, NB-3, STA-NB-9, and SK-N-MC, and a heterogeneous GD2 pattern (i.e. both positive and negative cells) for SJNB-12 and GI-M-EN (not shown).
As the above mentioned cell lines clustered together with the PNET family tumor SK-N-MC, the lines were tested for 19 specific solid tumor gene fusions by means of a real-time multiplex RT-PCR as described[22]. Besides the confirmative finding of a *FLI1-EWS* fusion in SK-N-MC, no other specific translocations were detected. Based on the above presented data we decided to exclude NN-1, NB-3, STA-NB-9, GI-M-EN and SJNB-12 for further analysis of neuroblastoma specific gene expression patterns.

Identification of deletion related gene expression signatures
To identify genes whose expression pattern is related to specific genetic defects in neuroblastoma, we dichotomized the cell line panel with respect to presence or absence of deletion of 11q or 3p (see Table 1). Stratification for deletion of 1p was not possible as only 2 cell lines contained intact 1p chromosomes. For identification of deletion related genes, we tested which genes had a significant ($p<0.05$) different mean expression in the two cell line groups (Table 3), and eliminated sporadic genes that were included due to presence of one or two strong outlying values.
Two genes were found to be higher expressed in 3p deleted cell lines, and 3 were decreased, one of which is the *VHL* tumor suppressor gene on 3p25. Scatterplot analysis indicated that 3p deleted cell lines group together in the bottom left section characterized by low *VHL* and *NME1* expression (Figure 3A).
With respect to the 11q status, three genes were found to be higher expressed in deleted cell lines, and 5 genes (of which 3 are located on 11q23~q24) were significantly decreased in expression. PCA analysis of the expression levels of these 8 genes in 19 neuroblastoma cell lines allowed a perfect classification of the cell lines based on their 11q status (Figure 3B). The expression pattern of two representative genes (*IGF2* and *MCAM*) is depicted in Figure 3C.

Identification of *MYCN* downstream genes
Using the same strategy as outlined above, we identified 19 and 13 genes that were significantly differentially expressed in *MYCN* amplified vs. single copy neuroblastoma cell lines and primary tumor samples, respectively (Table 3). In parallel, supervised SAM analysis with a quantitative response metric (i.e. *MYCN* expression level) was applied, and yielded a similar set of genes (not shown).
In order to provide further clues for identification of MYCN transcriptional target genes or their downstream effectors, we compared the expression level in SK-N-SH and SKMYC2 cells. The latter cell line consists of stably transfected SK-N-SH cells with a constitutive *MYCN* expression vector[23], and it was shown that these cells displayed a 500 fold increase in *MYCN* expression compared to the parental cells, a level which is similar to the transcript abundance in the *MYCN* amplified IMR-32 cells (data not shown). Of 70 genes tested, 28 displayed a more than 2-fold expression difference (13 upregulated, and 15 downregulated), of which 10 were also differentially expressed in *MYCN* amplified vs. single copy cell lines, tumors or both (Table 4, Figure 4).

Survival analysis
Twenty-seven neuroblastoma patients for which high-quality RNA was available from tumor samples prior to therapy were subjected to SAM censored survival analysis. Twelve genes were identified that might be correlated with patient survival probability (q-value < 0.05). Kaplan-Meier survival analysis of the tumor samples dichotomized with respect to the median expression level of these genes confirmed the prognostic value for 8 of the 12 genes (log rank statistic < 0.05: Hs.28462, *MEIS1*, *GAP43*, *CALM2*; <0.01: *MYCN*, *VHL*, *DKK3*, *CD44*) (Figure 5, middle). Complete linkage hierarchical cluster analysis based on the Spearman rank correlation coefficient as a similarity measure showed three patient clusters (Figure 5, top). Cluster 1 contains 8 patients (all stage 3 or 4) with a 100% mortality rate. Cluster 2 comprises 8 patients, of which 3 died of disease (i.e. 3/3 stage 4 tumors in this cluster). Interesting to note, 2 of these 3 patients survived more than 6 years after initial diagnosis (see Table 2). Cluster 3 contains 11 patients that are still alive, and which all have a favorable stage of

disease (1, 2 or 4S) (median follow-up 54 months). Principal component analysis demonstrated that the first two components (explaining 61.3% of the expression variation) were able to classify 24/27 patients according to disease outcome (Figure 5, bottom right). To investigate the independent prognostic power of these 12 survival correlated genes, Cox regression analysis was performed. Forward conditional entering of the genes indicated that *MYCN* and *VHL* were the most significantly independent prognostic predictors, while backward entering retained the *VHL*, *DKK3*, *MEIS2* and *NPY* genes (Figure5, bottom left)

Identification of novel amplified and overexpressed transcripts

In addition to the isolation of the 3 known co-amplified genes located at 2p24 in cell line IMR-32 (i.e. *MYCN*, *DDX1* and *NAG*, see above), 16 other partial cDNA clones in the SSH library were shown to be amplified and overexpressed in cell line IMR32. One clone was part of the *MEIS1* homeobox gene (2p14) that was recently shown to be amplified in IMR-32[24, 25]. Extensive transcript mapping, homology searches and EST contig building indicated that 11 other cDNA clones presumably belonged to 2 novel genes. One is located close to the *MEIS1* gene, but appears to be only highly expressed in IMR-32. A second transcript is located 500 kb telomeric to *NAG*, and is amplified in 12% of 75 studied *MYCN* amplified neuroblastomas. The 4 remaining clones are located in the large 150 kb intron of *NAG* between exon 4 and 5, and were shown to be amplified and overexpressed in 45% of the *MYCN* amplified neuroblastomas. BLAST analysis of the human EST database with exon 4 and 5 of the *NAG* gene as a query sequence failed to identify an EST clone that contained both exons, whereas multiple clones were picked-up that contained either exon 4 or exon 5. Furthermore, RT-PCR with a forward primer in exon 4 and a reverse primer in exon 7 failed to yield the expected band of 341 bp in IMR-32 or SK-N-SH. In contrast, a sharp and single band of approximately 3 kb was amplified. Furthermore, Northern blot analysis estimated the *NAG* transcript size to be 2.5 kb longer compared to the published sequence. Sequence contig assembly using our 4 SSH clones, public ESTs selected by BLAST, and the human genome sequence allowed in silico cloning of a 2.7 kb transcript fragment between exon 4 and 5. These data indicate that the published *NAG* gene is probably misannotated and should contain 21 more exons between former exon 4 and 5. The elongated *NAG* gene sequence is predicted to contain an upstream start codon resulting in in-frame addition of 537 amino acids in front of the former protein sequence. Further characterization of these novel transcripts and curated *NAG* gene, and determination of their relevance in neuroblastoma is currently ongoing.

DISCUSSION

Despite recent new insights in the genetic heterogeneity of neuroblastoma, most of the genes as well as the developmental and differentiation pathways involved in its pathogenesis remain to be elucidated. As recognition of the underlying molecular defects and their downstream effects is of great importance for better diagnosis, classification, outcome prediction and development of tailored treatment protocols and new drugs, we sought to identify additional relevant neuroblastoma genes. For this purpose, a subtractive cDNA cloning strategy was applied to isolate differentially expressed genes by comparing two neuroblastoma cell lines belonging to different genetic subgroups (i.e. with or without *MYCN* amplification, and deletion of 1p and 11q). A non-redundant set of 300 cDNA clones was isolated, for which extrapolated Northern blot results indicated that 75% of the clones represent true differentially expressed transcripts. Here we report on the expression pattern of 50 of these clones, in conjunction with literature based candidate genes, prognostic markers, or genes with a reported differential expression pattern in neuroblastoma.

We adopted a supervised strategy for identification of aberration and prognosis related gene expression signatures in a validated and representative panel of neuroblastoma cell lines and primary tumors. In an attempt to understand the molecular switches that are responsible for the oncogenetic properties of *MYCN* overexpression, we identified 12 and 18 genes that were shown to have a significantly altered expression in *MYCN* amplified vs. single copy number tumors and cell lines, respectively. In this list are two novel transcripts included with unknown function and no homology to other genes, and located in critical regions of loss in high stage tumors (UniGene clusters Hs.28462 at 11q23.3, and Hs.182594 at 14q32). The majority of the genes identified in this study have not been reported in the context of neuroblastoma biology nor *MYCN* amplification. Increased expression of *NCL* and *RPS25* has been described in a SAGE profiling study of the MYCN model system SH-EP[26], and *BCAT1* is a known transcriptional target of MYC[27].
Cell lines and tumors have only 4 genes in common that are differentially expressed with respect to the *MYCN* status (*SOS1*, *CALM2*, *DKK3* and *MYCN* itself). In addition to *MYCN*, these 3 genes might represent true and relevant differential expression markers that discriminate between *MYCN* amplified and single copy neuroblastomas, and might help explain the biological differences between these two genetic subgroups. In this respect, the decreased expression of the *human son of sevenless homolog 1* (*SOS1*), which is amongst others involved in RAS mediated NGF signalling, is in keeping with the observed decreased or absent expression of the high affinity NGF receptor *NTRK1* in advanced stage *MYCN* amplified neuroblastomas. Further evidence that an altered RAS pathway might play a role in *MYCN* amplified tumors is provided by the observed decreased *calmodulin* (*CALM2)* expression, a gene which is implicated in RASGRF1 mediated RAS activation[28]. Furthermore, high *HRAS* expression has been associated with low *MYCN* expression and favorable patient outcome[29, 30], and was recently suggested to play a role in the spontaneous regression of neuroblastoma[31].

To determine which of the above identified genes are MYCN downstream targets, we tested their expression level in a *MYCN* cell line model system, that consists of stably *MYCN* transfected cells and their parental non-amplified counterparts with a 500 fold lower *MYCN* expression. As positive controls for both MYCN dependent induction and repression of gene expression, two additional genes (i.e. *INHBA* and *ID2*) were quantified. As expected, the angiogenesis inhibitor *activin A* (*INHBA*) was strongly downregulated in the SKMYC2 cells[32]. *ID2* gene expression levels however remained unchanged, in contrast to a reported MYCN dependent induction[33]. Similar contrasting observations in another laboratory prompted us to analyze the relation between ID2 and MYCN content in further detail in neuroblastoma cell lines and primary tumors, demonstrating a clear lack of correlation between ID2 and MYCN, and absence of prognosis related predictive power of *ID2* expression levels (manuscript in preparation[34]).
In general, MYCN appears to be a more potent transcriptional silencer, with 7 genes being repressed by more than 15-fold, while no gene was induced more than 6.5 fold. The upregulation of three ribosomal proteins *RPS25*, *RPL13A* and *RPL11* is in keeping with

published data, where a role for MYCN in enhanced expression of a large set of genes functioning in ribosome biogenesis and protein synthesis has been described[26]. The finding that some genes involved in neuronal differentiation are induced (*NEUROD1*, *CHGA*, *STMN2*) with increased *MYCN* expression, while others are repressed (*NPY*, *GAP43*) is puzzling and deserves further study. In this context, it is noteworthy that there are apparently conflicting reports on the role of MYCN in cellular differentiation, with some studies indicating preferential *MYCN* expression during organogenesis and cell differentiation[35, 36], while others describing that exogenous *MYCN* overexpression inhibits induced differentiation of neuroblastoma cells[37, 38].
Overall, our expression data provide possible insight into the way MYCN exerts it malignant effects, i.e. by promotion of angiogenesis (*INHBA)* and cell proliferation *(DKK3, CDKN1C),* by inhibition of apoptosis (*TGM2*), and by altering adhesion properties (*CD44*, *HXB*), possibly leading to enhanced invasive capacity. Another possible very interesting *MYCN* target gene identified in this study is the mortalization related and candidate tumor suppressor gene *DKK3*. An almost 6 fold reduction in expression level has been observed in SKMYC2 cells, with a general decreased expression in both *MYCN* amplified cell lines and tumors. DKK3 belongs to a family of secretory glycoproteins, with some members having the ability to antagonize WNT proto-oncogene signalling. DKK3 is down-regulated in a series of different immortalized and tumor-derived cell lines, and primary tumor samples, in part by promoter hypermethylation[39, 40]. Exogenous *DKK3* over-expression in tumor cells was shown to inhibit cell growth[41]. Further evidence that this gene might play an important role in the biology of specific neuroblastoma subgroups, comes from the observed strong independent predictive power for patient outcome, as determined in the panel of primary tumors (see further). Further studies are required to confirm a mechanistic link between *MYCN* and the *DKK3* gene (as well as the other identified putative transcriptional target genes), and to determine the biological consequences of an altered expression level.

Upon the search for deletion related class I and II tumor suppressor genes, five genes were found to be differentially expressed in neuroblastoma cell lines harboring a 3p deletion compared to cell lines without this genetic defect. The gene that displayed the most significantly reduced expression level in deleted cell lines is the Von Hippel Lindau (*VHL*) tumor suppressor gene. In view of the location of this gene in the –still large- critical region of 3p loss in neuroblastoma[42], its established role in pheochromocytoma[43] (like neuroblastoma a neural crest derived tumor), and its demonstrated strong independent prognostic power in multivariate analysis of primary tumor samples (see further), we propose this gene as a potential target of 3p loss in neuroblastoma. Preliminary mutation analysis however yielded no basepair alteration in the *VHL* coding region of 26 neuroblastoma tumors, nor aberrant *VHL* promoter methylation (Hoebeeck et al., unpublished results). In analogy with recent reports of haploinsufficiency of other suppressor genes involved in familial cancer syndromes (i.e. *APC* and *PTEN*[44, 45]), the observed 2-3 fold expression difference suggests that a similar mechanism could play a role in this subset of 3p deleted neuroblastomas.
With respect to 11q, a set of 8 genes was found that perfectly classified the neuroblastoma cell lines based on their 11q deletion status. Interestingly, 3 of the identified genes are located on chromosome region 11q23-q24 (*NCAM*, *MCAM*, and *SRPR*), which is commonly lost in metastatic neuroblastoma tumors. In view of the delineation of a shortest region of overlap between markers D11S1340 and D11S1299[46], the melanoma cell adhesion molecule *MCAM* with a putative role in neural crest development is a good positional and functional candidate tumor suppressor gene for the 11q23 locus. However, it has been reported that increased MCAM expression is correlated with development of metastatic melanoma[47], in which 11q23 LOH has been reported as a late event[48]. Further study is required to clarify this apparent discrepancy. In addition, it remains to be determined whether these gene expression changes are relevant to the specific genetic subgroups of neuroblastoma, or merely reflect a bystander dosage effect due to loss of one allele.

In analogy to recent reports where microarray based gene expression profiling is used to predict the clinical outcome of patients with various types of cancer, a supervised learning method was applied to search for specific predictor genes for survival probability. Twelve genes were identified, of which only 3 were previously shown to be correlated with prognosis

in neuroblastoma (*CD44*, *NTRK1*, and *MYCN*). Depending on the feeding mechanism, multivariate regression analyses attributed independent prognostic power to 4 new markers (*VHL*, *DKK3*, *NPY* and *MEIS2*). Subsequent hierarchical cluster and principal component analysis allowed reliable classification of 24/27 patients according to outcome, which outperforms any current system based on a single gene or genetic defect. Still, some deceased patients were mistakenly classified in the prognostic favorable group. As it turned out, patient 9 had a very slow growing primary tumor that could be controlled for more than 5 years by repeated MIBG therapy. Patient 41 was originally diagnosed with a stage 4S tumor, which was later revised to stage 4. This patient was in complete remission for more than 5 years, after which a new and aggressive stage 4 tumor was diagnosed resulting in death of the patient. The first diagnosed tumor was analyzed in this study. The clinical course of these patients could partially explain their classification in the favorable group. Clearly, additional markers are needed to identify the patients at risk which now mistakenly clustered. The next step will be to test the predictive power of the identified expression signature on an extended series of primary tumors, and to develop a robust classifier for accurate disease course prediction.

Using a combination of primary tumor samples, cancer cell lines, and a transfected model system, we have identified a substantial number of relevant neuroblastoma genes which deserve further study. As reported in other human cancers, we also observed expression patterns differences between cell lines and primary tumors, which might be explained by sampling differences, in vitro effects, and the heterogeneity of tumor tissue compared tot relatively homogenous cell line populations. More important in this study, the observed discrepancy might be attributed to a fundamental biological difference between *MYCN* single copy cell lines and tumors, with the former being derived from aggressively growing and metastasizing cells, while the latter include a large fraction of prognostically favorable localized tumors. Likewise, the observation that not all putative *MYCN* downstream genes found in SKMYC2 cells are differentially expressed in *MYCN* amplified vs. single copy cell lines and/or tumors probably indicates a certain tissue or cell specific effect of MYCN overexpression (due to presence or absence of the appropriate cofactor proteins, in part depending on the differentiation status of the cells). The importance of the cellular context for MYCN to exert its transcriptional effect is underscored by the current lack of any consistent marker that is differentially expressed in *MYCN* amplified vs. single copy tumors, with the exception of the recently identified *minichromosome maintenance protein MCM7*[49]. Caution has therefore to be taken not to restrict to specific cell line model systems, and to apply a level of validation that includes clinical tumor samples.

In view of the importance of amplified oncogenes in the development of many types of tumors, the identification of novel overexpressed genes in cell line IMR-32 might be of particular importance. Although we recently demonstrated that the frequently co-amplified *DDX1* and *NAG* genes do not result in diminished event-free or overall survival probability compared to MNA tumors without amplification of these genes[13], the possibility remains that co-amplified and overexpressed genes influence the malignant phenotype of the MNA tumors. The presence of the 4 known and 2 novel amplified genes in the IMR-32 SSH cDNA library, and the identification of not yet annotated *NAG* exons, clearly illustrate the power and efficiency of the applied subtractive methodology to clone amplified and overexpressed genes in tumors.

In conclusion, we demonstrated the combinatorial power of subtractive cDNA cloning and real-time PCR expression profiling to identify several genes previously unknown to be involved in neuroblastoma biology, and to designate specific gene expression patterns in the different genetic subgroups of this childhood neoplasm. We provided evidence that the *VHL* tumor suppressor gene and the *MCAM* adhesion molecule might be the critical targets of 3p and 11q loss, respectively. Furthermore, insight was gained into the mechanisms responsible for the specific malignant phenotype associated with *MYCN* amplification, including a consistent downregulation of the mortalization related DKK3 gene. Finally, several new prognostic marker genes were identified and allowed reliable patient classification with respect to survival probability.

ACKNOWLEDGMENTS

We would like to thank Kristin Strumane for her excellent technical assistance with the SSH procedure and Northern blot analysis, Lieven Thorrez for sequencing and establishment of the non-redundant database, Sven Påhlman for helpful discussions, Katrien Swerts and Jan Philippe for immunochemical assays, and Olivier Delattre and Martine Peter for multiplex PCR analysis of fusion genes. Lloyd Culp (Cleveland, USA), Rogier Versteeg (Amsterdam, The Netherlands), Peter Ambros (Vienna, Austria), Patrick Reynolds (Los Angeles, USA), Garret Brodeur (Philadelphia, USA), Thomas Look (Boston, USA), Susan Cohn (Chicago, USA) and Valérie Combaret (Lyon, France) are gratefully acknowledged for providing us with neuroblastoma cell lines.

FIGURES

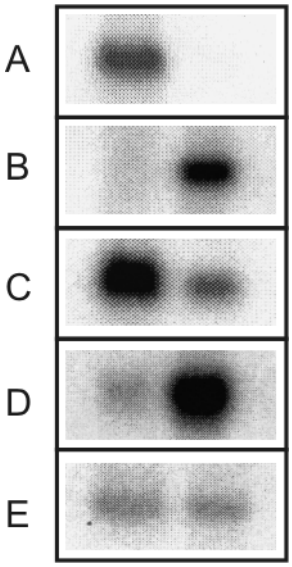

Figure 1: Five representative Northern blot results from 36 tested SSH clones hybridized to IMR-32 (right lane) and SK-N-SH (left). A: *MME*, SK-N-SH specific expression (found for 5/36 clones); B: *DDX1*, IMR-32 specific expression (7/36); C: *MEIS2*, >3 fold higher expression in SK-N-SH (13/36); D: *NAG*, >3 fold higher expression in IMR-32 (3/36); and E: *MTCO2*, equal abundance (8/36).

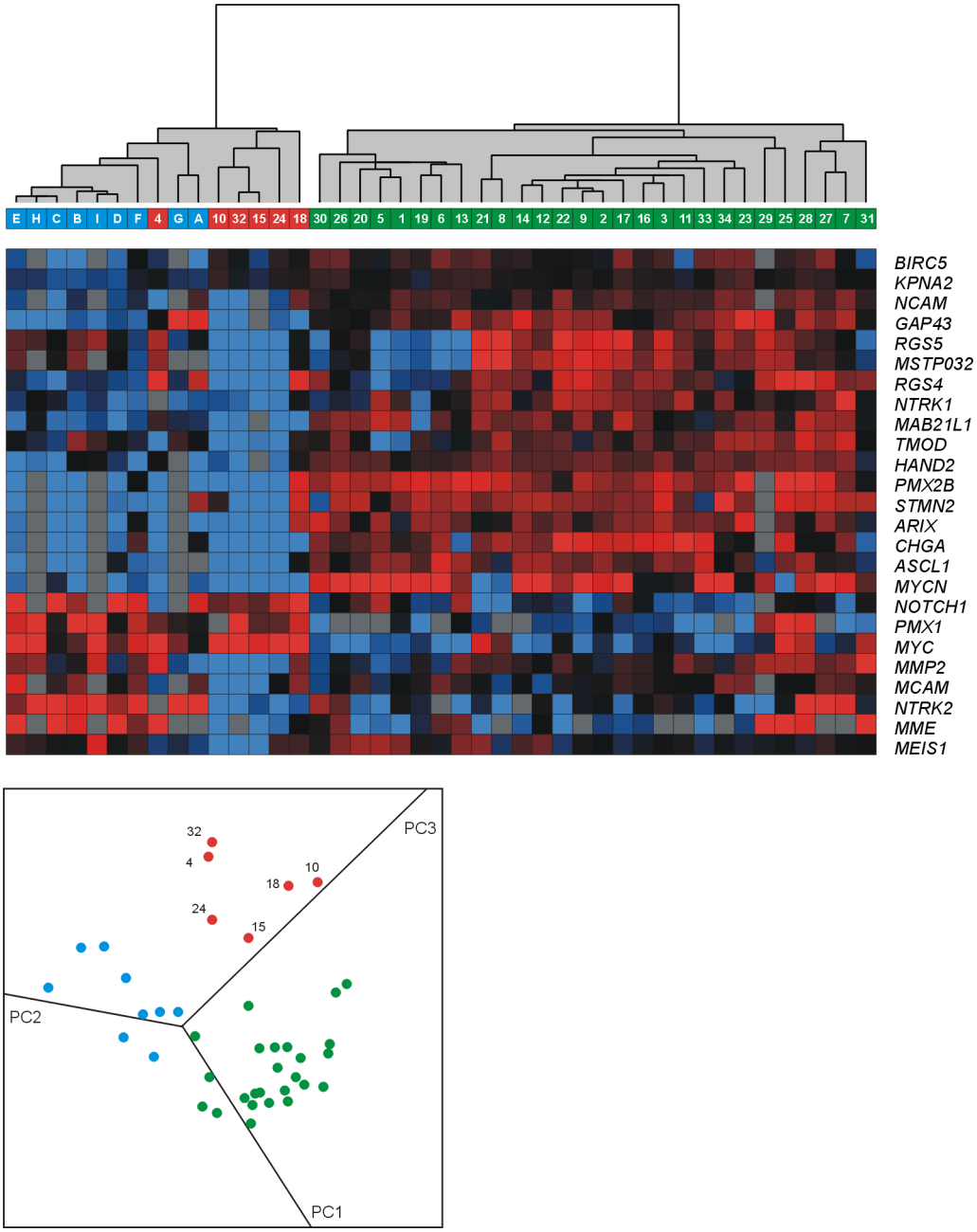

Figure 2:
Top: Average linkage hierarchical cluster analysis of neuroblastoma cell lines and normal tissues (columns) for 25 genes (rows) identified by SAM as tissue of origin classifiers (red: high expression, blue: low expression, gray: missing value; see Table 1 for names and genetic features of the cell lines) (normal tissues: adult brain (A), heart (B), kidney (C), liver (D), lung (E), trachea (F), fetal brain (G), mammary gland (H), and uterus (I)
Bottom: 3D projection of the same cell lines and normal tissues on the three major principal components (PC) of the 25 genes used for hierarchical clustering (blue: normal human tissues, green: neuroblastoma cell lines, red: atypical or non-neuroblastoma cell lines)

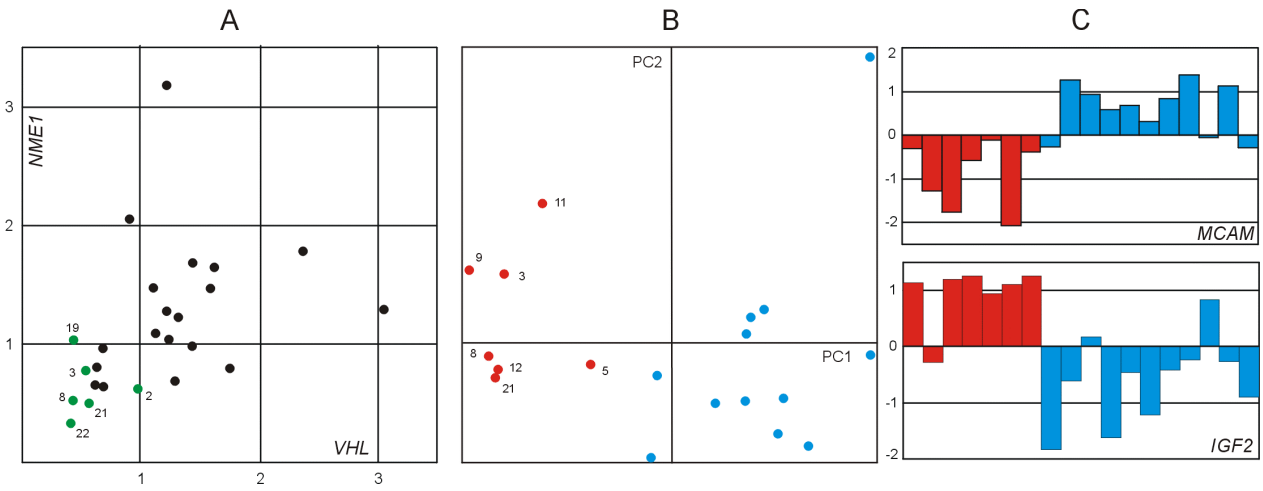

Figure 3:
A: Scatterplot of neuroblastoma cell lines according to their *VHL* and *NME1* expression level (green: 3p deleted; black: intact 3p).
B: Projection of neuroblastoma cell lines on the first two principal components (PC) that capture 53.1% variance of the 8 genes that displayed a significantly differential expression level with respect to the 11q status (see Table 3) (red: 11q deleted; blue: intact 11q).
C: Log transformed and mean centered expression level of two genes from the set that was used in panel B for PCA analysis (red: expression level in cell lines with 11q deletion; blue: intact 11q).

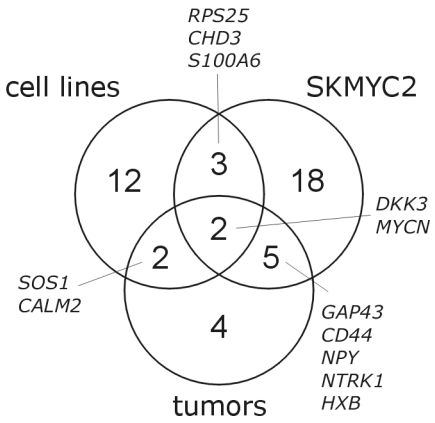

Figure 4:
Overview of the number of genes that were found to be significantly ($p<0.05$) differentially expressed between *MYCN* amplified vs. single copy cell lines (19/76 tested genes) or primary tumor biopsies (13/37), or that displayed a more than 2-fold expression difference when comparing stably MYCN transfected SKMYC2 cells with the parental single copy MYCN cell line SK-N-SH (28/70 tested genes). Genes that were differentially expressed in more than one system (i.e. cell lines, tumors, or transfected SKMYC2 cells) are indicated in the respective Venn diagram intersections

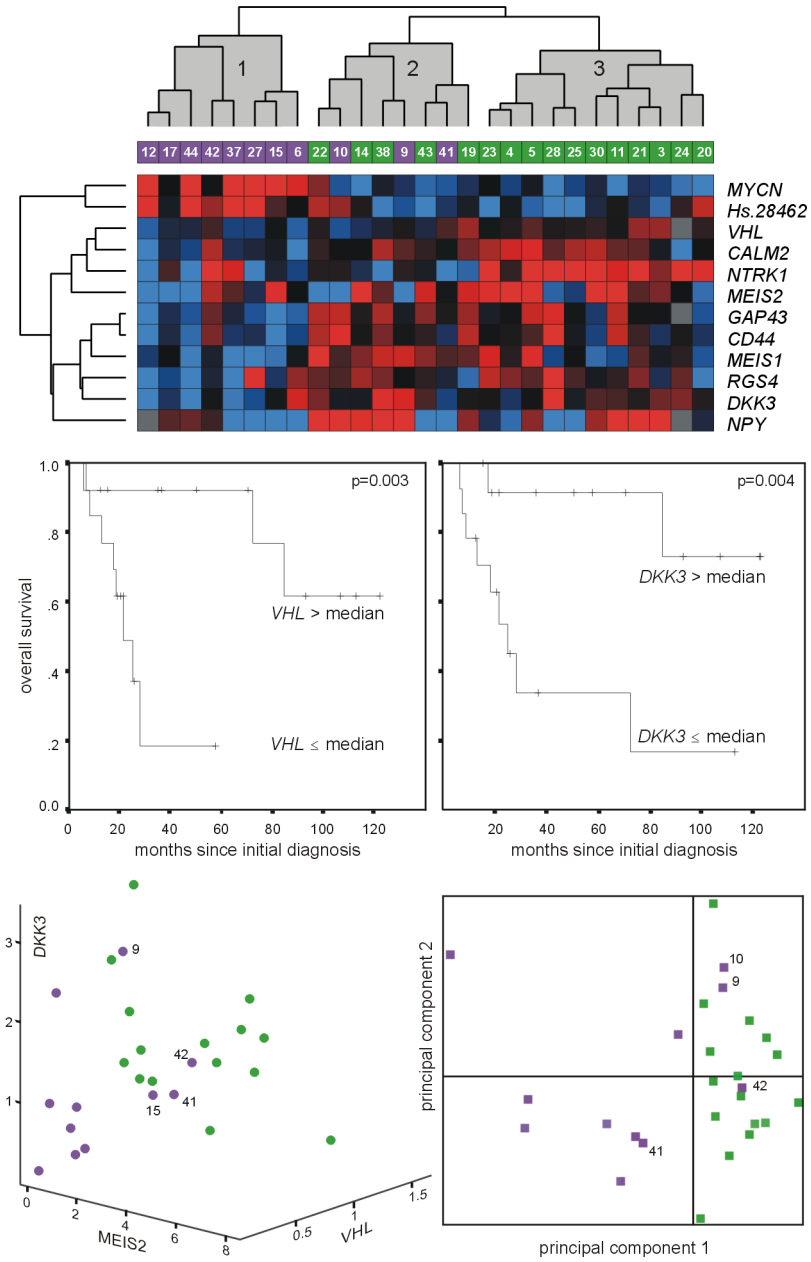

Figure 5:
Top: complete linkage hierarchical cluster analysis of primary tumor samples (columns) for 12 genes (rows) identified by SAM as prognostic predictors (top) (red: high expression, blue: low expression; green: alive, purple: dead; see Table 2 for clinical and genetic features of patients and tumors).
Middle: Kaplan-Meier survival curves for two representative genes, patients are dichotomized with respect to the median gene expression.
Bottom right: Projection of the patients to the first two principal components of the 12 genes used for hierarchical clustering (green: alive; purple: dead)
Bottom left: 3D scatterplot of patients according to the tumoral expression of 3 genes identified by backward Cox regression analysis as most independent predictors for patient outcome (green: alive, purple: dead).

Table 1: Genetic features of studied cell lines

number	name	MNA [a]	1p del [b]	3p del [b]	11q del [b]
1	CHP 134	amp	del	no	no
2	CHP 901	amp	del	del	-
3	CLB-GA	no	-	del	del
4	GI-ME-N	no	del	no	del
5	IMR-32	amp	del	no	del
6	LA-N-1	amp	del	no	no
7	LA-N-5	amp	del	no	no
8	LA-N-6	no	del	del	del
9	N206	amp	del	no	del
10	NB-3	no	-	no	-
11	NBL-S	no	-	no	del
12	NGP	amp	del	no	del
13	NLF	amp	del	-	no
14	NMB	amp	del	no	-
15	NN-1	no	no	no	no
16	SJNB-1	no	del	no	-
17	SJNB-10	amp	del	-	no
18	SJNB-12	no	del	del	no
19	SJNB-6	amp	del	del	no
20	SJNB-8	amp	del	no	no
21	SK-N-AS	no	del	del	del
22	SK-N-BE	amp	del	del	-
23	SK-N-FI	no	no	no	no
24	SK-N-MC	no	del	del	-
25	SK-N-SH	no	no	no	no
26	SMS-KAN	amp	del	no	no
27	SMS-KCNR	amp	del	no	no
28	STA-NB-10	amp	del	no	-
29	STA-NB-12	amp	del	no	no
30	STA-NB-3	amp	del	no	-
31	STA-NB-8	amp	del	no	-
32	STA-NB-9	no	no	no	-
33	TR-14	amp	del	no	-
34	UHG-NP	amp	del	no	-

a: MNA: *MYCN* amplification; amp: amplification; no: normal
b: del: deletion; no: normal; - not tested or not informative

Table 2: Clinical and genetic features of neuroblastoma patients

sample	stage [a]	1p del [b]	MNA [c]	age [d]	status	OS [e]
PT_5	1	no	no	0.92	alive	36.76
PT_21	1	no	no	17.17	alive	122.33
PT_22	1	no	no	5.69	alive	35.63
PT_23	1	no	no	3.42	alive	20.75
PT_24	1	no	no	6.64	alive	122.90
PT_25	1	no	no	1.45	alive	12.92
PT_38	1	no	no	13.25	alive	21.57
PT_43	1	no	no	4.34	alive	19.13
PT_3	2	no	no	10.62	alive	107.07
PT_11	2	no	no	14.53	alive	57.63
PT_19	2	del	no	10.98	alive	93.27
PT_20	2	no	no	18.74	alive	50.33
PT_6	3	del	amp	22.39	dead	17.82
PT_14	3	no	no	62.83	alive	25.91
PT_28	3	no	no	7.50	alive	70.47
PT_30	3	no	no	7.43	alive	15.77
PT_42	3	no	amp	17.13	dead	7.43
PT_9	4	no	no	63.83	dead	84.80
PT_10	4	no	no	56.82	dead	21.60
PT_12	4	del	amp	57.51	dead	25.10
PT_15	4	del	amp	34.20	dead	28.17
PT_17	4	no	no	50.21	dead	18.67
PT_27	4	del	amp	19.60	dead	6.63
PT_37	4	del	amp	46.50	dead	8.90
PT_41	4	no	no	3.26	dead	72.23
PT_44	4	del	amp	11.77	dead	13.51
PT_4	4S	no	no	2.47	alive	112.97

a: INSS stage[14]
b: MNA: *MYCN* amplification; amp: amplification; no: normal
c: del: deletion; no: normal
d: age at diagnosis (in months)
e: overall survival (in months from diagnosis till death or last follow-up)

Table 3: Genetic aberration related gene expression differences

11q deletion related	p value [a]	change [b]
IGF2	0.002	up
MCAM	0.002	down
NTRK1	0.011	up
SRPR	0.011	down
MME	0.030	down
CHGA	0.030	up
NCAM	0.037	down
PIM1	0.046	down
3p deletion related	p value	change
VHL	<0.001	down
RGS5	0.006	up
NME1	0.007	down
MSTP032	0.011	up
CTNNB1	0.028	down
MNA related (T) [c]	p value	change
MYCN°*	<0.001	up
*GAP43**	<0.001	down
*CD44**	<0.001	down
Hs.28462	<0.001	up
CALM2°	<0.001	down
MEIS1	0.001	down
VHL	0.003	down
SOS1°	0.004	down
HAND2	0.009	down
*NTRK1**	0.014	down
DKK3°*	0.025	down
*HXB**	0.030	down
*NPY**	0.037	down
MNA related (C) [d]	p value	change
MYCN°*	<0.001	up
Hs.182594	0.001	up
NCL-	0.001	up
BCAT1	0.002	up
SOS1°	0.006	down
NME1-	0.006	up
MYC	0.007	down
RPS25-*	0.007	up
TNFRSF10B	0.014	up
HRY#-	0.014	down
CHD3-*	0.017	up
IGF2	0.020	down
CALM2°	0.027	down
MSTP032-	0.027	down
PMX2B#-	0.031	down
CTNNB1-	0.036	up
DKK3°*	0.042	down
RGS5	0.042	down
*S100A6**	0.048	down

a: Mann-Whitney exact significance (2 times the one-sided p statistic)
b: up: higher expression in samples with the genetic effect; down: decreased expression in samples with the genetic defect under study

c: MNA: *MYCN* amplification; T: primary tumor samples; *: also differentially expressed in SKMYC2 (see Table 4); °: differentially expressed in both cell lines and primary tumor samples
d: C: cell lines; -: not tested in primary tumor samples; #: not tested in SKMYC2 cells (see Table 4)

Table 4: Differentially expressed genes in SKMYC2 vs. SK-N-SH [a]

downregulated [b]	ratio [c]
PMX1	1921.14
TGFBI	443.04
NPY (T)	69.83
TGM2	48.36
INHBA	31.41
HXB (T)	16.97
CD44 (T)	16.17
DKK3 (T,C)	5.68
S100A6 (C)	5.06
GAP43 (T)	4.69
CDKN1C	3.09
IGF2	2.80
NTRK2	2.77
NTRK1 (T)	2.70
LTBP1	2.50
upregulated [b]	ratio [d]
MYCN (T,C)	490.33
ASCL1	6.58
NEUROD1	5.72
CHGA	4.57
RPL13A	3.85
STMN2	2.79
RPS25 (C)	2.68
MEIS2	2.52
RGS5	2.35
CHD3 (C)	2.28
TMOD	2.21
MAB21L1	2.18
RPL11	2.13

a: only genes with an expression difference of more than 2 fold are listed; two independent RNA extractions were performed (coefficient of variation for ratio's < 35%)
b: also differentially expressed in *MYCN* amplified vs. single copy cell lines (C), or primary tumors (T)
c: SK-N-SH/SKMYC2
d: SKMYC2/SK-N-SH

REFERENCES

1. Brodeur, G.M., Seeger, R.C., Schwab, M., Varmus, H.E. & Bishop, J.M. Amplification of N-myc in untreated human neuroblastomas correlates with advanced disease stage. *Science* **224**, 1121-1124 (1984).
2. Teitz, T. et al. Caspase 8 is deleted or silenced preferentially in childhood neuroblastomas with amplification of MYCN. *Nat Med* **6**, 529-535 (2000).
3. Bown, N. et al. Gain of chromosome arm 17q and adverse outcome in patients with neuroblastoma. *N Engl J Med* **340**, 1954-1961 (1999).
4. White, P.S. & Versteeg, R. in Neuroblastoma. (eds. G.M. Brodeur, T. Sawada, Y. Tsuchida & P. Voûte) 57-74 (Elsevier, Amsterdam; 2000).
5. Luttikhuis, M.E. et al. Neuroblastomas with chromosome 11q loss and single copy MYCN comprise a biologically distinct group of tumours with adverse prognosis. *Br J Cancer* **85**, 531-537 (2001).
6. Plantaz, D. et al. Comparative genomic hybridization (CGH) analysis of stage 4 neuroblastoma reveals high frequency of 11q deletion in tumors lacking MYCN amplification. *Int J Cancer* **91**, 680-686 (2001).
7. Vandesompele, J. et al. Genetic heterogeneity of neuroblastoma studied by comparative genomic hybridization. *Genes Chromosomes Cancer* **23**, 141-152 (1998).
8. Diatchenko, L. et al. Suppression subtractive hybridization: a method for generating differentially regulated or tissue-specific cDNA probes and libraries. *Proc Natl Acad Sci U S A* **93**, 6025-6030 (1996).
9. Van Roy, N. et al. 1;17 translocations and other chromosome 17 rearrangements in human primary neuroblastoma tumors and cell lines. *Genes Chromosomes Cancer* **10**, 103-114 (1994).
10. Van Roy, N. et al. Molecular cytogenetic analysis of 1;17 translocations in neuroblastoma. *Eur J Cancer* **31A**, 530-535 (1995).
11. Van Roy, N. et al. Combined M-FISH and CGH analysis allows comprehensive description of genetic alterations in neuroblastoma cell lines. *Genes Chromosomes Cancer* **32**, 126-135 (2001).
12. Van Roy, N. et al. Comparative genomic hybridization analysis of human neuroblastomas: detection of distal 1p deletions and further molecular genetic characterization of neuroblastoma cell lines. *Cancer Genet Cytogenet* **97**, 135-142 (1997).
13. De Preter, K. et al. Quantification of MYCN, DDX1, and NAG Gene Copy Number in Neuroblastoma Using a Real-Time Quantitative PCR Assay. *Mod Pathol* **15**, 159-166 (2002).
14. Brodeur, G.M. et al. Revisions of the international criteria for neuroblastoma diagnosis, staging, and response to treatment. *J Clin Oncol* **11**, 1466-1477 (1993).
15. Hall, T.A. BioEdit: a user-friendly biological sequence alignment editor and analysis program for Windows 95/98/NT. *Nucleic Acids Symp Ser* **41**, 95-98 (1999).
16. Vandesompele, J., De Paepe, A. & Speleman, F. Elimination of primer-dimer artefacts and genomic co-amplification using a two-step SYBR Green I real-time RT-PCR. *Anal Biochem* (2002).
17. Vandesompele, J. et al. Accurate normalization of real-time quantitative RT-PCR data by geometric averaging of multiple internal control genes. *Genome Biology* (submitted).
18. Eisen, M.B., Spellman, P.T., Brown, P.O. & Botstein, D. Cluster analysis and display of genome-wide expression patterns. *Proc Natl Acad Sci U S A* **95**, 14863-14868 (1998).
19. Tusher, V.G., Tibshirani, R. & Chu, G. Significance analysis of microarrays applied to the ionizing radiation response. *Proc Natl Acad Sci U S A* **98**, 5116-5121 (2001).
20. Dysvik, B. & Jonassen, I. J-Express: exploring gene expression data using Java. *Bioinformatics* **17**, 369-370 (2001).
21. Gestblom, C. et al. The basic helix-loop-helix transcription factor dHAND, a marker gene for the developing human sympathetic nervous system, is expressed in both high- and low-stage neuroblastomas. *Lab Invest* **79**, 67-79 (1999).
22. Peter, M., Gilbert, E. & Delattre, O. A multiplex real-time pcr assay for the detection of gene fusions observed in solid tumors. *Lab Invest* **81**, 905-912 (2001).

23. Judware, R. & Culp, L.A. Over-expression of transfected N-myc oncogene in human SKNSH neuroblastoma cells down-regulates expression of beta 1 integrin subunit. *Oncogene* **11**, 2599-2607 (1995).
24. Jones, T.A., Flomen, R.H., Senger, G., Nizetic, D. & Sheer, D. The homeobox gene MEIS1 is amplified in IMR-32 and highly expressed in other neuroblastoma cell lines. *Eur J Cancer* **36**, 2368-2374 (2000).
25. Spieker, N. et al. The MEIS1 oncogene is highly expressed in neuroblastoma and amplified in cell line IMR32. *Genomics* **71**, 214-221 (2001).
26. Boon, K. et al. N-myc enhances the expression of a large set of genes functioning in ribosome biogenesis and protein synthesis. *Embo J* **20**, 1383-1393 (2001).
27. Schuldiner, O. et al. ECA39, a conserved gene regulated by c-Myc in mice, is involved in G1/S cell cycle regulation in yeast. *Proc Natl Acad Sci U S A* **93**, 7143-7148 (1996).
28. Farnsworth, C.L. et al. Calcium activation of Ras mediated by neuronal exchange factor Ras-GRF. *Nature* **376**, 524-527 (1995).
29. Tanaka, T. et al. A significant association of Ha-ras p21 in neuroblastoma cells with patient prognosis. A retrospective study of 103 cases. *Cancer* **68**, 1296-1302 (1991).
30. Nakada, K., Fujioka, T., Kitagawa, H., Takakuwa, T. & Yamate, N. Expressions of N-myc and ras oncogene products in neuroblastoma and their correlations with prognosis. *Jpn J Clin Oncol* **23**, 149-155 (1993).
31. Kitanaka, C. et al. Increased ras expression and caspase-independent neuroblastoma cell death: possible mechanism of spontaneous neuroblastoma regression. *J Natl Cancer Inst* **94**, 358-368 (2002).
32. Breit, S. et al. The N-myc oncogene in human neuroblastoma cells: down-regulation of an angiogenesis inhibitor identified as activin A. *Cancer Res* **60**, 4596-4601 (2000).
33. Lasorella, A., Noseda, M., Beyna, M., Yokota, Y. & Iavarone, A. Id2 is a retinoblastoma protein target and mediates signalling by Myc oncoproteins. *Nature* **407**, 592-598 (2000).
34. Vandesompele, J., Anders, E., Axelson, H., Speleman, F. & Pahlman, S. Lack of correlation between ID2 and MYCN expression in neuroblastoma cell lines and tumors. (in preparation).
35. Mugrauer, G., Alt, F.W. & Ekblom, P. N-myc proto-oncogene expression during organogenesis in the developing mouse as revealed by in situ hybridization. *J Cell Biol* **107**, 1325-1335 (1988).
36. Jakobovits, A., Schwab, M., Bishop, J.M. & Martin, G.R. Expression of N-myc in teratocarcinoma stem cells and mouse embryos. *Nature* **318**, 188-191 (1985).
37. Peverali, F.A. et al. Retinoic acid-induced growth arrest and differentiation of neuroblastoma cells are counteracted by N-myc and enhanced by max overexpressions. *Oncogene* **12**, 457-462 (1996).
38. Bogenmann, E., Torres, M. & Matsushima, H. Constitutive N-myc gene expression inhibits trkA mediated neuronal differentiation. *Oncogene* **10**, 1915-1925 (1995).
39. Kobayashi, K. et al. Reduced expression of the REIC/Dkk-3 gene by promoter-hypermethylation in human tumor cells. *Gene* **282**, 151-158 (2002).
40. Tsuji, T., Miyazaki, M., Sakaguchi, M., Inoue, Y. & Namba, M. A REIC gene shows down-regulation in human immortalized cells and human tumor-derived cell lines. *Biochem Biophys Res Commun* **268**, 20-24 (2000).
41. Tsuji, T. et al. Antiproliferative activity of REIC/Dkk-3 and its significant down-regulation in non-small-cell lung carcinomas. *Biochem Biophys Res Commun* **289**, 257-263 (2001).
42. Ejeskar, K., Aburatani, H., Abrahamsson, J., Kogner, P. & Martinsson, T. Loss of heterozygosity of 3p markers in neuroblastoma tumours implicate a tumour-suppressor locus distal to the FHIT gene. *Br J Cancer* **77**, 1787-1791 (1998).
43. Koch, C.A. et al. Genetic aspects of pheochromocytoma. *Endocr Regul* **35**, 43-52 (2001).
44. Yan, H. et al. Small changes in expression affect predisposition to tumorigenesis. *Nat Genet* **30**, 25-26 (2002).
45. Kwabi-Addo, B. et al. Haploinsufficiency of the Pten tumor suppressor gene promotes prostate cancer progression. *Proc Natl Acad Sci U S A* **98**, 11563-11568 (2001).

46. Guo, C. et al. Allelic deletion at 11q23 is common in MYCN single copy neuroblastomas. *Oncogene* **18**, 4948-4957 (1999).
47. Lehmann, J.M., Riethmuller, G. & Johnson, J.P. MUC18, a marker of tumor progression in human melanoma, shows sequence similarity to the neural cell adhesion molecules of the immunoglobulin superfamily. *Proc Natl Acad Sci U S A* **86**, 9891-9895 (1989).
48. Herbst, R.A. et al. Identification of two distinct deletion targets at 11q23 in cutaneous malignant melanoma. *Int J Cancer* **80**, 205-209 (1999).
49. Shohet, J.M. et al. Minichromosome maintenance protein MCM7 is a direct target of the MYCN transcription factor in neuroblastoma. *Cancer Res* **62**, 1123-1128 (2002).

DISCUSSION

Gene expression analysis plays an increasingly important role in many fields of biological research. Two recently developed methods to measure transcript levels have gained much popularity and are frequently applied. Microarrays permit the parallel analysis of thousands of genes in two differentially labeled RNA populations, while real-time reverse transcriptase PCR (RT-PCR) provides the simultaneous measurement of gene expression in many different samples for a limited number of genes, and is especially suited when only a small number of cells are available, e.g. small tumor biopsies or microdissected cells. Both techniques have the advantage of speed, throughput and a high degree of potential automation compared to conventional quantification methods, such as Northern blot analysis, ribonuclease protection assay, or competitive RT-PCR. Real-time PCR has additional advantages over the conventional and former PCR based quantification methods in terms of accuracy, sensitivity, dynamic range of quantification, and absence of post-PCR manipulations.

Since the initial description of the real-time PCR methodology, sequence-specific fluorescence-labeled probes have been considered as a standard detection format in many diagnostic and research applications[1, 2]. However, these probes –due to the relatively high cost- are not suited for quantification of multiple sequences. In Paper V of this thesis, we therefore optimized and validated a real-time PCR assay using the SYBR Green I dye, which is a much more economical alternative to quantify any given sequence because it is a non-specific DNA minor-groove binder that fluoresces when bound to double-stranded DNA. The lack of additional specificity -otherwise provided by a sequence-specific probe- can be compensated for by melting curve analysis, which allows accurate assessment of PCR specificity[3].
Although advertised for by many leading life science companies, we discovered that a one-step RT-PCR using SYBR Green I for online monitoring of PCR cycle progression might obscure the true result in quantitative assays. Indeed, we observed that the reverse transcriptase enzyme and gene-specific primers conspire to produce primer-dimer (PD) artefacts that are efficiently co-amplified with the target (and detected by the generic binding dye SYBR Green I) during the PCR phase. For samples where the gene of interest is of low abundance (and PD are readily formed), this problem is of particular importance. So far, extensive primer-dimer formation during one-step RT-PCR has not been described yet, because most one-step assays use specific probes as a detection format. However, caution has to be taken, as these probes do not allow to the experimenter to determine the effect of PD on the quantitative results. The introduction of a two-step RT-PCR (i.e. cDNA synthesis using random hexamer or oligo(dT) primers, and PCR are performed in separate tubes) completely eliminated this problem.
Further validation of the real-time PCR illustrated the prerequisite -and efficacy- of DNase treatment of RNA prior to cDNA synthesis, to ensure that data are not confounded by genomic contamination and the inevitable presence of pseudogenes. This step also significantly facilitated primer design, as there is no further need to exclude the possibility of genomic contamination during RT-PCR. Determination of the intra- and inter-assay variation of our established method showed that DNase treatment, cDNA synthesis and RT-PCR were very reproducible. In conclusion, we provided evidence that a two-step real-time quantitative RT-PCR based on SYBR Green I detection chemistry and DNase treated RNA as template is the method of choice for sensitive and reproducible transcript abundance measurements for a large series of different genes.

With the advent of sensitive and accurate gene expression technologies such as the above described real-time quantitative RT-PCR, the requirements for a proper internal control or so-called housekeeping gene have become increasingly stringent. Although many studies have reported that housekeeping gene expression can vary considerably, no study has systematically addressed the critical issues of using housekeeping genes, nor proposed an adequate workaround. In Paper VI of this thesis, we rigorously measured the expression level of 10 common housekeeping genes in 85 samples from 13 different human tissues. Special attention was paid to select genes that belong to different functional and abundance classes, which significantly reduced the fact that genes might be co-regulated. We firmly demonstrated that the common practice of using a single housekeeping gene for normalization (such as *beta actin*, or *glyceraldehyde-3-phosphate dehydrogenase*), can result in erroneous normalization by at least a factor 3 in 25% of any tested samples. In order to address the expression stability of a given control gene in a series of tissue samples, we developed a conceptually novel and robust gene expression stability measure, and outlined an algorithm to determine the most stable and hence reliable housekeepers in a given tissue panel. The algorithm is based on repeated gene stability measurements and subsequent elimination of the least stable control gene. To handle the large amount of calculations, a Visual Basic application for Microsoft Excel (termed *geNorm)* was developed and is freely available from the authors on request (Figure 1).

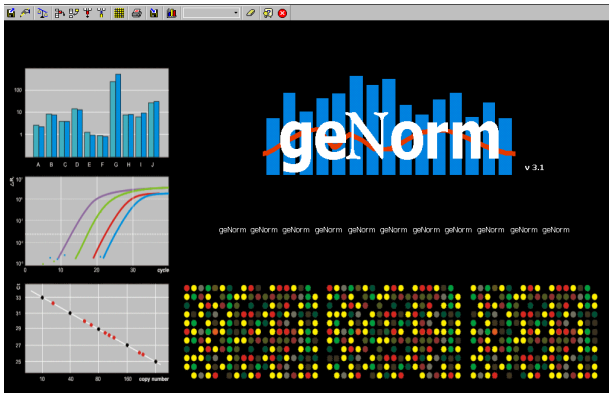

Figure 1: Splash screen of the *geNorm* applet during startup from Microsoft Excel.

We also presented a procedure to determine how many control genes are required for reliable normalization. It turned out that 3 genes sufficed for samples with relatively low expression variation, but that other tissues or cell types required a fourth or fifth control gene to deal with the observed expression variation. Finally, we validated the expression stability measure and the geNorm algorithm on two levels. First, we showed that most non-specific expression variation (which should be completely absent after perfect normalization conditions) was removed when stable control genes (as determined by geNorm) were used for normalization, in contrast to the use of random housekeeping genes. Further validation based on publicly available microarray data demonstrated that our proposed normalization factor was equivalent to frequently applied microarray normalization factors.
In conclusion, we described and validated a procedure to identify the most stable control genes in a given set of tissue samples, and to determine the optimal number of genes required for reliable normalization of RT-PCR data. The presented strategy can be applied to any number or kind of genes or tissues, and should allow more accurate gene expression profiling. This is of utmost importance for studying the biological significance of subtle expression differences.

The power of genome-wide expression profiling in the study of cancer is demonstrated by an ever increasing number of high impact papers that describe the presence of specific gene expression signatures that allow more accurate diagnosis[4, 5], tumor classification[6-10], and patient outcome prediction[11-13], compared to current clinical-genetic or morphology based criteria. Two major strategies are being used to accomplish a genome-wide cancer transcriptome profile, i.e. serial analysis of gene expression (SAGE[14]) and microarray analysis[15], with real-time quantitative PCR technology being most frequently used to confirm and extend obtained results. From a conceptual point of view, the SAGE methodology is superior, as it generates absolute data, which can easily be integrated into existing SAGE databases, for further data mining and comparison with other transcriptomes. However, the significant amount of workload to generate a SAGE based transcriptome excludes its general application to study complex biological problems that require testing of multiple samples to draw significant conclusions (such as the aforementioned applications). In contrast, microarrays permit the parallel analysis of thousands of genes in a way that allows study of a far greater number of samples (up to 300 different samples in a recent report[4]). With the advent of these high-throughput technologies and the generation of vast amounts of data, a new era of computing based biological data mining has emerged. Whereas until recently mainly exploratory tools were used (such as hierarchical clustering[16] or self organizing maps[17]), analysis is now more and more shifted towards supervised learning strategies, like neural networking[5] and harvesting of expression trees[18].

With respect to the genome wide expression analysis of neuroblastoma, only a limited number of reports have been published. Two studies aimed at identification of *MYCN* downstream genes and their effectors by comparing the expression profile of *MYCN* amplified neuroblastoma cells with single copy tumor cells. A SAGE based study revealed a list of genes involved in ribosome biogenesis and protein synthesis, demonstrating that MYCN functions in part as a regulator of cell growth[19]. Filter array hybridization analysis of 3 neuroblastoma cell lines and various other *MYC* amplified cancer cell lines identified both *MYCN* and *MYC* putative target genes, the majority of which involved in cell cycle regulation[20]. A more global expression profiling analysis of predominantly neuroblastoma cell lines was performed in a microarray study where an artificial neural network model was developed for classification and diagnostic prediction of small round blue cell tumors, which are childhood neoplasms with a similar histological appearance (see Chapter 1)[5]. Several marker genes not previously associated with neuroblastoma were identified.
Although the above cited studies yielded valuable information, they do not provide significant insight into the molecular basis of the various genetic subgroups of neuroblastoma, nor do they propose new marker genes for improved classification or patient outcome prediction.

In Paper VII of this thesis, we therefore attempted to identify relevant neuroblastoma genes on a transcriptome wide basis, using a combination of subtractive cDNA cloning of differentially expressed genes, and subsequent real-time PCR profiling of both neuroblastoma cell lines and primary tumors. Typical gene

expression signatures were found associated with major genetic defects and patient outcome. Combination of differential analysis of *MYCN* amplified versus single copy cell lines and tumors, and a *MYCN* overexpressing cell line model system identified the mortalization related *DKK3* gene as a strong candidate *MYCN* transcriptionally repressed gene, in part responsible for the oncogenic mechanism associated with *MCYN* overexpression. In view of the observed decreased expression in 3p or 11q deleted cell lines, the *VHL* and *MCAM* genes were suggested to be candidate neuroblastoma tumor suppressor genes for the 3p and 11q critical region, respectively. Further evidence that *VHL* might play an important role in a subgroup of neuroblastoma, comes from its observed independent predictive power in a set of 12 genes that allowed improved prediction of patient survival probability.

The majority of the genes identified in this study have not been reported in the context of neuroblastoma biology, and underscore the efficacy of subtractive expression profiling in the study of cancer. In view of the rather surprising limited number of differentially expressed genes observed in SAGE profiling studies of cancerous vs. normal tissues (i.e. a few hundred transcripts) (reviewed in ref. [21]), our non-redundant library of 300 clones might contain already a significant fraction of the relevant neuroblastoma genes, and thus holds great promise for our planned microarray based identification and further study of potential new targets for diagnosis, prognosis and therapy of neuroblastoma. Overall, subtractive cDNA cloning proves to be a very valuable and economic strategy for generating relevant differentially expressed clones for downstream applications such as microarray profiling. This is in contrast to common microarray based screening strategies, where typically 5.000 to 10.000 random clones are studied to end up with a set of a few tens to hundreds of genes of putative interest. Furthermore, current cDNA arrays are somewhat limited in a way that predominantly known genes and isolated EST clones with a moderate to high abundance are present. However, microarrays based on subtractive cDNA libraries would be enriched for both differentially expressed and low abundant transcripts, thus maximizing the efficiency for identification of relevant and new genes. Future research strategies in our laboratory therefore include the generation of additional subtractive cDNA libraries based on different model systems (e.g. microcell mediated chromosome transferred cell lines, and normal neuroblast precursors vs. malignant tumor cells). Subsequent custom microarray expression profiling of well characterized neuroblastoma samples is aimed at elucidation of the pathways disturbed in the different genetic subgroups, and identification of a prognostic set of marker genes that allow sensitive discrimination of patients that require intensive treatment, and others that benefit with milder therapeutic interventions, resulting in significantly decreased adverse treatment side-effects.

REFERENCES

1. Lie, Y.S. & Petropoulos, C.J. Advances in quantitative PCR technology: 5' nuclease assays. *Curr Opin Biotechnol* **9**, 43-48. (1998).
2. Bustin, S.A. Absolute quantification of mRNA using real-time reverse transcription polymerase chain reaction assays. *J Mol Endocrinol* **25**, 169-193. (2000).
3. Ririe, K.M., Rasmussen, R.P. & Wittwer, C.T. Product differentiation by analysis of DNA melting curves during the polymerase chain reaction. *Anal Biochem* **245**, 154-160. (1997).
4. Ramaswamy, S. et al. Multiclass cancer diagnosis using tumor gene expression signatures. *Proc Natl Acad Sci U S A* **98**, 15149-15154 (2001).
5. Khan, J. et al. Classification and diagnostic prediction of cancers using gene expression profiling and artificial neural networks. *Nat Med* **7**, 673-679 (2001).
6. Hedenfalk, I. et al. Gene-expression profiles in hereditary breast cancer. *N Engl J Med* **344**, 539-548 (2001).
7. Armstrong, S.A. et al. MLL translocations specify a distinct gene expression profile that distinguishes a unique leukemia. *Nat Genet* **30**, 41-47 (2002).
8. Alizadeh, A.A. et al. Distinct types of diffuse large B-cell lymphoma identified by gene expression profiling. *Nature* **403**, 503-511 (2000).
9. Golub, T.R. et al. Molecular classification of cancer: class discovery and class prediction by gene expression monitoring. *Science* **286**, 531-537 (1999).
10. Bhattacharjee, A. et al. Classification of human lung carcinomas by mRNA expression profiling reveals distinct adenocarcinoma subclasses. *Proc Natl Acad Sci U S A* **98**, 13790-13795 (2001).
11. Shipp, M.A. et al. Diffuse large B-cell lymphoma outcome prediction by gene-expression profiling and supervised machine learning. *Nat Med* **8**, 68-74 (2002).
12. van 't Veer, L.J. et al. Gene expression profiling predicts clinical outcome of breast cancer. *Nature* **415**, 530-536 (2002).
13. Pomeroy, S.L. et al. Prediction of central nervous system embryonal tumour outcome based on gene expression. *Nature* **415**, 436-442 (2002).

14. Velculescu, V.E., Zhang, L., Vogelstein, B. & Kinzler, K.W. Serial analysis of gene expression. *Science* **270**, 484-487 (1995).
15. Schena, M., Shalon, D., Davis, R.W. & Brown, P.O. Quantitative monitoring of gene expression patterns with a complementary DNA microarray. *Science* **270**, 467-470. (1995).
16. Eisen, M.B., Spellman, P.T., Brown, P.O. & Botstein, D. Cluster analysis and display of genome-wide expression patterns. *Proc Natl Acad Sci U S A* **95**, 14863-14868 (1998).
17. Tamayo, P. et al. Interpreting patterns of gene expression with self-organizing maps: methods and application to hematopoietic differentiation. *Proc Natl Acad Sci U S A* **96**, 2907-2912 (1999).
18. Hastie, T., Tibshirani, R., Botstein, D. & Brown, P. Supervised harvesting of expression trees. *Genome Biol* **2**, RESEARCH0003 (2001).
19. Boon, K. et al. N-myc enhances the expression of a large set of genes functioning in ribosome biogenesis and protein synthesis. *Embo J* **20**, 1383-1393 (2001).
20. Schuldiner, O. & Benvenisty, N. A DNA microarray screen for genes involved in c-MYC and N-MYC oncogenesis in human tumors. *Oncogene* **20**, 4984-4994 (2001).
21. Polyak, K. & Riggins, G.J. Gene discovery using the serial analysis of gene expression technique: implications for cancer research. *J Clin Oncol* **19**, 2948-2958 (2001).

SUMMARY

Neuroblastoma is defined as one disease, but there's increasing evidence that it may comprise several biological subtypes. Indeed, this enigmatic childhood tumor displays a remarkably variable clinical course, ranging from spontaneous regression or maturation into benign ganglioneuroma, to aggressive proliferation with widespread metastasis and fatal outcome of the patient. This hallmark of clinical variability reflects the underlying genetic heterogeneity of the tumoral cells.
In the first part of this thesis, we illustrated the power of comparative genomic hybridization in whole genome screening for structural and numerical chromosome aberrations in neuroblastoma, in particular for the analysis of localized tumors and high stage neuroblastomas lacking *MYCN* amplification, for which little genetic information was available. One of the major findings was the presence of a nonrandom pattern of whole chromosome gains and losses in low stage, prognostically favorable tumors, while high stage tumors mainly displayed partial chromosome imbalances. In keeping with this, extra chromosomes 17 or unbalanced 17q gain was found to be the most frequently genetic abnormality in low and high stage tumors, respectively, suggesting a possible gene dosage effect of one or more genes on 17q in neuroblastoma pathogenesis. Further study indicated that the 17q status was the most significant predictor for clinical outcome, and should therefore be incorporated in future clinical trials. Finally, a new genetic subgroup of aggressive neuroblastoma tumors was delineated, characterized by the presence of deletions of the long arm of chromosome 11, often in association with loss of 3p, but typically without *MYCN* amplification.

In the second part of this thesis, we attempted to identify relevant neuroblastoma genes on a transcriptome wide basis, using a combination of subtractive cDNA cloning of differentially expressed genes, and subsequent real time PCR profiling in both neuroblastoma cell lines and primary tumors. To this purpose, we first optimized the PCR assay, and demonstrated that a two-step real time quantitative RT-PCR based on SYBR Green I detection chemistry and DNase treated RNA as template is the method of choice for sensitive and reproducible transcript abundance measurements for a large series of different genes. Furthermore, we provided an adequate workaround for an old problem in gene expression studies, i.e. normalization of expression levels. We developed a conceptually novel and robust gene expression stability measure, outlined an algorithm to determine the most stable and hence reliable housekeepers in a given tissue panel, and presented a procedure to determine the optimal number of genes required for reliable normalization of RT-PCR data. This strategy should allow more accurate gene expression profiling, which is of utmost importance for studying the biological significance of subtle expression differences.
Gene expression data mining revealed typical expression signatures that were associated with major genetic defects and patient outcome. Several candidate MYCN transcriptional target genes were identified based on a combination of expression profiling of cell lines, primary biopsies, and a transfected MYCN overexpressing cell line, and might shed light on the way MYCN exerts its oncogenetic effects. Furthermore, putative class I and II tumor suppressor genes were identified for the critical regions of loss on chromosome arms 3p and 11q. Finally, several new prognostic marker genes were identified and allowed reliable patient classification with respect to survival probability.

In conclusion, we have provided significant new insights in the genetic heterogeneity of neuroblastoma, which resulted in a more accurate and detailed genetic subgroup classification, and identification of a strong predictive factor for patient outcome. Additionally, we have identified a substantial number of relevant neuroblastoma genes that deserve further study, and provided a technical framework for future isolation and analysis of differentially expressed genes in other genetic subgroups of neuroblastoma.

RÉSUMÉ

L'étude du neuroblastome est de grand intérêt puisqu'il comprend différents sous-types biologiques. En effet, chez l'enfant il est énigmatique et connaît une évolution clinique imprévisible pouvant aller d'une régression spontanée ou d'une maturation jusqu'à la formation d'un ganglioneurome bénin ou encore d'une prolifération agressive avec des métastases généralisées à l'issue fatale. Cette variabilité clinique reflète l'hétérogénéité génétique des cellules tumorales.
Cette thèse présente dans sa première partie l'intérêt de l'hybridation génomique comparative pour l'étude du caryotype. L'étude des aberrations de nombre et de structure des chromosomes du neuroblastome est particulièrement intéressante dans les tumeurs localisées et surtout dans les neuroblastomes à un stade avancé qui n'ont pas d'amplification *MYCN*. Grâce à la CGH l'identification d'anomalies de nombres, de pertes et de gains des chromosomes est possible dans des tumeurs localisés à pronostic favorable ainsi que la détection de déséquilibres de structures dans les tumeurs avancées. Spécifiquement, un chromosome 17 en extra ou un gain du bras 17q est l'anomalie cytogénétique la plus courante dans les tumeurs qu'elles soient localisées ou avancées. Ceci suggère que le 17q est impliqué dans la pathogénèse du neuroblastome. Des études ultérieures démontrent l'importance d'un contrôle du 17q comme élément prédictif de l'évolution clinique. La présence de délétion cytogénétique dans le bras 11q associé à la perte du bras 3p montre un nouveau sous-groupe et se retrouve dans les neuroblastomes agressifs qui n'ont pas d'amplification *MYCN*.

Dans la seconde partie de cette thèse nous avons comme but l'identification des gènes relevants du neuroblastome. Pour cette détection de gènes nous combinons le clonage subtractif des gènes exprimés différemment et de PCR en temps réel de lignées de neuroblastomes en de tumeurs primaires. L'optimisation de la technique PCR, par RT-PCR quantitative en 2 temps avec détection en SYBR Green I précédé d'un traitement DNAse de l'ARN, a prouvé être de grande reproduction dans une méthode sensible pour la mesure de transcrits d'une large série de gènes. Ensuite, nous avons trouvé la solution adéquate d'un vieux problème dans l'étude de l 'expression de gènes en normalisant les niveaux de l' expression. Pour cela, nous avons conçu un nouveau paramètre pour mesurer la stabilité de l 'expression d'un gène, tout comme un algorithme pour identifier dans une série d'échantillons les gènes les plus stables et aussi les plus fiables dans un tissu bien déterminé. Nous présentons également une technique de détermination du nombre idéal de gènes nécessaires à une bonne normalisation de la RT-PCR. La méthode présentée offre la possibilité de mesurer de façon plus précise les niveaux d'expression génique. Ceci est de grande importance dans l'étude de l'importance biologique de différences subtiles d'expression.
Les analyses démontrent que des signatures spécifiques d'expression peuvent être associées aux principaux défauts génétiques et aussi à un pronostic pour les patients. Un nombre de gènes candidats réglés par MYCN ont été identifié en combinant l'analyse de lignées cellulaires, de biopsies de tumeurs primaires, et d'une lignée transfectée ayant MYCN en surexpression. Ce travail a permis de mettre en évidence les méchanismes moléculaires des effets oncogénétiques de la protéine MYCN. Ensuite les gènes candidats suppresseurs de tumeurs de la classe I et II pour la région critique de perte en 3p et 11q ont été identifiés. Enfin, nous avons également identifié une série de gènes marqueurs d'intérêt pronostique afin de classifier les patients selon leur espérance de vie.

En conclusion, nous apportons de nouvelles perspectives dans l'hétérogénéité génétique du neuroblastome qui aboutissent à une classification plus exacte et détaillée des différents sous-groupes, et à l'identification d'un facteur conclusif pour le pronostic.
Ensuite nous avons identifié un nombre considérable de gènes neuroblastomes importants qui méritent une étude plus approfondie. Finalement nous avons développé un encadrement technique qui permet d'isoler et d'analyser d'autres gènes différentiels dans d'autres sous-groupes de neuroblastomes.

SAMENVATTING

Neuroblastoom wordt gedefinieerd als één tumortype, maar meer en meer lijkt het erop dat deze vorm van kanker verschillende biologische subtypes omvat. Neuroblastoom komt voor bij kinderen en vertoont een merkwaardig variabel klinisch verloop, gaande van spontane regressie of maturatie naar een goedaardig ganglioneuroom bij de ene patiënt, tot een agressief groeiende tumor met wijdverspreide uitzaaiingen en snel overlijden bij de andere patiënt. Deze typische klinische variabiliteit reflecteert ten dele de genetische heterogeniteit van de tumorcellen.
In het eerste deel van deze thesis hebben we de kracht geïllustreerd van vergelijkende genoomhybridisatie bij de studie van structurele en numerieke chromosoomafwijkingen in neuroblastoom. Deze methodologie is voornamelijk interessant gebleken voor de analyse van gelokaliseerde tumoren en metastaserende neuroblastomen zonder amplificatie van het *MYCN* proto-oncogen, voor dewelke voorheen slechts weinig genetische informatie beschikbaar was. Een belangrijke bevinding was de aanwezigheid van een specifiek patroon van numerieke chromosoomafwijkingen in prognostisch gunstige lage stadia tumoren, tegenover voornamelijk partiële chromosoomdefecten in hoge stadia neuroblastomen. Daarnaast werd aangetoond dat een extra chromosoom 17 of ongebalanceerde 17q toename de meest frequente genetische afwijking vormt in respectievelijk lage en hoge stadia neuroblastomen. Een verder doorgedreven analyse resulteerde in de identificatie van de 17q status als de meest significante voorspellende parameter voor de overlevingskansen van de patiënt, wat suggereert dat dit genetisch kenmerk in toekomstige klinische studies zou moeten geïncorporeerd worden. Tot slot werd een nieuwe genetische subgroep van agressieve neuroblastomen afgebakend, die gekenmerkt worden door een deletie van de lange arm van chromosoom 11, vaak in combinatie met een deletie van de korte arm van chromosoom 3, en zonder amplificatie van *MYCN*.

In het tweede deel van deze thesis beoogden we relevante neuroblastoomgenen te identificeren op basis van een combinatie van subtractieve cDNA klonering van differentieel geëxprimeerde genen en *real time* PCR profilering van neuroblastoom cellijnen en primaire tumoren. Hiertoe hebben we eerst de PCR methode geoptimaliseerd, waarbij aangetoond werd dat een tweestaps *real time* kwantitatieve RT-PCR op basis van SYBR Green I detectie en voorafgaande DNase-behandeling van het RNA, de aangewezen methode is voor gevoelige en reproduceerbare metingen van transcriptniveaus van een grote reeks verschillende genen. Verder hebben we een doeltreffende oplossing aangeboden voor een oud zeer bij expressiestudies, namelijk de normalisatie van expressieniveaus. We hebben een robuuste en conceptueel nieuwe genexpressie-stabiliteitsparameter ontwikkeld, gekoppeld aan een algoritme om de meest stabiele en dus betrouwbare huishoudgenen in een gegeven stalenreeks te identificeren. Daarnaast werd een procedure voorgesteld om het optimaal aantal genen te bepalen nodig voor een betrouwbare normalisatie van RT-PCR resultaten. De voorgestelde methode biedt de mogelijkheid om correct genexpressieniveaus te meten, wat van groot belang is voor de studie van de biologische significantie van subtiele expressieverschillen.
Data-analyse toonde aan dat typische genexpressie-signaturen geassocieerd konden worden aan de belangrijkste genetische defecten en aan de prognose van de neuroblastoompatiënten. Een aantal kandidaat *MYCN* transcriptionele doelwitgenen werden geïdentificeerd op basis van een gecombineerde analyse van cellijnen, primaire tumorbiopsiën, en een stabiel getransfecteerde cellijn waarin *MYCN* tot overexpressie komt. Deze bevindingen bieden mogelijks inzicht in de moleculaire mechanismen waarop het MYCN proteïne zijn oncogenetische effecten uitoefent. Verder werden mogelijke klasse I en II tumorsuppressor-genen voor de kritische regio's van verlies op chromosoomarmen 3p and 11q geïdentificeerd. Tenslotte werd ook een reeks van prognostische merkergenen geïdentificeerd, die de mogelijkheid bieden om op een betrouwbare wijze patiënten te classificeren volgens hun overlevingskansen.

Samengevat kunnen we stellen dat we belangrijke nieuwe inzichten gekregen hebben in de genetische heterogeniteit van neuroblastoom, wat resulteerde in een meer nauwkeurige en gedetailleerde subgroepclassificatie, alsook de identificatie van een sterke prognostische parameter. Bijkomend hebben we een substantieel aantal relevante neuroblastoomgenen geïdentificeerd die verdere studie verdienen, en een technisch kader ontwikkeld voor toekomstige isolaties en analyses van differentieel geëxprimeerde genen in andere genetische subgroepen van neuroblastoom.

ABBREVIATIONS

bHLH-LZ	basic Helix-Loop-Helix/Leucine Zipper
CGH	Comparative Genomic Hybridization
cM	centiMorgan
CNS	Central Nervous System
EFS	Event Free Survival
FISH	Fluorescent In Situ Hybridization
HVA	Homovanillic Acid
INPC	International Neuroblastoma Pathology Classification
kb	kilobases (one thousand basepairs)
LOH	Loss Of Heterozygosity
Mb	Megabases (one million basepairs)
M-FISH	Multicolour FISH
MKI	Mitosis-Karyorrhexis Index
MNA	*MYCN* Amplification
NB	Neuroblastoma
OS	Overall Survival
PCA	Principle Component Analysis
PCR	Polymerase Chain Reaction
PD	Primer Dimers
PNET	Primitive Neuroectodermal Tumor
PNS	Peripheral Nervous System
RT	Reverse Transcriptase
SAM	Significance Analysis of Microarray data
SIF	Small Intensely Fluorescent
SNS	Sympathetic Nervous System
SRO	Shortest Region of Overlap
SSH	Suppression Subtractive Hybridization
VMA	Vanillylmandelic Acid

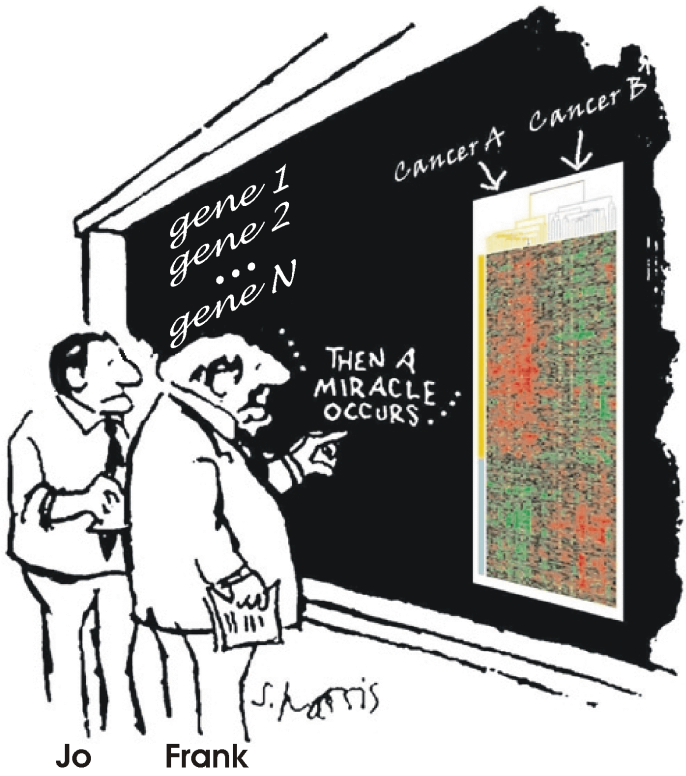

two weeks before the Ph.D. thesis is due
« I think you have to be a little more specific here in step two … »

ACKNOWLEDGMENTS

"Science is built up with facts, as a house is with stones. But a collection of facts is no more science than a heap of stones is a house." (Jules Henri Poincairé)

With the completion of this little house, I would like to express my gratitude to all construction workers who helped me trail and stack the building stones of this thesis.

Frank Speleman and Anne De Paepe, thank you for giving me the opportunity to join the neuroblastoma research team, and to grow as a young investigator. I really appreciated the atmosphere of trust, support, and enthusiasm in which I could develop the necessary research skills to 'build' my own thesis. Thank you for inspiring ideas, and encouragements.

All members of the neuroblastoma research team, Nadine Van Roy, Mireille Van Gele, Katleen De Preter, Els De Smet and Jasmien Hoebeeck, and colleague Ph.D. students, Bruce Poppe, Heidi Van Limbergen, Elfride De Baere, Ineke Vandenbroecke, and Katleen Claes, for collection of data, wet lab work, cheerfull discussions, collaborative papers, and nice lab ambiance.

Geneviève Laureys and all other pediatric oncologists for sample and data collection; I admire your work, and value the helpful discussions and interest in our work. All patients and parents for participating in our studies.

Former team member Katherine Mortier, and former students I had the chance to supervise, Lieven Thorrez, Katleen De Preter, Johann Iso-Oja, Filip Pattyn, and Jasmien Hoebeeck. Thank you all for your tremendous help in the lab, and cheerfull moments.

All members of the cytogenetics lab for their general interest, friendly conversations, and birthday cakes; especially Geert De Vos and Peter Degraeve for dedicated cell culture and help with karyotyping. All staff members of our service, and especially Sylvia De Bie, for her trust, and IT discussions; and all current and past members of the secretary office, for their administrative help, and friendly talks.

Frans Van Roy, Geert Berx, Kristin Strumane, and Katrien Staes for giving me the opportunity to spend some months in their lab, amongst others to do my very first PCR, for helping me with the subtractive cloning and Northern blot hybridizations, and for interesting discussions.

Romain Pauwels, and Ines Carromuino, for introducing us in the world of real time PCR, and to allow access to the ABI7700 machine, which was probably one of the first installed in Belgium.

I would also like to thank our European CGH collaborators, Dominique Plantaz, Valérie Combaret, Nick Bown, Maria Łastowska, Christian Brinkschmidt, Holger Christiansen, Peter Ambros, James Nicholson, Andy Pearson, and Olivier Delattre, for sharing data, samples and ideas. This nice multicenter collaboration resulted in three publications included in this thesis.

Sven Påhlman, and Anders Edsjö, new friends from Sweden, for enjoyable but thorough discussions, and sharing their ideas and interesting points of vue on neuroblastoma. I hope we will continue to meet and exchange ideas in the future.

Marie-Rose Verschraegen-Spae and Rita Dendooven, for blurring the fact that my French is not much better than my Russian.

Bio-Rad and Eurogentec, for the fine collaboration and financial support of this thesis; and all other people whom I forget to mention, apologies and double thanks!

My parents, for their education, limitless opportunities, and interest in what I do.
And above all, Ellen, for her infinite love, understanding and support; I could not have managed without her!

CURRICULUM VITAE

Jo VANDESOMPELE
Ghent University Hospital
Center for Medical Genetics, 1K5
De Pintelaan 185, B-9000 Ghent
09 2405518 (phone), 09 2404970 (fax), joke.vandesompele@rug.ac.be

Education

1986-1992	Latin-Sciences, H.-Hartcollege, Waregem
1992-1997	Bio-engineer in cell and gene technology Ghent University, Faculty of Agricultural and Applied Biological Sciences thesis: "Comparative genomic hybridization of neuroblastoma tumors"
1997-2002	Ph.D. training, Ghent University, Faculty of Medicine and Health Sciences

Professional record

1997-2001	Ph.D. candidate with IWT-specialisation grant
2001-2002	Ph.D. candidate with RUG finalisation grant

Publications *Articles in international journals with referee system*

Van Gele M, Speleman F, Vandesompele J, Van Roy, Leonard JH (1998): Characteristic pattern of chromosomal gains and losses in Merkel cell carcinoma detected by comparative genomic hybridization. Cancer Research, 58: 1503-1508.

Van Gele M, Van Roy N, Ronan SG, Messiaen L, Vandesompele J, Geerts ML, Naeyaert JM, Blennow E, Bar-Am I, Das Gupta TK, Leonard JH, Speleman F (1998): Molecular characterization of 1p36 breakpoints in two Merkel cell carcinomas. Genes, Chromosomes and Cancer, 23: 67-71.

Vandesompele J, Van Roy N, Van Gele M, Laureys G, Ambros P, Heimann P, Devalck C, Schuuring E, Brock P, Otten J, Gyselinck J, De Paepe A, Speleman F (1998): Genetic heterogeneity of neuroblastoma studied by comparative genomic hybridization. Genes, Chromosomes and Cancer, 23: 141-152.

Bown N, Cotterill S, Lastowska M, O'Neill S, Pearson ADJ, Nicholson J, Plantaz D, Meddeb M, Danglot G, Bernheim A, Brinkschmidt C, Christiansen H, Betts D, Vandesompele J, Van Roy N, Speleman F (1999): Gain of chromosome arm 17q and adverse outcome in patients with neuroblastoma. N Eng J Med, 340:1954-1961.

Judson H, Van Roy N, Vandesompele J, Van Gele M, Speleman F, Bonthron DT: Structure and mutation analysis of the gene encoding caspase-activated nuclease, a candidate neuroblastoma tumour suppressor gene (2000):
Hum Genet, 106(4):406-13.

Vandesompele J, Speleman F, Van Roy N, Laureys G, Brinkschmidt C, Christiansen H, Lampert F, Lastowska M, Bown N, Pearson A, Nicholson J, Ross F , Combaret V, Delattre O, Feuerstein BG, Plantaz D (2001): Multicentre analysis of patterns of DNA gains and losses in 204 neuroblastoma tumours: How many genetic subgroups are there? Medical Pediatric Oncology, 36:5-10.

Plantaz D, Vandesompele J, Laureys G, Bown N, Lastowska M, Brinkschmidt C, Nicholson J, Combaret V, Delattre O, Bénard J, Caron H, Feuerstein BG, Speleman F (2001): Deletion of chromosome 11q is the most frequent deletion detetected by CGH in stage 4 neuroblastoma lacking MYCN amplification and 1p deletion. Int J Cancer, 91:680-686

Vandenbroucke I, Vandesompele J, De Paepe A, Messiaen L (2001): Quantification of splice variants using real-time PCR. Nucleic Acids Research, 29(13):E68

Van Roy N, Van Limbergen H, Vandesompele J, Van Gele M, Boppe B, Salwen H, Laureys G, Manoel N, De Paepe A, Speleman F (2001): Combined M-FISH and CGH analysis allows comprehensive description of genetic alterations in neuroblastoma cell lines. Genes, Chromosomes and Cancer, 32(2):126-135

De Preter K, Speleman F, Combaret V, Lunec J, Laureys G, Francotte N, Board J, Pearson A, De Paepe A, Van Roy N, Vandesompele J (2002): Quantification of MYCN, DDX1 and NAG copy number in neuroblastoma using a real-time quantitative PCR assay. Modern Pathology, 15(2):159-166

Vandesompele J, De Paepe A, Speleman F (2002): Elimination of primer-dimer artefacts and genomic co-amplification using a two-step SYBR Green I real-time RT-PCR. Analytical Biochemistry, 303(1):95-98

Vandesompele J, Speleman F (2002)
A brief commentary on "Chromosomal aberrations in neuroblastoma cell lines identified by cross species color banding and chromosome painting" (Letter-to-the-editor). Cancer Genetics Cytogenetics, 135(2):178-178

Van Roy N, Vandesompele J, Berx G, Staes K, Van Gele M, De Smet E, De Paepe A, Laureys G, van der Drift P, Versteeg R, Van Roy F, Speleman F: Localisation of the 17q breakpoint of a constitutional 1;17 translocation in a patient with neuroblastoma within a 25 kb segment located between the ACCN1 and TLK2 genes and near the distal breakpoints of two microdeletions in NF1 patients. Genes, Chromosomes and Cancer (in press)

Vandesompele J, De Preter K, Pattyn F, Poppe B, Van Roy N, De Paepe A, Speleman F
Accurate normalization of real-time quantitative RT-PCR data by geometric averaging of multiple internal control genes. GenomeBiology (in press)

Claes K, Vandesompele J, Poppe B, Dahan K, Coene A, De Paepe A, Messiaen L
Pathological splice mutations outside the invariant AG/GT splice sites of BRCA1 exon 5 increase alternative transcripts levels in the 5' end of the BRCA1 gene. Oncogene (accepted)

Oral presentations

Evaluation of SSH for identification of differentially expressed genes in neuroblastoma. Vandesompele J, Van Roy N, Thorrez L, Berx G, De Paepe A, Van Roy F, Laureys G, Speleman F. 32nd Meeting of the International Society of Paediatric Oncology (SIOP), October 5th, 2000, Amsterdam, The Netherlands. Medical and Paediatric Oncology 35(3):169-183, 2000

Subtractive expression profiling between two genetic subgroups of neuroblastoma. Vandesompele J, Pattyn F, De Preter K, Van Roy N, Swerts K, Hoebeeck J, Laureys G, De Paepe A, Philippe J, Speleman F. Advances in Neuroblastoma Research, June 17-19, 2002, Paris, France

Congresses, workshops and meetings

First European Symposium on Applied Genome Research, November 26-27, 1998, Brussels, Belgium (poster)

Advances in Neuroblastoma Research, June 15-17, 1998, Bath, UK (poster)

Belgian Association for Cancer Research, January 30th, 1999, Antwerp, Belgium (poster)

Introduction to PCR and Real Time PCR analysis, December 10th, 1999, Affligem, Belgium

Genomics and Proteomics - Highways to Functional Biology, May 7th, 1999, Ghent, Belgium

Eighth International Workshop on Chromosomes in Solid Tumors, January 30-February 1, 2000, Tucson, Arizona, USA (poster)

Advances in Neuroblastoma Research, May 16-18, 2000, Philadelphia, USA (poster)

From Genomics to Proteomics, May 25th, 2000, Beerse, Belgium

CGH task force The Netherlands-Belgium, August 3, 2000, Rotterdam, The Netherlands (oral presentation "Neuroblastoma: from CGH to expression profiling")

32nd Meeting of the International Society of Paediatric Oncology (SIOP), October 5, 2000, Amsterdam, The Netherlands (oral presentation "Evaluation of SSH for identification of differentially expressed genes in neuroblastoma")

Pediatric Oncology Staff Meeting, December 21, 2000, Ghent, Belgium (oral presentation "Evaluation of SSH for identification of differentially expressed genes in neuroblastoma")

Oncogenomics, Januari 25-27, 2001, Tucson, USA (poster)

First annual meeting of the Belgian Society for Human Genetics, February 9, 2001, Brussels, Belgium (poster)

Sequence Detection Software user meeting (Applied Biosystems), January 18, 2001 Rotterdam, The Netherlands (invited speaker "Quantification and normalization of gene expression using SYBR Green I real-time RT-PCR")

The second Euroconference on Quantitative Molecular Cytogenetics, April 26-28, 2001, Salamanca, Spain (poster)

Signal transduction in cell death and gene induction: From cells to physiology & strategies for discovery, November 10-11, 2000, Ghent, Belgium

The 31st annual meeting of the European Environmental Mutagen Society, September 1-5, 2001, Ghent, Belgium

Quantitative PCR seminar (Bio-Rad), March 14, 2002 Affligem, Belgium (invited speaker "Quantification and normalization of gene expression using SYBR Green I real-time RT-PCR: methodology & applications")